



UNIVERSITAT DE
BARCELONA

**Administration of chitosan-tripolyphosphate-DNA
nanoparticles overexpressing key enzymes to improve
omega-3 long-chain polyunsaturated fatty acid synthesis
in gilthead sea bream (*Sparus aurata*)**

Yuanbing Wu



Aquesta tesi doctoral està subjecta a la llicència **Reconeixement- NoComercial – SenseObraDerivada 4.0. Espanya de Creative Commons.**

Esta tesis doctoral está sujeta a la licencia **Reconocimiento - NoComercial – SinObraDerivada 4.0. España de Creative Commons.**

This doctoral thesis is licensed under the **Creative Commons Attribution-NonCommercial-NoDerivs 4.0. Spain License.**



UNIVERSITAT_{DE}
BARCELONA

UNIVERSITAT DE BARCELONA

**ADMINISTRATION OF CHITOSAN-TRIPOLYPHOSPHATE-DNA
NANOPARTICLES OVEREXPRESSING KEY ENZYMES TO IMPROVE
OMEGA-3 LONG-CHAIN POLYUNSATURATED FATTY ACID SYNTHESIS IN
GILTHEAD SEA BREAM (*SPARUS AURATA*)**

YUANBING WU



UNIVERSITAT DE
BARCELONA

UNIVERSITAT DE BARCELONA

FACULTAT DE FARMÀCIA I CIÈNCIES DE L'ALIMENTACIÓ

DEPARTAMENT DE BIOQUÍMICA I FISIOLOGIA
SECCIÓ DE BIOQUÍMICA I BIOLOGIA MOLECULAR

PROGRAMA DE DOCTORAT EN BIOTECNOLOGIA

**ADMINISTRATION OF CHITOSAN-TRIPOLYPHOSPHATE-DNA
NANOPARTICLES OVEREXPRESSING KEY ENZYMES TO IMPROVE
OMEGA-3 LONG-CHAIN POLYUNSATURATED FATTY ACID SYNTHESIS IN
GILTHEAD SEA BREAM (*SPARUS AURATA*)**

YUANBING WU
Barcelona 2023



UNIVERSITAT DE
BARCELONA

UNIVERSITAT DE BARCELONA

FACULTAT DE FARMÀCIA I CIÈNCIES DE L'ALIMENTACIÓ

DEPARTAMENT DE BIOQUÍMICA I FISIOLOGIA
SECCIÓ DE BIOQUÍMICA I BIOLOGIA MOLECULAR

PROGRAMA DE DOCTORAT EN BIOTECNOLOGIA

**ADMINISTRATION OF CHITOSAN-TRIPOLYPHOSPHATE-DNA
NANOPARTICLES OVEREXPRESSING KEY ENZYMES TO IMPROVE
OMEGA-3 LONG-CHAIN POLYUNSATURATED FATTY ACID SYNTHESIS IN
GILTHEAD SEA BREAM (*SPARUS AURATA*)**

Memòria presentada per Yuanbing Wu per a optar al títol de doctor per la
Universitat de Barcelona

Isidoro Metón Teijeiro
Director

Yuanbing Wu
Doctorand

Barcelona 2023

Acknowledgements

I would like to express my sincere gratitude to my supervisor, Dr. Isidoro Metón, for his invaluable guidance throughout my doctoral studies. Dr. Metón's rigorous approach to experimental practice and results, logical problem-solving abilities, patience in data analysis, insightful comments on the relationship between results, and his warm and cordial personality have been instrumental in shaping my research and will undoubtedly prove invaluable in my future research endeavors.

Additionally, I extend my thanks to Prof. María Pilar Almajano for providing me with access to experimental equipment and offering valuable feedback and suggestions during my doctoral studies.

I am also grateful to my colleagues Ania Rashidpour, Lab technician Christopher Dominguez Vela and Ignasi Mata Saumell, and all other members at the department of Biochemistry and Physiology, for their unwavering support and warm concern during my doctoral studies.

Special thanks go to my roommates, XuFei Lu, Xiangbo Bu, Yu Yin, and Yang Wang, whose assistance and companionship have lessened my nostalgia and enriched my life abroad. I cherish their friendship dearly.

Thanks to the China Scholarship Council for supporting my living expenses during my PhD studies.

Finally, the love and support from my family and girlfriend are beyond words.

Yuanbing Wu
2023.02.28, Barcelona, Spain

Abstract

Eicosapentaenoic acid (20:5 n -3, EPA) and docosahexaenoic acid (22:6 n -3, DHA) are omega-3 long-chain polyunsaturated fatty acids (n -3 LC-PUFA) known to prevent atherosclerosis, stroke, obesity, type-2 diabetes, inflammation and autoimmune disease, among others. Few organisms, such as *Caenorhabditis elegans* and some invertebrates, can synthesize the n -3 fatty acid series in significant amounts, and marine fish and shellfish, which acquire pre-formed LC-PUFA by trophic transfer, are the major sources of n -3 LC-PUFA in the human diet. However, substitution of fish oil by vegetable oils in aquafeeds reduces healthy n -3 LC-PUFA in cultured fish, while increases proinflammatory n -6 fatty acids. The present study aimed to empower *Sparus aurata* to boost endogenous synthesis of n -3 LC-PUFA by transient expression of fish codon-optimized *Caenorhabditis elegans* $\Delta 12/n$ -6 (FAT-2) and $\Delta 15/n$ -3 (FAT-1) fatty acid desaturases using chitosan-tripolyphosphate (TPP) nanoparticles as DNA delivery system. Growth performance, body composition, serum metabolites, fatty acid profile and expression of key enzymes in intermediary metabolism were evaluated in *Sparus aurata* juveniles 72 hours after a single intraperitoneal injection of chitosan-TPP nanoparticles encapsulated with expression plasmids encoding fish codon-optimized *C. elegans* FAT-1 and FAT-2 (short-term effect) and in 70-day treated fish that were periodically administered with chitosan-TPP-DNA nanoparticles (long-term sustained effect).

For the short-term study, increased levels of FAT-1 and FAT-2 mRNAs (> 10-fold) were detected 72 hours post-injection in the *S. aurata* liver. Expression of FAT-1 elevated hepatic EPA and total n -3 PUFA. In addition to reduced serum triglycerides, co-expression of FAT-1 and FAT-2 also induced proportions of DHA and PUFA in the *S. aurata* liver. Compared to control fish, treatment with FAT-1, FAT-2 and FAT-1 + FAT-2 downregulated expression of hepatic key genes in glycolysis and lipogenesis, including *g6pd*, *pfk1*, *pk*, *pfkfb1*, *acaca*, *acacb*, *fasn*, *scd1a* and *fads2*. In addition, co-expression of FAT-1 and FAT-2 significantly upregulated the activity of rate-limiting enzymes in glycolysis and the pentose phosphate pathway. Fish expressing FAT-2 and FAT-1 + FAT-2 showed lower hepatic expression of *pparg* and *srebfl*, and higher of *bnf4a*. Treatment with FAT-1 and FAT-2 alone downregulated *srebfl* and upregulated *ppara*, respectively, in the *S. aurata* liver.

To study long-term sustained expression of FAT-1, FAT-2 and FAT-1 + FAT-2, chitosan-TPP-DNA nanoparticles were provided to fish every 4 weeks (3 doses in total). After 70 days of treatment, tissue distribution analysis showed high expression levels for FAT-1 and FAT-2 in the liver (>200-fold) followed by the intestine (10 to 25-fold), while no differential expression occurred in the skeletal muscle and brain. Expression of FAT-1 and FAT-1 + FAT-2 increased weight gain. Fatty acid methyl esters assay revealed that co-expression of FAT-1 and FAT-2 increased liver production and muscle accumulation of EPA, DHA and total n -3 LC-PUFA, while decreased the n -6/ n -3 ratio. Co-expression of FAT-1 and FAT-2 downregulated *srebfl* and genes encoding rate-limiting enzymes for *de novo* lipogenesis in the liver, leading to decreased circulating triglycerides and cholesterol. In contrast, FAT-2 and FAT-1 + FAT-2 upregulated hepatic *bnf4a*, *nr1h3* and key enzymes in glycolysis and the pentose phosphate pathway.

Our findings demonstrate that administration of chitosan-TPP-DNA nanoparticles, a

methodology that circumvents obtention of genetically modified organisms, is a proper gene delivery method for sustained expression of exogenous enzymes in the liver of *Sparus aurata*. Specifically, co-expression of FAT-1 and FAT-2 enabled the production of functional fish for human consumption, rich in *n*-3 LC-PUFA, notably EPA and DHA, and with decreased *n*-6/*n*-3 fatty acids ratio. In addition, co-expression of FAT-1 and FAT-2 increased weight gain and the specific growth rate in *Sparus aurata*.

CONTENTS

TABLE OF CONTENTS

1 INTRODUCTION	1
1.1 LC-PUFA, health and aquaculture	3
1.1.1 LC-PUFA	3
1.1.2 LC-PUFA and health	3
1.1.3 LC-PUFA and aquaculture	5
1.2 Carbohydrate metabolism in fish	8
1.3 Amino acid metabolism in fish.....	11
1.4 LC-PUFA synthesis in fish.....	13
1.4.1 LC-PUFA transport and absorption	13
1.4.2 DNL	14
1.4.3 Fatty acid elongation and desaturation	15
1.4.4 The regulation of LC-PUFA synthesis.....	17
1.4.5 FAT-1 and FAT-2 in <i>Caenorhabditis elegans</i>	20
1.5 Chitosan as a nuclear acid delivery vector	21
1.5.1 Chitosan-TPP-DNA nanoparticle properties.....	21
1.5.2 Ionic gelation methods.....	23
2 OBJECTIVES	25
2.1 General objective	27
2.2 Specific objectives.....	28
3 MATERIALS AND METHODS.....	29
3.1 Animals.....	31
3.1.1 Animal maintenance and sampling.....	31
3.1.2 Experiments	33
3.1.3 Growth performance.....	34
3.2 Plasmids.....	35
3.3 Oligonucleotides	35
3.4 Design of fish codon-optimized cDNAs.....	38
3.5 Preparation of DH5 α competent <i>Escherichia coli</i>	38
3.6 Transformation of DH5 α competent cells.....	39
3.7 Isolation of plasmids.....	41
3.8 Restriction endonuclease digestion.....	41
3.9 DNA ligation.....	44
3.10 PCR screening of positive ligation products	44
3.11 DNA gel electrophoresis.....	46
3.12 Cycle sequencing.....	47
3.13 RNA extraction.....	48
3.14 Reverse transcription.....	48

3.15	Quantitative real-time PCR.....	49
3.16	Eukaryotic cell culture and transformation.....	50
3.16.1	HepG2 culture.....	51
3.16.2	Subculture.....	51
3.16.3	Freezing cells.....	52
3.16.4	Thawing cells.....	52
3.17	Calcium phosphate-DNA co-precipitation.....	53
3.18	Serum metabolites.....	54
3.19	Enzyme activity assays.....	56
3.19.1	Total soluble protein content.....	57
3.19.2	Pfkl.....	58
3.19.3	Fbp1.....	59
3.19.4	Pklr.....	60
3.19.5	G6pd.....	62
3.19.6	Pgd.....	62
3.19.7	Idh.....	63
3.19.8	Ogdh.....	64
3.19.9	Alt.....	65
3.19.10	Ast.....	66
3.20	Body composition.....	67
3.21	Fatty acids extraction.....	70
3.22	Gas chromatography.....	71
3.23	Chitosan-TPP-plasmid nanoparticles.....	71
3.23.1	Preparation of Chitosan-TPP-plasmid nanoparticles.....	71
3.23.2	Characterization of nanoparticle size and zeta potential.....	73
3.24	Statistical analysis.....	73
4	RESULTS.....	75
4.1	Construction of pSG5-FAT-1.....	77
4.1.1	Fish codon-optimized sequence of FAT-1.....	77
4.1.2	Enzyme digestion of pMA-T-FAT-1 and pSG5.....	78
4.1.3	PCR colony screening of pSG5-FAT-1.....	79
4.1.4	Sequencing pSG5-FAT-1.....	80
4.2	Construction of pSG5-FAT-2.....	81
4.2.1	Fish codon-optimized sequence of FAT-2.....	81
4.2.2	Enzyme digestion of pMA-T-FAT-2 and pSG5.....	82
4.2.3	PCR colony screening of pSG5-FAT-2.....	83
4.2.4	Sequencing pSG5-FAT-2.....	84
4.3	Characterization of chitosan-TPP-plasmid nanoparticles.....	85

4.4 Effect of <i>in vitro</i> expression of pSG5-FAT-1 and pSG5-FAT-2	85
4.4.1 Transient transfection with pSG5-FAT-1 and pSG5-FAT-2 increases FAT-1 and FAT-2 mRNA levels in HepG2.....	86
4.4.2 Transient transfection with pSG5-FAT-1 and pSG5-FAT-2 affects the fatty acid profile in HepG2 cells.....	87
4.5 Short-term effects of expressing fish codon-optimized <i>C. elegans</i> FAT-1 and FAT-2 in <i>S.</i> <i>aurata</i>	88
4.5.1 Hepatic expression of exogenous enzymes, FAT-1 and FAT-2.....	88
4.5.2 Effect on serum metabolites	89
4.5.3 Effects on hepatic fatty acid profile.....	90
4.5.4 Effect on hepatic expression of <i>DNL</i> and LC-PUFA synthesis related genes..	92
4.5.5 Effect on hepatic expression of glucose metabolism related genes.....	94
4.5.6 Effect on hepatic activity of intermediary and glucose metabolism related enzymes	95
4.5.7 Effect of short-term nanoparticle administration on hepatic expression of glucose and lipid metabolism related transcription factors.....	98
4.6 Long-term detection of fish codon-optimized <i>C. elegans</i> FAT-1 and FAT-2 mRNA levels in the liver of <i>S. aurata</i> after a single dose of chitosan-TPP-DNA nanoparticles	99
4.7 Effects of periodical intraperitoneal doses of chitosan-TPP nanoparticles complexed with pSG5-FAT-1 and pSG5-FAT-2 on the intermediary metabolism, fatty acid profile and growth parameters in <i>S. aurata</i>	100
4.7.1 Effect of periodical nanoparticle administration on tissue distribution of FAT-1 and FAT-2.....	100
4.7.2 Effect of periodical nanoparticle administration on body composition and growth performance.....	101
4.7.3 Effect of periodical nanoparticle administration on serum metabolites	102
4.7.4 Effect of periodical nanoparticle administration on hepatic fatty acid profile.	103
4.7.5 Effect of periodical nanoparticle administration on muscle fatty acid profile.	105
4.7.6 Effect of periodical nanoparticle administration on hepatic expression of <i>DNL</i> and LC-PUFA synthesis related genes	107
4.7.7 Effect of periodical nanoparticle administration on the hepatic expression of glucose metabolism related genes	109
4.7.8 Effect of periodical nanoparticle administration on hepatic activity of intermediary and glucose metabolism related enzymes.....	110
4.7.9 Effect of periodical nanoparticle administration on hepatic expression of glucose and lipid metabolism related transcription factors	113
5 DISCUSSION	115
5.1 Expression of fish codon-optimized <i>C. elegans</i> FAT-1 and FAT-2 in HepG2 cells	117

5.2 Delivery of chitosan-TPP complexed with fish codon-optimized FAT-1 and FAT-2 nanoparticles to <i>S. aurata</i>	118
5.2.1 Effects of FAT-1 and FAT-2 expression on body composition and growth performance.....	119
5.2.2 Effects of FAT-1 and FAT-2 expression on serum metabolites.....	120
5.2.3 Effects of FAT-1 and FAT-2 expression on hepatic and muscular fatty acid profiles in <i>S. aurata</i>	121
5.2.4 Effects of FAT-1 and FAT-2 expression on lipid metabolism.....	123
5.2.5 Effects of FAT-1 and FAT-2 expression on glycolysis-gluconeogenesis, PPP, the Krebs cycle and amino acid metabolism.....	126
6 CONCLUSIONS.....	131
7 REFERENCES.....	137
8 APPENDIX.....	163

LIST OF FIGURES

Figure	Description
Figure 1.1.1	Structures of palmitic acid and oleic acid
Figure 1.2	Schematic overview of hepatic glycolysis, gluconeogenesis and the Krebs cycle.
Figure 1.3.3	Biosynthetic pathways of LC-PUFA in vertebrates (black arrows)
Figure 1.5.1	Deacetylation of chitin to chitosan
Figure 1.5.2	Ionic gelation of chitosan-TPP-DNA nanoparticles
Figure 4.1.1	Fish codon-optimized <i>C. elegans</i> FAT-1 cDNA sequence
Figure 4.1.2A	Gel electrophoresis of pMA-T-FAT-1 digested with <i>Eco</i> RI and <i>Kpn</i> I
Figure 4.1.2B	Gel electrophoresis of pSG5 digested with <i>Eco</i> RI and <i>Kpn</i> I
Figure 4.1.3	PCR screening of pSG5-FAT-1
Figure 4.1.4a	pSG5-FAT-1 sequencing with T7 forward primer
Figure 4.1.4b	pSG5-FAT-1 sequencing with pSG5rev reverse primer
Figure 4.2.1	Fish codon-optimized <i>C. elegans</i> FAT-2 cDNA sequence
Figure 4.2.2A	Gel electrophoresis of pMA-T-FAT-2 digested with <i>Eco</i> RI and <i>Bam</i> HI
Figure 4.2.2B	Gel electrophoresis of pSG5 digested by <i>Eco</i> RI and <i>Bam</i> HI
Figure 4.2.3	PCR screening of pSG5-FAT-2
Figure 4.2.4A	pSG5-FAT-2 sequencing with T7 forward primer
Figure 4.2.4B	pSG5-FAT-2 sequencing with pSG5rev reverse primer
Figure 4.4.1	Effect of transient transfection with pSG5 (control), pSG5-FAT-1, pSG5-FAT-2, and pSG5-FAT-1 + pSG5-FAT-2 plasmids on the mRNA levels of fish codon-optimized FAT-1 and FAT-2 in HepG2 cells
Figure 4.5.1	Short-term effect of chitosan-TPP nanoparticles encapsulated with pSG5 (control), pSG5-FAT-1, pSG5-FAT-2 and pSG5-FAT-1 + pSG5-FAT-2 on the mRNA levels of fish-codon optimized <i>C. elegans</i> FAT-1 (A) and FAT-2 (B) in the <i>S. aurata</i> liver
Figure 4.5.2	Short-term effect of chitosan-TPP nanoparticles encapsulated with pSG5 (control), pSG5-FAT-1, pSG5-FAT-2 and pSG5-FAT-1 + pSG5-FAT-2 on serum glucose (A), triglycerides (B) and cholesterol (C) in <i>S. aurata</i>
Figure 4.5.4	Short-term effects of chitosan-TPP nanoparticles encapsulated with pSG5 (control), pSG5-FAT-1, pSG5-FAT-2 and pSG5-FAT-1 + pSG5-FAT-2 on the expression of key genes in DNL and LC-PUFA synthesis in the liver of <i>S. aurata</i>
Figure 4.5.5	Short-term effects of chitosan-TPP nanoparticles encapsulated with pSG5 (control), pSG5-FAT-1, pSG5-FAT-2 and pSG5-FAT-1 + pSG5-FAT-2 on the mRNA levels of glucose metabolism genes in the <i>S. aurata</i> liver
Figure 4.5.6	Short-term effects of chitosan-TPP nanoparticles complexed with pSG5 (control), pSG5-FAT-1, pSG5-FAT-2 and pSG5-FAT-1 + pSG5-FAT-2 on key enzymes in glycolysis-gluconeogenesis, PPP, the Krebs cycle and amino acid

	metabolism in the liver of <i>S. aurata</i>
Figure 4.5.7	Short-term effects of chitosan-TPP nanoparticles encapsulated with pSG5 (control), pSG5-FAT-1, pSG5-FAT-2 and pSG5-FAT-1 + pSG5-FAT-2 on the expression of key transcription factors involved in glucose and lipid metabolism in the liver of <i>S. aurata</i> .
Figure 4.6	Effect of single dose of chitosan-TPP nanoparticles complexed with pSG5 (control), pSG5-FAT-1, pSG5-FAT-2 and pSG5-FAT-1 + pSG5-FAT-2 on the mRNA levels of fish-codon optimized <i>C. elegans</i> FAT-1 and FAT-2 in <i>S. aurata</i> liver
Figure 4.7.1	Effect of periodical administration of chitosan-TPP nanoparticles complexed with pSG5 (control), pSG5-FAT-1, pSG5-FAT-2 and pSG5-FAT-1 + pSG5-FAT-2 on the mRNA levels of fish-codon optimized <i>C. elegans</i> FAT-1 and FAT-2 in <i>S. aurata</i> tissues
Figure 4.7.3	Effect of periodical nanoparticle administration of chitosan-TPP nanoparticles complexed with pSG5 (control), pSG5-FAT-1, pSG5-FAT-2 and pSG5-FAT-1 + pSG5-FAT-2 on serum glucose (A), triglycerides (B) and cholesterol (C) in <i>S. aurata</i>
Figure 4.7.6	Effect of periodical administration of chitosan-TPP nanoparticles complexed with pSG5 (control), pSG5-FAT-1, pSG5-FAT-2 and pSG5-FAT-1 + pSG5-FAT-2 on the expression of key genes in DNL and LC-PUFA synthesis in the liver of <i>S. aurata</i>
Figure 4.7.7	Effect of periodical administration of chitosan-TPP nanoparticles complexed with pSG5 (control), pSG5-FAT-1, pSG5-FAT-2 and pSG5-FAT-1 + pSG5-FAT-2 on the mRNA levels of glucose metabolism genes in <i>S. aurata</i> liver
Figure 4.7.8	Effect of periodical administration of chitosan-TPP nanoparticles complexed with pSG5 (control), pSG5-FAT-1, pSG5-FAT-2 and pSG5-FAT-1 + pSG5-FAT-2 on key enzymes in glycolysis-gluconeogenesis, PPP, the Krebs cycle and amino acid metabolism in the liver of <i>S. aurata</i>
Figure 4.7.9	Effect of periodical administration of chitosan-TPP nanoparticles complexed with pSG5 (control), pSG5-FAT-1, pSG5-FAT-2 and pSG5-FAT-1 + pSG5-FAT-2 on the expression of key transcription factors involved in glucose and lipid metabolism in the liver of <i>S. aurata</i>

LIST OF TABLES

Table	Description
Table 1.1.3.1a	Common terrestrial sources of dietary LC-PUFA
Table 1.1.3.1b	Common fish sources of dietary LC-PUFA
Table 3.1.1	Microbaq 16S diet composition
Table 3.3	Oligonucleotides
Table 3.5	LB broth
Table 3.6	LB agar plate
Table 3.8a	Enzyme digestion of pMA-T-FAT-1 and pSG5 plasmids with <i>EcoRI</i>
Table 3.8b	Enzyme digestion of pMA-T-FAT-1 and pSG5 plasmids with <i>KpnI</i>
Table 3.8c	Enzyme digestion of pMA-T-FAT-2 and pSG5 plasmids with <i>EcoRI</i> and <i>BamHI</i>
Table 3.9	DNA ligation system for assembling insert and vector
Table 3.10a	PCR reaction system for screening positive pSG5 colonies (volume per colony)
Table 3.10b	PCR reaction program
Table 3.11a	50X TAE (Tris-acetate-EDTA) buffer
Table 3.11b	1 % agarose (w/v)
Table 3.14a	Components for reverse transcription
Table 3.14b	Components for reverse transcription
Table 3.15b	Components of master mix for qPCR
Table 3.15c	qPCR running program
Table 3.16.2	10X PBS stock solution
Table 3.17	2X BBS sub solutions
Table 3.18	Standard for determination of serum metabolites
Table 3.19	Homogenization buffer for liver crude extract
Table 3.19.2	Reaction system for measuring hepatic Pfkf activity
Table 3.19.3	Reaction system for measuring hepatic Fbp1 activity
Table 3.19.4	Reaction system for measuring hepatic Pklr activity
Table 3.19.5	Reaction system for measuring hepatic G6pd activity
Table 3.19.6	Reaction system for measuring hepatic Pgd activity
Table 3.19.7	Reaction system for measuring hepatic Idh activity
Table 3.19.8	Reaction system for measuring hepatic Ogdh activity
Table 3.19.9	Reaction system for measuring hepatic Alt activity
Table 3.19.10	Reaction system for measuring hepatic Ast activity
Table 4.3	Characteristics of chitosan-TPP and chitosan-TPP-DNA nanoparticles
Table 4.4.2	Effect of pSG5 (control), pSG5-FAT-1, pSG5-FAT-2, and pSG5-FAT-1 + pSG5-FAT-2 plasmids on the fatty acid profile of HepG2 cells.
Table 4.5.3	Effects of chitosan-TPP nanoparticles complexed with pSG5 (control), pSG5-

	FAT-1, pSG5-FAT-2 and pSG5-FAT-1 + pSG5-FAT-2 on the fatty acid composition of <i>S. aurata</i> liver.
Table 4.7.2	Growth performance, nutrient retention and body composition of <i>S. aurata</i> after periodical administration of chitosan-TPP nanoparticles complexed with empty vector (pSG5, control), pSG5-FAT-1, pSG5-FAT-2 and pSG5-FAT-1 + pSG5-FAT-2.
Table 4.7.4	Effect of periodical administration of chitosan-TPP nanoparticles complexed with pSG5 (control), with empty vector (pSG5, control), pSG5-FAT-1, pSG5-FAT-2 and pSG5-FAT-1 + pSG5-FAT-2 on the fatty acid profile of <i>S. aurata</i> liver.
Table 4.7.5	Effect of periodical administration of chitosan-TPP nanoparticles complexed with pSG5 (control), with empty vector (pSG5, control), pSG5-FAT-1, pSG5-FAT-2 and pSG5-FAT-1 + pSG5-FAT-2 on the fatty acid profile of <i>S. aurata</i> skeletal muscle.

ABBREVIATIONS

Abbreviation	Full name	Abbreviation	Full name
18s	ribosomal subunit 18s	HMGCR	3-hydroxy-3-methyl-glutaryl-coenzyme a reductase
6PG	6-phosphogluconate	HNF4A	hepatocyte nuclear factor 4 alpha
α -KG	alpha-ketoglutarate	HSI	hepatosomatic index
ACAC	acetyl-CoA carboxylases	HUFA	high unsaturated fatty acids
ACACA	acetyl-CoA carboxylase alpha	IDH	isocitrate dehydrogenase
ACACB	acetyl-CoA carboxylase beta	INSIG1	insulin-induced genes 1
Acetyl-CoA	acetyl coenzyme A	LA	linoleic acid
ACTB	beta-actin	LB	Luria Bertani
ADP	adenosine diphosphate	LC-PUFA	long-chain polyunsaturated fatty acid
ALA	alpha-linolenic acid	LPL	lipoprotein lipase
Ala	alanine	LR	lipid retention
ALT	alanine transaminase	LXR	liver x receptor
Apo	apolipoprotein	LXRE	liver x receptor response element
ARA	arachidonic acid	MQ	milli-q
Asp	aspartic acid	MS-222	tricaine methansulfonate
AST	aspartate transaminase	MUFA	monounsaturated fatty acid
ATP	adenosine triphosphate	NADPH	reduced nicotinamide adenine dinucleotide phosphate
BBS	BES-buffered saline	ND	not determined
BES	2-(bis[2-hydroxyethyl]amino)ethanesulfonic acid	NR1H3	nuclear receptor subfamily 1 group h member 3
bHLH-LZ	basic helix-loop-helix leucine zipper	OA	oleic acid
bp	base pair	OAA	oxaloacetate
BW	body weight	OGDH	alpha-ketoglutarate dehydrogenase
CCiTUB	the Centres Científics i Tecnològics Universitat de Barcelona	PA	palmitic acid
CM	chylomicron	PBS	phosphate-buffered saline
CPT1A	carnitine palmitoyl transferase	PCK1	phosphoenolpyruvate

	1A		carboxykinase
CVD	cardiovascular disease	PEP	phosphoenolpyruvate
DGAT	diglyceride acyltransferase	PER	protein efficiency ratio
DHA	docosahexaenoic acid	PFKFB	6-phosphofructo-2-kinase/fructose-2,6-bisphosphatase
DHAP	dihydroxyacetone phosphate	PFKL	Phosphofructokinase liver type
DMEM	Dulbecco's modified eagle medium	PGD	6-phosphogluconate dehydrogenase
DNL	de novo lipogenesis	PKLR	pyruvate kinase L/R
EDTA	ethylenediaminetetraacetic acid	PPARA	peroxisome proliferator-activated receptor alpha
EEF1A	elongation factor 1 alpha	PPARG	peroxisome proliferator-activated receptor gamma
EFA	essential fatty acids	PPP	pentose phosphate pathway
EGTA	ethylene glycol-bis(beta-aminoethyl ether)-n,n',n'-tetraacetic acid	PR	protein retention
ELOVL	elongation of very long chain fatty acids protein	PUFA	polyunsaturated fatty acid
EP tube	Eppendorf tube	qPCR	quantitative real time PCR
EPA	eicosapentaenoic acid	Ref	reference
ER	endoplasmic reticulum	Rib-5-P	ribose-5-phosphate
FADS	fatty acid desaturase	rpm	revolutions per minute
FAO	the Food and Agriculture Organization of the United Nations	SA	stearic acid
FASN	fatty acid synthase	SCAP	cleavage-activating protein
FAT-1	$\Delta 15/n-3$ desaturase	SCD	stearoyl-CoA desaturase
FAT-2	$\Delta 12/n-6$ desaturase	SEM	standard error of the mean
FATPs	fatty acid transport proteins	SFA	saturated fatty acid
FBP1	fructose 1,6-bisphosphatase	SGR	specific growth rate
FBS	fetal bovine serum	SREBF1	sterol regulatory element binding transcription factor 1
FCR	feed conversion ratio	SREBP	sterol regulatory element binding protein
Fru-2,6-P ₂	fructose 2,6-bisphosphate	SREs	sterol regulatory elements

Fru-6-P	fructose 6-phosphate	TAE	tris-acetate-EDTA
G6PC	Glucose-6-phosphatase catalytic unit	TE	tris-EDTA buffer
G6PD	glucose-6-phosphate dehydrogenase	TF	transcription factors
GAP	glyceraldehyde 3-phosphate	TG	triglycerides
GCK	glucokinase	TPP	tripolyphosphate
Glu-6-P	glucose-6-phosphate	TSPC	total soluble protein content
GRAS	generally recognized as safe	VLDL	very low-density lipoprotein

1 INTRODUCTION

1.1 LC-PUFA, health and aquaculture

1.1.1 LC-PUFA

Fatty acids are a sort of carboxylic acids with an aliphatic chain. Fatty acids that contain no double bonds are termed saturated (SFA). SFA are further classified into 4 subclasses based on the chain lengths: short (4-10 carbon atoms), medium (12-14 carbon atoms), long (16-18 carbon atoms) and very long (20 or more carbon atoms). When considering the number of double bonds, fatty acids are termed monounsaturated (MUFA, 1 double bond) and polyunsaturated (PUFA, more than 1 double bond). For example, long-chain polyunsaturated fatty acids (LC-PUFA) are fatty acids that contain 14-20 carbon atoms and 2 or more double bonds. When there are more than 2 double bonds exist, LC-PUFA are also termed highly unsaturated fatty acids (HUFA), such as eicosapentaenoic acid (EPA) and docosahexaenoic acid (DHA). In addition, according to the International Union of Pure and Applied Chemistry, abbreviation notation of each specific fatty acid is expressed as “C:D*n*-x”, where “C” stands for the number of carbon atoms, “D” for the number of double bonds, “*n*-x” for the methyl-end carbon atom position of the first double bond. For example, palmitic acid (PA) and oleic acid (OA) are the common names that correspond to the abbreviation notation of “16:0” and “18:1*n*-9”, respectively (figure 1.1.1). Apart from this, carbon atom position can be also marked as “delta (Δ) x”, where “x” indicates the carbon number from carboxyl end. For example, the double bond position of OA is at Δ 9 position.

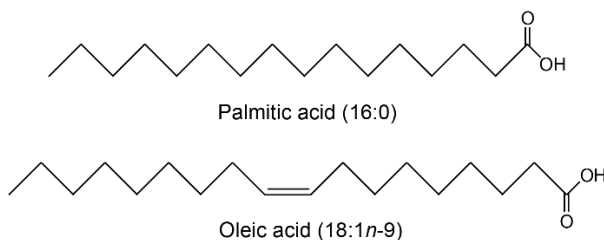


Figure 1.1.1 Structures of palmitic acid and oleic acid.

1.1.2 LC-PUFA and health

In 1929, Burr and Burr reported a severe deficiency syndrome in rats caused by exclusion of fats

from the diet (Burr and Burr, 1929), which led the discovery of the *n*-3 and *n*-6 essential fatty acids (EFA): linoleic acid (LA) and α -linolenic acid (ALA), respectively. The two fatty acids found as essential in rats were further confirmed for primates, including human beings. Later, the metabolic reasons for the essential role of LA and ALA were revealed in humans, as well as other vertebrates: the lack of Δ 12 and Δ 15 desaturases, which convert OA and LA into LA and ALA, respectively. Once overcome this obstacle, LA and ALA are further metabolized into *n*-6 and *n*-3 LC-PUFA, respectively, by a sort of desaturases and elongases in vertebrates (figure 1.3.3).

In addition to storing energy, LC-PUFA and their derivatives are also essential for growth and development acting as bioactive components of membrane phospholipids, substrates for signalling molecules and modulators of gene expression (Zhang et al., 2016). Apart from this, the impact of *n*-3 and *n*-6 PUFA series that cannot be interconverted draws different effects of the two fatty acids and the *n*-6/*n*-3 ratio, on health in vertebrates.

Evidence from clinical and laboratory research supports a general beneficial effect of *n*-3 PUFA, especially EPA and DHA, on inflammation, cardiovascular diseases (CVD), and neural development among others. In randomized double-blind trials, oral supplement of 2 g EPA + DHA for 25 weeks reduced plasma concentrations of C-reactive protein, a marker for systemic inflammation, and expression of other inflammation factors in maternal adipose and the placental tissue of overweight pregnant women (Haghiac et al., 2015). The effect of *n*-3 PUFA on inflammation was also suggested by a study on obese adolescents provided with 1.2 g/day *n*-3 PUFA (EPA + DHA) (Dangardt et al., 2010). The anti-inflammation effect of *n*-3 PUFA has been shown in other pathological processes, such as rheumatoid arthritis and inflammatory bowel disease, which was well reviewed by Calder (Calder, 2017). Interestingly, the *n*-3 PUFA EPA has high affinity for cyclooxygenases, which are known to convert the *n*-6 PUFA arachidonic acid (ARA) into the pro-inflammatory factor prostaglandin E2 (Ricciotti and Fitzgerald, 2011), and fish oil supplementation decreases by 50 % the production of the pro-inflammatory factor with tissue EPA/ARA ratios above 0.2 (L. Dong et al., 2016). Besides, several *n*-3 PUFA derivatives such as, resolvins, maresins and protectins, are also involved in the process of inflammation resolution (Serhan and Petasis, 2011). CVD can cause mortality of 28 % to 43 % in Europe countries according to a recent study (Timmis et al., 2020). *n*-3 PUFA has shown its protective effect against CVD. Clinical studies have provided evidence that the risk of CVD was significantly lower by daily intake of the *n*-3 PUFA EPA (Bhatt et al., 2019). It is worth noting that lack of the benefits of *n*-3 PUFA has been reported in some studies (Nicholls et al.,

2020), which may be due to a low dose of EPA. On the other hand, the *n*-3 PUFA DHA presents the highest body concentration in the brain (Svennerholm, 1968), suggesting that it serves important neural functions. Indeed, DHA was shown to promote neurogenesis (Kawakita et al., 2006) and neuroprotection (Belayev et al., 2009). Although debate exists as to whether endogenous synthesis of DHA from its precursor is sufficient for the adult brain (Domenichiello et al., 2015), women in pregnancy and lactation is recommended to ingest 200-300 mg/day of DHA (Guesnet and Alessandri, 2011), a number that is higher than the estimated daily intake for most population in the world (Forsyth et al., 2016).

LA, the precursor of the *n*-6 PUFA family, is a structural component of membrane known to maintain the epidermal water permeability barrier. The direct oxidized derivative of LA (Niki, 2009), 9-hydroxyoctadecadiene acid, which generation increases under oxidative stress such as nonalcoholic fatty liver disease (Feldstein et al., 2010), has been shown to promote inflammation (Hattori et al., 2008). Besides, competitive relationship has been found between the two EFA when converting to downstream PUFAs due to shared enzymes (Tu et al., 2010). Thus, effect of the ratio between *n*-3 and *n*-6 PUFA on health has gained more and more attention. From a historical perspective, dietary ratio of *n*-6/*n*-3 PUFA is thought to be changed from about 1 to 20 in about 200 years since the Industrial Revolution, which is considered too short for body evolutionary adaptation (Simopoulos, 2016). High ratios of *n*-6/*n*-3 PUFA have been shown to be associated with CVD (Shoji et al., 2013), cancer (Williams et al., 2011) and hepatic steatosis (Sertoglu et al., 2015), for instance. On the other hand, low ratios of *n*-6/*n*-3 PUFA benefit reducing oxidative stress and inflammation (Yang et al., 2016).

1.1.3 LC-PUFA and aquaculture

1.1.3.1 Aquaculture, the source of dietary *n*-3 LC-PUFA

The common source of dietary LC-PUFA is generally derived from vegetables and meat. In most vegetable oils, LA represents a high proportion while ALA is relatively low (table 1.1.3.1a). Similarly, meat from terrestrial animals also present high LA to ALA ratio (table 1.1.3.1a). In contrast, fish, especially marine fish, contains higher levels of *n*-3 LC-PUFA (table 1.1.3.1b) than the terrestrial sources. EPA and DHA rarely exist in the terrestrial sources but are ample in fish. Indeed, ecological research reveals a strong prevalence of *n*-3 LC-PUFA, especially EPA and DHA, in aquatic organisms

(Colombo et al., 2017). The high content of *n*-3 LC-PUFA in fish may ascribe to the aquatic trophic chain and the ingestion of organisms with high levels of *n*-3 LC-PUFA. Apart from this, marine fish in general retains more *n*-3 LC-PUFA than freshwater fish. Genetic studies showed that marine fish, which are mainly carnivorous, exhibit limited ability to biosynthesize *n*-3 LC-PUFA and require preformed HUFA in their diet (Tocher, 2010). However, freshwater fish and anadromous are highly capable of converting 18-C PUFA from both *n*-3 and *n*-6 series to HUFA (Mock et al., 2019; Xie et al., 2022). Due to the high content of LC-PUFA in microalgae and other organisms presented in the natural diet of marine fish, the content of LC-PUFA in marine fish is generally higher than freshwater fish (Li et al., 2011).

Arguably, fish are considered the most important dietary source of *n*-3 LC-PUFA, especially EPA and DHA, for most of the world human population. Global apparent fish consumption *per capita* increased from 9.0 kg in 1950 to 20.5 kg in 2018, which corresponds to an average annual growing rate of 3.1 % and 1 % higher than all other animal-derived protein for human consumption (Guenard, 2020). Even so, aquaculture still has huge growth potential when considering differences in regional development. In developed countries, the consumption reached 24.4 kg *per capita* in 2017, a number that in developing, the least developed and low-income food-deficit countries, which in total represent 83 % of the world population, are 19.4 kg, 12.6 kg and 9.3 kg, respectively (Guenard, 2020). Concomitantly, the source of fish on market, either from captures or aquaculture, has changed dramatically (Guenard, 2020). World capture fisheries production almost stopped growing since the mid-1980s due to that many fishing grounds have apparently reached the upper limit of production. Paradoxically, significant proportions of wild fish captures are processed into fishmeal and fish oil, and added to aquafeeds as predominant protein and lipid sources for fish farming. Meanwhile, worldwide aquaculture contribution to fish production increased from 25.7 % in 2000 to 46.0 % in 2018, among which fish farmed in marine waters accounts for about one-third of the total production. Although world growth rate of aquaculture fish production quantity was about 4 % in 2016-2018, notably, the growth rate has decreased by 2 % when compared with values in 2001-2005. Thus, it is reasonable to speculate that nutritional quality of aquaculture fish production will receive more and more attention. Indeed, the rapid growth of aquaculture is causing problems regarding to fish quality such as low EPA and DHA content in fish fillets.

Table 1.1.3.1a Common terrestrial sources of dietary LC-PUFA

INTRODUCTION

	LA	ALA	EPA	DHA	NDB Number
Vegetable oil					
Corn	51.900	1.040	0	0	4518
Olive	9.710	0.607	0.001	0	100258
Soybean	50.900	6.620	0	0	4044
Sunflower	20.500	0.163	0.002	0	100262
Rapeseed	17.800	7.450	0	0	4582
Animal fat					
Chicken	0.598	0.026	0.004	0.07	5746
Beef	0.625	0.078	0.003	0	7022
Pork	4.310	0.175	0.005	0.003	7089
Lamb	0.140	0.117	0.017	0.020	17371
Butter	1.890	0.308	0.024	0.002	1001

Data from U.S. Department of Agriculture, query in 2022. Numbers represent g in 100 g portion.

Table 1.1.3.1b Common fish sources of dietary LC-PUFA

	LA	ALA	EPA	DHA	NDB Number / Reference
Freshwater fish					
Carp	0.517	0.270	0.238	0.114	15008
Tilapia	0.158	0.033	0.005	0.086	15261
Catfish	0.755	0.054	0.017	0.057	15234
Rainbow trout	0.466	0.059	0.217	0.516	15240
Marine fish					
Atlantic cod	0.005	0.001	0.064	0.12	15015
Flatfish	0.043	0.017	0.137	0.108	15028
Seabass	0.088	0.034	0.161	0.322	Ref (Prato and Biandolino, 2012)
Seabream	0.082	0.042	0.269	0.620	Ref (Prato and Biandolino, 2012)
Salmon	0.122	0.089	1.010	0.944	15078

Data from U.S. Department of Agriculture, query in 2022 or publications. Numbers represent g in 100 g portion.

1.1.3.2 Decline of *n*-3 LC-PUFA in aquaculture products

Feed nutrients are closely related to fillet quality. In contrast to feeds for terrestrial animals (Peters et al., 2014), aquafeeds require not only higher proportions of fishmeal but also the presence of fish oil for optimal fish growth and quality (Oliva-Teles et al., 2015). However, worldwide suppliers of fish oil have reached their sustainable limits since the mid-1980s. Aquaculture industry must compromise to the reduction of the amount of fish oil addition in aquafeeds and seek for other oil sources. Vegetable oil is a viable alternative due to the large production. However, replacement of fish oil with vegetable oil significantly reduces *n*-3 LC-PUFA, specially EPA and DHA, in fish's flesh (Pang et al., 2014). A recent study on temporal variations of farmed Atlantic salmon has shown that median contents of EPA + DHA decreased more than 60 % since 2005 (Moxness Reksten et al., 2022). Thus, a considerable amount of studies have focused on genetic modification of terrestrial oil crops in order to produce more *n*-3 LC-PUFA, notably EPA and DHA, for aquafeeds (Napier et al., 2015). However, genetic modified crop oil still has high content of *n*-6 PUFA, such as LA, which would reflect in the quality of fillet (Lundebye et al., 2017) and affect human health as mentioned above. For instance, with the limitation of fish oil supply, research efforts have been made to alleviate the dependence on fish oil in aquafeed for gilthead sea bream (*Sparus aurata*), which constitutes one of the most cultured marine fish in Europe (Vasconi et al., 2017). Substitution in *S. aurata* feeds by vegetable oils reshapes the fillet fatty acids profiles. In *S. aurata*, the content of moisture, protein and ash are stable in general, whereas lipids content as well as fatty acid profiles are strikingly flexible (Grigorakis, 2007). An investigation on wild *S. aurata* fillets has shown that the total lipid is about 1.4 % in winter and 8.1 % in summer (Yildiz et al., 2008). The farmed *S. aurata* generally contains higher total lipid content and *n*-6 LC-PUFA when compared with wild fish (Vasconi et al., 2017).

1.2 Carbohydrate metabolism in fish

Among macronutrients, carbohydrate-derived acetyl-CoA commonly satisfies *de novo* lipogenesis (DNL) in the liver (figure 1.2). Once transported into cytosol, glucose is phosphorylated to glucose-6-phosphate (Glu-6-P) by glucokinase (GCK). Glu-6-P is the initial substrate for glycogenesis, glycolysis, and pentose phosphate pathway (PPP). Glucose oxidation through glycolysis and PPP generates pyruvate, which is further converted into acetyl-CoA and NADPH, compounds that could be diverted to DNL. In glycolysis, the main rate-limiting steps are catalyzed by: GCK; phosphofructokinase liver type (PFKL), converting hepatic fructose 6-phosphate (Fru-6-P) into

INTRODUCTION

fructose 1,6-bisphosphate; and pyruvate kinase L/R (PKLR), catalyzing the conversion of phosphoenolpyruvate (PEP) into pyruvate. Glucose-6-phosphatase catalytic unit (G6PC) and fructose-bisphosphatase (FBP) catalyze the opposite reactions than GCK and PFKL, respectively. 6-Phosphofructo-2-kinase/fructose-2,6-bisphosphatase (PFKFB) converts Fru-6-P into fructose 2,6-bisphosphate (Fru-2,6-P₂), a potent allosteric activator of PFKL and inhibitor of FBP. Pyruvate produced by glycolysis in cytosol is transported into mitochondria and converted into acetyl-CoA by pyruvate dehydrogenase. After conversion of acetyl-CoA into citrate, further oxidation can proceed through the Krebs cycle, where the main rate-limiting reactions are catalyzed by citrate synthase, isocitrate dehydrogenase (IDH) and oxoglutarate dehydrogenase (OGDH). From mitochondria, citrate can be also transported into cytosol, and converted into acetyl-CoA for DNL. In the PPP, Glu-6-P is catalyzed by two key enzymes, glucose-6-phosphate dehydrogenase (G6PD) and phosphogluconate dehydrogenase (PGD) that generate NADPH.

In general, fish, especially carnivorous fish, are more vulnerable to utilizing carbohydrates for energy than mammals. In other words, carnivorous fish has low efficiency of serum glucose clearance. Carnivorous fish intolerance to dietary glucose may result from evolutionary adaptation to the natural protein-rich diet and low availability of carbohydrate digestion. In contrast to mammals, where postprandial plasma glucose returns to resting state within an hour, glucose clearance in carnivorous fish consumes hours and exhibits glucose intolerance (Kamalam et al., 2017). Physiological characteristics including carbohydrate digestion, glucose transport and metabolism limit carnivorous fish utilizing dietary starch.

Fish, especially the carnivores, have lower activity levels of enzymes for carbohydrate digestion in addition to the shorter digestive tract when compared with non-carnivorous animals. Activity of amylase in the digestive tract of carnivorous fish is 10 times lower than in non-carnivores (Hidalgo et al., 1999; H. Liu et al., 2016). On the other hand, the activity of digestive enzymes had marginal alteration in response to dietary carbohydrates (Castro et al., 2019). Several kinds of bacteria in gut also produce enzymes for carbohydrate digestion. Dietary supplement of these bacteria resulted in higher activities of amylase and cellulase (Lazado et al., 2012). Thus, the specific microbiota in fish may also ascribe to its limited ability of carbohydrate digestion. Following the digestion, carbohydrates are hydrolyzed into short chain products and transported from intestine to the blood stream. When compared with herbivorous elevation of the expression of glucose transporters in the intestine, carnivorous fish showed greater delay in response to oral starch administration (Su et al., 2020).

INTRODUCTION

Additionally, dysregulation of glycolysis when responding to starch challenge was found in carnivorous fish. For example, significant decrease of activity and expression of G6pc was reported in herbivorous fish after oral starch administration, whereas the responses in carnivorous fish were subtle (Su et al., 2020). Studies in the carnivorous *S. aurata* also reported sluggish postprandial inductions of hepatic *gck* and *g6pc* (Caseras et al., 2000; Panserat et al., 2002). Insulin exerts a major role in mediating glucose catabolism. Characterization of muscular insulin-binding capacity found that carnivorous fish had significant lower binding capacity than the herbivorous (Parrizas et al., 1994).

Dietary supplement of *n*-3 LC-PUFA has influences on glucose metabolism, which can vary depending on the specific fatty acid. Differences of glycogen deposition were observed between diets composed of fish oil and land animal fats in the hepatocytes of European seabass (Monteiro et al., 2018). However, *n*-3 LC-PUFA scarcely affect resting-state circulatory glucose levels of carnivorous fish (Magalhães et al., 2021). Even though, replacement of dietary fish oil with vegetable oil showed different serum postprandial glucose levels in gilthead sea bream (Bouraoui et al., 2011). Thus, intake of *n*-3 LC-PUFA may modify basal metabolic rate of glucose in fish. Indeed, in Atlantic salmon, meanwhile EPA shows positive association with insulin signaling and PPP activation, DHA was related with induced glycolytic flux (Horn et al., 2019). Dietary inclusion of linseed oil, rich in ALA, was related to lower activity of G6pd in the liver of *S. aurata* (Menoyo et al., 2004).

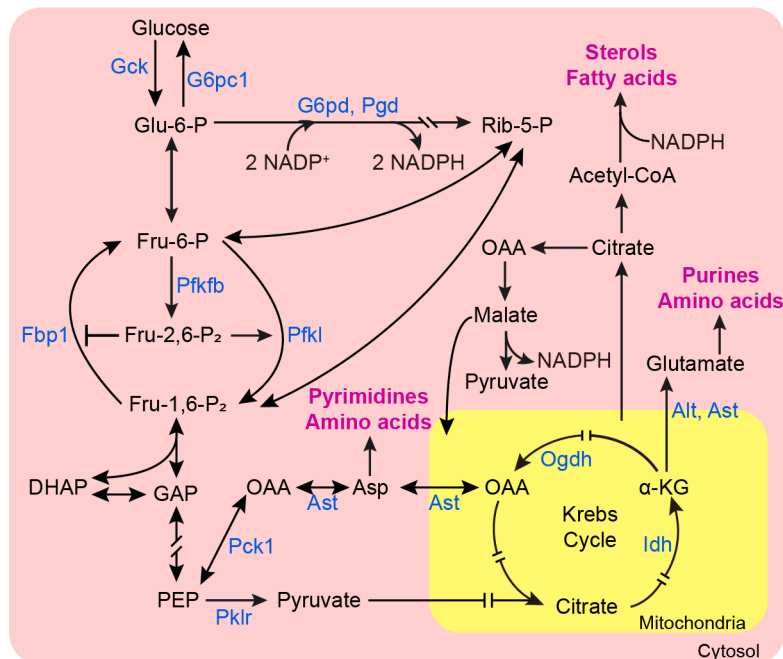


Figure 1.2 Schematic overview of hepatic glycolysis, gluconeogenesis and the Krebs cycle. Gck, glucokinase; G6pc1, glucose-6-phosphatases, catalytic subunit 1; G6pd, glucose-6-phosphate dehydrogenase; Pgd, 6-phosphogluconate dehydrogenase; Pfkfb, 6-phosphofructo-2-kinase/fructose-2,6-bisphosphatase; Fbp1, fructose 1,6-bisphosphatase; Pfkf, phosphofructokinase, liver type; Pck1, phosphoenolpyruvate carboxykinase; Pk1r, pyruvate kinase L/R; Alt, alanine transaminase; Ast, aspartate transaminase; Ogdh, α -ketoglutarate dehydrogenase; Idh, isocitrate dehydrogenase; Glu-6-P, glucose-6-phosphate; Rib-5-P, ribose-5-phosphate; Fru-6-P, fructose-6-phosphate; Fru-2,6-P₂, fructose-2,6-bisphosphate; GAP, glyceraldehyde 3-phosphate; DHAP, dihydroxyacetone phosphate; PEP, 2-phosphoenolpyruvate; Ala, alanine; OAA, oxaloacetate; α -KG, alpha ketoglutarate; Asp, aspartic acid. Letters in blue are enzymes.

1.3 Amino acid metabolism in fish

Fish digest dietary proteins in the gastrointestinal tract and absorb into the blood stream in a process similar to monogastric animals. Generally, fish dietary protein requirement is between 36 % and 46 %, depending on their trophic levels (2 to 4.7) (Teles et al., 2020). Fish, especially the carnivores, trend to directly utilize amino acids as energy source, which is different from terrestrial animals that preferably utilize carbohydrates for energy (Jia et al., 2017). Although amino acids are less efficient than glucose in producing energy, the preference of amino acids conforms the poikilothermic and ammoniotelic mode of aquatic life. Fish gill is an efficient system for excretion of the toxic byproduct ammonia from protein catabolism for energy (Wilkie, 2002). Apart from the preference, fish body protein shows scarcely difference with terrestrial animals regarding protein contents and amino acids profiles (Uhe et al., 1992).

Similar to terrestrial animals, physiological processes of fish utilizing amino acids for energy are oxidative deamination, ammonia release and conversion of amino acids into α -keto acids. Thus, α -keto acids such as pyruvate are involved in the Krebs cycle and provide energy for cells. Nevertheless, α -keto acids also contribute to fatty acid synthesis and gluconeogenesis. Glutamine, the degraded product glutamate, and leucine represent the most abundant ATP sources from amino acids in fish (Jia et al., 2017). In presence of glutamate dehydrogenase, glutamate is catalyzed into α -ketoglutarate. Another pathway to generate α -keto acids is transamination, for example alanine is transaminated into pyruvate by glutamic--pyruvic transaminase (ALT) and aspartate is transaminated into oxaloacetate by glutamic-oxaloacetic transaminase (AST).

The effect of dietary *n*-3 LC-PUFA may benefit protein retention of carnivorous fish. Dietary replacement of fish oil with vegetable oil showed marginal effects on protein retention of both carnivorous and herbivorous fish (Magalhães et al., 2020; Wang et al., 2018). However, in grass carp, Du *et al.* reported not only a negative correlation between dietary fish oil levels and protein retention values, but also a lower protein retention in fish oil diets comparing to plant and lard sources (Du et al., 2008). In carnivorous fish, higher protein deposition was found with diets free of fish oil than with 15 % fish oil supplementation (Glencross et al., 2016). In contrast, fish oil based diet generated higher crude protein than ALA-rich diets (linseed oil) in rainbow trout (Turchini et al., 2018). Similarly, dietary supplement of *n*-3 LC-PUFA induced protein retention in silvery-black porgy juveniles (Mozanzadeh et al., 2015).

Several mechanisms of dietary *n*-3 LC-PUFA affecting amino acid synthesis have been addressed. In terrestrial animals and humans, studies showed that *n*-3 LC-PUFA facilitating protein synthesis may be achieved through insulin-mediated mechanistic target of rapamycin kinase (MTOR) pathway and reduction of amino acid oxidation (Gingras et al., 2007). In carnivorous fish, replacement of dietary fish oil with linseed oil generated retarded growth performance and reduction of Mtor signaling pathway (Qin et al., 2020). On the other hand, increased dietary lipids (fish oil + soybean oil) are related with induced hepatic expression of genes involved in Mtor pathway in coho salmon (Yu et al., 2022). However, another study in gilthead sea bream found no difference of hepatic *mtor* expression between fish diets rich in ARA and DHA (Magalhães et al., 2020). A study in rat reported that dietary fish oil increased the plasma levels of some amino acids, possibly via peroxisome proliferator activated receptor alpha (PPARA) (Bjørndal et al., 2013). As mentioned in section 1.4.4, the effect of dietary fish oil on PPARA expression is controversial. Thus, whether *n*-3 LC-PUFA favor fish protein synthesis via Ppara remains unclear. *n*-3 LC-PUFA regulating amino acid metabolism may also through transamination. In juvenile starry flounder, higher serum Alt and Ast activities were observed in fish supplied with DHA (Ma et al., 2014). Whereas, dietary replacement of fish oil with vegetable oils reduced hepatic Alt and Ast in tilapia (Li et al., 2016; Peng et al., 2016). On the other hand, dietary supplement of ARA has been shown to decrease serum Ast activity of juvenile yellow catfish (Ma et al., 2018). However, in juvenile Asian seabass, dietary fish oil showed rarely difference with vegetable oil regarding hepatic glutamate dehydrogenase activity and Alt expression (Glencross et al., 2016).

1.4 LC-PUFA synthesis in fish

In the presence of EFA, *i.e.*, LA and ALA, fish can synthesize LC-PUFA in general through chain elongation and desaturation. Dietary presence of LA and ALA can satisfy growth requirement of freshwater fish (Tocher, 2010). However, marine fish also require dietary EPA and DHA due to the limited synthesis ability (Tocher, 2010).

1.4.1 LC-PUFA transport and absorption

Circulatory transportation of fatty acids is mainly in form of triglycerides (TG), composed by 3 molecules of fatty acids and 1 of glycerol. TG are neutral lipid and insoluble in the aqueous bloodstream. Thus, the transportation further relies on lipoproteins, such as very low-density lipoproteins (VLDL) and chylomicrons (CM). TG from either endogenous synthesis or intestinal ingestion are assembled into VLDL and CM, respectively. Triglycerides stands for the most proportion of lipids in VLDL and CM.

Dietary TG assembled into CM are secreted into the lymphatic system via intestinal lacteals, transported to the thoracic duct and entered the bloodstream. CM are suggested to be the only pathway for dietary TG absorption (Hussain, 2014). Plasma CM and TG increased after meal and returned to normal state within hours. Postprandial TG is mainly entered into and utilized by peripheral tissues instead of liver. In detail, about 80 to 90 % of CM-carried TG are hydrolyzed by lipoprotein lipase (LPL) at the capillary endothelium of peripheral organs. Another main source of plasma TG is derived from VLDL. Like CM, VLDL-carried TG are also hydrolyzed by LPL and released at local endothelial cells. Therefore, the clearance of plasma TG is closely related to the activity of peripheral LPL. In general, LPL activity is regulated at transcriptional and post-translational levels by nutritional status and physical exercise (Kersten, 2014). Once TG are hydrolyzed by LPL, free fatty acids including LC-PUFA are released and supplied to the cells. Although fatty acids are able to cross cell membranes by passive diffusion, such protein-independent manner may not be sufficient for tissue requirement (Vusse, 2009).

Dietary intake of *n*-3 LC-PUFA has been associated with a remarkable decrease of plasma TG in both postprandial and fasting states of mammals (Park and Harris, 2003; Qi et al., 2008). Such TG-

lowering effect is also conservative in fish (Liu et al., 2018). Several mechanisms, either reduction of TG synthesis or induction of plasma TG clearance, have been suggested for the TG-lowering effect. Supplements of EPA and DHA were associated with lower plasma apolipoprotein (APO) C-III (Sahebkar et al., 2018), a peptide which exists in CM and VLDL and has potent inhibitory effects on LPL-mediated TG hydrolysis (Larsson et al., 2017). Therefore, the TG-lowering effect may be due to high activity of local hydrolysis of TG by LPL under *n*-3 LC-PUFA-associated to low APO C-III presence in plasma. Conservatively, dietary *n*-3 LC-PUFA also associated with high LPL activity in fish muscle and adipose tissue (Bouraoui et al., 2011; Richard et al., 2006a). The suppression of *n*-3 LC-PUFA on fatty acids synthesis via transcription factors, which is described in detail in section 1.4.2, may also ascribe to the TG-lowering effect.

1.4.2 DNL

In vertebrates, LC-PUFA cannot be synthesized by DNL and requires EFA as substrates due to lack of *n*-3 and *n*-6 desaturases. However, it is still worthwhile to briefly describe the DNL pathway. In vertebrates, the fatty acid synthesis starts from the substrate acetyl-CoA and the enzymatic catalysis by acetyl-CoA carboxylases (ACAC) and fatty acid synthase (FASN). Acetyl-CoA is an one-carbon thioester as well as an intermediate that exists in (or bridges) many critical biological pathways, such as the catabolism of glucose, fatty acids and amino acids. ACAC initialize the biosynthetic via catalyzing the ATP-dependent irreversible carboxylation of acetyl-CoA to malonyl-CoA, which is further converted by FASN to the first DNL product, PA (16:0). Following the 16-carbon saturated PA, other fatty acids are synthesized through elongation and desaturation, which is reviewed in later sections. Vertebrates tend to utilize available fatty acids for metabolic demand and the activation of DNL is more a response to cellular acetyl-CoA excess, in conditions with low fat and high carbohydrate diets.

In mammals and fish, two ACAC isoforms exist and differ in the subcellular location and tissue distribution. The cytosolic ACACA is abundant in the liver and adipose tissue, whilst ACACB is located in the mitochondrion and highly expressed in the muscle and also present in the liver (Abu-Elheiga et al., 2000). Although, the two isoforms catalyze the same reaction, ACACB-synthesized malonyl-CoA functions in reducing mitochondrial β -oxidation rather than in DNL (Abu-Elheiga et al., 2001). ACACA is regulated in multiple manners involving transcriptional regulation, post-translational modification and allosteric control (Hunkeler et al., 2018) by factors such as citrate, malonyl-CoA, palmitoyl-CoA, and sterol regulatory element binding transcription factor 1 (SREBF1). FASN, a

cytosolic protein, exists in a broad range of tissues such as liver, adipose tissue, lung and kidney (Semenkovich et al., 1995). Apart from malonyl-CoA as substrate, FASN-mediated PA synthesis also requires acetyl-CoA and the reducing power of NADPH. FASN is also transcriptionally and post-transcriptionally regulated by factors such as glucose and SREBF1.

1.4.3 Fatty acid elongation and desaturation

In vertebrates, DNL produces C16 fatty acids, which are converted into LC-PUFA by elongases and desaturases (Figure 1.3.3).

The elongation involves elongases catalyzing four sequential steps: condensation, reduction, dehydration and reduction. In the first step, fatty acid-CoA is condensed with malonyl-CoA, which provides two carbons for elongating the carbon chain, and turned into 3-ketoacyl-CoA. Secondly, 3-ketoacyl-CoA is reduced to 3-hydroxyacyl-CoA with the participation of NADPH. The third step is a dehydration where 3-hydroxyacyl-CoA is converted into enoyl-CoA. Finally, enoyl-CoA is reduced to fatty acid-CoA via NADPH. Thus, each of the four-step cycle elongates fatty acids for 2 carbons. To date, eight ELOVL fatty acid elongases (ELOVL1-8) have been identified in animals, which differed in tissue distribution and substrate preference (Castro et al., 2016; Li et al., 2020). For example, *ELOVL4* shows high mRNA levels in eye and catalytic preference to 24:0 and 26:0, whilst *elovl5* mRNA is highly expressed in the liver and preferably acts on to 18:2, 18:3 n -3, 18:3 n -6 and 20:4 fatty acids (Monroig et al., 2012; Ohno et al., 2010)

In teleost fish, all elongases except Elov13 and Elov17 have been reported. Among which, Elov12 is limited to freshwater and diadromous fish (Xie et al., 2021). Elov12 shows preference towards C20 and C22 fatty acids (Xie et al., 2021). The absence of Elov12 in marine fish may partially explain that EPA and DHA are EFA for these animals. Nevertheless, the existence of Elov14, with two gene paralogs identified (*elov14a* and *elov14b*), raises the possibility for marine fish to endogenously synthesize DHA (Ferraz et al., 2020).

MUFA and PUFA are produced from SFA desaturation: two hydrogen atoms are removed creating one carbon-carbon double bond by fatty acid desaturases (FADS), during which NADPH is supplied as reducing power. Based on the inserted carbon atom from either carboxyl or methyl end of fatty acyl chain, desaturases can be classified as “delta (Δ) x desaturase” or “ ω x desaturase”. For

example, $\Delta 12$ desaturase and $\omega 3$ desaturase can insert a double bond at the twelfth carbon atom from the carboxy end and the third carbon atom from the methyl end, respectively. In addition to the terms “delta (Δ) x desaturase” and “ ω x desaturase”, “v+x” is also applied for classifying desaturases that insert double bonds based on the position of preexisting double bonds in the substrate. For example, v+3 desaturation of 16:1 n -7 produces 16:2 n -10. In vertebrates, four FADS (1-4) have been identified. Each of these FADS differed in the catalytic site preference depending on the species (Costa et al., 2012; Marquardt et al., 2000) Following DNL, stearic acid (SA, 18:0) is desaturated into OA by stearoyl-CoA desaturase (SCD). Stepwise desaturation of OA produces LA and ALA. However, the two enzymes, $\Delta 12/n-6$ desaturase (FAT-2) and $\Delta 15/n-3$ desaturase (FAT-1), that for catalyze the reaction have only been found in lower class eukaryotes such as *Caenorhabditis elegans* (Spsychalla et al., 1997; Zhou et al., 2011).

Teleost fish species except the *Elopomorpha* are believed to express only Fads2 (Xie et al., 2021). Nevertheless, diverse *fads2* genes differing in few amino acids positions and different carbon site activities, have been found in fish (Hamid et al., 2016). In teleost, activity sites of Fads2 have been reported at $\Delta 4$, $\Delta 5$, $\Delta 6$ and $\Delta 8$ carbons, among which carnivorous marine fish only showed $\Delta 6$ activity (Xie et al., 2021). The absence of $\Delta 4$ and $\Delta 5$ activity limits carnivorous fish to synthesize EPA and DHA.

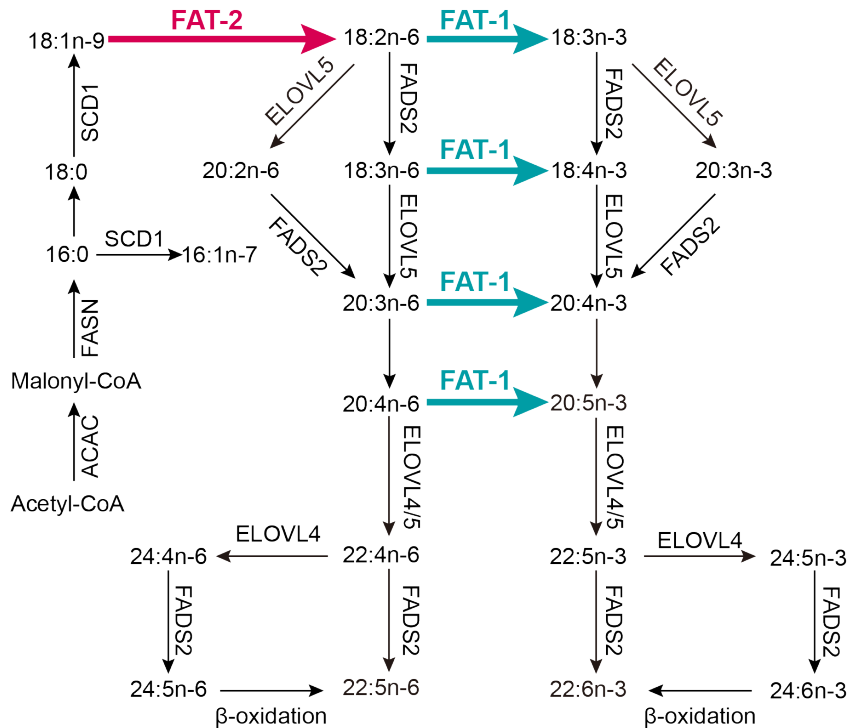


Figure 1.3.3 Biosynthetic pathways of LC-PUFA in vertebrates (black arrows). ACAC, acetyl-CoA carboxylases; ELOVL, elongation of very long chain fatty acids protein; FADS2, fatty acid desaturase 2; FASN, fatty acid synthase; FAT-1, $\Delta^{15}/n-3$ desaturase (blue arrows); FAT-2, $\Delta^{12}/n-6$ desaturase (red arrows); SCD1, stearoyl-CoA desaturase.

1.4.4 The regulation of LC-PUFA synthesis

In health state, LC-PUFA synthesis is tightly regulated in a feedback manner that combines sense of cellular LC-PUFA levels and regulation of the activity of lipogenic enzymes. The sensing and regulation of LC-PUFA is mainly achieved by the binding of several transcription factors (TF) to specific nucleotide sequences in the promoter region of genes coding lipogenic enzymes, leading to transcriptional activation or inhibition.

SREBF1 is one of the TF that was initially identified in HeLa cells with three overlapping partial cDNAs, namely *SREBF1a*, *SREBF1b* and *SREBF1c* (Yokoyama et al., 1993), which turned to be two isoforms produced by the SREBF1 gene. Due to alternative promoter usage, the two isoforms, which differed from their first exons, are designated SREBF1a and SREBF1c (Soyal et al., 2015). SREBF1a

and SREBF1c have similar protein structure consisting of three parts: N-terminal transcription factor domain which contains a basic helix-loop-helix leucine zipper (bHLH-LZ) for the binding to enhancers of lipogenic genes; two membrane-spanning regions; and a regulatory domain at the C-terminus (Soyal et al., 2015). The synthesized *SREBF1* precursors are bound to the endoplasmic reticulum (ER) membrane. In low sterol and fatty acid state, insulin induced gene (INSIG) 1 dissociates from SREBF cleavage-activating protein, which in turn facilitates transport of SREBF cleavage-activating protein-SREBF1 complex to the Golgi apparatus, where the bHLH of SREBF1 is proteolyzed and the transcription factor domain is released to the nucleus (Soyal et al., 2015). Thus, mature SREBF1 binds to sterol regulatory elements (SREs) in lipogenic genes and induce their expression (Soyal et al., 2015). SREBF1 have been shown to promote fatty acid, triglycerides and cholesterol synthesis. The SREs have been reported in genes for fatty acid, triglycerides and cholesterol synthesis, such as *ACACA*, *ACACB*, *FASN*, *SCD*, *FADS2*, *ELOVL5* and 3-hydroxy-3-methylglutaryl-CoA reductase (*HMGCR*) (Knebel et al., 2012). In addition, SREBF1 is also involved in the regulation of glycolysis. For instance, in *S. aurata* *Sreb1* was proven to transactivate *pfkfb* and *gck* (Egea et al., 2008; Metón et al., 2006). On the other hand, PUFA can inhibit the induction of SREBF1 on these lipogenic genes at transcriptional and posttranscriptional level. The transcriptional suppression can be achieved by antagonizing liver X receptor (LXR), a nuclear receptor that induces *SREBF1* expression via binding the LXR response element (LXRE) in the *SREBF1* promoter (Repa et al., 2000). Proteolytic activation of SREBF1 is inhibited by PUFA and MUFA via blocking the degradation of INSIG1, a process which impedes SREBF1 transport and maturation (Joon et al., 2008; Kim et al., 2013). In addition, *n*-3 LC-PUFA has been shown to reduce lipogenic genes expression (Muhlhausler et al., 2010), which may due to alteration of ER membrane lipids and inhibit SREBF1 from proteolysis and further nuclear release (Hishikawa et al., 2020). Besides, while *n*-3 and *n*-6 LC-PUFA have similar reduction on *SREBF1* mRNA and precursor abundance, the most potent reduction on mature SREBF1 levels promoted by the *n*-3 LC-PUFA DHA may result from a contemporary suppression of *Insig2* mRNA (López-Soldado et al., 2009). In fish, SREBF1 has been identified in several species (Xie et al., 2021) and its functions are conservative in inducing the expression of lipogenic genes (Xie et al., 2021).

LXR has two isotypes, LXR α and LXR β , that are encoded by *NR1H3* and *NR1H2* genes, the nuclear receptor subfamily 1 group H members, respectively. Human LXR α and LXR β share 77 % of homology. In fish, only one *NR1H* gene has been identified, which is similar to mammalian *NR1H3*. The absence of fish *nr1h2* may due to evolutionary loss (Bertrand et al., 2004). LXR has significant

roles in maintaining cholesterol homeostasis via reducing the biosynthesis and inducing the excretion in the liver (Wang and Tontonoz, 2018). Apart from this, LXR also modulates lipogenesis in the liver. LXR stimulates expression of lipogenic genes mainly via binding LXRE in the *SREBF1* promoter. Additionally, LXR also directly activates lipogenic genes including hepatic *ACAC*, *FASN*, *SCD*, *FADS1*, *FADS2* and *ELOVL5* via binding LXRE in their promoter (Gao et al., 2013; Jalil et al., 2019). In fish, *elov5* is suggested to directly respond to LXR α in head kidney tissue (Minghetti et al., 2011). PUFA, rather than SFA and MUFA, can suppress LXR-mediated *SREBF1* expression by competition with LXR ligands as mentioned above.

Hepatocyte nuclear factor 4 alpha (HNF4A) is a nuclear receptor that is essential for maintaining lipid homeostasis, including lipogenesis and lipoprotein secretion. Deficiency in hepatic *Hnf4a* results in reduced expression of *Fasn* as well as diglyceride acyltransferase and apolipoproteins (Yin et al., 2011). In mammals and fish, HNF4A binds and transactivates lipogenic genes including *FASN* (Adamson et al., 2006), *FADS2* ($\Delta 4$, $\Delta 5$ and $\Delta 6$) (Dong et al., 2020; Y. Dong et al., 2016) and *ELOVL5* (Y. Li et al., 2018). Besides, genes related to glucose metabolism including phosphoenolpyruvate carboxykinase (*PCK*) and *G6PC* are also induced by HNF4A activation, which may also be involved in the response to lipogenesis (Gonzalez, 2008). On the other hand, binding with SFA has been shown to activate HNF4A, whereas few LC-PUFA showed suppression on HNF4A activity and expression as well as that of downstream genes (Bordoni et al., 2006; López-Soldado et al., 2009). In regard to glucose metabolism, SFA showed no effect while PUFA is able to inhibit G6PC promoter activity (Rajas et al., 2002).

PPARA is a well investigated nuclear receptor that is highly expressed in the liver and which exerts crucial roles in a broad range of functions including fatty acid uptake, transport and oxidation, and lipogenesis, in a manner of ligand-controlled transactivation of target genes (Bougarne et al., 2018a). Direct PPARA targets include fatty acid transport proteins, transferases such as carnitine palmitoyltransferase 1A (CPT1A) and fatty acyl-CoA dehydrogenases (Bougarne et al., 2018a), through which it can maintain fuel supply in low energy state. PPARA not only induces fatty acid oxidation but also increases lipogenesis mainly via SREBF1 (Fernández-Alvarez et al., 2011). The endogenous ligands of PPARA include fatty acids and their derivatives, for instance eicosanoids, endocannabinoids, and phospholipids (Chakravarthy et al., 2009). In contrast to the poor affinity of SFA, unsaturated fatty acids especially LC-PUFA including LA, ALA, GLA, ARA and EPA are effective to activate PPARA and induce the expression of downstream genes (Forman et al., 1997). Such activation is not

only derived from the binding effect but also from induction of *Ppara* expression (Tapia et al., 2014). In addition, *n*-3 LC-PUFA are suggested to be more potent than *n*-6 LC-PUFA in activating PPARA (Echeverría et al., 2016). In fish, two homologous forms, *ppara1* and *ppara2*, have been identified, and the response to fatty acid varies from species and within the two homologs. For example, dietary replacement of fish oil with vegetable oil increased the expression of *ppara2* in the liver of rainbow trout while decreased in Japanese seabass (Dong et al., 2017). In Japanese seabass, diet-enriched ALA or fish oil inhibited hepatic *ppara1* while upregulated *ppara2* mRNA levels when compared with PA or OA diets (Dong et al., 2015).

Peroxisome proliferator activated receptor gamma (PPARG) belongs to the same nuclear receptor family than PPARA, although with a much lower expression level in the liver (Ahmadian et al., 2013). Similar to PPARA, activation of PPARG is also involved in a broad range of functions including hepatic TG storage and gluconeogenesis via transcriptional increase of genes such as *Acaca*, *Scd* and *Fasn* (Wang et al., 2020). Besides, activation of PPARG trends to decrease *FADS2* ($\Delta 6$) along with an increase of *PPARG* mRNA levels (Gu et al., 2002). A study on fish hepatocytes also shows that activation of *Pparg* decreases the expression of *fads2* ($\Delta 5$ and $\Delta 6$), while increases *pparg*, *elovl5* and *srebflc* expression (You et al., 2017). Fatty acids and its derivatives are able to bind PPARG and affect the downstream genes expression (Marion-Letellier et al., 2016). While SFA with either short or long chain length are unable to bind PPARG (Xu et al., 1999), *n*-3 and *n*-6 LC-PUFA such as LA, ARA, EPA and DHA have shown binding affinity with PPARG (Xu et al., 1999; Zhao et al., 2011). In spite of this, decreased expression of *PPARG* is associated with dietary LC-PUFA (Tian et al., 2014; Wang et al., 2012), indicating a feedback control of PPARG activation by these fatty acids. However, the decrease of *pparg* expression by LC-PUFA is inconsistent between fish species (You et al., 2017), which may due to the existence of two isoforms encoded from the same gene with different promoters (Lee et al., 2018).

1.4.5 FAT-1 and FAT-2 in *Caenorhabditis elegans*

As mentioned above, vertebrates lack the enzymes FAT-1 and FAT-2, and therefore they cannot synthesize *de novo* PUFA and require dietary supplement of EFA. However, the two enzymes have been identified in some invertebrates such as the roundworm *Caenorhabditis elegans*.

C. elegans FAT-1 is a *n*-3 desaturase with activity at $\Delta 15$ and $\Delta 17$ fatty acid substrates (Figure

1.3.3). For example, FAT-1 deficiency in *C. elegans* leads to a decrease of 18:3 n -3, 20:4 n -3, 20:5 n -3 and increase of 18:2 n -6, 20:3 n -6 and 20:4 n -6 proportions (Kahn-Kirby et al., 2004; Watts and Browse, 2002). Heterologous expression of *C. elegans* FAT-1 also confirmed the above-mentioned activities. Transgenic expression of *C. elegans* FAT-1 in mammalian cells decreases a series of n -6 LC-PUFA including 18:2 n -6, 20:2 n -6, 20:3 n -6, 20:4 n -6, 22:4 n -6 and 22:5 n -6, while increases 18:3 n -3, 20:4 n -3, 20:5 n -3, 22:5 n -3 and 22:6 n -3 (Kang et al., 2001).

C. elegans FAT-2 acts mainly at Δ 12 of fatty acid substrates. FAT-2 deficiency in *C. elegans* produced a noticeable accumulation of 18:1 n -9 and complete loss of PUFA proportions (Watts and Browse, 2002). When expressed in yeast cells, *C. elegans* FAT-2 act as v+3 desaturase which inserted double bonds sequentially at the Δ 12 and Δ 15 positions in substrates with preexisting Δ 9 double bond, such as 14:1 n -9, 15:1 n -9, 16:1 n -9, 16:2 n -9, 17:1 n -9, 18:1 n -9, 18:2 n -9 and 18:3 n -6 (Zhou et al., 2011).

1.5 Chitosan as a nuclear acid delivery vector

Naked nucleic acid receives high rate of clearance *in vivo* (HE et al., 2012), but delivered by vectors either viral or non-viral ones overcome such drawback. Nevertheless, viral vectors provoke immunogenicity and acute inflammation, which encourage the development of non-viral gene delivery systems using physical and chemical methods (Nayerossadat et al., 2012). While physical approaches such as microinjection and electroporation are generally limited to *ex vivo* delivery, chemical methods including cationic liposomes and cationic polymers are more practical for *in vivo* applications (Nayerossadat et al., 2012). Chemical methods utilize biocompatible materials that carry positive charges to form nanoscale particles with the anionic cargo nuclear acid. Chitosan is a type of cationic polymer increasingly used for delivering nucleic acids *in vivo* due to its well-known advantages such as low toxicity, mucoadhesion, biodegradability and biocompatibility (Wu et al., 2020a). Ionic gelation is one of the methods for chitosan nanoparticles preparation, based on electrostatic complexation of chitosan, ionic cross-linkers such as tripolyphosphate (TPP), and nucleic acids (Csaba et al., 2009).

1.5.1 Chitosan-TPP-DNA nanoparticle properties

Chitosan-TPP-DNA nanoparticles allows efficient DNA encapsulation, are cost-effective and easy to prepare. Chitosan is made from the second most abundant natural polysaccharide: chitin. It is

obtained from crustaceans, insects and microorganisms (Rinaudo, 2006). The structure of chitin is poly (*N*-acetyl-b-D glucosamine), which deacetylation results in the linear polysaccharide with poly (D-glucosamine) repeat units, chitosan (Figure 1.5.1). Chitosan refers to a product of about 50 % deacetylation of chitin, a degree that makes it soluble in aqueous acid at pH lower than 6 (Rinaudo, 2006). The water-solubility relies on the degree of deacetylation, molecular weight and the p*K*_a value of the amine group in D-glucosamine, which is about 6.5 (Strand et al., 2001). Commercially available chitosan is heterogeneous in the degree of deacetylation and molecular weight. In acidic conditions, chitosan amine groups are protonated and able to complex into polyplexes electrostatically with the phosphate groups of DNA. However, chitosan-DNA nanoparticles have limitations in isolation, storage, physical shapes and DNA-dependence (Chew et al., 2003; Csaba et al., 2009). To overcome these drawbacks, ionic cross-linkers such as TPP has been introduced into the system (Csaba et al., 2009). Like chitosan, the multivalent polyanion TPP is also easy to obtain and it is classified as Generally Recognized As Safe (GRAS, conditionally). Cross-link between chitosan and TPP depends on the positive charged amino groups of chitosan and negative charged TPP. Chitosan-TPP nanoparticles are formed immediately after dropwise adding of TPP into chitosan solution. Presence of TPP tunes chitosan-DNA nanoparticles (chitosan-TPP-DNA) more compact and stable, which is due to an additional trapping of DNA by the chitosan-TPP complex, besides the electrostatic effect (Katas and Alpar, 2006; Santos-Carballal et al., 2018). In general, the particle size of chitosan-TPP is around 300 nm with positive surface charges (zeta potential) around 30 mV, whilst loading DNA can slightly increase the size and decrease the zeta potential (Wu et al., 2020a).

In addition to the above-mentioned properties, chitosan-TPP-DNA nanoparticles have additional advantages such as low toxicity, biodegradability, and sustained release. Besides the consensus of GRAS of chitosan and TPP, toxicity concerns of chitosan-TPP-DNA nanoparticle are driven by the nanoscale feature that enables chitosan to cross organismal barriers, and the biodegradability of chitosan-TPP complex, which may cause short- and long-term toxicity, respectively (Islam et al., 2019; Jeevanandam et al., 2018). Nevertheless, toxicity evaluation of chitosan-TPP nanoparticles using multiple modes including cells and embryos indicates a negligible toxicity at certain doses (De Campos et al., 2004; Hu et al., 2011; Rampino et al., 2013). Although more investigation is required on the toxicity of chitosan-TPP nanoparticles, it is believed to be a highly promising carrier (Islam et al., 2019). Biodegradability is an important parameter for administration routes like subcutaneous and intraperitoneal in comparison with oral. Biodegradation depends on the features of chitosan-TPP nanoparticles and the exposed environment. The degradation can be classified as

hydrolytic, enzymatic and oxidative reactions (Marin et al., 2013). Chitosan cross-linking TPP slows the hydrolytic and enzymatic degradation (Islam et al., 2019). Chitosan-TPP-DNA nanoparticles prolonging cargo gene expression *in vivo* mainly relies on enzymatic rather than hydrolytic degradation (Csaba et al., 2009).

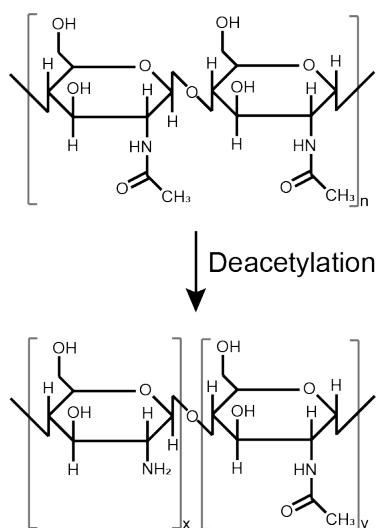


Figure 1.5.1 Deacetylation of chitin to chitosan

1.5.2 Ionic gelation methods

The preparation conditions for chitosan-TPP-DNA nanoparticles by ionic gelation are simple and mild, which favors the maintenance of the bioactivity of encapsulated compound (Figure 1.5.2). The nanoparticles are formed instantaneously upon the mix of aqueous solutions of chitosan and TPP-DNA under stirring at room temperature (Csaba et al., 2009). Nevertheless, nanoparticle characteristics, especially size, zeta potential and dispersity, are dominated by the preparation parameters including pH of solutions, molecular weight of chitosan, chitosan/TPP mass ratio and stirring speed (Bozkir and Saka, 2004; Carrillo et al., 2014; Fàbregas et al., 2013; Gan et al., 2005; Nasti et al., 2009). In general, particle size is positively associated with chitosan molecular weight, chitosan concentration, pH and stirring speed. Zeta potential is induced by lower pH, chitosan molecular weight and chitosan concentration. The dispersity of chitosan-TPP nanoparticles is affected by chitosan molecular weight, pH and chitosan/TPP concentrations.

INTRODUCTION

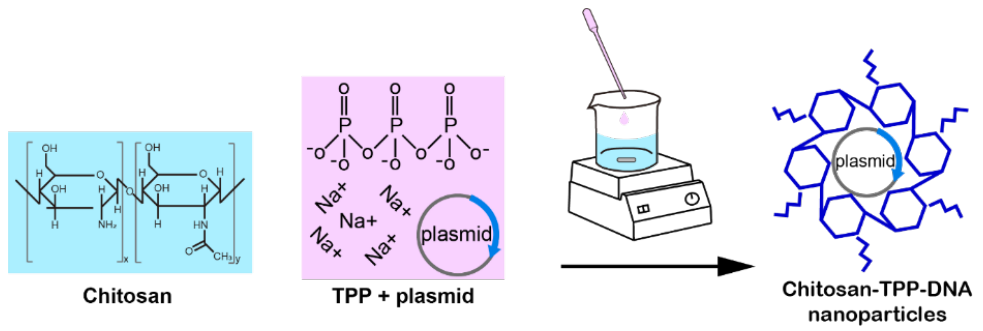


Figure 1.5.2 Ionic gelation of chitosan-TPP-DNA nanoparticles. TPP, tripolyphosphate.

2 OBJECTIVES

2.1 General objective

LC-PUFA and their derivatives are essential for growth and development acting as bioactive components of membrane phospholipids, being substrates for signalling molecules and modulators of gene expression (Zhang et al., 2016). Fish can not *de novo* synthesize LC-PUFA efficiently and require dietary supplementation due to the lack of $\Delta 12/n-6$ and $\Delta 15/n-3$ desaturases. However, shortage of fish oil, the major source of LC-PUFA, in aquafeeds is nowadays a major challenge in aquaculture due to dietary requirements of fish and the growing size of the industry. Vegetable oil is an alternative to fish oil that is currently being included in aquafeeds due to the large production. However, replacement of fish oil with vegetable oil significantly reduces *n-3* LC-PUFA, specially EPA and DHA, and increases the *n-6/n-3* fatty acid ratio in the fish's flesh (Pang et al., 2014), which would subsequently negatively affect human health. Thus, a considerable amount of studies focus on obtention of genetically modified organism such as terrestrial oil crops in order to produce more *n-3* LC-PUFA, notably EPA and DHA, for aquafeeds (Napier et al., 2015). Even so, antinutritional factors that exist in terrestrial plants challenge this strategy (Osmond and Colombo, 2019).

To alleviate fish oil dependency of aquafeeds, emerging efforts are also made to promote endogenous expression of FAT-1 and FAT-2 activities in fish mainly by obtaining transgenic animals. Efficient conversion of *n-6* PUFA to *n-3* PUFA has been reported in transgenic models expressing codon-optimized *C. elegans* FAT-1 and FAT-2, including zebrafish (Sun et al., 2020a) and common carp (X. Zhang et al., 2018). The *n-3* LC-PUFA content is improved by double transgenesis of FAT-1 and FAT-2 in zebrafish (Pang et al., 2014) and pig (Tang et al., 2019). However, the transgenic strategy is in a long-running debate with major concerns of genetic pollution to natural organisms as well as consumer acceptance of genetically modified organisms (Tocher et al., 2019). Alternatively, the use of chitosan as a nucleic acids' vector for gene therapy applications *in vivo* has been receiving increasing interest in the last years due to its mild processing conditions, nanoscale production and cost-effective merits in gene delivery applications (Wu et al., 2020a).

In view of the foregoing, we hypothesized that transient overexpression of FAT-1 and FAT-2 in the liver of *Sparus aurata* could boost the synthesis of *n-3* LC-PUFA, mainly EPA and DHA. To this end, the main objective of the study was to address metabolic and growth effects of a single dose and periodical administration of chitosan-TPP-DNA nanoparticles expressing *C. elegans* FAT-1 and FAT-2 in *S. aurata*.

2.2 Specific objectives

To address the main goal of the PhD thesis, the specific objectives were:

- 1) Construction of plasmids expressing fish codon-optimized *C. elegans* FAT-1 (pSG5-FAT-1) and FAT-2 (pSG5-FAT-2).
- 2) Obtention of chitosan-TPP nanoparticles complexed with pSG5-FAT-1, pSG5-FAT-2 and empty vector (pSG5, control).
- 3) Acute effects of a single intraperitoneal dose of chitosan-TPP-DNA nanoparticles on blood metabolites and liver intermediary metabolism and fatty acid profile in *S. aurata*.
- 4) Long-term detection of fish codon-optimized *C. elegans* FAT-1 and FAT-2 mRNA levels in the liver of *S. aurata* after a single dose of chitosan-TPP-DNA nanoparticles.
- 5) Effects of periodical intraperitoneal doses of chitosan-TPP-DNA nanoparticles on blood metabolites, liver intermediary metabolism, liver and muscle fatty acid profile and growth parameters in *S. aurata*.

3 MATERIALS AND METHODS

3.1 Animals

Gilthead sea bream (*Sparus aurata* Linnaeus 1758) belongs to the family *Sparidae*. It has oval body with moderately deep and compressed, regular curved head and a golden frontal stain between two small eyes, low mouth and thick lips, 4 to 6 canine-like teeth anteriorly in each jaw, followed posteriorly by blunter teeth which become progressively molar-like and are arranged in 2 to 4 rows, scales along lateral line 73 to 85 and a large black blotch at origin of lateral line (Yúfera et al., 2011; Carpenter and De Angelis, 2016). In aquaculture, *S. aurata* is the second largest cultured marine fish in Europe, accounting for 42.2 % of total European aquaculture production of marine fish according to the Food and Agriculture Organization 2022 year report (Circular, 2022).

S. aurata is commonly found over both rocky and soft bottoms along the Mediterranean and Atlantic coast of Europe and Africa, primarily in shallow waters (0-2 m) and gradually descending to deeper waters (> 50 m) with optimum growth temperature between 25-26 °C (Kir, 2020). The carnivorous fish *S. aurata* mainly feeds on arthropods and molluscs in nature (Hadj Taieb et al., 2013). The *Sparidae* family commonly exhibits hermaphroditism. *S. aurata* is a protandrous hermaphroditic species. It remains sexually immature during the first year of existence. Thereafter, individuals develop as functional males for another year. In most cases, during the third year of life sex reversal occurs and it is accompanied by resorption of spermatogonia and development of the ovarian tissue, while a percentage of the population remains as males (Zohar et al., 1978).

3.1.1 Animal maintenance and sampling

S. aurata juveniles were obtained from Piscimar (Burriana, Castellón, Spain) and transported to the Aquatic Animal facility at the Scientific and Technological Centers from the Universitat de Barcelona (CCiTUB). The experimental facilities provide constant control of room temperature at 20.0 °C, marine water and 250-liter aquariums. The aquariums are equipped with closed-circuit water system consisting of pump filters (eXperience 250, EHEIM, Germany), UV sterilisers (reeflexUV 800, EHEIM, Germany), air pumps (air100, EHEIM, Germany) and fixed photoperiod of 12 h light-12 h dark. Fish were assigned randomly to experimental aquariums (17-22 fishes/aquarium). Diet (Microbaq 165, Dibaq, Spain, table 3.1.1) was provided to fish twice daily at 9:00 and 19:00 after 3 days of the assignment. Fish weight of 6 g was estimated for feeding regime at a ratio of 5 % body weight per day during acclimatation. After at least 2 weeks of acclimatation, fish were weighed (ACBplus-150,

Adam Equipment, USA) and diet was adjusted to 3 % of BW per day for fish approximating 7-8 g of average weight. Every 2 weeks fish were weighted to readjust the diet.

Table 3.1.1 Microbaq 165 diet composition

Ingredients (% Weight)	
Brown fish meal	60.5
Fish oil	13.5
Wheat meal	11.4
Wheat gluten	8.3
Soluble fish extract	2.5
Mineral mixture	1.7
Yeast extract	1.0
Soy lecithin	1.0
Vitamin mixture	0.1
Nutritional composition (% Weight)	
Protein	52.0
Lipid	18
Carbohydrates	12
Ash	10
Moisture	8
Gross energy(kJ/g)	21.3

Fish were anesthetized by tricaine methanesulfonate (MS-222, Code 118000500, Thermo Scientific Acros, China) at a concentration of 70 mg/L in marine water before weighing and sampling. Ethical treatment of fish followed the guidelines of the University of Barcelona's Animal Welfare Committee (proceeding #10811, Generalitat de Catalunya), in accordance with the local legislation (RD 53/2013) and European Union Directive (2010/63/EU) for animal experiments.

The sampling process was as follows:

Preliminary steps

- Fasting fish for 24 hours before sampling or intraperitoneal injection.
- Fill a container with seawater at rearing temperature which capacity is suitable for the size

and number of fish.

- Dissolve the anaesthetic agent MS-222 at 70 mg/L.
- Transfer 10 fish into the container and wait until they are sedated (about 5 min).
- Proceed to sacrifice and tissue sampling or perform intraperitoneal injection.

Formal steps

- Fish were sacrificed by cervical section.
- Blood was collected with glass Pasteur pipettes (Code 1154-6963, Fisher Scientific, Germany) pre-soaked in 3 % w/v trisodium citrate (Code 131655, Panreac, Spain) to inhibit coagulation.
- Tissues were detached following the order: liver, intestine, skeletal muscle, and brain.
- To remove attached blood and other body fluids, tissues were washed with 0.9% saline before package.
- Immediate after saline wash, tissues were frozen by immersion in liquid nitrogen and kept at -80 °C until use.
- The blood was stand on ice for about 3 hours followed by centrifugation at 500 g and 4 °C for 10 min.
- Supernatant after the centrifugation was collected and stored at - 20 °C for metabolites analysis.

3.1.2 Experiments

3.1.2.1 Short-term administration of a single dose of chitosan-TPP-plasmid nanoparticles

After 2 weeks of acclimatation, fish were anesthetized and weighed. Chitosan-TPP-plasmid

nanoparticles were resuspended with saline (0.9 % w/v) to 2 mg plasmid/mL and intraperitoneally injected to fish at 10 µg plasmid/g of BW. Four groups of fish were treated to receive chitosan-TPP-pSG5 (pSG5; control), chitosan-TPP-pSG5-FAT-1 (FAT-1), chitosan-TPP-pSG5-FAT-2 (FAT-2) or chitosan-TPP-pSG5-FAT-1 + chitosan-TPP-pSG5-FAT-2 (FAT-1 + FAT-2) nanoparticles. Diet was administered twice a day at a ration of 3 % BW and fish were reared for 72 hours before sampling.

3.1.2.2 Long-term detection of fish codon-optimized *C. elegans* FAT-1 and FAT-2 mRNA levels in the liver of *S. aurata* after a single dose of chitosan-TPP-DNA nanoparticles

For verifying the lasting efficiency of the plasmid-delivery nanoparticles in the liver, the effect of a single dose chitosan-TPP-plasmid nanoparticles was evaluated 1 month after the treatment. After 2 weeks of acclimatation, fish were anesthetized and weighed. Two groups of fish were intraperitoneally injected with FAT-1 or FAT-1 + FAT-2 at 10 µg plasmid/g of BW. Diet was administered twice a day at a ration of 3 % BW and fish were reared for 4 weeks before sampling.

3.1.2.3 Long-term effect of periodical administration of chitosan-TPP-plasmid nanoparticles

After 2 weeks of acclimatation, fish were anesthetized and weighed. Four groups of fish were intraperitoneally injected up to 3 times (once every 4 weeks) with pSG5, FAT-1, FAT-2 or FAT-1 + FAT-2 nanoparticles. Every single administration consisted of 10 µg plasmid per gram BW. Fish was weighed and the diet was readjusted every 14 days. Fish were fed twice a day at a ration of 3 % BW. Seventy days after the first injection (14 days after the last injection) fish were sacrificed and sampled.

3.1.3 Growth performance

Specific growth rate (SGR), feed conversion ratio (FCR), hepatosomatic index (HSI), protein retention (PR), lipid retention (LR) and protein efficiency ratio (PER) were calculated according to the following equations:

$SGR = (\ln W_f - \ln W_i) * 100 / T$; where W_f and W_i are mean final and initial body fresh weight (g), and T is time (days)

$FCR = \text{dry feed intake (g)} / \text{wet weight gain (g)}$

HSI = liver fresh weight (g)*100 / fish body weight (g)

PR = body protein gain (g)*100 / protein intake (g)

LR = body lipid gain (g)*100 / lipid intake (g)

PER = weight gain (g) / feed protein provided (g)

3.2 Plasmids

pCMVβ is a mammalian reporter vector that was used for evaluating transient transfection efficiency in eukaryotic cell culture experiments.

pMA-T-FAT-1 is a vector backbone for assembling synthetic fish codon-optimized *C. elegans* FAT-1 cDNA. The plasmid was purchased from ThermoFisher Scientific (see section 3.4).

pMA-T-FAT-2 is a vector backbone for assembling synthetic fish codon-optimized *C. elegans* FAT-2 cDNA. The plasmid was purchased from ThermoFisher Scientific (see section 3.4).

pSG5, a modified form of the eukaryotic expression vector pSG5 (Stratagene) was used. The modification includes addition of several restriction sites at the multicloning site for facilitating the subcloning process. pSG5 has promoter SV40, β-globin intron II and a polyadenylation signal to allow expression of eukaryotic inserts *in vivo*.

pSG5-FAT-1 was constructed by digestion of pMA-T-FAT-1 and pSG5 using *EcoRI* and *KpnI*, and ligation of the digested products, fish codon-optimized *C. elegans* FAT-1 cDNA and pSG5.

pSG5-FAT-2 was constructed by digestion of pMA-T-FAT-2 and pSG5 using *EcoRI* and *BamHI*, and ligation of the digested products, fish codon-optimized *C. elegans* FAT-2 cDNA and pSG5.

3.3 Oligonucleotides

Oligonucleotides listed in table 3.3 were intended for quantifying mRNA levels (real-time quantitative polymerase chain reaction, qPCR), except T7 and pSG5rev, which were used for PCR

colony screening.

Table 3.3 Oligonucleotides

Gene	Code	F/R	Sequences (5' to 3')	GenBank Accession
<i>18s</i>	JDRT18s	F	TTACGCCCATGTTGTCCTGAG	AM490061
	JDRT18as	R	AGGATTCTGCATGATGGTCACC	
<i>acaca</i>	RT_ACC1TV 1_F	F	CCCAACTTCTTCTACCACAG	JX073712
	RT_ACC1TV 1_R	R	GAACTGGAActCTACTACAC	
<i>acacb</i>	RT_ACC2_F	F	TGACATGAGTCCTGTGCTGG	JX073714
	RT_ACC2_R	R	GCCTCAGTTCGTATGATGGT	
<i>actb</i>	qBActin.F	F	CTGGCATCACACCTTCTACAACGAG	X89920
	qBActin.R	R	GCGGGGGTGTGAAGGTCTC	
<i>cpt1a</i>	JS-qCPT1A-F	F	GAAGGGCAGATAAAGAGGGGC	JQ308822
	JS-qCPT1A-R	R	GCATCGATCGCTGCATTCAGC	
<i>ef1a</i>	AS-EF1Fw	F	CCCGCTCTGTGCTTCG	AF184170
	AS-EF1Rv	R	CAGCAGTGTGGTTCGTTAGC	
<i>elov14a</i>	YW2111	F	AAGAACAGAGAGCCCTCCAG	MK610320
	YW2112	R	TGCCACCCTGACTTCATTG	
<i>elov14b</i>	YW2113	F	TCTACACAGGCTGCCATTC	MK610321
	YW2114	R	CGAAGAGGATGATGAAGGTGAC	
<i>elov15</i>	JS-qFAE-F	F	GGGATGGCTACTGCTCGACA	AY660879
	JS-qFAE-R	R	CAGGAGAGTGAGGCCAGAT	
<i>fads2</i>	JS1615	F	CACTATGCTGGAGAGGATGCC	AY055749
	JS1616	R	TATTTCCGGTCTGGCTGGGC	
<i>fasn</i>	JS-qFAS-F	F	GTAGAGGACACGCCATCGAT	JQ277708
	JS-qFAS-R	R	TGCGTATGACCTCTTGGTGTGCT	
FAT-1	YW2001	F	TTCACCCCATTCCTTTCAGCG	--
	YW2002	R	TAGGCGCACACGCAGCAGCA	
FAT-2	YW2003	F	AAGAGGACTACAACAACAGAACCGC CA	--
	YW2004	R	CGAACAGTCTGCTCCAAGGCCAA	
<i>fbp1</i>	AE5	F	CAGATGGTGAGCCGTGTGAGAAGG ATG	AF427867
	AE6	R	GCCGTACAGAGCGTAACCAGCTGCC	

MATERIALS AND METHODS

<i>g6pc1</i>	CO1701	F	GCGTATTGGTGGCTGAGGTCG	AF151718
	CO1702	R	AAGGAGAGGGTGGTGTGGAAG	
<i>g6pd</i>	RT_G6PD_F	F	TGATGATCCAACAGTTCCTA	JX073711
	RT_G6PD_R	R	GCTCGTTCTGACACACTGA	
<i>gck</i>	JYA-GK-F1	F	TGTGTCAGCTCTCAACTCGACC	AF169368
	JYA-GK-R1	R	AGGATCTGCTCTACCATGTGGAT	
<i>hmgr</i>	JS1601	F	ACTGATGGCTGCTCTGGCTG	MN047456
	JS1602	R	GGGACTGAGGGATGACGCAC	
<i>hnf4a</i>	YW2119	F	GTGGACAAAGACAAGCGAAATC	FJ360721
	YW2120	R	GCATTGATGGATGGTAAACTGC	
<i>nr1h3</i>	YW2109	F	GCATCTGGACGAGGCTGAATAC	FJ502320
	YW2110	R	ACTTAGTGTGCGAAGGCTCACC	
<i>pck1</i>	AE15	F	CAGCGATGGAGGAGTGTGGTGGG	AF427868
	AE16	R	GCCCATCCCAATCCCGCTTCTGTG CTCCGGCTGGTCAGTGT	
<i>pfkl</i>	JYA03F1	F	TGCTGGGGACAAAACGAACTCTTCC	KF857580
	JYA04R1	R	AAACCCTCCGACTACAAGCAGAGCT	
<i>pfkfb1</i>	JS1507	F	TGCTGATGGTGGGACTGCCG	U84724
	JS1508	R	CTCGGCGTTGTCGGCTCTGAAG	
<i>pklr</i>	MG1301q	F	CAAAGTGGAAAGCCGGCAAGGG	KF857579
	MG1302q	R	GTCGCCCCTGGCAACCATAAC	
<i>pCMVβ</i>	JDRTpcmvbS	F	CCCATTACGGTCAATCCGC	--
	JDRTpcmvbA S	R	ACAACCCGTCGGATTCTCC	
<i>ppara</i>	LS_1701	F	GTGAGTCTTGTGAGTGAGGGGTTG	AY590299
	LS_1702	R	AGTGGGGATGGTGGGCTG	
<i>pparg</i>	JS1603	F	TGCGAGGGCTGTAAGGGTTTC	AY590304
	JS1604	R	GTTTCTCCTTCTCCGCCTGGG	
<i>scd1a</i>	YW2117	F	TCCCTTCCGCATCTCCTTTG	JQ277703
	YW2118	R	TTGTGGTGAACCCTGTGGTCTC	
<i>srebfl</i>	JS1406	F	CAGCAGCCCGAACACCTACA	JQ277709
	JS1407	R	TTGTGGTCAGCCCTTGGAGTTG	
--	T7	F	TAATACGACTCACTATAGGG	--
--	pSG5rev	R	CGGAGCCTATGGAAAAACG	--

F, Forward; R, Reverse.

3.4 Design of fish codon-optimized cDNAs

C. elegans FAT-1 and FAT-2 coding DNA sequences were uploaded to GeneArt Instant Designer and optimized by *Danio rerio* codon usage (ThermoFisher Scientific, USA). The fish codon-optimized *C. elegans* FAT-1 and FAT-2 cDNAs were commercially manufactured and inserted into pMA-T (ThermoFisher Scientific, USA). Upon arrival, 5 µg of the delivered pMA-T-FAT-1 and pMA-T-FAT-2 constructs were both resuspended in 10 µL of 10 mM Tris-HCl buffer, by gently pipetting up and down several times and stored at -80 °C until use. Identity of pMA-T-FAT-1 and pMA-T-FAT-2 was confirmed by sequencing (see 3.12).

3.5 Preparation of DH5α competent *Escherichia coli*

The *E. coli* strain DH5α, which has high transformation efficiency, is applied for molecular cloning of plasmids and ligation products. The protocol followed to prepare DH5α competent cells was:

- Prepare 100 mM MgCl₂ (Code 141396, Panreac, Spain) and 100 mM CaCl₂ (C7902-500G, Sigma, USA) for following usage.
- Autoclave (Code 4004372, J. P. Selecta, Spain) the two solutions above mentioned and store them at 4 °C for following usage.
- Mix 25 mL of 100 mM CaCl₂ solution with 4.4 mL of glycerine (Cat G7757, Sigma-Aldrich, USA), autoclave it and store it at 4 °C for following usage.
- Prepare 60 mL LB broth according to table 3.5 for following usage

Table 3.5 LB broth

Component	Quantity	Reference
Tryptone	10 g	Cat 1612.00, Pronadisa, Spain
NaCl	10 g	131659.1214, Panreac, Spain
Yeast extract	5 g	Cat 1702.00, Pronadisa, Spain

Dissolve the components with 1 liter of distilled water, adjust the pH to 7.0 with NaOH, and autoclave for 20 min at 15 psi (1.05 kg/cm²).

- Seeding 50 µL of original DH5α competent cells in 5 mL of LB broth.

- Culture the cells in a shaker (New Brunswick™ Excella® E25, Eppendorf, Germany) at 220 rpm and 37 °C overnight.
- Add 5 mL of the overnight culture into 50 mL LB broth and culture overnight again as above.
- Centrifuge the 50 mL culture at 2500 g and 10 °C for 10 min (Centrifuge 5415R, Eppendorf, Germany). Withdraw the supernatant.
- Resuspend the pellet with 50 mL of ice-cold 100 mM MgCl₂.
- Centrifuge the MgCl₂ resuspension at 2500 g and 10 °C for 10 min and withdraw the supernatant.
- Resuspend the pellet with 10 mL of ice-cold 100 mM MgCl₂.
- Add 100 mL of ice-cold 100 mM CaCl₂ that prepared before and keep the mixture on ice for 90 min.
- Centrifuge the culture under 2500 g and 10 °C for 10 min and withdraw the supernatant.
- Resuspend the pellet in 12.5 mL of resuspension solution (*i.e.*, the mixture of CaCl₂ and glycerin).
- Store as 200 µL aliquots at -80 °C until use.

3.6 Transformation of DH5α competent cells

Plasmids and ligation products* were transferred into DH5α by heat shock. Single colonies containing the transferred product are allowed to grow for further amplification in liquid medium. The steps were as follow:

- Thaw 50 µL DH5α competent cells on ice and mix it with 0.25 µg plasmids in sterile tubes.
- Incubate the cells on ice for 15 min.

- Incubate the cells in water bath at 42 °C for 2 min and 45 sec.
- Incubate the cells on ice for 3 min.
- Mix 400 µL antibiotic free LB broth with the cells.
- Incubate the cells in water bath at 37 °C for 1 hour.
- Centrifuge the cells at 5000 g for 30 seconds.
- Withdraw 400 µL of the supernatant and resuspend the cells with the rest liquid near the Bunsen burner.
- Transfer 5 µL of the resuspension from above into a LB agar plate (table 3.6).

Table 3.6 LB agar plate

Component	Quantity	Reference
Tryptone	10 g	Cat 1612.00, Pronadisa, Spain
NaCl	10 g	131659.1214, Panreac, Spain
Yeast extract	5 g	Cat 1702.00, Pronadisa, Spain
Agarose	20 g	Cat 1802.00, Pronadisa, Spain

Dissolve the components with 1 liter of distilled water, adjust the pH to 7.0 with NaOH, and autoclave for 20 min at 15 psi (1.05 kg/cm²) on liquid cycle. Cool to 60 °C and add antibiotics according to plasmid-mediated resistance. Different concentrations were applied according to antibiotics. For pCMVβ, pMA-T and pSG5-mediated resistance, ampicillin (100 µg/mL) was used. Pour 30 mL of the above mixture per 90-mm plate, cool at room temperature until gelification was completed and store the plate at 4°C.

- Spread the cells evenly over the plate using a sterilized glass stick near to flame.
- Keep the plate at room temperature for 15 min.
- Upside down the plate and incubate at 37 °C overnight (Type INB500, Memmert, Germany).

*For transformation of ligation products, 200 μ L of DH5 α cells and 5 μ L of ligation product were used.

3.7 Isolation of plasmids

To amplify and obtain suitable amounts of plasmid, either miniprep (Ref.740588.250, Macherey-Nagel, Germany), midiprep (Ref. K0481, ThermoFisher Scientific, USA) or gigaprep (Ref.740593, Macherey-Nagel, Germany) were performed according to the corresponding manuals of the commercial kits. The basic procedure was reported by Birnboim and Doly (Birnboim and Doly, 1979). General steps for amplification and extraction of plasmid DNA were:

- Set up an overnight DH5 α *E. coli* bacterial culture (New Brunswick Biological Shaker Excella E25, Eppendorf, USA) by inoculating a single plasmid-transformed colony picked from a freshly streaked plate into appropriate volume of LB broth containing the antibiotic corresponding to the plasmid resistance.
- Harvest DH5 α cells by centrifugation at 4500-6000 g and 4 °C for 15 min.
- Resuspend the cell pellet with the suspension solution provided by the kit. Generally, suspension solution provides an optimal pH for subsequent lysis.
- Break down cell membrane and denature DNA by alkaline solution (lysis).
- Precipitate chromosomal DNA and other cellular compounds in acid medium, where plasmid DNA reverts to its supercoiled structure and remains in solution.
- Clarify the lysate by centrifugation at room temperature.
- Load the cleared lysate into a column with anion-exchange resin for binding plasmid DNA.
- Plasmid DNA is eluted after washing the column and dissolved in TE buffer for further use.

3.8 Restriction endonuclease digestion

Restriction endonucleases recognize and cut double-stranded DNA at specific sites. Restriction

digestion results in the formation of either blunt or sticky DNA ends, which facilitate the ligation of linear double-strand DNA fragments. The digestion process for subcloning FAT-1 and FAT-2 cDNAs into pSG5 were as follow:

- Digest pMA-T-FAT-1 and pSG5 plasmids with *EcoRI* at 37 °C in water bath for 4.5 hour (table 3.8a). Every 1.5 hour, additional 5 U more of enzyme were added.

Table 3.8a Enzyme digestion of pMA-T-FAT-1 and pSG5 plasmids with *EcoRI*

Component (concentration)	Volume/amount	Reference
Plasmid	2 µg	--
Buffer (10X)	8	Thermo Scientific, ref.#B12, USA
MQ Water	--	Merck KGaA, ref.SYNSVHFWW, Germany
<i>EcoRI</i> (10 U/µL)	2	Thermo Scientific, ref.#ER0271, USA
Final volume	80 µL	--

The amount of plasmid for digestion depends on the recovery rate of products after purification of the reaction system and the requirement for ligation (see 3.9).

- Purification of digested products from the above step using the High Pure PCR product Purification Kit (Ref.11732668001, Roche, Germany).
- Digest the purified products by *KpnI* with water bath at 37 °C for 4.5 hour (table 3.8b). Additional 5 U of enzyme were added every 1.5 hour.

Table 3.8b Enzyme digestion of pMA-T-FAT-1 and pSG5 plasmids with *KpnI*

Component (concentration)	Volume (µL)	Reference
Product of <i>EcoRI</i> digestion	30	
Buffer (10X)	8	Thermo Scientific, ref.#B29, USA
MQ Water	40	Merck KGaA, ref.SYNSVHFWW, Germany
<i>KpnI</i> (10 U/µL)	2	Thermo Scientific, ref.#ER0521, USA
Final volume	80	--

- Purify the *EcoRI/KpnI* product using the High Pure PCR product Purification Kit (Ref.11732668001, Roche, Germany).
- The product of pMA-T-FAT-1 *EcoRI/KpnI* digestion was submitted to gel electrophoresis (see

section 3.11), in order to separate FAT-1 and pMA-T and purify the band gel corresponding to FAT-1 cDNA (1231bp) using the High Pure PCR product Purification Kit (Ref.11732668001, Roche, Germany).

- Purified pSG5 and FAT-1 were ready for ligation.

Enzyme digestion of pMA-T-FAT-2 and pSG5 (for assembling FAT-2) were completed by one-step digestion. Briefly:

- Digest pMA-T-FAT-2 and pSG5 plasmids by *EcoRI* and *BamHI* at 37 °C water bath for 4.5 hour (table 3.8c). Additional 5 U of enzyme were added every 1.5 hour.

Table 3.8c Enzyme digestion of pMA-T-FAT-2 and pSG5 plasmids with *EcoRI* and *BamHI*

Component (concentration)	Volume/amount	Reference
Plasmids	2 µg	--
Buffer (10X)	8 µL	Thermo Scientific, ref.#B57, USA
MQ Water	--	Merck KGaA, ref.SYNSVHFVW, Germany
<i>EcoRI</i> (10 U / µL)	2 µL	Thermo Scientific, ref.#ER0271, USA
<i>BamHI</i> (10 U / µL)	2 µL	Thermo Scientific, ref.#ER0051, USA
Final volume	80 µL	--

The amount of plasmid for digestion depends on the recovery rate of products after purification of the reaction system and the requirement for ligation (see 3.9).

- The products from *EcoRI/BamHI* digestion were purified by the High Pure PCR product Purification Kit (Ref.11732668001, Roche, Germany).
- The product of pMA-T-FAT-2 digestion was submitted to gel electrophoresis (see section 3.11), in order to separate FAT-2 and pMA-T and purify the band gel corresponding to FAT-2 cDNA (1153bp) using the High Pure PCR product Purification Kit (Ref.11732668001, Roche, Germany).
- Purified pSG5 and FAT-2 were ready for the following ligation.

3.9 DNA ligation

DNA ligation allowed to join DNA vector/plasmid with a gene of interest. The resulting recombinant plasmid contains the gene of interest for further applications, such as sequencing and complexing with chitosan-TPP. Upon obtaining FAT-1, FAT-2 and pSG5 fragments, a LigaFast™ Rapid DNA Ligation System (Part# 9PIM822, Promega, USA) was processed for construction of pSG5-FAT-1 and pSG5-FAT-2 plasmids following the manufacturer instructions. Briefly:

- Thaw and mix well of pre-allocated ligation buffer for 1.5 min.
- Add components into the buffer tube according to table 3.9.

Table 3.9 DNA ligation system for assembling insert and vector

Components	Concentration	Final Volume
2X rapid ligation buffer	1 X	5 μ L
Insert sequence (FAT-1/FAT-2)	4 μ L in total	require calculation*
Plasmid (pSG5)		require calculation*
Ligase	3 U/ μ L	1 μ L

Calculation: $[(\text{ng of plasmid} \times \text{kb size of insert}) / \text{kb size of plasmid}] \times \text{molar ratio of insert: plasmid} = \text{ng of insert}$. A molar ratio of 1:3 was used. Optimal amount of plasmid is 50 ng. To adjust plasmid + insert to a final volume of 4 μ L in total, the following equation was applied: Let, i = Insert sequence, p = Plasmid, C = Concentration (ng/ μ L), L = Length (bp), V = Volume. Then, $V_p (\mu\text{L}) = 4 V_p / (V_p + V_i)$, $V_i (\mu\text{L}) = 4 V_i / (V_p + V_i)$.

- Incubate the reaction system at room temperature for 1 hour and then at 10 °C overnight.
- Amplify the amount of pSG5-FAT-1 and pSG5-FAT-2 using miniprep (see section 3.7) for restriction analysis and sequencing.

3.10 PCR screening of positive ligation products

PCR screening was applied for identifying positive ligation products using primers designed from the surrounding sequences of the insert location in the vector. Successful ligated plasmids result in the

expected size of PCR products after visualization of agarose gel electrophoresis. PCR screening was as follows:

- Transformation and amplification of ligation products with DH5 α competent cells (see section 3.6).
- Prepare PCR reaction mixture (table 3.10a).

Table 3.10a PCR reaction system for screening positive pSG5 colonies (volume per colony)

Component (concentration)	Volume (μ L)	Reference
T7 primer (10 μ M)	0.3	--
pSG5rev primer (10 μ M)	0.3	--
dNTPs (100 μ M)	dATP (25 μ M)	P/N 55082, Thermo Fisher Scientific, USA
	dGTP (25 μ M)	P/N 55084, Thermo Fisher Scientific, USA
	dTTP (25 μ M)	P/N 55085, Thermo Fisher Scientific, USA
	dCTP (25 μ M)	P/N 55083, Thermo Fisher Scientific, USA
Taqpol polymerase buffer with MgCl ₂ (10X)	1.5	--
Taq polymerase (5U/ μ L)	0.09	10.003, Biotools, Spain
MQ water	12.41	--

- Allocate the mixture into PCR tubes.
- Mark and pick colonies randomly from the transformation plate by using sterile pipette tips (10 μ L size) and pipetting into the PCR tubes under Bunsen burner. Part of each of the colonies should be retained in the plate further for amplification after identifying positive colonies.
- After short centrifugation of the PCR reaction mixture, process PCR reaction program as table 3.10b.

Table 3.10b PCR reaction program

Cycle	Temperature (°C)	Time (min)
--	95	1
	95	0.5
35	55	0.5
	72	2
--	72	5

- PCR products were analyzed by gel electrophoresis (see section 3.11)
- Upon identification of positive colonies (*i.e.*, pSG5-FAT-1 and pSG5-FAT-2), the remaining part of corresponding colonies were processed to perform minipreps (see section 3.7).
- After purification from minipreps, the plasmids were sent for sequencing (see section 3.13) to precisely confirm the nucleotide sequences of the recombinant plasmids.

3.11 DNA gel electrophoresis

This method is based on the motion of negatively charged DNA in agarose gels submitted to an electric field. DNA gel electrophoresis is used for separation and identification of DNA sequences according to DNA sizes. Gel electrophoresis was applied as follows:

- Prepare and autoclave 50X TAE (Tris-acetate-EDTA) buffer at pH = 8.2.

Table 3.11a 50X TAE (Tris-acetate-EDTA) buffer

Component	Concentration	Reference
Tris base	2.0 M	T1503-1KG, Sigma, USA
Acetic acid	1.0 M	141008, Panreac, Spain
EDTA	0.05 M	ED2SS-500G, Sigma-Aldrich, USA

Table 3.11b 1 % agarose (w/v)

Component	Amount	Reference
Agarose	0.5 g	AG-0500, Ecogen, Spain
50X TAE	1 mL	--

Distilled water	49 mL	--
-----------------	-------	----

- Melt the agarose-buffer mixture using microwave until completely dissolved.
- Cool the agarose to 65 °C and add 6 µL SYBR Safe DNA gel stain (Ref.S33102, Thermo Fisher Scientific, USA).
- Pour the agarose into a gel tray with the well comb in place and cool at room temperature for gelification (about 50 min).
- Immerse the gel into a horizontal electrophoresis chamber (Ref.1704467EDU, Bio-Rad, USA) that filled with 1X TAE buffer.
- Load 5 µL DNA sample with 1 µL 6X Orange DNA Loading Dye (Ref.R0631, Thermo Fisher Scientific, USA).
- Load 5 µL of appropriate DNA Ladder (Ref.SM0311, Thermo Scientific, USA).
- Gel electrophoresis exercised under power supplied at 100 volts (Model453, ISCO, USA) until dye line reached about 80 % of the gel length.
- Visualize the gel electrophoresis results by the Gel DocTM EZ Imager (Ref.10000076956, Bio-Rad, USA).

*Visualize the gel electrophoresis on platform of UV device (Model TFP-M/WL, Biotech, Spain) and cut the desired size band if needed.

3.12 Cycle sequencing

Cycle sequencing based on the Sanger sequencing method is applied for precisely verifying DNA sequences. Sequence analysis was performed at the CCiTUB. Preparation before sending to the sequencing service was as follows:

- Pre-heat incubator (Model D1100, Labnet, USA) to 85 °C.

- Add suitable volume of product in a PCR tube: 100 ng for every 1000 bp DNA length.
- Add 10 μ M of T7 and pSG5rev primers.
- Incubate the tube at 85 °C for 15 min with the tap open.
- Store at – 20 °C before sequencing.
- After analysis and confirmation of pSG5-FAT-1 and pSG5-FAT-2 constructs, remaining solutions from the miniprep were used to amplify the plasmid by midiprep or gigaprep (see section 3.7) for further applications.

3.13 RNA extraction

RNA extraction is the purification of RNA from biological samples. Total RNA from samples were extracted using HigherPurity Tissue Total RNA Purification kit (Ref AN0152-XL, Canvax, Cordoba Spain) according to the manufacturer’s protocol. Absorbance of the RNA at 260 nm and 280 nm were measured by the NanoDrop 1000 Spectrophotometer (Thermo Fisher Scientific, USA) and a ratio of 260/280 around 2.0 is generally accepted for following steps, such as reverse transcription.

3.14 Reverse transcription

Reverse transcription is a process where complementary DNA (cDNA) is synthesized from a single-stranded RNA template by reverse transcriptase. The steps were as follows:

- Prepare the mixture in table 3.14a.

Table 3.14a Components for reverse transcription

Components	Concentration	Reference
dNTPs	0.5mM	See table 3.10a
Random Hexamers	6.25ng/ μ L	SO142, Thermo Scientific, USA
Total RNA	2 μ g	--
MQ water	Up to 16 μ L	--

- Incubate the mixture for 5 min at 65 °C.
- Chill the mixture on ice for 1 min, briefly centrifuge and place on ice.
- Add following mixture to make the final volume of 20 μL (table 3.14b).

Table 3.14b Components for reverse transcription

Components	Concentration	Reference
OPTIZYME M-MLV RT buffer	1X	P0073-XL, Canvax, Spain
Ribonuclease Inhibitor	1U/ μL	BP3222-1, Fisher Scientific, USA
OPTIZYME M-MLV Reverse Transcriptase	10U/ μL	P0073-XL, Canvax, Spain

- Incubate the mixture at room temperature for 10 min and 37 °C for 50 min.
- Heat the mixture 15 min at 70 °C to inactivate the M-MLV reverse transcriptase.
- Store cDNA product at – 20 °C before downstream applications.

3.15 Quantitative real-time PCR

For RNA quantification, quantitative real-time PCR (qPCR) was adopted. Once intercalated to DNA, SYBR Green becomes less mobile and releases its energy as fluorescence, which intensity is directly associated with the concentration of double-stranded DNA, allowing detection and quantification of real-time DNA transcripts in PCR.

- Prepare master mix as in table 3.15b.

Table 3.15b Components of master mix for qPCR

Components	Concentration	Volume	Reference
Forward primer	10 μM	1 μL	--
Reverse primer	10 μM	1 μL	--
SYBR Green Master Mix	--	12.5 μL	A25743, Thermo Fisher Scientific, USA
qPCR Water	--	8.5 μL	--

- Dilute 10 times cDNA samples from the liver, brain, and intestine with MQ water before use.
- Add 2 μL of cDNA sample in the master mix.
- Allocate 10 μL of the mixture in each of duplicate reaction tubes (4358293, Life technologies, USA).
- Cover the tubes with caps (4323032, Life technologies, USA) and centrifuge at 1000 rpm for 1 min (FC5714, Ohaus, Switzerland).
- Insert the tubes in QuantStudio™ 3 Real-Time PCR System (A28131, Thermo Fisher Scientific, USA) and run the program as follow:

Table 3.15c qPCR running program

Temperature ($^{\circ}\text{C}$)	Time (min)	Cycle
95	10	--
95	0.25	40
62	1	

Dissociation curves were applied after each experiment to confirm the amplification of single products. Serial dilutions of control cDNA were used to generate standard curves in order to determine the efficiency of the amplification reaction for each gene. The mRNA levels for genes were normalized using *S. aurata* ribosomal subunit 18s (*18s*), β -actin (*actb*) and elongation factor 1 alpha (*eef1a*) as endogenous controls. The standard $\Delta\Delta\text{CT}$ method was used to calculate variations in gene expression (Livak and Schmittgen, 2001).

3.16 Eukaryotic cell culture and transformation

HepG2 cells transfection was applied for validating the constructed expression plasmids and their effects on fatty acid synthesis by 48-hour transient transfection using the method of calcium phosphate-DHA co-precipitation. HepG2 cells from the same batch were seeded in 24 culture dishes. Twelve dishes of cells received pSG5 (control), pSG5-FAT-1, pSG5-FAT-2 or pSG5-FAT-1 + pSG5-FAT-2 for validating the expression of FAT-1 and FAT-2 ($n=3$). The other twelve dishes of cells also received the four treatments ($n=3$) for evaluation of fatty acid profiles.

3.16.1 HepG2 culture

The cells were cultured in 100 mm tissue culture dishes (Ref. 130182, ThermoScientific, Korea) using water jacketed CO₂ incubator (Forma Series ii, Thermo Scientific, USA) with temperature at 37 °C and 5 % CO₂.

The culture medium was composed of Dulbecco's Modified Eagle Medium (DMEM) (Ref.41966-029, Gibco, UK) supplemented with 10 % fetal bovine serum (FBS) (Ref. 10500-064, Gibco, Germany) and 1 % antibiotics (Ref. 15140-122, gibco, USA). The medium was replaced every 2-3 days by aspirating and adding prewarmed (37 °C) fresh medium.

3.16.2 Subculture

When cells reached about 80 % confluence, subcultures were processed. For 100 mm culture dishes, the medium is aspirated, and the cells are gently rinsed with 5 mL of 1X phosphate buffered saline (PBS, see table 3.16.2) in order to remove FBS, which can inhibit trypsin activity. Discard the rinsing PBS, add 1 mL trypsin (Ref.12605-028, Gibco, Denmark) and incubate at 37 °C for 2-3 min.

After incubation, tap the side of the dish to detach the cells from the plastic surface. Add 10 mL prewarmed (37 °C) fresh medium and subdivide the cells into new dishes (or collect the cells for cryopreservation, see 3.16.3). Count cells prior to subculture.

For counting the cells, mix 10 µL of the trypsinized cells with 10 µL Trypan Blue (Ref. T10282, Invitrogen, USA). Load 10 µL of the mixture inside a counting chamber slide (Ref. C10283, Invitrogen, USA) and insert the slide into Countess™ (Invitrogen, USA) for analyzing cell concentration.

2.2×10⁶ cells are subdivided into a new 100 mm culture dish. Add fresh medium to compensate the total culture volume into 10 mL. Culture the cells as in 3.16.1.

Table 3.16.2 10X PBS stock solution

Component	Concentration (M)	Reference
NaCl	1.37	131659.1214, Panreac, Spain
KCl	0.027	4936, Merck, Germany

Na ₂ HPO ₄	0.1	122507.1211, Panreac, Spain
KH ₂ PO ₄	0.018	4873, Merck, Germany

Adjust pH = 7.40 with HCl; autoclave for 20 min at 15 psi (1.05 kg/cm²); store at room temperature.

3.16.3 Freezing cells

Steps below are followed for cryopreservation:

- Prepare freezing medium: 70% DMEM + 20% FBS + 10% dimethyl sulfoxide (Ref. D4540-500ML, Sigma, USA)
- Label cryovials with the date, name of researcher, passage number and cell type.
- Transfer trypsinized cells into 15 mL falcon and centrifuge at 1000 rpm and room temperature for 5 min.
- Remove the supernatant and loosen the pellet by gentle tapping the tube bottom.
- Add the freezing media till required cell density, which for mammalian cells is usually 10⁶/mL. Cells should not be at room temperature in freezing media for more than 10 min.
- Transfer the cryovials into a CoolCell (at room temperature) and put into a -80 °C freezer. The CoolCell decreases the cryovials temperature steadily by 1 °C/min.
- After approximately 24 h, remove the cryovials from the CoolCell and transfer into liquid nitrogen for long-term storage.

3.16.4 Thawing cells

Steps below are followed for thawing cells:

- Remove cryovial from liquid nitrogen storage and place in 37°C water bath until about 80% defrosted (this should take no longer than 1 min).

- Transfer the cells into a 15 mL falcon containing 10 mL of prewarmed culture medium.
- Centrifuge at 1000 rpm and room temperature for 5 min.
- Discard the supernatant and resuspend in appropriate amount of cell culture medium.
- Transfer cells into a culture dish and grow in incubator.

3.17 Calcium phosphate-DNA co-precipitation

This method is aimed for introducing foreign DNA into eukaryotic cells. Before *in vivo* employment of chitosan-TPP-plasmid nanoparticles, validation of the constructed plasmids expressing FAT-1 and FAT-2 was performed by transient transfection of both plasmids into HepG2 cells using the phosphate-DNA co-precipitation method:

1. Prepare 50 mL 2× BBS (BES-buffered saline) by mixing 25 mL, 2.8 mL, 150 µL and 22.05 mL, respectively, of solution No.1, 2, 3 and MQ water (table 3.17).

Table 3.17 2X BBS sub solutions

Solution No.	Component	Concentration (M)	Reference
1	BES	0.1	A1062.0100, AppliChem, Germany
2	NaCl	5	131659.1214, Panreac, Spain
3	Na ₂ HPO ₄ ·2H ₂ O	0.5	122507.1211, Panreac, Spain

Adjust BES solution pH = 7.00 with NaOH. The three solutions are prepared with MQ water.

2. Adjust the pH of BBS solution to several points around 7.00, take 55 µL of the BBS solution at each pH point for 'BBS Effectiveness test' (step 3-5). Effective pH theoretically at 6.95 to 6.98.
3. Add 2 µL plasmid (1 µg/µL), 41 µL MQ water and 5 µL CaCl₂ (2.5M), vortex very well.
4. Dropwise 50 µL of BBS solution into the solution from step 3 under vortexing.
5. Add 1 µL of the above solution on a glass slide and check under 100X microscope to see which pH of BBS solution generates the most even and granular precipitates.

6. Adjust the BBS solution again to the pH that produced the bigger precipitate.
7. Filter the BBS solution by sterile filter (Ref. 10462200, Whatman, Germany) in a vertical laminar flow workbench (AV-30/70, Telstar, Japan) and store at 4 °C until use.
8. Prepare suitable amount dishes of cells at about 40% confluence.
9. Change medium 2 hours before transfection.
10. Pre-check if the BBS solution still produce precipitate (step 5).
11. Add 1 µg of internal control plasmid (pCMVβ) + 20 µL of target plasmid (1 µg/µL) + 450 µL of MQ sterile water and mix with 50 µL of CaCl₂ (2.5M) by vortexing.
12. Keep vortexing the above solution while dropwise adding 500 µL 2×BBS solution slowly within 20 sec.
13. Check if the precipitate exists using 1 µL of the mixture from step 12.
14. Add the solution dropwise to the dishes of cells and swirling gently to mix well.
15. Grow the cells for 48 hours.
16. Cell pellets are collected by trypsinization and centrifugation for expression and fatty acid analysis.

3.18 Serum metabolites

Enzymatic colorimetric methods were applied for quantitative measurements of glucose (ref. 1129010, Liner chemicals, Spain), triglycerides (ref. 1155010, Liner chemicals, Spain) and cholesterol (ref. 41022, Spinreact, Spain) with commercial kits. The principles are:

β-D-glucose + H₂O + O₂ = D-gluconate + H₂O₂, catalyzed by glucose oxidase

4-aminoantipyrine + phenol + H₂O₂ = quinoneimine + H₂O, catalyzed by peroxidase

Triglycerides + 3 H₂O = glycerol + 3 free fatty acids, catalyzed by lipoprotein lipase

glycerol + ATP = glycerol-3-phosphate + ADP, catalyzed by glycerolkinase

glycerol-3-phosphate + O₂ = dihydroxyacetone phosphate + H₂O₂, catalyzed by glycerophosphate oxidase

4-aminoantipyrine + phenol = quinoneimine + H₂O, catalyzed by peroxidase

Cholesterol esters + H₂O = cholesterol + fatty acids, catalyzed by cholesterol esterase

cholesterol + O₂ = 4-cholestenona + H₂O₂, cholesterol oxidase

4-aminoantipyrine + phenol = quinoneimine + H₂O, catalyzed by peroxidase

Absorbance of quinoneimine at 500 nm linearly correlated with concentration of the substrate at certain range. Thus, concentration of metabolites in serum are compared and calculated with standard references. The protocols for determining glucose, triglycerides and cholesterol were:

- Prepare standard samples for references. Standards and reagents were provided with the kits.

Table 3.18 Standard for determination of serum metabolites

No.	Standard* (200 mg/dL, μL)	H ₂ O (add to 5 μL)	Reagent (μL)
1	5	0	495
2	2.5	2.5	495
3	1.25	3.75	495
4	0.625	4.375	495
5	0	5	495

* Formula in the table is applied for preparing standard of serum glucose, triglycerides and cholesterol.

- Incubate the standards of glucose and cholesterol at room temperature for 10 min, and triglycerides for 15 min.
- Measure the absorbance of the standards at 500 nm (UV 1800, SHIMADZU, Japan) and create

standard curves.

- Mix 5 μL sample and 495 μL reagent, incubate and measure at 500 nm as the standards.
- (Optional) Dilute sample with distilled water when the absorbance of sample surpassed the values of standard no. 1.
- Calculate glucose, triglycerides, and cholesterol concentrations according to the standard curves.

3.19 Enzyme activity assays

Hepatic enzymes activities involved in glycolysis gluconeogenesis, PPP, Krebs cycle and amino acid metabolism were measured, including Pfkf, Fbp1, Pklr, G6pd, Pgd, Idh, Ogdh, Alt and Ast. Hepatic total soluble protein content was also measured for expressing specific enzyme activity (U/g total soluble protein).

For measuring the enzyme activity and protein content, liver crude extracts were prepared as indicated below. All the components for the measurement were kept cold on ice before incubation.

- Prepare homogenization buffer according to table 3.19.
- Weigh 50 to 100 mg liver samples previously that stored at $-80\text{ }^{\circ}\text{C}$.
- Add homogenization buffer to the sample (5:1 volume/weight, $\mu\text{L}/\text{mg}$).
- Homogenize the samples using Polytron-PT 10-35 (Kinematica, Switzerland) at position 3 for about 15 seconds.
- Centrifuge the samples at 10000 g and $4\text{ }^{\circ}\text{C}$ for 30 min.
- Transfer liver crude extracts (*i.e.*, the clear central layer) into new tubes for analysis.
- The specific enzyme activity assay and protein content were detected by Varioskan Lux multimode microplate reader (Ref VL0000D0, ThermoScientific, USA) (see following sections).

Table 3.19 Homogenization buffer for liver crude extract

Component	Final concentration	Reference
Tris-HCl, pH = 7.5	50 mM	T1503-1KG, Sigma, USA
EDTA	4 mM	ED2SS-500G, Sigma-Aldrich, USA
NaF	50 mM	106449, Merck, Germany
Sucrose	250 mM	107651, Merck, Germany
Phenylmethylsulfonyl fluoride	0.5 mM	P-7626, Sigma, USA
1.4-Dithiothritol	1 mM	10197777001, Roche, Germany

Stock solution consisted of Tris-HCl, EDTA and NaF was prepared 10 X before use. Sucrose, phenylmethylsulfonyl fluoride and 1.4-dithiothritol were freshly added to the diluted solution. Phenylmethylsulfonyl fluoride was dissolved in 1-propanol at 200 mM as stock.

3.19.1 Total soluble protein content

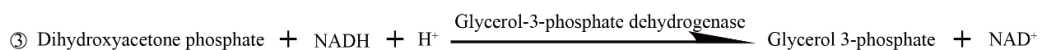
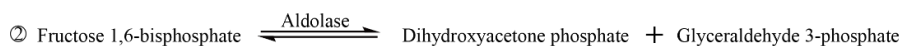
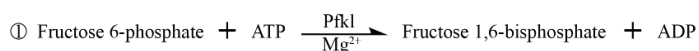
To calculate the specific enzyme activity, the total soluble protein was determined by the Bradford method (Kruger, 1996) using bovine serum albumin (BSA, No. A-6003, Sigma, USA) as standard reference. Total soluble protein content (TSPC) in each sample was measured and calculated according to the reference. The protocol was as indicated below:

- Prepare 2 mg/mL BSA aqueous solution (standard solution).
- Dilute the standard solution to a range of concentrations: 1 mg/mL, 0.5 mg/mL, 0.25 mg/mL, 0.125 mg/mL and 0.0625 mg/mL.
- Dilute Bradford Reagent (Cat. 5000006, Bio-Rad, Germany) 5 times with distilled water.
- Mix 196 μ L of diluted Bradford Reagent and 4 μ L of BSA solution in 96-well plate. Perform the analysis in duplicate.
- Incubate the mixture at 30 °C for 5 min and read the absorbance at 595 nm.
- Create a correlation curve from the serial concentration of BSA and corresponding absorbances.
- Dilute crude extracts 25-fold using distilled water.

- Mix 196 μL of diluted Bradford Reagent and 4 μL of the diluted crude extract in 96-well plate.
- Add the 0.5 mg/mL BSA solution in the same plate as positive control.
- Assay liver extracts by duplicate.
- Incubate the mixture at 30 $^{\circ}\text{C}$ for 5 min and read the absorbance at 595 nm.
- Calculate TSPC according to the standard reference.

3.19.2 Pfk1

Reactions designed for determining Pfk1 activity are described below. One unit of Pfk1 activity was considered to catalyse the conversion of 2 μmol of NADH to NAD^+ per minute.



To perform the determination, R1 and R2 mixtures (table 3.19.2) were separately prepared and the procedure was as follow:

- Add 4 μL of crude extract and 176 μL of R1 into 96-well plate (Cat.167008, Thermo Scientific, USA) and brief mix by multi-channel pipette.
- Incubate the mixture at 30 $^{\circ}\text{C}$ for 3 min.
- Add 20 μL R2 and briefly mix. Incubate the mixture at 30 $^{\circ}\text{C}$ for 1 min.
- Read the plate 15 seconds per round for 24 rounds at 340 nm.
- Beer Lambert law was used for calculating enzyme activity: $A = \epsilon bC$, where A = absorbance, ϵ = the molar extinction coefficient of NADH ($6220 \text{ mol}^{-1} \text{ cm}^{-1}$), b = pathlength of light = height

of 200 μL mixture in 96-well plate (0.56 cm) and C = concentration of the absorbing species (NADH, mol). Thus, PfkI activity = $2 \cdot \Delta C \cdot \text{min}^{-1} = 2 \cdot \Delta A \cdot \epsilon^{-1} \cdot b^{-1} \cdot \text{min}^{-1}$. PfkI specific activity (U/g) = PfkI activity / TSPC.

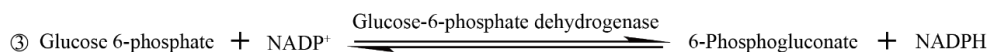
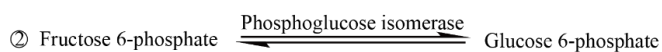
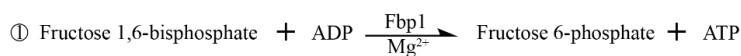
Table 3.19.2 Reaction system for measuring hepatic PfkI activity

Component	Concentration	Reference
R1		
Tris-HCl ¹	100 mM	T1503-1KG, Sigma, USA
MgCl ₂	5 mM	M2670-100G, Sigma-Aldrich, USA
KCl	50 mM	4936, Merck, Germany
NADH	0.15 mM	128015, Boehringer Mannheim, Germany
Ammonium sulfate	4 mM	1217, Merck, Germany
2-mercaptoethanol	12 mM	M3148-250ML, Sigma, USA
Fructose-6-phosphate	10 mM	F3627-1G, Sigma, USA
Glucose-6-phosphate	30 mM	G7879-5G, Sigma, USA
Aldolase ²	0.675 U / mL	A8811-1KU, Sigma, USA
Triosephosphate isomerase ²	5 U / mL	T2391-2MGM, Sigma, USA
Glycerol-3-phosphate dehydrogenase ²	2 U / mL	127752, Boehringer Mannheim, Germany
R2		
ATP	1 mM	A2383-1G, Sigma, USA

¹pH = 8.25. ²Mix the three enzymes and centrifuge at 10000 g and 4 °C for 2 min. Resuspend the enzyme pellet in Tris-HCl (pH = 8.25) buffer.

3.19.3 Fbp1

Reactions designed for determining Fbp1 activity are indicated below. One unit of Fbp1 activity catalyzes the conversion of 1 μmol of NADP⁺ to NADPH per minute.



To perform the determination, R1 mixture (table 3.19.3) was prepared, and the procedure was as follows.

Table 3.19.3 Reaction system for measuring hepatic Fbp1 activity

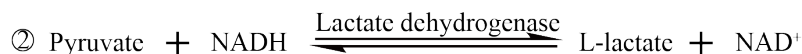
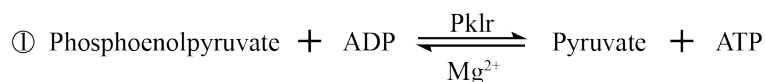
Component	Concentration	Reference
R1		
Imidazole ¹	85 mM	I0125-100G, Sigma, USA
MgCl ₂	5 mM	M2670-100G, Sigma-Aldrich, USA
NADP ⁺	0.5 mM	10128058001, Roche, USA
2-mercaptoethanol	12 mM	M3148-250ML, Sigma, USA
Fructose 1,6-phosphate	12 mM	104795, Boehringer Mannheim, Germany
Phosphoglucose isomerase ²	2.5 U / mL	F2668-4ML, Sigma, USA
Glucose-6-phosphate dehydrogenase ²	0.5 U / mL	G7877-1KU, Sigma, USA

¹pH = 7.70. ²Mix the two enzymes and use directly.

- Add 4 µL of crude extract and 196 µL R1 mixture into 96-well plate and brief mix by multi-channel pipette.
- Incubate the mixture at 30 °C for 30 second.
- Read the plate 15 seconds per round for 24 rounds at 340 nm.
- Beer Lambert law (see 3.19.2) was used for calculating Fbp1 activity: Fbp1 specific activity (U/g) = $\Delta A \cdot \epsilon^{-1} \cdot b^{-1} \cdot \text{min}^{-1} \cdot \text{TSPC}^{-1}$, where ϵ and b are the same as in section 3.19.2.

3.19.4 Pklr

Reactions designed for determining Pklr activity are indicated below. One unit of Pklr activity catalyzes the conversion of 1 µmole of NADH to NAD⁺ per minute.



To perform the determination, R1 and R2 mixtures (table 3.19.4) were separately prepared, and the procedure was as indicated below.

Table 3.19.4 Reaction system for measuring hepatic Pklr activity

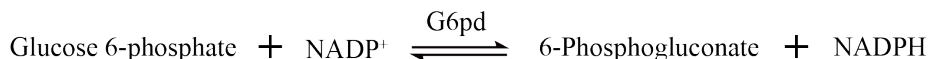
Component	Concentration	Reference
R1		
Glycylglycine ¹	70 mM	G1002-25G, Sigma, USA
MgCl ₂	10 mM	M2670-100G, Sigma-Aldrich, USA
KCl	100 mM	4936, Merck, Germany
NADH	0.15 mM	128015, Boehringer Mannheim, Germany
Phosphoenolpyruvate	2.8 mM	860077-1G, Sigma, USA
Lactate dehydrogenase ²	21 U / mL	L2500-25KU, Sigma, USA
R2		
ADP	2.5 mM	A2754-1G, Sigma, USA

¹pH = 7.40. ²Mix the three enzymes and centrifuge at 10000 g and 4 °C for 2 min. Resuspend enzyme pellet in glycylglycine (pH = 7.40) buffer.

- Add 2 µL of crude extract and 181.44 µL R1 mixture into 96-well plate (Cat.167008, Thermo Scientific, USA) and brief mix it by multi-channel pipette.
- Incubate the mixture at 30 °C for 5 min.
- Add 16.56 µL R2 mixture and brief mix. Incubate at 30 °C for 1 min.
- Read the plate 15 seconds per round for 24 rounds at 340 nm.
- Beer Lambert law was used for calculating enzyme activity: Pklr specific activity (U/g) = $\Delta A \cdot \epsilon^{-1} \cdot b^{-1} \cdot \text{min}^{-1} \cdot \text{TSPC}^{-1}$, where ϵ and b are the same as in section 3.19.2.

3.19.5 G6pd

Reactions designed for determining G6pd activity are below. One unit of G6pd activity catalyzes the conversion of 1 μmol of NADP^+ to NADPH per minute.



To perform the determination, R1 mixture (table 3.19.5) was prepared and the procedure was as described below.

Table 3.19.5 Reaction system for measuring hepatic G6pd activity

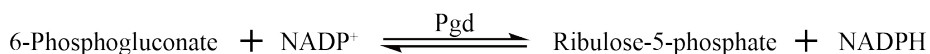
Component	Concentration	Reference
R1		
Imidazole ¹	77.5 mM	I0125-100G, Sigma, USA
MgCl ₂	5 mM	M2670-100G, Sigma-Aldrich, USA
NADP ⁺	1 mM	10128058001, Roche, USA
Glucose-6-phosphate	1 mM	G7879-5G, Sigma, USA

¹pH = 7.70.

- Add 4 μL of crude extract and 196 μL R1 mixture into 96-well plate and brief mix by multi-channel pipette.
- Incubate the mixture at 30 °C for 30 second.
- Read the plate 15 seconds per round for 24 rounds at 340 nm.
- Beer Lambert law was used for calculating G6pd activity: G6pd specific activity (U/g) = $\Delta A \cdot \epsilon^{-1} \cdot b^{-1} \cdot \text{min}^{-1} \cdot \text{TSPC}^{-1}$, where ϵ and b are the same as in section 3.19.5.

3.19.6 Pgd

Reactions designed for determining Pgd activity are below. One unit of Pgd activity was considered to catalyze the conversion of 1 μmol of NADPH to NADP^+ per minute.



To perform the determination, R1 mixture (table 3.19.6) was prepared, and the procedure was as described below.

Table 3.19.6 Reaction system for measuring hepatic Pgd activity

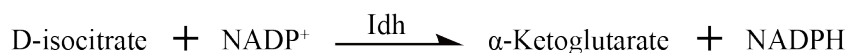
Component	Concentration	Reference
R1		
Imidazole ¹	82.7 mM	I0125-100G, Sigma, USA
MgCl ₂	3 mM	M2670-100G, Sigma-Aldrich, USA
NADP ⁺	0.5 mM	10128058001, Roche, USA
6-Phosphogluconate	2 mM	127604, Roche, USA

¹pH = 7.70.

- Add 4 μL of crude extract and 196 μL R1 mixture into 96-well plate and brief mix by multi-channel pipette.
- Incubate the mixture at 30 °C for 30 second.
- Read the plate 15 seconds per round for 24 rounds at 340 nm.
- Beer Lambert law was used for calculating Pgd activity: Pgd specific activity (U/g) = $\Delta A \cdot \epsilon^{-1} \cdot b^{-1} \cdot \text{min}^{-1} \cdot \text{TSPC}^{-1}$, where ϵ and b are the same as in section 3.19.2.

3.19.7 Idh

Reactions designed for determining Idh activity are below. One unit of Idh activity catalyzes the conversion of 1 μmol of NADP⁺ to NADPH per minute.



To perform the determination, R1 and R2 mixtures (table 3.19.7) were separately prepared and the procedure was as below.

- Add 4 μL of crude extract and 183 μL R1 mixture into 96-well plate and brief mix by multi-channel pipette.
- Incubate the mixture at 30 $^{\circ}\text{C}$ for 3 min.
- Add 13 μL R2 mixture and briefly mix. Incubate at 30 $^{\circ}\text{C}$ for 1 min.
- Read the plate 15 seconds per round for 24 rounds at 340 nm.

Beer Lambert law was used for calculating enzyme activity: Idh specific activity (U/g) = $\Delta A \cdot \epsilon^{-1} \cdot b^{-1} \cdot \text{min}^{-1} \cdot \text{TSPC}^{-1}$, where ϵ and b are the same as in section 3.19.2.

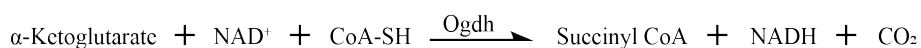
Table 3.19.7 Reaction system for measuring hepatic Idh activity

Component	Concentration	Reference
R1		
Triethanolamine ¹	80 mM	127426, Boehringer Mannheim, Germany
NaCl	42 mM	131659.1214, Panreac, Spain
DL-Isocitrate	3.7 mM	I1252-1G, Sigma, USA
MQ water ²	--	--
R2		
MnSO ₄	3.9 mM	131413, Panreac, Spain
NADP ⁺	0.325 mM	10128058001, Roche, USA

¹pH = 7.5. ²Add 12.6 μL MQ water per test.

3.19.8 Ogdh

Reactions designed for determining Ogdh activity are below. One unit of Ogdh activity catalyzes the conversion of 1 μmol of NAD⁺ to NADH per minute.



To perform the determination, R1 and R2 mixtures (table 3.19.8) were separately prepared and the procedure was as below.

- Add 4 μL of crude extract and 188 μL R1 mixture into 96-well plate and brief mix by multi-channel pipette.
- Incubate the mixture at 30 $^{\circ}\text{C}$ for 3 min.
- Add 8 μL R2 mixture and briefly mix. Incubate at 30 $^{\circ}\text{C}$ for 1 min.
- Read the plate 15 seconds per round for 24 rounds at 340 nm.

Beer Lambert law was used for calculating enzyme activity: Ogdh specific activity (U/g) = $\Delta\Lambda \cdot \epsilon^{-1} \cdot b^{-1} \cdot \text{min}^{-1} \cdot \text{TSPC}^{-1}$, where ϵ and b are the same as in section 3.19.2.

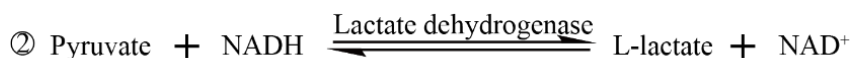
Table 3.19.8 Reaction system for measuring hepatic Ogdh activity

Component	Concentration	Reference
R1		
Phosphate buffer ¹	50 mM	106346.1000, Merck, Germany 122507.1211, Panreac, Spain
MgCl ₂	2 mM	M2670-100G, Sigma-Aldrich, USA
Thiamine pyrophosphate	0.6 mM	C8754-1G, Sigma, USA
NAD ⁺	2 mM	N7004-1G, Sigma, USA
α -ketoglutarate	10 mM	K1875-5G, Sigma, USA
EGTA ²	0.2 mM	E4378-10G, Sigma, USA
ADP	0.4 mM	A2754-1G, Sigma, USA
R2		
CoA-SH	0.12 mM	100493, MP Biomedicals, Germany

¹pH = 7.40. ²EGTA, ethylene glycol-bis(β -aminoethyl ether)-N,N,N',N'-tetraacetic acid.

3.19.9 Alt

Reactions designed for determining Alt activity are below. One unit of Alt activity catalyzes the conversion of 1 μmol of NADH to NAD⁺ per minute.



To perform the determination, R1 and R2 mixtures (table 3.19.9) were separately prepared and the procedure was as below.

- Dilute crude extract 20 times with MQ water.
- Add 5 μL of crude extract, 149.8 μL R1 mixture and 45.2 μL R2 mixture into 96-well plate and brief mix by multi-channel pipette.
- Incubate the mixture at 30 $^{\circ}\text{C}$ for 1 min.
- Read the plate 15 seconds per round for 24 rounds at 340 nm.

Beer Lambert law was used for calculating enzyme activity: Alt specific activity (U/g) = $\Delta A \cdot \epsilon^{-1} \cdot b^{-1} \cdot \text{min}^{-1} \cdot \text{TSPC}^{-1}$, where ϵ and b are the same as in section 3.19.2.

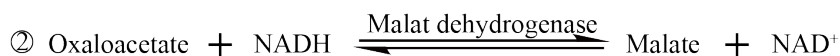
Table 3.19.9 Reaction system for measuring hepatic Alt activity

Component	Concentration	Reference
R1		
Tris-HCl ¹	112.5 mM	T1503-1KG, Sigma, USA
L-Alanine	562.5 mM	A7627, Sigma, USA
Lactate dehydrogenase ²	1012.5 U / L	L2500-25KU, Sigma, USA
MQ water ³	--	--
R2		
NADH	0.26 mM	128015, Boehringer Mannheim, Germany
α -Ketoglutarate	15 mM	K1875-5G, Sigma, USA

¹pH = 7.30. ²Centrifuge at 10000 g and 4 $^{\circ}\text{C}$ for 2 min. Resuspend enzyme pellet in Tris-HCl (pH = 7.30) buffer. ³Add 12.64 μL MQ water per test.

3.19.10 Ast

Reactions designed for determining Ast activity are below. One unit of Ast activity catalyzes the conversion of 1 μmol of NADH to NAD^+ per minute.



To perform the determination, R1 and R2 mixtures (table 3.19.10) were separately prepared and the procedure was as below.

- Dilute crude extract 20 times with MQ water.
- Add 5 μL of crude extract, 149.8 μL R1 mixture and 45.2 μL R2 mixture into 96-well plate and brief mix by multi-channel pipette.
- Incubate the mixture at 30 $^{\circ}\text{C}$ for 1 min.
- Read the plate 15 seconds per round for 24 rounds at 340 nm.

Beer Lambert law was used for calculating enzyme activity: Ast specific activity (U/g) = $\Delta A \cdot \epsilon^{-1} \cdot b^{-1} \cdot \text{min}^{-1} \cdot \text{TSPC}^{-1}$, where ϵ and b are the same as in section 3.19.2.

Table 3.19.10 Reaction system for measuring hepatic Ast activity

Component	Concentration	Reference
R1		
Tris-HCl ¹	90.75 mM	T1503-1KG, Sigma, USA
L-Aspartate	271.5 mM	A9256, Sigma, USA
Malat dehydrogenase ²	345 U / L	127256, Boehringer Mannheim, Germany
MQ water ³	--	--
R2		
NADH	0.26 mM	128015, Boehringer Mannheim, Germany
α -Ketoglutarate	15 mM	K1875-5G, Sigma, USA

¹pH = 7.80. ²Centrifuge at 10000 g and 4 $^{\circ}\text{C}$ for 2 min. Resuspend enzyme pellet in Tris-HCl (pH = 7.80) buffer. ³Add 76.20 μL MQ water per test.

3.20 Body composition

Fish whole-body compositions, including moisture, crude protein, crude fat, and ash, were

analyzed (Busacker et al., 1990)(Lucas, 1996).

Moisture content was measured as follows:

- Weigh empty glass dishes.
- Defrost the stored fish on ice for 1 hour.
- Wipe fish surface water, place the fish in dishes and weigh net fresh fish.
- Place the dishes + fish in oven (E50, Heraeus, Germany) at 85 °C.
- Cool the dish + fish in desiccator to room temperature for about 1 hour.
- Weighed the dish + fish every 24 hours until the last two weights are constant.
- Moisture content % = $100 \times [\text{fresh fish weight} - (\text{dry dish} + \text{fish weight} - \text{dry dish weight})] / \text{fresh fish weight}$.
- The dried samples were grinded into fine particles and stored in desiccator for further analysis of crude protein, crude fat, and ash contents.

Crude fat content was measured by the Soxhlet method as follows:

- Cellulose extraction thimbles (Ref. E022080, Part Dumas, France) were weighed after dried at 80 °C overnight.
- Weigh about 2000 mg of the grinded sample and load it into the thimble.
- Insert the sample-loaded thimble into a Soxhlet extractor.
- Add about 100 mL petroleum ether (Ref. 131315.0314, Panreac, Spain) into the 150-mL round bottom flask of Soxhlet extraction apparatus.
- Assemble the extraction units and seal interfaces with polytetrafluoroethylene film tape.

- Pass tap water through the condenser.
- Heat the round bottom flask with electric heating mantle (Mode XC-250, R.Espinar, Spain).
- Adjusted the heat source so that petroleum ether was condensed at about 5 drops / second.
- Conduct the extraction till consistent weight of the thimble with sample reached, which was about 3 hours according to pre-test result.
- Pull out the thimble and place it in fume hood for about 10 min and in oven at 80 °C for 30 min to evaporate petroleum ether and dry the thimble.
- Weigh the thimble.
- Crude fat content % = $100 \times [\text{weight of pre-extracted sample} - (\text{weight of post-extracted thimble with sample} - \text{thimble weight})] / \text{weight of pre-extracted sample}$.

Crude protein content was calculated using the protein-nitrogen conversion factor $(6.25) \times$ Nitrogen content, which was determined as follows:

- Place 1.00 to 2.00 mg of the sample into a tin capsule (D1002, Elemental Microanalysis, United Kingdom) and weigh using microbalance according to the manual (MX5, Mettler Toledo, USA).
- Weighed and determined each sample for triplicates.
- Package the capsule with sample into a tight cube and send to the CCiTUB for nitrogen content analysis (FlashEA 1112 NC Analyzer, ThermoFisher Scientific, USA).

Ash content was determined as follows:

- Mark ceramic porcelain boats (length \times width \times height, 77 \times 13 \times 8 mm) with pencil and heat in a muffle furnace (Hobersal 12PR/300, Hobersal, Spain) at 550 °C overnight.
- Keep the boats in the furnace for 3 hours after the heating.

- Take the boats out and cool the boats to room temperature in a desiccator for about 1 hour.
- Weigh the boats.
- Weigh about 1.00 g of fish sample and place into the boat.
- Insert the sample-loaded boat into the same furnace and heat at 550 °C overnight.
- Keep the boats in the furnace for 3 hours after the heating.
- Take the boats out and cool the boats to room temperature in a desiccator for 1 hour.
- Weigh the boat with sample.
- Ash content = $100 \times (\text{post-heat weight of boat with sample} - \text{boat weight}) / \text{pre-heat weight of sample}$.

3.21 Fatty acids extraction

Fatty acid of liver and muscle samples were extracted by the Bligh and Dyer method (Bligh and Dyer, 1959), as indicated below:

- Prepare fresh mixture of methanol (A3493-5000, Panreac, Spain) + chloroform (194002, MP Biomedicals, USA) at a volume ratio of 2:1 and place on ice.
- Dissolve 2M KOH (131515, Panreac, Spain) in methanol.
- Weigh about 50 mg liver or muscle sample from -80 °C and keep in glass tube (99445-10, Pyrex, USA) sitting on ice.
- Add 1.5 mL of the ice-cold methanol-chloroform mixture and vortex for 2 min.
- Add 0.5 mL ice-cold chloroform using glass pipette and vortex for 0.5 min.
- Add 0.5 mL ice-cold distilled water and vortex for 0.5 min.

- Centrifuge at 4 °C and 1000 g for 15 min.
- Transfer the middle layer into brown glass tubes and keep on ice.
- Volatilize solvent in the brown glass tubes completely under gentle N₂ flux (0.5 to 1 psi) using Sample Concentrator device.
- Add 0.5 mL n-hexane (104367.2500, Merck, Germany) and vortex to dissolve precipitate.
- Add 0.2 mL of the 2M KOH-methanol solution, vortex for 0.5 min, and incubate at room temperature for 3 min to trans-esterify fatty acids.
- Transfer the samples into a 1.5 ml Eppendorf tube and centrifuge at 2000 g and 4 °C for 5 min.
- Save the upper phase in gas chromatography vials (SV02-A20-100, Labbox, Spain) at -20 °C until gas chromatography analysis.

3.22 Gas chromatography

HepG2 cells and *S. aurata* liver and muscle samples were applied for fatty acids composition analysis by gas chromatography with flame ionization detection (GC-2025, Shimadzu, Japan) equipped with capillary column BPX70, 30 m × 0.25 mm × 0.25 μm (Trajan Scientific and Medical, Australia). The oven temperature was held 1 min at 60 °C and then raised to 260 °C by 6 °C/min. Injector (AOC-20i, Shimadzu, Japan) and detector temperatures were set at 260 °C and 280 °C, respectively. One microliter of sample was injected with helium as carrier gas and split ratio 1:20. Supelco 37 Component FAME Mix (CRM47885, Sigma-Aldrich, USA) was introduced as references for identifying fatty acids. Gas chromatography data was analyzed by OpenchromV13 and expressed as percentage of content.

3.23 Chitosan-TPP-plasmid nanoparticles

3.23.1 Preparation of Chitosan-TPP-plasmid nanoparticles

Chitosan-TPP nanoparticles complexed with pSG5 (empty vector), pSG5-FAT-1, or pSG5-FAT-2 were prepared by the ionic gelation method. Chitosan solution (2 mg/mL) was prepared as follows:

MATERIALS AND METHODS

- Prepare 500 mL of 0.1M glacial acetic acid: add 2859.5 μ L glacial acetic acid (141008, Panreac, Spain) into 400 mL MQ water, mix it well and fix the final volume to 500 mL.
- Prepare 100 mL of 0.1M sodium acetate: add 1360.8 mg (HR-150AZ, A&D, Japan) sodium acetate 3-hydrate (Code 478137, Analyticals, Italy) into 80 mL MQ water. Stirring to mix it and fix the final volume to 100 mL.
- Add 1 g chitosan (Ref. 448869-50G, Sigma, USA) into a mixture composed of 423.50 mL of the glacial acetic acid and 76.50 mL of the sodium acetate solutions. Magnetic stirring at 1000 rpm for 4.5 hours to dissolve chitosan (MR 3000, Heidolph, Germany). Filter the dissolved solution through qualitative analysis filter paper (ref. 1300/80, Filter-Lab, Spain).

For preparing TPP solution (0.84 mg/mL), dissolve 420 mg TPP with 400 mL MQ water, mix and fix the final volume to 500 mL. Filter the solution through qualitative analysis filter paper.

Mannitol solution (2 % w / v) was prepared by dissolving 10.0 g mannitol (ref. M4125-500g, Sigma, USA) into 400 mL MQ water. Mix and fix the final volume to 500 mL.

Chitosan-TPP-plasmid nanoparticles were prepared with the above solutions as follow:

- Mix 4000.0 μ L TPP solution and 1000.0 μ L plasmid (1mg/mL) through a brief vortex.
- Add 10000.0 μ L chitosan solution in a 25 mL breaker and stirring the solution at 800 rpm with a 2.5 \times 0.5 cm fluoropolymer coating stirrer.
- Dropwise the TPP-plasmid mixture into chitosan solution using Pasteur pipette at about 3 sec/drop (about 6 min in total).
- Keep stirring 10 min more for gelation.
- Centrifuge the above mixture at 36000 g and 15 °C for 20 mins (Model L-90K, Beckman Coulter, USA).
- Discard supernatant and wash the precipitate (nanoparticles) twice with 1 mL MQ water (avoid

directly onto the white precipitate).

- Resuspended the nanoparticles with 2 mL of the mannitol solution by pipetting.
- Freeze-drying the nanoparticles by lyophilization (Cryodos 50, IMA-Telstar, Spain) at -47 °C for 48 hours.
- Store the prepared nanoparticles at 4 °C until use.
- Resuspended the nanoparticles with 0.9% saline solution before *in vivo* experiment.

3.23.2 Characterization of nanoparticle size and zeta potential

Solutions taken from the end of the gelation process were used for nanoparticles characterization by dynamic light scattering and laser Doppler electrophoresis using Malvern Instrument (Malvern Panalytical, UK) as follows:

- Pipette 1 mL of the solution into disposable cuvettes and insert the cuvettes into the instruments. Folded capillary zeta cells were used for determining zeta potential.
- The Standard Operating Procedures of the instrument were taken for particle size and zeta potential measurement.
- Dilute the samples with MQ water to optimal concentration, if necessary, for particle size and zeta potential characterization.

3.24 Statistical analysis

To identify significant differences between treatments, the SPSS Version 25 software (IBM, Armonk, NY, USA) was used to submit experimental data to unpaired Student's t-test (2 groups) and one-way analysis of variance followed by the Duncan post-hoc test (> 2 groups). Statistical significance was considered when $P < 0.05$.

4 RESULTS

4.1 Construction of pSG5-FAT-1

4.1.1 Fish codon-optimized sequence of FAT-1

Fish codon-optimized FAT-1 cDNA sequence (GenBank No. ON374024) was designed using GeneArt Instant Designer (ThermoFisher Scientific, USA) and optimized according to *Danio rerio* codon usage. The synthetic FAT-1 is composed by 1231 base pair (bp) including an upstream *EcoRI* restriction endonuclease site, a Kozak sequence at the translation initiation site and a downstream *KpnI* restriction endonuclease site (figure 4.1.1). The deduced amino acid sequence of fish codon-optimized FAT-1 is 402 amino acids, which exhibit 100 % homology wild type *C. elegans* FAT-1 (figure 4.1.1).

```

gggaattcgccacc atg gtc gct cac agc agc gag gga ctt agc gct aca gct cct gtg aca
      .....M V A H S S E G L S A T A P V T
ggc gga gat gtg ctg gtg gac gct aga gct agc ctg gaa gag aaa gag gct cct cgc gac
G G D V L V D A R A S L E E K E A P R D
gtc aac gcc aac acc aag cag gct acc acc gag gaa cct aga atc cag ctg cct acc gtg
V N A N T K Q A T T E P R I Q L P T V
gac gcc ttc aga agg gct atc cct gct cac tgt ttc gag aga gat ctg gtc aag agc atc
D A F R R A I P A H C F E R D L V K S I
aga tac ctg gtg cag gac ttc gcc gct ctg acc atc ctg tac ttc gcc ctg cct gcc ttc
R Y L V Q D F A A L T I L Y F A L P A F
gag tac ttc gga ctg ttc gga tac ctc gtg tgg aac atc ttc atg gga gtg ttc gga ttc
E Y F G L F G Y L V W N I F M G V F G F
gcc ctg ttc gtc gtg gga cac gac tgt ctg cac gga agc ttc agc gac aac cag aac ctg
A L F V V G H D C L H G S F S D N Q N L
aac gac ttc atc gcc cat atc gct ttc agc cct ctg ttc agc cct tac ttc cct tgg cag
N D F I G H I A F S P L F S P Y F P W Q
aaa agc cac aag ctg cac cac gcc ttc acc aac cac atc gac aag gac cac gga cac gtg
K S H K L H H A F T N H I D K D H G H V
tgg atc cag gac aag gac tgg gaa gcc atg cct agc tgg aaa aga tgg ttc aac ccc att
W I Q D K D W E A M P S W K R W F N P I
cct ttc agc gcc tgg ctg aag tgg ttc cct gtg tac acc ctg ttt gga ttc tgt gac gga
P F S G W L K W F P V Y T L F G F C D G
agc cac ttc tgg cct tac agc agc ctg ttc gtg cgc aac tct gag cgc gtg cag tgt gtg
S H F W P Y S S L F V R N S E R V Q C V
atc agc gga atc tgc tgc tgc gtg tgc gcc tat atc gcc ctg aca atc gcc gga agc tac
I S G I C C C V C A Y I A L T I A G S Y
agc aac tgg ttc tgg tac tac tgg gtg ccc ctg agc ttc ttc gcc ctg atg ctg gtc atc
S N W F W Y Y W V P L S F F G L M L V I
gtg acc tac ctg cag cac gtg gac gat gtg gct gag gtg tac gag gct gac gag tgg tct
V T Y L Q H V D D V A E V Y E A D E W S
ttt gtg cgc gga cag acc cag acc atc gac cgc tat tat gga ctg gga ctc gac acc acc
F V R G Q T Q T I D R Y Y G L G L D T T
atg cac cac atc acc gac gga cat gtg gcc cac cac ttt ttc aac aag atc cct cac tac
M H H I T D G H V A H H F F N K I P H Y
cac ctg atc gag gcc acc gag gcc gtg aag aaa gtg ctg gaa cct ctg agc gac acc cag
H L I E A T E G V K K V L E P L S D T Q
tac gga tac aag agc caa gtg aac tac gac ttc ttc gcc aga ttc ctg tgg ttc aac tac
Y G Y K S Q V N Y D F F A R F L W F N Y
aag ctg gac tac ctg gtc cac aag acc gcc gga atc atg cag ttc aga acc aca ctg gaa
K L D Y L V H K T A G I M Q F R T T L E
gaa aag gcg aag gcc aag tga ggtaccgg
E K A K A K -

```

Figure 4.1.1 Fish codon-optimized *C. elegans* FAT-1 cDNA sequence. Dotted and solid underlined letters indicate restriction endonuclease sites and Kozak sequence, respectively. Lower case letters between restriction endonuclease sites correspond to the coding sequence of FAT-1. Uppercase letters show the deduced amino acid sequence of FAT-1, where “-” indicates the stop codon.

4.1.2 Enzyme digestion of pMA-T-FAT-1 and pSG5

In order to obtain the expression construct pSG5-FAT-1, both pMA-T-FAT-1 and pSG5 were digested with *EcoRI* and *KpnI*. Gel electrophoresis results showed that pMA-T-FAT-1 digestion resulted in two bands with expected sizes, around 3609 bp (pMA-T) and 1231 bp (FAT-1 cDNA) (figure 4.1.2A). The digested pSG5 showed a major band of about 4086 bp (figure 4.1.2B). Digestion products corresponding to pSG5 and fish codon-optimized FAT-1 cDNA were further ligated in presence of T₄ DNA ligase (see section 3.9).

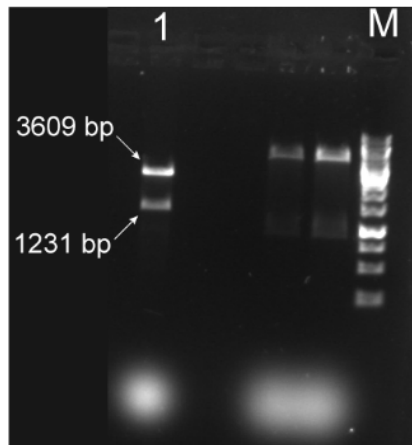


Figure 4.1.2A Gel electrophoresis of pMA-T-FAT-1 digested with *EcoRI* and *KpnI*. M, 1kb gene ruler; 1, pMA-T-FAT-1.

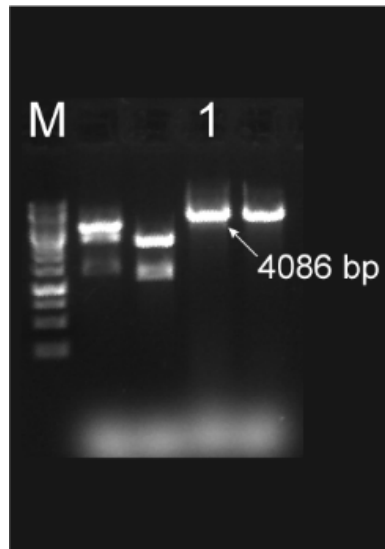


Figure 4.1.2B Gel electrophoresis of pSG5 digested with *EcoRI* and *KpnI*. M, 1kb gene ruler; 1, pSG5.

4.1.3 PCR colony screening of pSG5-FAT-1

Ligation products were used to transform competent DH5 α *E. coli* cells (see section 3.6), which were subsequently analyzed by PCR colony screening and showed 17 positive and 11 negative pSG5-FAT-1 colonies (figure 4.1.3). The expected size for positive and negative bands was 1656 bp and 425 bp, respectively (figure 4.1.3).

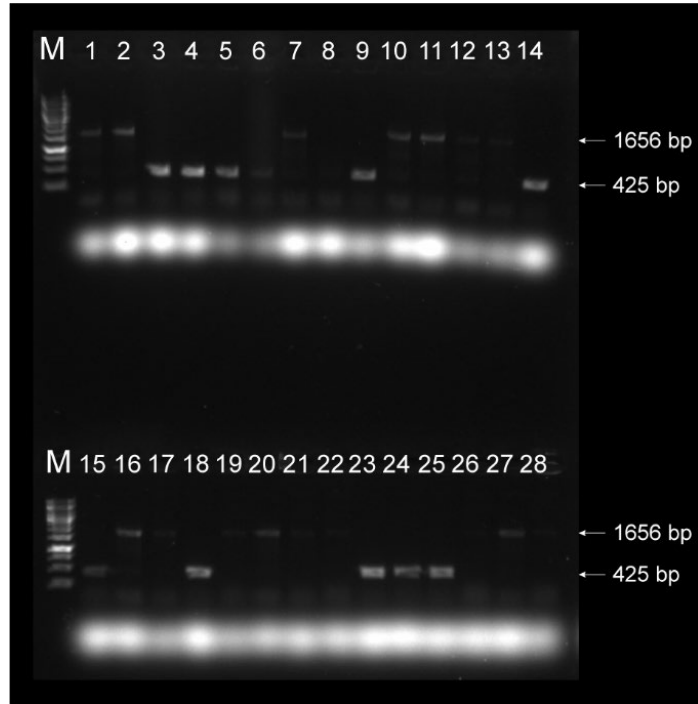


Figure 4.1.3 PCR screening of pSG5-FAT-1. Line with amplification bands of about 1656 bp were apparent positive colonies and those with 425 bp bands were considered as negative colonies. M, 1kb gene ruler; 1-28, colony number.

4.1.4 Sequencing pSG5-FAT-1

Apparent positive colonies no. 2, 11, 16, 20, and 27 were selected for sequencing (figure 4.1.3) using T7 and pSG5rev as forward and reverse primers, respectively. Fully sequence on both sides confirmed colonies no. 20 and 27 having no mutations and being fully consistent with the designed sequence. Figures 4.1.4A and 4.1.4B show representative electropherograms resulting from pSG5-FAT-1 sequencing with T7 and pSG5rev primers, respectively.

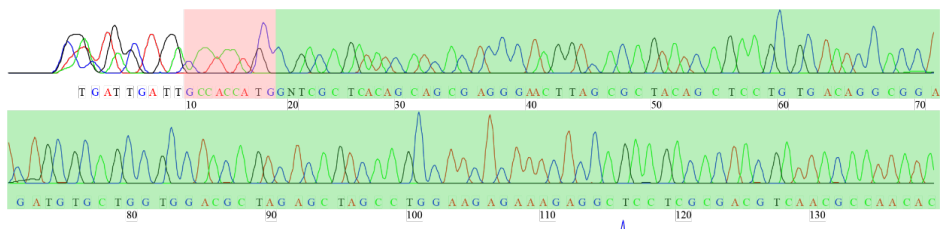


Figure 4.1.4A pSG5-FAT-1 sequencing with T7 forward primer. Pink box, Kozak sequence;

Green box, fish codon-optimized *C. elegans* FAT-1 cDNA (partial).

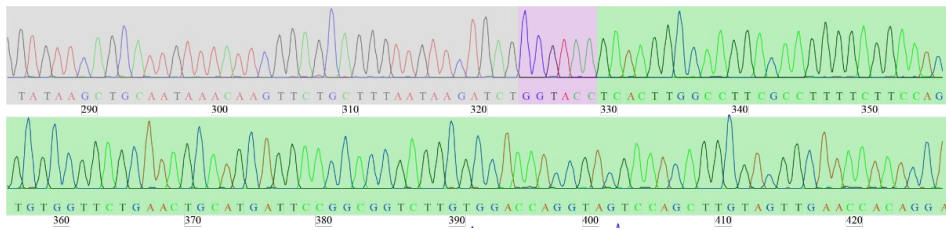


Figure 4.1.4B pSG5-FAT-1 sequencing with pSG5rev reverse primer. Gray box, pSG5 (partial); Purple box, *KpnI* restriction site; Green box, fish codon-optimized *C. elegans* FAT-1 cDNA (partial).

4.2 Construction of pSG5-FAT-2

4.2.1 Fish codon-optimized sequence of FAT-2

Fish codon-optimized sequence of FAT-2 cDNA sequence (GenBank No. ON374025) was designed using GeneArt Instant Designer (ThermoFisher, USA) and optimized according to *Danio rerio* codon usage. Fish codon-optimized FAT-2 consists of 1151 bp including upstream *EcoRI* restriction endonuclease site, Kozak sequence and downstream *BamHI* restriction endonuclease site (figure 4.2.1). The deduced amino acid sequence of fish codon-optimized FAT-2 is composed by 376 amino acids and has 100 % homology with wild type *C. elegans* FAT-2 (figure 4.2.1).

```

gggaattcgcacc atg aca atc gcc acc aaa gtg aac acc aac aag aag gac ctg gac acc
      M T I A T K V N T N K K D L D T
atc aag gtg cca gag ctg cct tct gtg gcc gct gtg aaa gct gct atc cct gag cac tgc
I K V P E L P S V A A V K A A I P E H C
ttc gtg aag gac cct ctg acc agc atc agc tac ctg atc aag gac tac gtg ctg ctg gcc
F V K D P L T S I S Y L I K D Y V L L A
gga ctg tac ttc gcc gtg cct tac atc gag cac tac ctc gga tgg atc gga ctg ctc gga
G L Y F A V P Y I E H Y L G W I G L L G
tgg tac tgg gcc atg gga atc gtg gga agc gct ctg ttc tgt gtg gga cac gac tgt gga
W Y W A M G I V G S A L F C V G H D C G
cac gga agc ttc agc gac tac gag tgg ctg aac gac ctg tgc gga cac ctg gct cac gct
H G S F S D Y E W L N D L C G H L A H A
cct atc ctg gct cca ttc tgg cct tgg cag aaa agc cac aga cag cac cac cag tac acc
P I L A P F W P W Q K S H R Q H Q Y T
agc cac gtg gaa aag gac aag gga cac cct tgg gtc acc gaa gag gac tac aac aac aga
S H V E K D K G H P W V T E E D Y N N R
acc gcc atc gag aaa tac ttc gct gtg atc cct atc agc gga tgg ctg aga tgg aac cct
T A I E K Y F A V I P I S G W L R W N P
atc tac acc atc gtg gga ctg cct gac gga agc cac ttt tgg cct tgg agc aga ctg ttc
I Y T I V G L P D G S H F W P W S R L F
gag aca acc gag gac aga gtg aag tgc gcc gtt agc gga gtg gct tgc gcc atc tgc gcc
E T T E D R V K C A V S G V A C A I C A
tat atc gct ttc gtg ctg tgc gac tac agc gtg tac aca ttc gtg aag tac tac tac atc
Y I A F V L C D Y S V Y T F V K Y Y Y I
ccg ctg ctg ttc cag gga ctg atc ctg gtc atc atc acc tac ctg cag cac cag aac gag
P L L F Q G L I L V I I T Y L Q H Q N E
gac atc gag gtg tac gag gct gac gag tgg gga ttt gtg cgc gga cag acc cag acc atc
D I E V Y E A D E W G F V R G Q T Q T I
gac aga cat tgg gga ttc gga ctg gac aac atc atc acc aac atc acc aac gga cac gtg
D R H W G F G L D N I M H N I T N G H V
gcc cac cac ttt ttc ttc aca aaa atc ccg cac tac cat ctg ctg gaa gct acc cct gcc
A H H F F F T K I P H Y H L L E A T P A
atc aag aag gct ctg gaa cct ctg aag gac acc cag tac gga tac aag aga gaa gtg aac
I K K A L E P L K D T Q Y G Y K R E V N
tac aac tgg ttc ttc aag tac ctg cac tac aac gtg acc ctg gac tac ctg aca cac aag
Y N W F F K Y L H Y N V T L D Y L T H K
gcc aag ggc gtg ctg cag tac aga agc gga gtc gag gcc gcc aag gct aag aaa gct cag
A K G V L Q Y R S G V E A A K A K K A Q
tga ggatccgg
-

```

Figure 4.2.1 Fish codon-optimized *C. elegans* FAT-2 cDNA sequence. Dotted and solid underlined letters indicate restriction endonuclease sites and Kozak sequence, respectively. Lower case letters between restriction endonuclease sites correspond to the coding sequence of FAT-2. Uppercase letters show the deduced amino acid sequence of FAT-2, where “-” indicates the stop codon.

4.2.2 Enzyme digestion of pMA-T-FAT-2 and pSG5

To construct pSG5-FAT-2, both pMA-T-FAT-2 and pSG5 were double digested with *Eco*RI and *Bam*HI. Gel electrophoresis of digested products resulted in the apparition of two bands around 3527 bp and 1151 bp for pMA-T-FAT-2 (figure 4.2.2A), and a major band of around 4104 bp for pSG5 (figure 4.2.2B). Digestion products corresponding to pSG5 and fish codon-optimized FAT-2 cDNA were further ligated in presence of T₄ DNA ligase (see section 3.9).

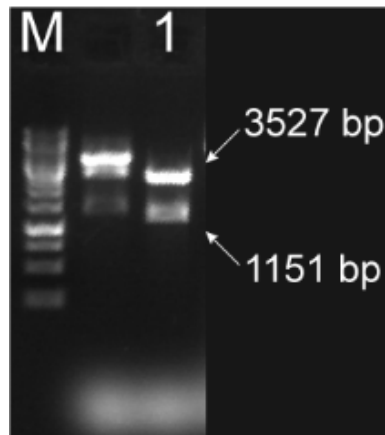


Figure 4.2.2A Gel electrophoresis of pMA-T-FAT-2 digested with *EcoRI* and *BamHI*. M, 1kb gene ruler; 1, pMA-T-FAT-2.

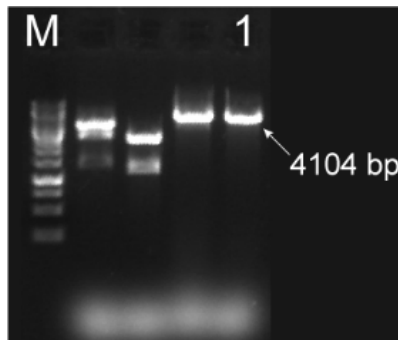


Figure 4.2.2B Gel electrophoresis of pSG5 digested by *EcoRI* and *BamHI*. M, 1kb gene ruler; 1, pSG5.

4.2.3 PCR colony screening of pSG5-FAT-2

Competent DH5 α *E. coli* cells were transformed with the ligation products following the procedure described in section section 3.6 and subsequently analyzed by PCR colony screening. PCR screening showed 12 apparent positive and 11 negative pSG5-FAT-2 colonies (figure 4.2.3). The expected sizes of the positive and negative bands were 1556 bp and 425 bp, respectively (figure 4.2.3).

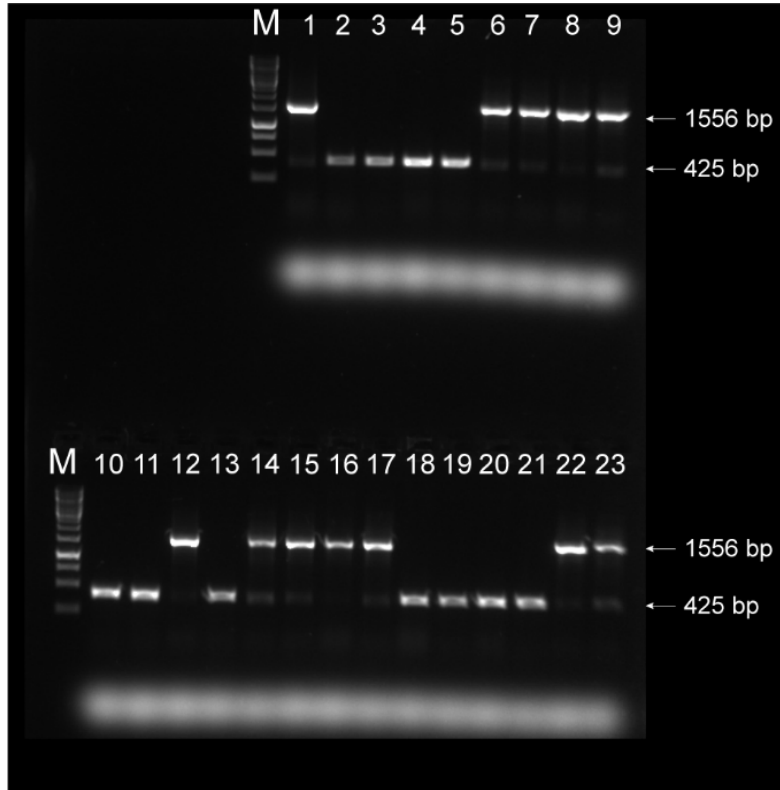


Figure 4.2.3 PCR screening of pSG5-FAT-2. Lines with a band of about 1556 bp were apparent positive colonies, while lines with a 425 bp band were considered as negative colonies. M, 1kb gene ruler; 1-23, colony number.

4.2.4 Sequencing pSG5-FAT-2

Apparent positive colonies no. 6 and 7 (figure 4.2.3) were selected for further sequencing using T7 and pSG5rev as forward and reverse primers, respectively. Fully sequence on both sides confirmed colonies no. 6 and 7 having no mutations and being totally consistent with the designed sequence. Figures 4.2.4A and 4.2.4B show representative electropherograms resulting from pSG5-FAT-2 sequencing with T7 and pSG5rev primers, respectively.

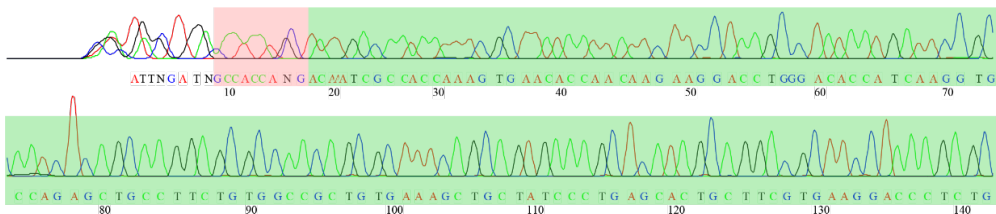


Figure 4.2.4A pSG5-FAT-2 sequencing with T7 forward primer. Pink box, Kozak sequence;

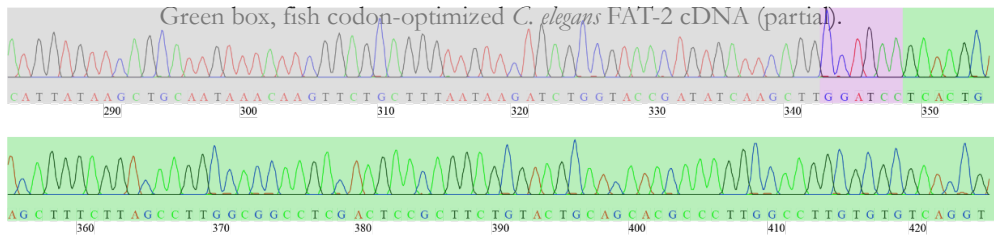


Figure 4.2.4B pSG5-FAT-2 sequencing with pSG5rev reverse primer. Gray box, pSG5 (partial); Purple box, *Bam*HI restriction site; Green box, fish codon-optimized *C. elegans* FAT-2 cDNA (partial).

4.3 Characterization of chitosan-TPP-plasmid nanoparticles

For hepatic delivery and expression of foreign proteins FAT-1 and FAT-2 in *Sparus aurata*, chitosan-TPP nanoparticles nude or complexed with DNA (empty pSG5, pSG5-FAT-1 or pSG5-FAT-2) were obtained following the ionic gelation method (see section 3.23). The resulting nanoparticles were characterized for particle size and zeta-potential (table 4.3). The results showed that the size of chitosan-TPP nanoparticles were 214.6 ± 20.2 nm and zeta potential was 37.6 ± 0.6 mV. Chitosan-TPP-DNA nanoparticles were 262.7 ± 74.0 nm and 12.0 ± 0.8 mV. The zeta-potential of chitosan-TPP-DNA was significantly lower than chitosan-TPP nanoparticles.

Table 4.3 Characteristics of chitosan-TPP and chitosan-TPP-DNA nanoparticles

Plasmid	Z-average \pm SEM (nm)	Zeta Potential (mV) \pm SEM
Chitosan-TPP	214.6 ± 20.2	37.6 ± 0.6
Chitosan-TPP-DNA	262.7 ± 74.0	$12.0^* \pm 0.8$

Z-average was measured by dynamic light scattering. Zeta potential values were determined by laser-Doppler anemometry. Data represents the mean \pm standard error of the mean (SEM), $n = 3$ measurements. Asterisk indicates significant differences between chitosan-TPP and chitosan-TPP-DNA ($P < 0.05$).

4.4 Effect of *in vitro* expression of pSG5-FAT-1 and pSG5-FAT-2

In order to validate functionality of pSG5-FAT-1 and pSG5-FAT-2 constructs previous to

chitosan-TPP encapsulation and performing *in vivo* experiments, both expression constructs were used to transfect liver-derived cells (HepG2) and analyze FAT-1 and FAT-2 mRNA levels as well as changes in fatty acid profile. To this end, HepG2 cells seeded in 100 mm culture dishes were transiently transfected with pSG5, pSG5-FAT-1, pSG5-FAT-2, and pSG5-FAT-1 + pSG5-FAT-2 plasmids (20 µg/dish), respectively, using the DNA calcium phosphate co-precipitation method.

4.4.1 Transient transfection with pSG5-FAT-1 and pSG5-FAT-2 increases FAT-1 and FAT-2 mRNA levels in HepG2

Forty-eight hours following transfection, cells were lysed, total RNA was isolated and submitted to RT-qPCR using primer pairs YW2001/YW2002, YW2003/YW2004 and JDRTpcmvbS/JDRTpcmvbAS (see section 3.14 and 3.15) for amplifying FAT-1, FAT-2 and pCMVβ, respectively, and normalized to pCMVβ mRNA levels. When compared with control cells transfected with empty pSG5, transfection of pSG5-FAT-1 and pSG5-FAT-2 significantly increased the mRNA levels of FAT-1 and FAT-2, respectively (figure 4.4.1). Compared to controls, cells transfected with pSG5-FAT-1 and pSG5-FAT-1 + pSG5-FAT-2 upregulated 2121.1 and 2430.1-fold FAT-1 mRNA levels, respectively. Similarly, FAT-2 mRNA abundance in the cells transfected with pSG5-FAT-2 and pSG5-FAT-1 + pSG5-FAT-2 was 4287.9 and 2454.2-fold higher than in control cells, respectively.

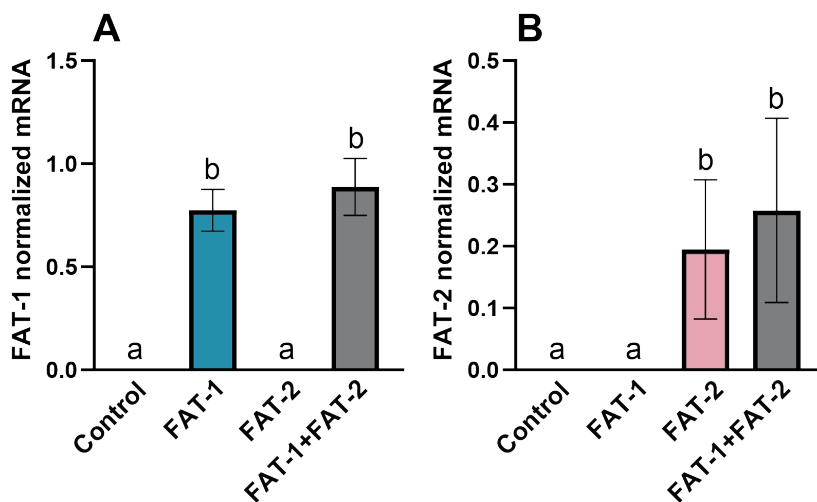


Figure 4.4.1 Effect of transient transfection with pSG5 (control), pSG5-FAT-1, pSG5-FAT-2, and pSG5-FAT-1 + pSG5-FAT-2 plasmids on the mRNA levels of fish codon-optimized FAT-

1 and FAT-2 in HepG2 cells. Forty-eight hours following transfection, FAT-1 and FAT-2 expression was determined by RT-qPCR and normalized to pCMV β mRNA levels. Expression levels are represented as mean \pm SEM ($n = 3$). Homogeneous subsets for the treatment are shown with different letters ($P < 0.05$).

4.4.2 Transient transfection with pSG5-FAT-1 and pSG5-FAT-2 affects the fatty acid profile in HepG2 cells

In addition to verify FAT-1 and FAT-2 expression, further confirmation of the functionality of the two enzymes was performed in HepG2 through analysis of changes in the fatty acid profile. Forty-eight hours following transfection with pSG5-FAT-1 and pSG5-FAT-2, HepG2 cells were collected to determine the fatty acid profile by gas chromatography (see section 3.22).

As shown in table 4.4.2, among 16 fatty acids identified in the present study, treatment with FAT-1 + FAT-2 significantly increased 1.4, 1.2, 1.1, 3.5, 1.6, 2.6, 1.6 and 1.2-fold the percentage of SA (18:0), OA (18:1 n -9c), LA (18:2 n -6c), ARA (20:4 n -6), PUFA, n -3 fatty acids, n -6 fatty acids and n -9 fatty acids, respectively. The treatment also decreased PA (16:0, to 94.4% of control values) and SFA (to 90.9%). A 2.2-fold increase of ARA (20:4 n -6) was also observed in both FAT-1 and FAT-2 treated cells. In addition, cells treated with FAT-1 alone showed a 1.1-fold increase of n -9 fatty acids. Although not significantly different, a 2.8- and 3.8-fold increase of DHA was observed after transfecting FAT-1 and FAT-1 + FAT-2, respectively.

Table 4.4.2 Effect of pSG5 (control), pSG5-FAT-1, pSG5-FAT-2, and pSG5-FAT-1 + pSG5-FAT-2 plasmids on the fatty acid profile of HepG2 cells.

Fatty acid	Control	FAT-1	FAT-2	FAT-1 + FAT-2
14:0	10.49 \pm 0.74	10 \pm 0.4	9.82 \pm 1.18	8.04 \pm 0.13
16:0	47.43 ^b \pm 0.36	46.34 ^{ab} \pm 0.43	46.29 ^{ab} \pm 1.19	44.77 ^a \pm 0.44
17:0	0.31 \pm 0.3	0.02 \pm 0.01	0 \pm 0	0.11 \pm 0.05
18:0	4.9 ^a \pm 0.16	5.57 ^a \pm 0.42	5.57 ^a \pm 0.45	7 ^b \pm 0.22
21:0	0.01 \pm 0	0.02 \pm 0.01	0.01 \pm 0	0.03 \pm 0.02
15:1 n -5	0 \pm 0	0.01 \pm 0	0 \pm 0	0.01 \pm 0
16:1 n -7	22.8 \pm 0.73	21.94 \pm 0.23	22.07 \pm 0.34	22.07 \pm 0.08
17:1 n -7	0.64 \pm 0.04	0.68 \pm 0.04	0.75 \pm 0.13	0.8 \pm 0.03
18:1 n -9c	9.8 ^a \pm 0.12	10.93 ^{ab} \pm 0.37	10.78 ^{ab} \pm 0.36	11.27 ^b \pm 0.28

RESULTS

20:1 n -9	0.05±0.01	0.12±0.04	0.1±0.05	0.15±0.01
18:2 n -6c	1.86 ^a ±0.08	1.91 ^a ±0.06	1.87 ^a ±0.03	2.11 ^b ±0.02
18:3 n -6	0.95±0.04	0.83±0.21	1.17±0.2	1.09±0.03
20:3 n -3	0.04±0.02	0.06±0.01	0.07±0.03	0.12±0.04
20:4 n -6	0.65 ^a ±0.16	1.45 ^b ±0.33	1.4 ^b ±0.22	2.25 ^c ±0.1
20:5 n -3	0.02±0.01	0.02±0.01	0.01±0	0.02±0
22:6 n -3	0.04±0.04	0.11±0.05	0.09±0.02	0.15±0.03
SFA	63.13 ^b ±0.8	61.95 ^b ±0.32	61.68 ^b ±0.5	59.95 ^a ±0.35
MUFA	33.29±0.64	33.68±0.27	33.71±0.83	34.3±0.26
PUFA	3.57 ^a ±0.2	4.37 ^a ±0.49	4.62 ^{ab} ±0.48	5.74 ^b ±0.09
n -3	0.11 ^a ±0.01	0.19 ^{ab} ±0.05	0.18 ^{ab} ±0.04	0.29 ^b ±0.05
n -6	3.46 ^a ±0.21	4.18 ^b ±0.45	4.44 ^{ab} ±0.44	5.45 ^b ±0.07
n -9	9.85 ^a ±0.13	11.05 ^b ±0.41	10.89 ^{ab} ±0.4	11.42 ^b ±0.29
n -6/ n -3	31.43±3.1	23.95±3.58	27.86±4.99	20.55±4.47

Data are expressed as percentage of total fatty acids and represented as mean ± SEM ($n = 3$). Different superscript letters indicate significant differences between groups ($P < 0.05$).

4.5 Short-term effects of expressing fish codon-optimized *C. elegans* FAT-1 and FAT-2 in *S. aurata*

4.5.1 Hepatic expression of exogenous enzymes, FAT-1 and FAT-2

Following successful verification of the functionality of pSG5-FAT-1 and pSG5-FAT-2 *in vitro*, the present study further introduced the two fish codon-optimized enzymes into *S. aurata* to study their potential for boosting n -3 LC-PUFA synthesis *in vivo*. Chitosan-TPP nanoparticles complexed with pSG5-FAT-1 and pSG5-FAT-2 were obtained for delivering the plasmids. This methodology was expected to facilitate the release *in vivo* and the function of the two enzymes in the liver of treated fish. Seventy-two hours after intraperitoneal administration of chitosan-TPP-DNA nanoparticles, the mRNA abundance of fish codon-optimized FAT-1 and FAT-2 was determined by RT-qPCR in *S. aurata* liver.

The results showed that when compared with control fish that received chitosan-TPP-pSG5 nanoparticles, chitosan-TPP complexed with pSG5-FAT-1 and pSG5-FAT-2 significantly induced the hepatic mRNA levels of FAT-1 and FAT-2, respectively (figure 4.5.1). In particular, the mRNA abundance of FAT-1 in fish treated with FAT-1 and FAT-1 + FAT-2 nanoparticles was 16.5 and 27.9-fold higher, respectively, than in control fish (figure 4.5.1A). Similarly, the mRNA levels of FAT-2 in

fish treated with FAT-2 and FAT-1 + FAT-2 nanoparticles were 21.2 and 16.4-fold higher than in control fish (figure 4.5.1B).

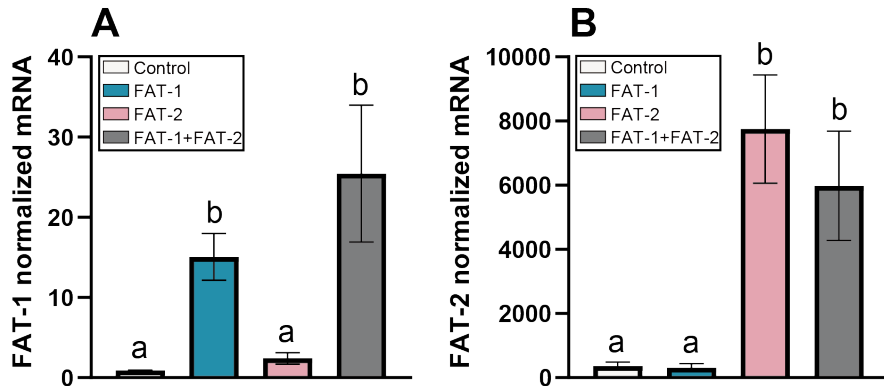


Figure 4.5.1 Short-term effect of chitosan-TPP nanoparticles encapsulated with pSG5 (control), pSG5-FAT-1, pSG5-FAT-2 and pSG5-FAT-1 + pSG5-FAT-2 on the mRNA levels of fish-codon optimized *C. elegans* FAT-1 (A) and FAT-2 (B) in the *S. aurata* liver. Seventy-two hours after nanoparticle administration and 24 h following the last meal, RNA was isolated and exogenous FAT-1 and FAT-2 expression was assayed by RT-qPCR. Values are represented as mean \pm SEM ($n = 3$) and were normalized to the *S. aurata* *18s*, *ef1a* and *actb* mRNA levels. Homogeneous subsets for the treatment are shown with different letters ($P < 0.05$).

4.5.2 Effect on serum metabolites

Previous reports indicated that transgenic expression of FAT-1 and FAT-2 reduced serum triglycerides in fish (Park and Harris, 2003; Qi et al., 2008). Thus, following the successful expression of the two exogenous enzymes in the liver of *S. aurata*, we further determined its effect on serum metabolites including glucose, triglycerides and cholesterol.

Figure 4.5.2 shows the short-term effect of FAT-1 and FAT-2 expression on serum glucose, triglycerides and cholesterol. For glucose and cholesterol, any treatment assayed promoted statistically significant differences compared to control values (figures 4.5.2A and C). However, co-expression of FAT-1 + FAT-2 significantly decreased triglycerides to 53.4 % of control values (figure 4.5.2B).

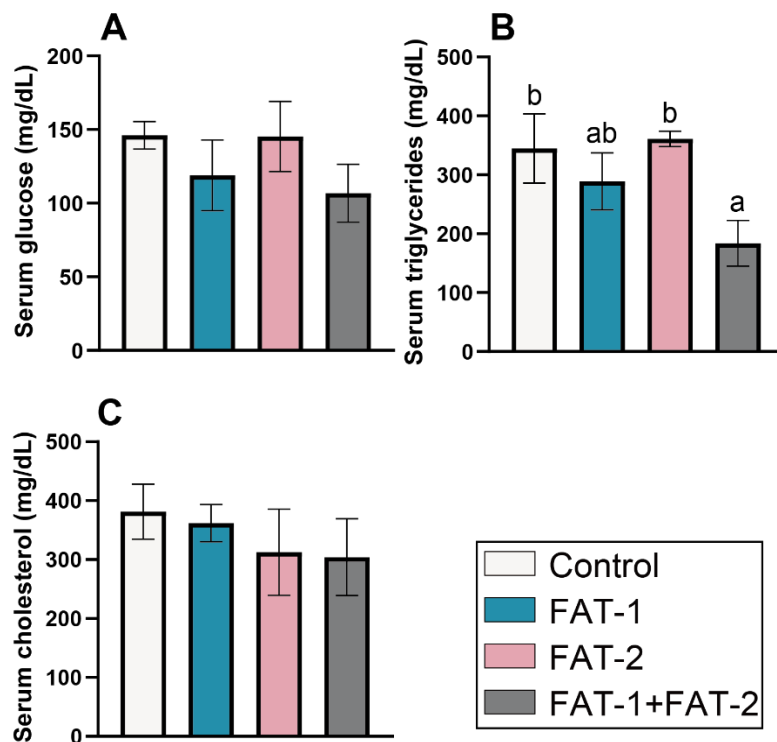


Figure 4.5.2 Short-term effect of chitosan-TPP nanoparticles encapsulated with pSG5 (control), pSG5-FAT-1, pSG5-FAT-2 and pSG5-FAT-1 + pSG5-FAT-2 on serum glucose (A), triglycerides (B) and cholesterol (C) in *S. aurata*. Seventy-two hours after nanoparticle administration and 24 h following the last meal, fish were sacrificed, and the blood was collected. Values are represented as mean \pm SEM ($n = 3 - 7$). Homogeneous subsets for the treatment are shown with different letters ($P < 0.05$).

4.5.3 Effects on hepatic fatty acid profile

FAT-1 is known to convert $n-6$ PUFA to $n-3$ PUFA, whereas FAT-2 converts OA to LA (Kang et al., 2001; Watts and Browse, 2002). Here, acute changes in the hepatic fatty acid profile resulting from the expression of fish codon-optimized FAT-1 and FAT-2 were analyzed by gas chromatography in the liver of treated fish 72-h post-administration of chitosan-TPP nanoparticles encapsulated with pSG5 (control), pSG5-FAT-1, pSG5-FAT-2 and pSG5-FAT-1 + pSG5-FAT-2 (table 4.5.3). Among 25 fatty acids identified, major fatty acids (each representing more than 1 % of total fatty acid composition), including SA (18:0), EPA (20:5 $n-3$), DHA (22:6 $n-3$), PUFA and total $n-3$ fatty acids, were significantly affected when compared to control levels. Specifically, expression of FAT-1 increased 1.3-fold both EPA and total $n-3$ fatty acids, while FAT-2 decreased SA to 69.7 % of control values.

RESULTS

Treatment of FAT-1 + FAT-2 increased 1.4-fold DHA and 1.1-fold PUFA compared to control fish, while decreased few marginal fatty acids that represent less than 1 % of total fatty acid composition, including heptadecenoic acid (17:1*n*-7), dihomo- γ -linolenic acid (20:3*n*-6) and nervonic acid (24:1*n*-9), to 9.5 %, 23 % and 25 % of the control values. Although not significant, treatment with FAT-1, FAT-2 and FAT-1 + FAT-2 showed a trend to decrease *n*-6/*n*-3 PUFA ratio to 76.4 %, 88.3 % and 88.8 %, respectively, of the values observed in control fish.

Table 4.5.3 Effects of chitosan-TPP nanoparticles complexed with pSG5 (control), pSG5-FAT-1, pSG5-FAT-2 and pSG5-FAT-1 + pSG5-FAT-2 on the fatty acid composition of *S. aurata* liver.

Fatty acid	pSG5	FAT-1	FAT-2	FAT-1 + FAT-2
14:0	8.61±0.2	9.47±0.69	10.35±1.13	8.09±0.84
15:0	0.13±0.13	0.11±0.11	0.1±0.1	0±0
16:0	28.98±1.2	26.45±1.06	26.42±0.87	26.68±1.19
17:0	0.1±0.04	0.07±0.02	0.07±0.03	0.11±0.02
18:0	4.39 ^b ±0.37	4.11 ^{ab} ±0.51	3.06 ^a ±0.29	4.31 ^{ab} ±0.39
20:0	0.17±0.17	0±0	0±0	0.34±0.2
21:0	0±0	0±0	0±0	0.04±0.02
15:1 <i>n</i> -5	0.04±0.03	0.01±0.01	0±0	0±0
16:1 <i>n</i> -7	4.42±1.18	5.49±0.11	6.38±0.33	5.3±0.27
17:1 <i>n</i> -7	0.21 ^b ±0.07	0.11 ^{ab} ±0.03	0.11 ^{ab} ±0.05	0.02 ^a ±0.01
18:1 <i>n</i> -9t	0.01±0.01	0.01±0	0.01±0	0±0
18:1 <i>n</i> -9	21.43±0.79	20.68±1.07	20.75±0.95	20.55±0.48
20:1 <i>n</i> -9	0.5±0.22	0.62±0.1	0.67±0.29	0.08±0.05
22:1 <i>n</i> -9	0.14±0.05	0.19±0.04	0.19±0.01	0.11±0.07
24:1 <i>n</i> -9	0.04 ^b ±0.01	0.02 ^{ab} ±0.01	0.01 ^{ab} ±0	0.01 ^a ±0
18:2 <i>n</i> -6t	0±0	0±0	0.01±0.01	0±0
18:2 <i>n</i> -6	23.7±1.23	23.62±0.55	23.84±0.94	26.26±0.98
20:2 <i>n</i> -6	0.06±0.03	0.09±0.02	0.12±0.02	0.09±0.06
18:3 <i>n</i> -3	1.35±0.48	1.64±0.34	1.26±0.23	1.13±0.19
18:3 <i>n</i> -6	0.07±0.06	0.2±0.2	0.37±0.07	0.19±0.08
20:3 <i>n</i> -6	0.52 ^b ±0.22	0.33 ^{ab} ±0.08	0.28 ^{ab} ±0.02	0.12 ^a ±0.07
20:3 <i>n</i> -3	0.08±0.05	0.01±0.01	0.02±0.01	0.12±0.05
20:4 <i>n</i> -6	0.18±0.06	0.29±0.03	0.23±0.01	0.17±0.1
20:5 <i>n</i> -3	2.31 ^a ±0.23	3.08 ^b ±0.26	2.66 ^{ab} ±0.11	2.73 ^{ab} ±0.24
22:6 <i>n</i> -3	2.55 ^a ±0.18	3.39 ^{ab} ±0.42	3.12 ^{ab} ±0.19	3.55 ^b ±0.26

RESULTS

SFA	42.39±1.1	40.2±1.02	39.99±1.6	39.57±1.61
MUFA	26.78±1.25	27.13±1.18	28.11±0.67	26.07±0.27
PUFA	30.83 ^a ±0.6	32.66 ^{ab} ±0.19	31.9 ^{ab} ±1.41	34.36 ^b ±1.44
<i>n</i> -3	6.29 ^a ±0.48	8.12 ^b ±0.49	7.06 ^{ab} ±0.48	7.53 ^{ab} ±0.39
<i>n</i> -6	24.54±1.01	24.54±0.44	24.84±0.98	26.83±1.09
<i>n</i> -9	22.11±0.75	21.52±1.16	21.62±0.86	20.75±0.48
<i>n</i> -6/ <i>n</i> -3	4.02±0.53	3.07±0.25	3.55±0.16	3.57±0.09

Data are expressed as percentage of total fatty acids and represented as mean ± SEM ($n = 4$). Different superscript letters indicate significant differences between groups ($P < 0.05$).

4.5.4 Effect on hepatic expression of *DNL* and LC-PUFA synthesis related genes

To gain insight into the short-term effects of FAT-1 and FAT-2 on lipid metabolism *in vivo*, the expression of enzymes exerting a major role in DNL and LC-PUFA synthesis was analyzed by RT-qPCR in the liver of *S. aurata*.

When compared to controls, the three treatments FAT-1, FAT-2 and FAT-1 + FAT-2 showed significant suppression on the mRNA levels of genes including *acaca* (to 5.9 %, 3.4 % and 4.4 % of control values, respectively), *acacb* (64.8 %, 72.3 % and 53.5 %), *fasn* (25.3 %, 23.3 % and 19.7 %), *scd1a* (18.2 %, 6.4 % and 8.5 %) and *fads2* (45.1 %, 12.2 % and 41.4 %) (figures 4.5.4A, B, C, D and E). Although not statistically significant for FAT-1 + FAT-2, the three treatments also decreased the expression of *hmgcr* to 21.7 %, 27.3 % and 64.5 % of the control values, respectively (figures 4.5.4J). In addition, the expression of *cpt1a* also showed an increase of 1.7-fold by the treatment with FAT-2 comparing to control fish (figure 4.5.4I).

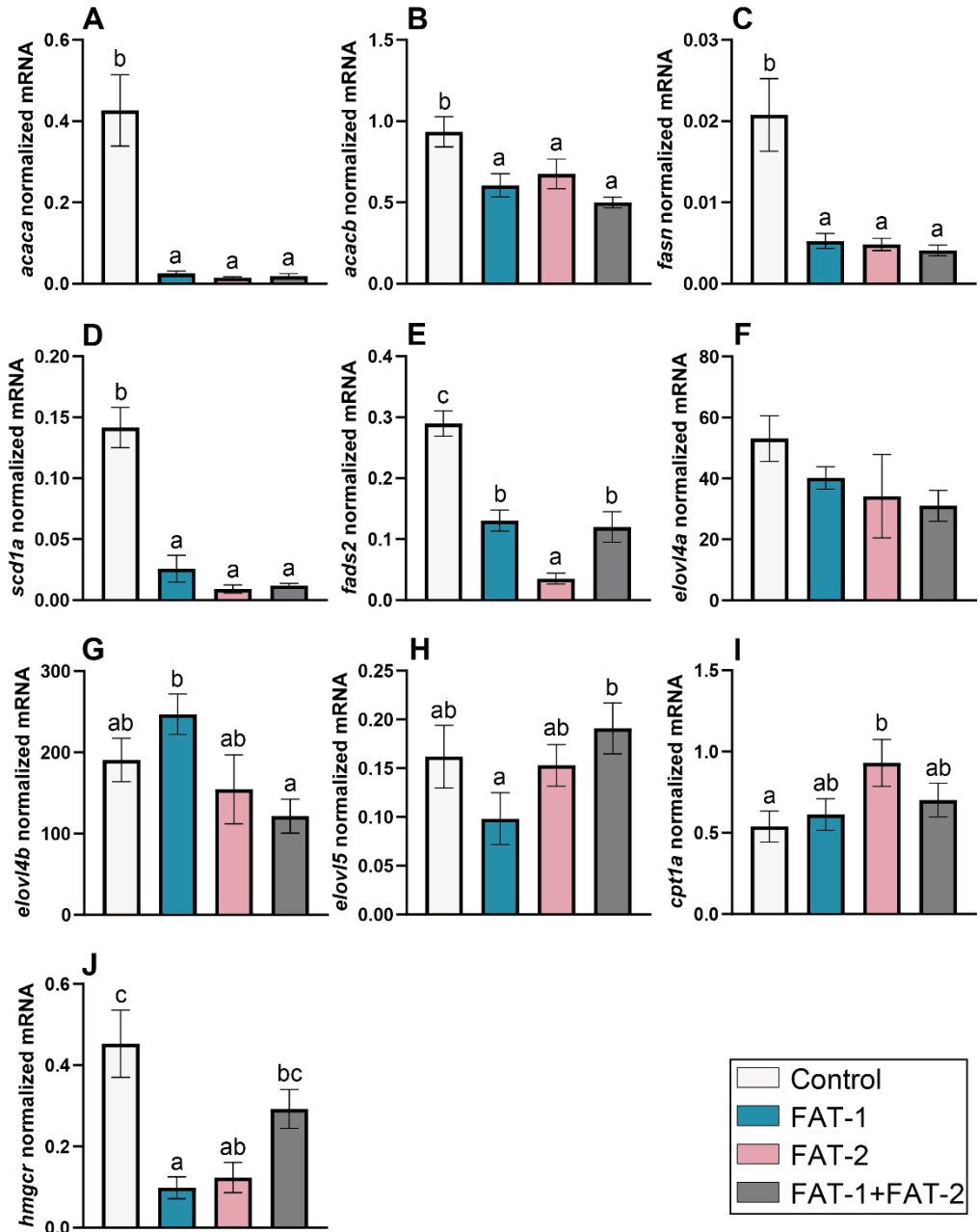


Figure 4.5.4 Short-term effects of chitosan-TPP nanoparticles encapsulated with pSG5 (control), pSG5-FAT-1, pSG5-FAT-2 and pSG5-FAT-1 + pSG5-FAT-2 on the expression of key genes in *DNL* and LC-PUFA synthesis in the liver of *S. aurata*. Seventy-two hours after nanoparticle administration and 24 h following the last meal, fish were sacrificed, the liver was collected, RNA isolated and gene expression was assayed by RT-qPCR. Data are means \pm SEM ($n = 4 - 6$). Expression data were normalized by the geometric mean of *S. aurata* *18s*, *actb* and *eef1a*

mRNA levels. Homogeneous subsets for the treatment are indicated with different letters ($P < 0.05$).

4.5.5 Effect on hepatic expression of glucose metabolism related genes

As above-mentioned, hepatic lipogenesis is tightly linked to glucose metabolism. Therefore, we also assayed transcript levels of key genes in glycolysis and PPP in response to FAT-1 and FAT-2 expression in the *S. aurata* liver.

Figures 4.5.5A-H show the effect of FAT-1 and FAT-2 on the hepatic expression of rate-limiting enzymes in glycolysis-gluconeogenesis and PPP 72 hours post-treatment. Treatment with FAT-1 significantly downregulated the mRNA levels of *g6pc1* (to 63.5 %) (figures 4.5.5B). The three treatments, FAT-1, FAT-2 and FAT-1 + FAT-2, increased the mRNA levels of *pfkl* 1.3-, 1.5- and 1.8-fold, respectively (figure 4.5.5D). The mRNA levels of *fbp1* were significant higher by the treatment of FAT-1 (1.4-fold) and FAT-2 (1.5-fold) than in control fish (figure 4.5.5D). FAT-2 also induced the mRNA abundance of *pkfr* 1.3-fold (figure 4.5.5F). Compared to control fish, treatment with FAT-1 and FAT-2 did not significantly modify the expression of *gck*, *pfkfb1*, *pck1* and *g6pd* (figures 4.5.5A, E, G and H).

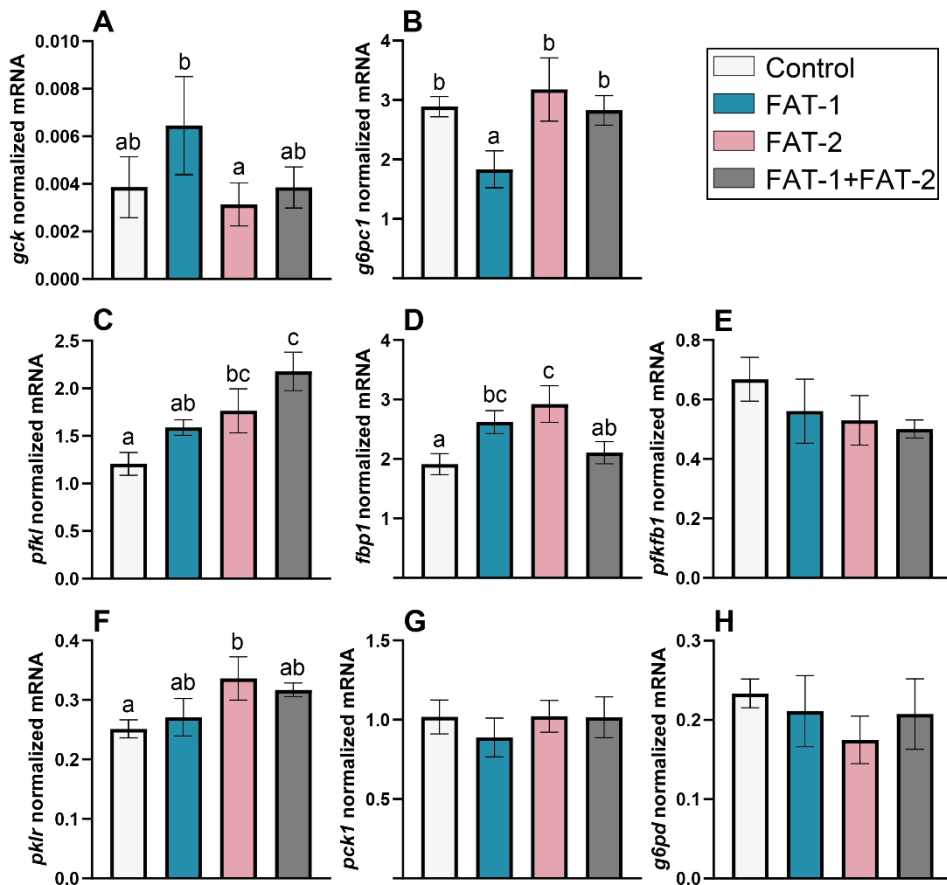


Figure 4.5.5 Short-term effects of chitosan-TPP nanoparticles encapsulated with pSG5 (control), pSG5-FAT-1, pSG5-FAT-2 and pSG5-FAT-1 + pSG5-FAT-2 on the mRNA levels of glucose metabolism genes in the *S. aurata* liver. Seventy-two hours after nanoparticle administration and 24 h following the last meal, RNA was isolated and gene expression was assayed by RT-qPCR, normalized to the *S. aurata* *18s*, *actb* and *ef1a* mRNA levels and expressed as mean \pm SEM ($n = 4 - 6$). Homogeneous subsets for the treatment are shown with different letters ($P < 0.05$).

4.5.6 Effect on hepatic activity of intermediary and glucose metabolism related enzymes

The present study also analyzed the effects of expressing FAT-1 and FAT-2 on the activity of key enzymes involved in hepatic glycolysis-gluconeogenesis, PPP, the Krebs cycle and amino acid metabolism.

Expression of FAT-1 significantly increased hepatic Ogdh activity (1.6-fold), while did not affect

RESULTS

the other assayed enzymes (figure 4.5.6H). Fish treated with FAT-2 showed a significant higher activity of Pfk1 (1.8-fold), Fbp1 (1.6-fold), Pklr (1.7-fold) and Pgd (1.4-fold) than control (figures 4.5.6A, B, D, F and J), while a significant lower value was found for Ogdh activity (39.9 % of the control values) (figure 4.5.7H). Co-expression of FAT-1 + FAT-2 induced the activity of Fbp1 (1.5-fold), Pklr (1.4-fold) and G6pd (1.3-fold) compared to the controls (figures 4.5.6B, D, E and I). Amino acid metabolism-related activities, Alt and Ast, were not affected by any of the treatments (figure 4.5.6I and J).

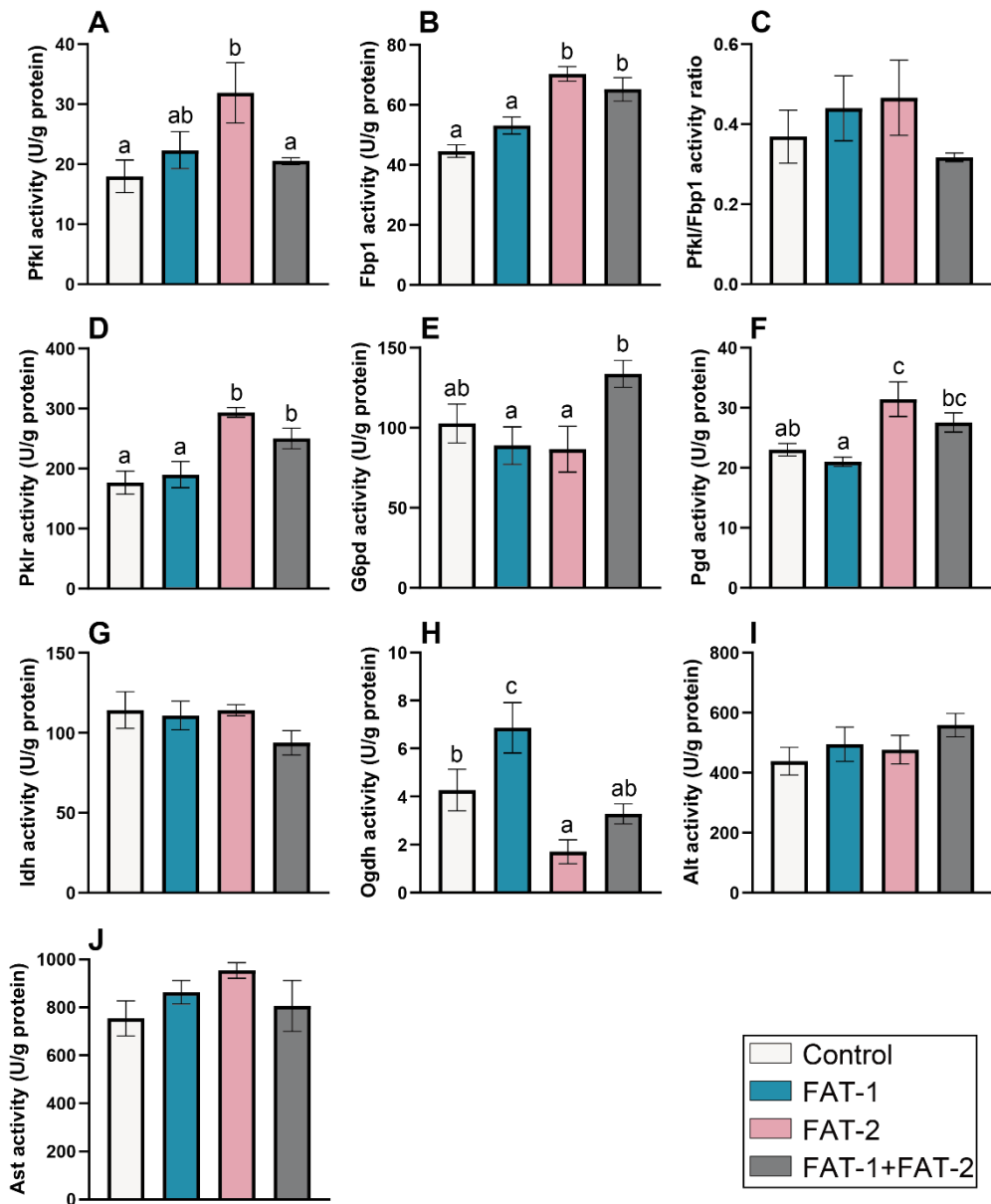


Figure 4.5.6 Short-term effects of chitosan-TPP nanoparticles complexed with pSG5 (control), pSG5-FAT-1, pSG5-FAT-2 and pSG5-FAT-1 + pSG5-FAT-2 on key enzymes in glycolysis-gluconeogenesis, PPP, the Krebs cycle and amino acid metabolism in the liver of *S. aurata*. Seventy-two hours after nanoparticle administration and 24 h following the last meal, the activity of hepatic key enzymes was analyzed and expressed as mean \pm SEM ($n = 4 - 6$). Homogeneous subsets for the treatment are shown with different letters ($P < 0.05$).

4.5.7 Effect of short-term nanoparticle administration on hepatic expression of glucose and lipid metabolism related transcription factors

To further address the acute effects of FAT-1 and FAT-2 on glucose and lipid metabolism, the mRNA levels of key transcription factors involved in controlling the expression of genes involved in glucose and lipid metabolism were evaluated.

The hepatic mRNA level of *ppara* was induced 1.3-fold by expression of FAT-2 (figure 4.5.7A). The treatments with FAT-2 and its co-expression with FAT-1 significantly decreased hepatic mRNA levels of *pparg* (to 48.6 % and 50.7 % of the control values, respectively) (figure 4.5.7B), while increased the mRNA levels of *hnf4a* (1.6-fold and 2.2-fold, respectively) (figure 4.5.7C). Expression of FAT-1, FAT-2 and FAT-1 + FAT-2 significantly downregulated *srebfl* to 60.5 %, 42.1 % and 35.6 % of control values, respectively (figure 4.5.7E).

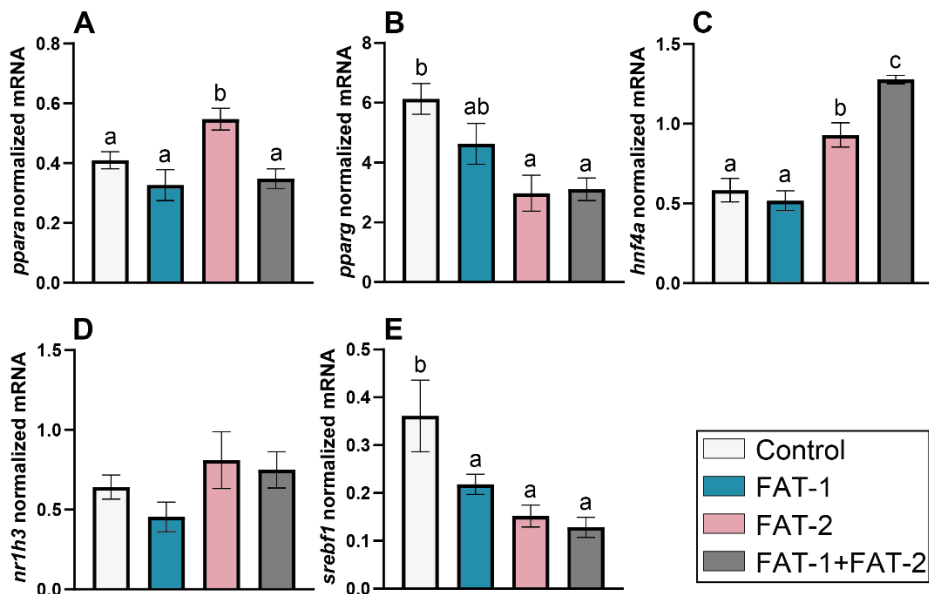


Figure 4.5.7 Short-term effects of chitosan-TPP nanoparticles encapsulated with pSG5 (control), pSG5-FAT-1, pSG5-FAT-2 and pSG5-FAT-1 + pSG5-FAT-2 on the expression of key transcription factors involved in glucose and lipid metabolism in the liver of *S. aurata*. Seventy-two hours after nanoparticle administration and 24 h following the last meal, fish were sacrificed, and the liver was collected. Data are means \pm SEM ($n = 6$). Expression data were normalized by the geometric mean of *S. aurata* *18s*, *actb* and *eefta* mRNA levels. Homogeneous subsets for the treatment are shown with different letters ($P < 0.05$).

4.6 Long-term detection of fish codon-optimized *C. elegans* FAT-1 and FAT-2 mRNA levels in the liver of *S. aurata* after a single dose of chitosan-TPP-DNA nanoparticles

As a preliminary step before studying the effects of periodical intraperitoneal doses of chitosan-TPP-DNA nanoparticles on growth and metabolism of *S. aurata*, the functionality of chitosan-TPP-DNA nanoparticles to sustain long-term expression of exogenous genes in *S. aurata* was addressed. To this end, the mRNA levels of fish codon-optimized *C. elegans* FAT-1 and FAT-2 were assayed in the liver of fish administered 28 days earlier with a single dose of chitosan-TPP-pSG5-FAT-1 and chitosan-TPP-pSG5-FAT-2 (10 µg/g BW of plasmid).

The results showed that at 28 days post-treatment, the hepatic mRNA levels of FAT-1 and FAT-2 were at levels even higher than those found at 72 h post-treatment. Expressed as mean \pm SEM ($n = 3$), fold increase over control values at 72 hours and 28 days post-treatment were 31.6 ± 4.1 and 74.8 ± 29.8 , respectively, for FAT-1 mRNA levels, while for FAT-2 mRNA levels fold increase was 20.3 ± 2.8 and 70.2 ± 7.0 , respectively.

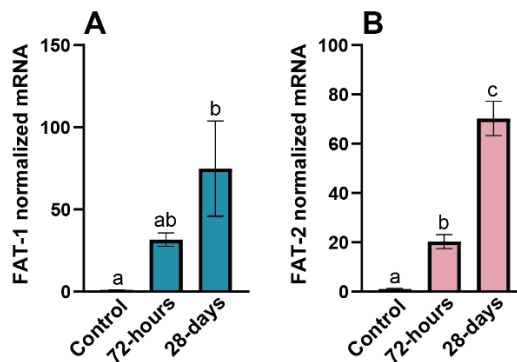


Figure 4.6 Effect of single dose of chitosan-TPP nanoparticles complexed with pSG5 (control), pSG5-FAT-1, pSG5-FAT-2 and pSG5-FAT-1 + pSG5-FAT-2 on the mRNA levels of fish-codon optimized *C. elegans* FAT-1 and FAT-2 in *S. aurata* liver. Seventy-two hours and twenty-eight days after nanoparticle administration, respectively, and 24 h following the last meal, RNA was isolated and exogenous FAT-1 and FAT-2 expression was assayed by RT-qPCR. Values are represented as mean \pm SEM ($n = 3$) and were normalized to the *S. aurata* *18s*, *ef1a* and *actb* mRNA levels. Homogeneous subsets for the treatment are shown with different letters ($P < 0.05$).

4.7 Effects of periodical intraperitoneal doses of chitosan-TPP nanoparticles complexed with pSG5-FAT-1 and pSG5-FAT-2 on the intermediary metabolism, fatty acid profile and growth parameters in *S. aurata*

4.7.1 Effect of periodical nanoparticle administration on tissue distribution of FAT-1 and FAT-2

To promote a long-term sustained expression of fish codon-optimized FAT-1 and FAT-2 in the liver of *S. aurata*, each experimental group of fish received every 4 weeks 3 intraperitoneal injections of chitosan-TPP complexed with 10 µg/g BW of the corresponding plasmid (pSG5, pSG5-FAT-1, pSG5-FAT-2 or pSG5-FAT-1 + pSG5-FAT-2) during a total period of 70 days. Nanoparticle administration was performed every 4 weeks. All administrations were performed 24 h before the last meal.

Following 70 days of treatment (14 days after the last injection and 24 h following the last meal), fish were sacrificed, and RNA was isolated for determining the mRNA levels of fish codon-optimized FAT-1 and FAT-2 by RT-qPCR in the liver, intestine, skeletal muscle and brain (figure 4.7.1). When compared with control fish, chitosan-TPP nanoparticles complexed with pSG5-FAT-1 and pSG5-FAT-2 significantly increased the mRNA levels of FAT-1 and FAT-2, respectively, in the liver and intestine of *S. aurata*. Specifically, FAT-1 mRNA abundance in the liver of fish administered with pSG5-FAT-1 was 201.8-fold higher than in control fish, while treatment with pSG5-FAT-2 upregulated FAT-2 297.4-fold. For the intestine, pSG5-FAT-1 and pSG5-FAT-2 upregulated 10.6-fold FAT-1 and 24.7-fold FAT-2, respectively. Nanoparticle administration did not exert effects on the skeletal muscle and brain.

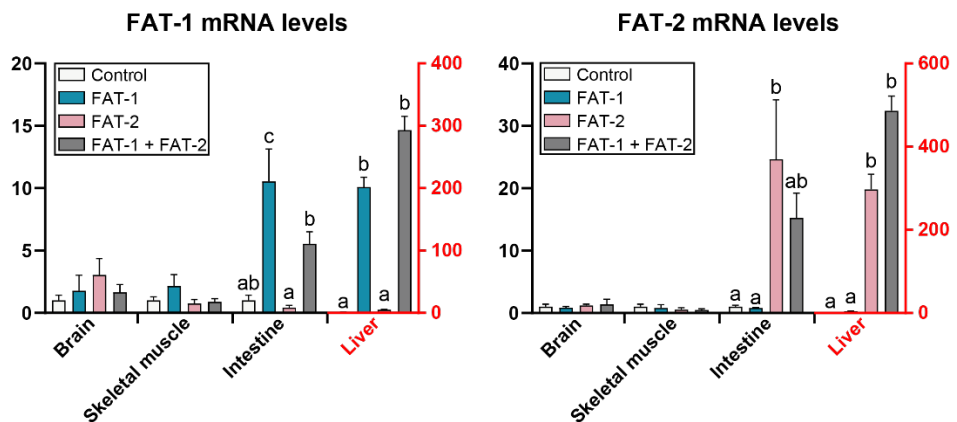


Figure 4.7.1 Effect of periodical administration of chitosan-TPP nanoparticles complexed with pSG5 (control), pSG5-FAT-1, pSG5-FAT-2 and pSG5-FAT-1 + pSG5-FAT-2 on the mRNA levels of fish-codon optimized *C. elegans* FAT-1 and FAT-2 in *S. aurata* tissues. Fish were treated 70 days with a total of 3 intraperitoneal injections (each administration every 4 weeks) of chitosan-TPP-DNA nanoparticle (10 µg/g BW of plasmid). Fourteen days after the last injection and 24 h following the last meal, exogenous FAT-1 and FAT-2 expression in brain, skeletal muscle, liver and intestine was assayed by RT-qPCR, normalized to the *S. aurata 18s* mRNA levels and represented as mean ± SEM ($n = 4$). For each tissue, homogeneous subsets for the treatment are shown with different letters ($P < 0.05$).

4.7.2 Effect of periodical nanoparticle administration on body composition and growth performance

Body composition of moisture, ash, crude fat and crude protein as well as fish growth performance parameters including SGR, FCR, HSI, PR, LR and PER were analyzed after periodical nanoparticle administration and sustained expression of FAT-1 and FAT-2 in *S. aurata*.

Long-term expression of fish codon-optimized FAT-1 + FAT-2 in the liver of *S. aurata* caused a moderate but significant 7.6 % decrease of whole-body crude protein values observed in control fish. No effect was observed in moisture, ash and crude lipid body composition (table 4.7.2). Analysis of growth performance parameters showed significantly increased weight gain values in fish expressing FAT-1 (18 % of increase) and FAT-1 + FAT-2 (26 % of increase) compared to control fish. No significant difference was found between controls and treatment with FAT-2. Similarly, the highest SGR was found in fish treated with FAT-1 + FAT-2, followed by fish treated with FAT-1, controls and fish treated with FAT-2. Fish expressing FAT-2 also presented the lowest PER. HSI significantly decreased in fish treated with FAT-1 and FAT-1 + FAT-2 to 72 % of control values. No significant differences were observed in PR and LR.

Table 4.7.2 Growth performance, nutrient retention and body composition of *S. aurata* after periodical administration of chitosan-TPP nanoparticles complexed with empty vector (pSG5, control), pSG5-FAT-1, pSG5-FAT-2 and pSG5-FAT-1 + pSG5-FAT-2.

	Control	FAT-1	FAT-2	FAT-1 + FAT-2
Initial body weight (g)	9.97±0.69	11.42±0.90	9.74±0.44	11.04±0.55
Final body weight (g)	34.64 ^a ±1.03	40.51 ^b ±1.63	31.46 ^a ±1.57	42.15 ^b ±1.25
Weight gain (g)	24.67 ^a ±0.51	29.09 ^b ±1.06	21.73 ^a ±1.23	31.11 ^b ±0.73

RESULTS

SGR (%)	1.79 ^{ab} ±0.05	1.85 ^{ab} ±0.08	1.59 ^a ±0.04	2.01 ^b ±0.03
FCR	1.40 ^{ab} ±0.03	1.36 ^{ab} ±0.04	1.53 ^b ±0.08	1.29 ^a ±0.03
HSI (%)	1.55 ^b ±0.12	1.12 ^a ±0.08	1.49 ^{ab} ±0.18	1.12 ^a ±0.15
PR (%)	24.98±3.24	21.96±0.85	18.90±2.45	21.81±1.56
LR (%)	28.00±7.50	31.47±1.12	25.17±2.03	26.24±2.02
PER	1.40 ^{ab} ±0.03	1.45 ^{ab} ±0.05	1.31 ^a ±0.07	1.52 ^b ±0.04
Moisture (%)	71.34±1.22	70.68±0.29	72.03±0.98	71.10±1.28
Ash (%)	13.72±1.47	13.93±0.12	13.07±0.73	12.94±0.45
Protein (%)	62.20 ^b ±3.88	58.81 ^{ab} ±1.80	57.98 ^{ab} ±1.04	57.50 ^a ±1.24
Lipid (%)	27.28±1.44	29.28±0.55	26.09±1.85	25.02±2.3

SGR, specific growth rate; FCR, feed conversion ratio; HSI, hepatosomatic index; PR, protein retention; LR, lipid retention; PER, protein efficiency ratio. Data are expressed as mean ± SEM ($n = 3$). Different superscript letters indicate significant differences between groups ($P < 0.05$).

4.7.3 Effect of periodical nanoparticle administration on serum metabolites

Following a periodic administration of 3 doses of FAT-1 and FAT-2 nanoparticles in 70 days, serum metabolites of glucose, triglycerides and cholesterol were analyzed in *S. aurata* using colorimetry as stated in section 3.18.

Serum glucose, triglycerides and cholesterol were determined in 70-day treated *S. aurata*. Any of the treatments assayed affected blood glucose levels. However, co-expression of FAT-1 + FAT-2 significantly decreased triglycerides and cholesterol to 41.6 % and 67.7 % of control values, respectively (figure 4.7.3).

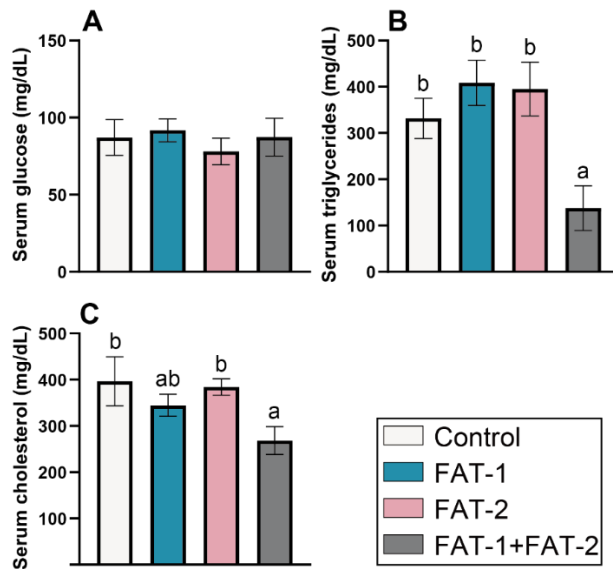


Figure 4.7.3 Effect of periodical nanoparticle administration of chitosan-TPP nanoparticles complexed with pSG5 (control), pSG5-FAT-1, pSG5-FAT-2 and pSG5-FAT-1 + pSG5-FAT-2 on serum glucose (A), triglycerides (B) and cholesterol (C) in *S. aurata*. Fish were treated 70 days with a total of 3 intraperitoneal injections (each administration every 4 weeks) of chitosan-TPP-DNA nanoparticle (10 $\mu\text{g/g}$ BW of plasmid). Fourteen days after the last injection and 24 h following the last meal, fish were sacrificed, and the blood was collected. Values are represented as mean \pm SEM ($n = 6-7$). Homogeneous subsets for the treatment are shown with different letters ($P < 0.05$).

4.7.4 Effect of periodical nanoparticle administration on hepatic fatty acid profile

Increasing the ratio of *n*-3 LC-PUFA through expression of FAT-1 and FAT-2 was one of the major objectives in the present study. Therefore, we analyzed the fatty acid profile in the *S. aurata* liver using gas chromatography after long-term sustained expression of the two enzymes.

Table 4.7.4 shows the fatty acid composition in the liver of *S. aurata* long-term treated with chitosan-TPP nanoparticles complexed with pSG5 (control), pSG5-FAT-1, pSG5-FAT-2, and pSG5-FAT-1 + pSG5-FAT-2. Among 30 different fatty acids identified in this study, treatment with FAT-1 and FAT-1 + FAT-2 significantly increased EPA (1.5-fold and 1.6-fold, respectively), DHA (2.4-fold and 2.3-fold, respectively) and total *n*-3 fatty acids (1.7-fold and 1.7-fold, respectively). The *n*-6/*n*-3

RESULTS

ratio significantly decreased in fish expressing FAT-1 (to 60.3 % of control values), FAT-2 (to 66.9 %) and FAT-1 + FAT-2 (to 63.7 %). A significant decrease of palmitoleic acid (16:1 n -7) to 58.4 % of control levels was also observed in FAT-1-treated fish.

Table 4.7.4 Effect of periodical administration of chitosan-TTP nanoparticles complexed with pSG5 (control), with empty vector (pSG5, control), pSG5-FAT-1, pSG5-FAT-2 and pSG5-FAT-1 + pSG5-FAT-2 on the fatty acid profile of *S. aurata* liver.

Fatty acid	Control	FAT-1	FAT-2	FAT-1 + FAT-2
14:0	9.38±0.46	7.31±1.45	7.43±0.60	7.40±1.45
15:0	0.10±0.10	0.32±0.12	0.37±0.13	0.32±0.11
16:0	27.49±0.66	27.09±3.37	26.33±1.42	25.29±2.50
17:0	0.21±0.03	0.11±0.04	0.22±0.11	0.11±0.04
18:0	3.73±0.39	3.88±0.30	4.20±0.38	4.03±0.33
20:0	0.02±0.02	0.20±0.13	0.08±0.03	0.08±0.04
21:0	0.06±0.06	0.16±0.06	0.12±0.07	0.11±0.04
22:0	0.00±0.00	0.06±0.04	0.11±0.04	0.05±0.05
23:0	0.02±0.02	0.01±0.01	0.00±0.00	0.01±0.01
24:0	0.01±0.01	0.03±0.02	0.06±0.02	0.04±0.02
14:1 n -5	0.06±0.05	0.00±0.00	0.14±0.09	0.13±0.04
15:1 n -5	0.06±0.02	0.02±0.01	0.05±0.03	0.05±0.02
16:1 n -7	6.93 ^b ±0.27	4.05 ^a ±1.23	5.58 ^{ab} ±0.48	5.38 ^{ab} ±0.42
17:1 n -7	0.20±0.02	0.22±0.00	0.26±0.02	0.23±0.01
18:1 n -9 _c	21.24±1.24	22.04±1.60	22.45±1.15	21.84±1.89
18:1 n -9 _t	0.06±0.03	0.04±0.01	0.08±0.02	0.04±0.01
20:1 n -9	0.58±0.08	0.83±0.02	0.71±0.13	0.72±0.14
22:1 n -9	0.17±0.03	0.30±0.08	0.25±0.05	0.31±0.08
24:1 n -9	0.00±0.00	0.07±0.05	0.07±0.03	0.05±0.03
18:2 n -6 _c	23.23±0.52	23.55±1.4	22.42±1.36	24.19±1.29
18:2 n -6 _t	0.26±0.22	0.09±0.03	0.09±0.04	0.13±0.05
20:2 n -6	0.17±0.05	0.25±0.03	0.21±0.05	0.19±0.07
22:2 n -6	0.01±0.01	0.02±0.01	0.02±0.01	0.02±0.01
18:3 n -3	1.29±0.10	1.26±0.25	1.76±0.45	1.16±0.20
18:3 n -6	0.76±0.17	0.65±0.14	0.81±0.06	0.72±0.14
20:3 n -3	0.00±0.00	0.06±0.06	0.00±0.00	0.07±0.07
20:3 n -6	0.23±0.04	0.29±0.06	0.21±0.06	0.25±0.02
20:4 n -6	0.22±0.02	0.29±0.10	0.40±0.14	0.30±0.11
20:5 n -3	1.79 ^a ±0.09	2.76 ^b ±0.29	2.43 ^{ab} ±0.26	2.89 ^b ±0.33

RESULTS

22:6 n -3	1.70 ^a ±0.15	4.02 ^b ±0.65	3.15 ^{ab} ±0.74	3.87 ^b ±0.66
SFA	41.02±0.58	39.18±4.49	38.92±1.64	37.45±3.54
MUFA	29.3±1.10	27.57±2.60	29.59±1.30	28.75±1.79
PUFA	29.67±0.60	33.25±2.51	31.49±1.39	33.80±1.94
n -3	4.78 ^a ±0.28	8.11 ^b ±0.99	7.34 ^{ab} ±0.99	8.00 ^b ±0.93
n -6	24.89±0.47	25.14±1.63	24.15±1.48	25.8±1.54
n -9	22.05±1.18	23.28±1.74	23.56±1.07	22.96±2.06
n -6/ n -3	5.26 ^b ±0.28	3.17 ^a ±0.26	3.52 ^a ±0.65	3.35 ^a ±0.42

Data are expressed as percentage of total fatty acids and represented as mean ± SEM ($n = 4$). Different superscript letters indicate significant differences between groups ($P < 0.05$).

4.7.5 Effect of periodical nanoparticle administration on muscle fatty acid profile

Following analysis of fatty acid composition in the liver, the profiles in the skeletal muscle were also determined by gas chromatography in order to confirm the effectiveness of FAT-1 and FAT-2 in elevating fish oil usage and improving fish fillet quality regarding muscle n -3 LC-PUFA content.

The effect of long-term hepatic expression of FAT-1, FAT-2 and FAT-1 + FAT-2 on the fatty acids profile in the skeletal muscle is shown in table 4.7.5. Twenty-one out of 29 fatty acids identified in the skeletal muscle were significantly affected by co-expression of FAT-1 and FAT-2. Total SFA significantly decreased to 57.1 % of controls, mostly resulting from the low content in myristic acid (14:0; 34.4 % of controls), PA (16:0; 56.3 % of controls) and margaric acid (17:0; 50.04 % of controls). In addition, treatment with FAT-1 and FAT-2 also decreased margaric acid to 50.04 % of control values, respectively. In contrast, longer SFA (with more than 17 carbons) presented increased values than in controls. Thus, SA (18:0) increased 1.2-fold, while arachidic acid (20:0), behenic acid (22:0), tricosylic acid (23:0) and lignoceric acid (24:0) raised from non-detectable levels in control fish to low but detectable levels in fish treated with FAT-1 + FAT-2.

MUFA, PUFA and total n -9, n -6 and n -3 fatty acids increased 1.3-fold, 1.3-fold, 1.5-fold, 1.1-fold and 2.2-fold, respectively, in the skeletal muscle of fish expressing FAT-1 + FAT-2. As a result of greater effect on n -3 series than in n -6 fatty acids, the n -6/ n -3 ratio significantly decreased to 52.0 % of control levels. Considering unsaturated fatty acids with a content greater than 1 % for any assayed treatment, expression of FAT-1 + FAT-2 significantly increased EPA (1.7-fold) and DHA (3.0-fold) from the n -3 series, LA (18:2 n -6c; 1.1-fold) and OA (18:1 n -9c; 1.5-fold), while decreased palmitoleic acid to 61.5 % of control levels. For less abundant unsaturated fatty acids (content between 0.1 % and

RESULTS

1 %), treatment with FAT-1 + FAT-2 also resulted in significant increases of *cis*-10-heptadecenoic acid (17:1*n*-7; 1.5-fold), gondoic acid (20:1*n*-9; 3.2-fold), erucic acid (22:1*n*-9; 5.2-fold), ARA (20:4*n*-6; 1.4-fold) and eicosadienoic acid (20:2*n*-6; 5.5-fold).

Table 4.7.5 Effect of periodical administration of chitosan-TPP nanoparticles complexed with pSG5 (control), with empty vector (pSG5, control), pSG5-FAT-1, pSG5-FAT-2 and pSG5-FAT-1 + pSG5-FAT-2 on the fatty acid profile of *S. aurata* skeletal muscle.

Fatty acid	Control	FAT-1	FAT-2	FAT-1 + FAT-2
14:0	8.83 ^b ±0.37	7.86 ^b ±1.39	7.44 ^b ±1.22	3.04 ^a ±0.10
15:0	0.00±0.00	0.00±0.00	0.00±0.00	0.00±0.00
16:0	29.58 ^b ±1.31	27.00 ^b ±3.05	26.93 ^b ±2.85	16.64 ^a ±0.34
17:0	0.18 ^b ±0.01	0.09 ^a ±0.00	0.09 ^a ±0.00	0.09 ^a ±0.00
18:0	2.77 ^a ±0.04	2.78 ^a ±0.15	2.96 ^a ±0.11	3.29 ^b ±0.08
20:0	0.00 ^a ±0.00	0.11 ^a ±0.07	0.09 ^a ±0.07	0.28 ^b ±0.03
22:0	0.00 ^a ±0.00	0.00 ^a ±0.00	0.00 ^a ±0.00	0.10 ^b ±0.01
23:0	0.00 ^a ±0.00	0.00 ^a ±0.00	0.00 ^a ±0.00	0.09 ^b ±0.03
24:0	0.00 ^a ±0.00	0.01 ^a ±0.01	0.02 ^a ±0.02	0.08 ^b ±0.00
14:1 <i>n</i> -5	0.01±0.01	0.01±0.01	0.01±0.01	0.02±0.00
15:1 <i>n</i> -5	0.02±0.02	0.04±0.02	0.06±0.02	0.05±0.00
16:1 <i>n</i> -7	6.63 ^b ±0.16	6.42 ^b ±0.68	6.14 ^b ±0.56	4.08 ^a ±0.05
17:1 <i>n</i> -7	0.16 ^a ±0.01	0.20 ^{ab} ±0.03	0.20 ^{ab} ±0.01	0.24 ^b ±0.00
18:1 <i>n</i> -9t	0.11 ^b ±0.04	0.06 ^{ab} ±0.03	0.11 ^b ±0.04	0.00 ^a ±0.00
18:1 <i>n</i> -9c	19.6 ^a ±0.53	21.98 ^a ±2.33	21.65 ^a ±2.01	28.45 ^b ±0.30
20:1 <i>n</i> -9	0.26 ^a ±0.16	0.48 ^{ab} ±0.12	0.54 ^{ab} ±0.10	0.84 ^b ±0.01
22:1 <i>n</i> -9	0.12 ^a ±0.01	0.20 ^a ±0.09	0.21 ^a ±0.09	0.62 ^b ±0.05
24:1 <i>n</i> -9	0.00 ^a ±0.00	0.01 ^a ±0.01	0.00 ^a ±0.00	0.08 ^b ±0.01
18:2 <i>n</i> -6t	0.40±0.23	0.16±0.16	0.17±0.17	0.00±0.00
18:2 <i>n</i> -6c	24.49 ^a ±0.62	24.57 ^a ±0.64	25.29 ^a ±0.67	27.98 ^b ±0.26
20:2 <i>n</i> -6	0.06 ^a ±0.02	0.12 ^a ±0.05	0.13 ^a ±0.04	0.33 ^b ±0.02
22:2 <i>n</i> -6	0.00 ^a ±0.00	0.01 ^a ±0.01	0.02 ^a ±0.02	0.10 ^b ±0.01
18:3 <i>n</i> -3	0.86±0.26	0.89±0.17	0.83±0.16	1.11±0.13
18:3 <i>n</i> -6	0.97±0.13	0.99±0.06	0.90±0.07	1.12±0.04
20:3 <i>n</i> -3	0.00±0.00	0.04±0.04	0.04±0.04	0.09±0.01
20:3 <i>n</i> -6	0.13±0.01	0.13±0.03	0.13±0.02	0.20±0.02
20:4 <i>n</i> -6	0.23 ^a ±0.01	0.24 ^a ±0.03	0.28 ^{ab} ±0.03	0.32 ^b ±0.01
20:5 <i>n</i> -3	2.36 ^a ±0.13	2.62 ^a ±0.44	2.79 ^a ±0.45	4.07 ^b ±0.03
22:6 <i>n</i> -3	2.25 ^a ±0.31	2.97 ^a ±0.99	2.98 ^a ±0.98	6.69 ^b ±0.21

RESULTS

SFA	41.36 ^b ±1.46	37.86 ^b ±4.21	37.53 ^b ±3.86	23.62 ^a ±0.38
MUFA	26.9 ^a ±0.80	29.39 ^a ±1.95	28.92 ^a ±1.68	34.38 ^b ±0.34
PUFA	31.75 ^a ±0.67	32.75 ^a ±2.26	33.55 ^a ±2.19	42.00 ^b ±0.38
<i>n</i> -3	5.47 ^a ±0.19	6.52 ^a ±1.59	6.64 ^a ±1.62	11.96 ^b ±0.16
<i>n</i> -6	26.27 ^a ±0.82	26.23 ^a ±0.74	26.91 ^a ±0.76	30.04 ^b ±0.26
<i>n</i> -9	20.09 ^a ±0.65	22.73 ^a ±2.53	22.51 ^a ±2.16	29.99 ^b ±0.32
<i>n</i> -6/ <i>n</i> -3	4.83 ^b ±0.30	4.52 ^b ±0.69	4.59 ^b ±0.76	2.51 ^a ±0.03

Data are expressed as percentage of total fatty acids and represented as mean ± SEM (*n* = 4). Different superscript letters indicate significant differences between groups (*P* < 0.05).

4.7.6 Effect of periodical nanoparticle administration on hepatic expression of *DNL* and LC-PUFA synthesis related genes

The effect of periodical nanoparticle administration of chitosan-TPP-DNA nanoparticles expressing FAT-1 and FAT-2 was also assessed on the hepatic expression of genes involved in DNL and LC-PUFA synthesis by RT-qPCR.

As shown in figure 4.7.6, treatment with FAT-1 significantly decreased the mRNA levels of *elov4a* (to 43.3 % of control values), *elov4b* (to 45.4 %) and *elov5* (to 62.3 %), while treatment with FAT-2 downregulated *elov5* to 43.6 % of control values (figures 4.7.8F, G and H). Co-expression of FAT-1 and FAT-2 also significantly downregulated *acaca* (to 31.4 % of control values), *acacb* (to 65.0 %), *fads2* (to 69.4 %), *elov4b* (to 59.1 %), *elov5* (to 41.8 %) and *hmgcr* (to 64.2 %) (figures 4.7.6A, B, E, G, H and J).

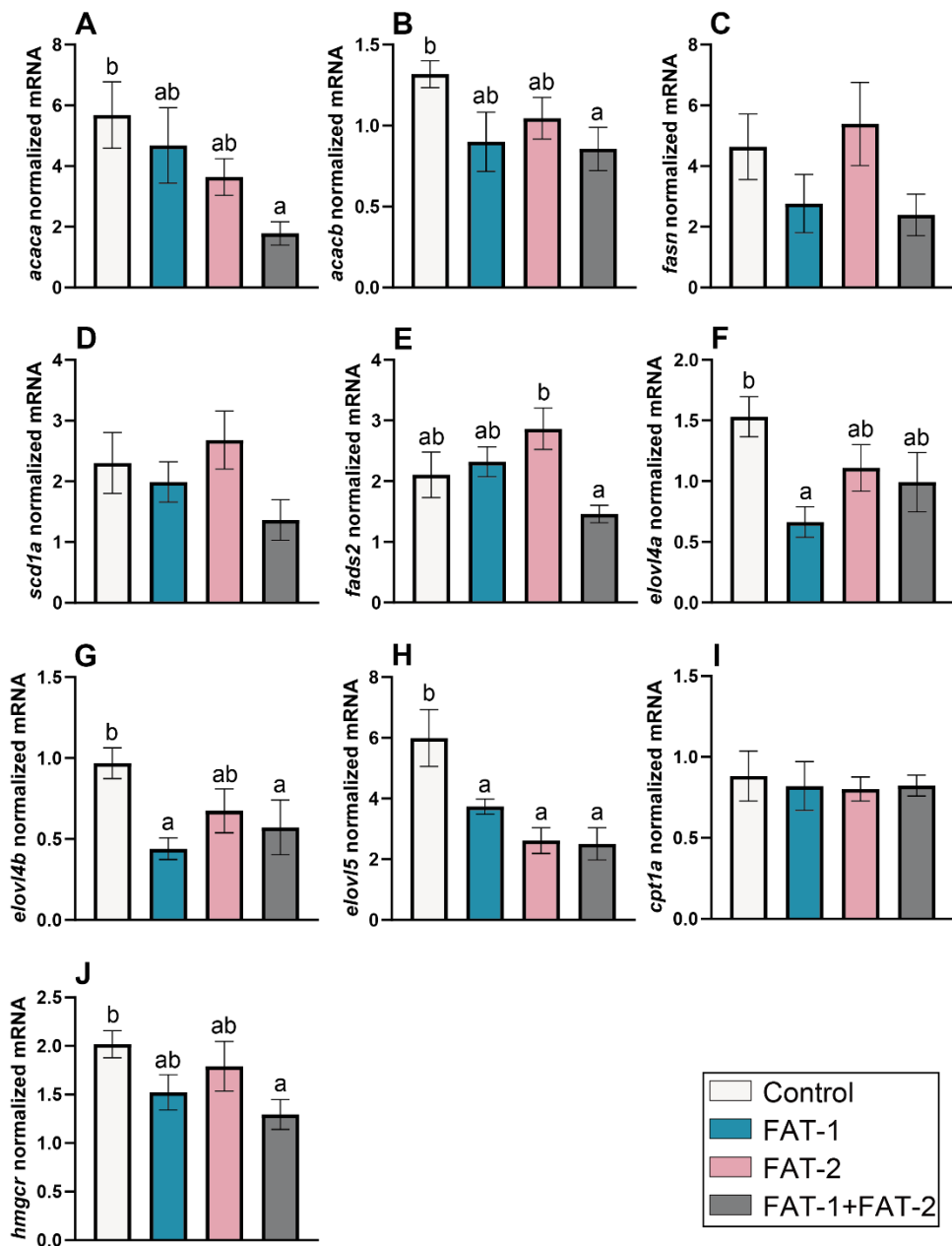


Figure 4.7.6 Effect of periodical administration of chitosan-TPP nanoparticles complexed with pSG5 (control), pSG5-FAT-1, pSG5-FAT-2 and pSG5-FAT-1 + pSG5-FAT-2 on the expression of key genes in DNL and LC-PUFA synthesis in the liver of *S. aurata*. Fish were treated 70 days with a total of 3 intraperitoneal injections (each administration every 4 weeks) of chitosan-TPP-DNA nanoparticle (10 $\mu\text{g/g}$ BW of plasmid). Fourteen days after the last injection and 24 h following the last meal, fish were sacrificed, and the liver was collected. Data are means \pm

SEM ($n = 6$). Expression data were normalized by the geometric mean of *S. aurata* *18s*, *actb* and *ef1a* mRNA levels. Homogeneous subsets for the treatment are shown with different letters ($P < 0.05$).

4.7.7 Effect of periodical nanoparticle administration on the hepatic expression of glucose metabolism related genes

Transcript levels of key genes related to glycolysis-gluconeogenesis and PPP in response to periodical nanoparticle administration and sustained long-term expression of FAT-1 and FAT-2 in *S. aurata* liver were also analyzed by RT-qPCR.

FAT-2 and its co-expression with FAT-1 significantly induced the hepatic mRNA levels of *pfkfb1* (1.4-fold), *pkfr* (1.5- and 1.9-fold) and *g6pd* (to 2.2- and 2.5-fold of the control values, respectively), when compared to controls (figures 4.7.7E, F and H).

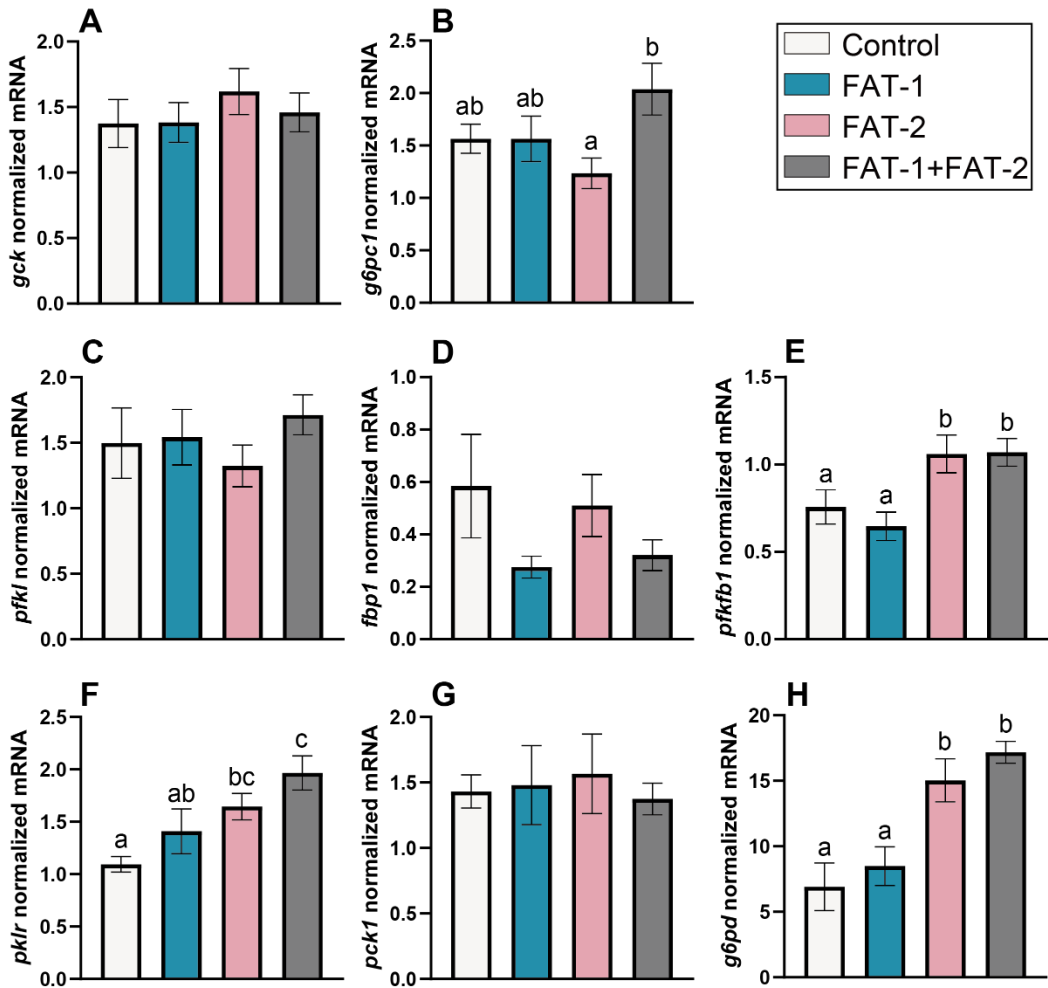


Figure 4.7.7 Effect of periodical administration of chitosan-TPP nanoparticles complexed with pSG5 (control), pSG5-FAT-1, pSG5-FAT-2 and pSG5-FAT-1 + pSG5-FAT-2 on the mRNA levels of glucose metabolism genes in *S. aurata* liver. Fish were treated 70 days with a total of 3 intraperitoneal injections (each administration every 4 weeks) of chitosan-TPP-DNA nanoparticle (10 $\mu\text{g/g}$ BW of plasmid). Fourteen days after the last injection and 24 h following the last meal, gene expression was assayed by RT-qPCR, normalized to the *S. aurata* *18s*, *actb* and *eef1a* mRNA levels and expressed as mean \pm SEM ($n = 4-6$). Homogeneous subsets for the treatment are shown with different letters ($P < 0.05$).

4.7.8 Effect of periodical nanoparticle administration on hepatic activity of intermediary and glucose metabolism related enzymes

To study the response of glucose metabolism to long-term expression of FAT-1 and FAT-2, the

activity of key enzymes of glycolysis-gluconeogenesis, PPP, the Krebs cycle and amino acid metabolism in *S. aurata* was determined.

Figure 4.7.8 shows the effect of long-term expression of fish codon-optimized FAT-1 and FAT-2 on the hepatic activity of rate-limiting enzymes involved in glycolysis-gluconeogenesis, PPP and the Krebs cycle. Fish treated with FAT-2 exhibited a significant induced activity of Pfkf (1.6-fold), Fbp1 (1.3-fold), Pklr (1.6-fold), G6pd (1.5-fold) and Pgd (1.6-fold), (figures 4.7.8A, B, D, E and F), while decreased activity of Ogdh (39 %) compared to control fish (figure 4.7.8H). Similarly, treatment with FAT-1 + FAT-2 increased Pklr activity (1.9-fold) compared to the control (figure 4.7.8D). When considering the Pfkf/Fbp1 activity ratio, fish treated with FAT-1 + FAT-2 exhibited an increased glycolytic flux (29.9 %) compared to control fish, respectively (Fig. 4.7.8C). FAT-1 and FAT-2 did not significantly affect neither the hepatic activity of Idh nor amino acid metabolism related enzymes (Alt and Ast).

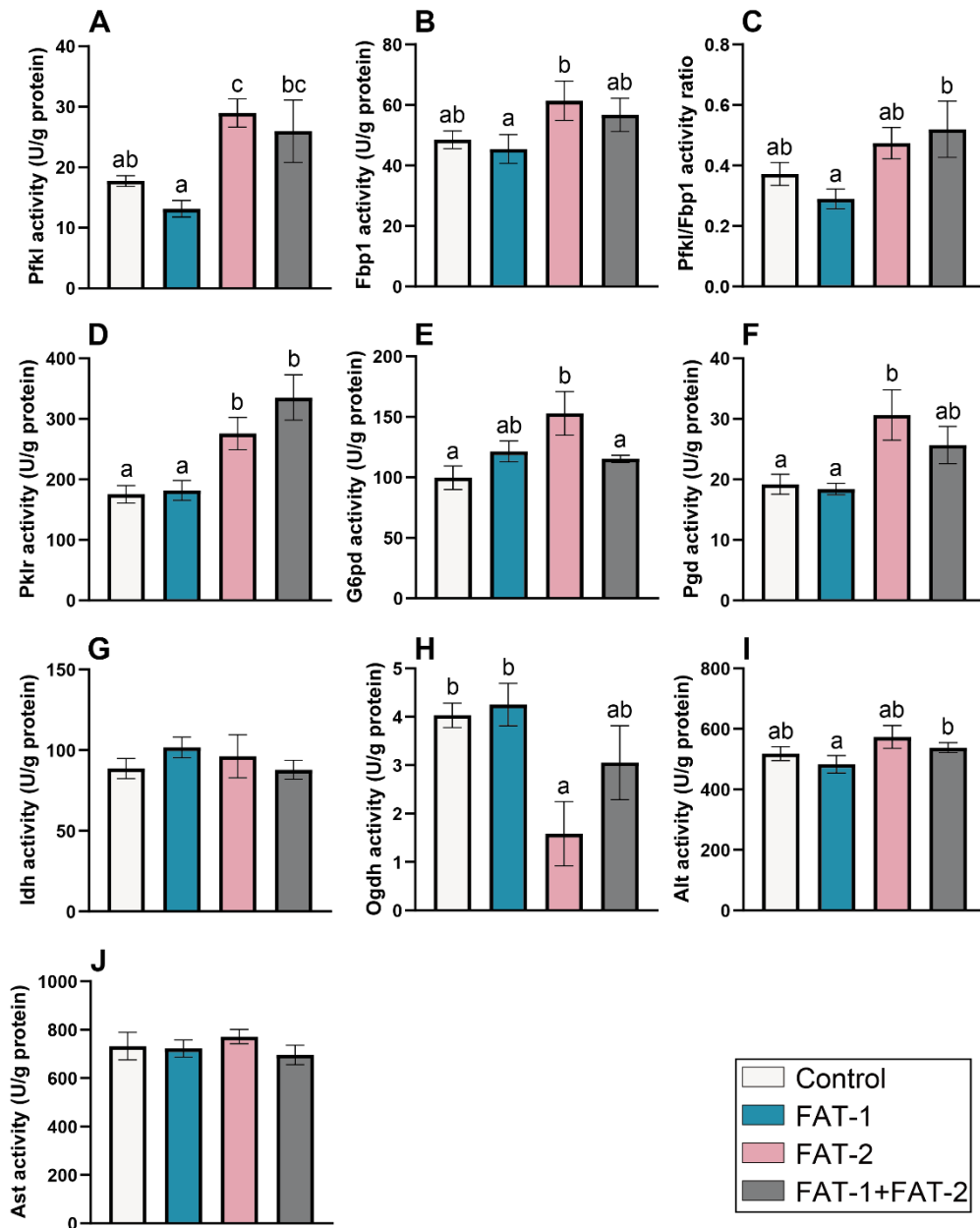


Figure 4.7.8 Effect of periodical administration of chitosan-TPP nanoparticles complexed with pSG5 (control), pSG5-FAT-1, pSG5-FAT-2 and pSG5-FAT-1 + pSG5-FAT-2 on key enzymes in glycolysis-gluconeogenesis, PPP, the Krebs cycle and amino acid metabolism in the liver of *S. aurata*. Fish were treated 70 days with a total of 3 intraperitoneal injections (each administration every 4 weeks) of chitosan-TPP-DNA nanoparticle (10 $\mu\text{g/g}$ BW of plasmid). Fourteen days after the last injection and 24 h following the last meal, fish were sacrificed, and the

liver was collected. Data are means \pm SEM ($n = 6$). Homogeneous subsets for the treatment are shown with different letters ($P < 0.05$).

4.7.9 Effect of periodical nanoparticle administration on hepatic expression of glucose and lipid metabolism related transcription factors

Transcription factors such as PPARA, PPARG, HNF4A, SREBF1 and NR1H3 are known to regulate glucose and lipid metabolism. Thus, here, we analyzed the expression of these transcription factors in response to sustained long-term expression of FAT-1 and FAT-2 by RT-qPCR in order to obtain further knowledge reasoning the changes caused by the two exogenous enzymes on *S. aurata* glucose and lipid metabolism.

In fish treated with FAT-1, the mRNA levels of *ppara* and *sreb1* were significantly reduced to 46.0 % of control values (figures 4.7.9A and E). Similarly, FAT-2 treatment also promoted a 56.3 % decrease of mRNA levels of *ppara* (figure 4.7.9A). Co-expression of FAT-1 + FAT-2 downregulated *pparg* and *sreb1* to 62.8 % and 41.8 % of control mRNA levels, respectively, while increased *nr1h3* mRNA levels 1.6-fold when compared to controls.

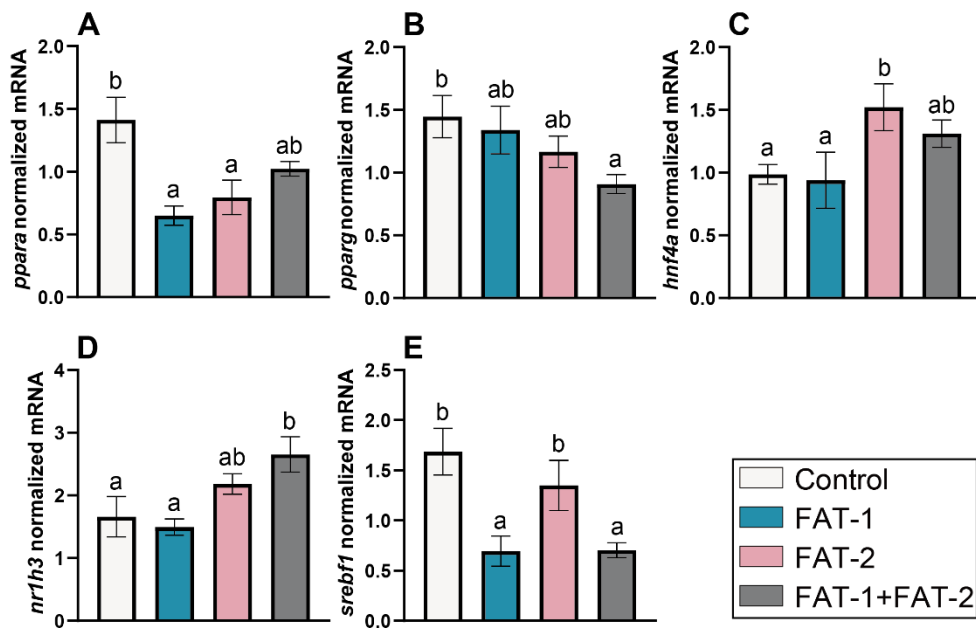


Figure 4.7.9 Effect of periodical administration of chitosan-TPP nanoparticles complexed

with pSG5 (control), pSG5-FAT-1, pSG5-FAT-2 and pSG5-FAT-1 + pSG5-FAT-2 on the expression of key transcription factors involved in glucose and lipid metabolism in the liver of *S. aurata*. Fish were treated 70 days with a total of 3 intraperitoneal injections (each administration every 4 weeks) of chitosan-TPP-DNA nanoparticle (10 µg/g BW of plasmid). Fourteen days after the last injection and 24 h following the last meal, fish were sacrificed, and the liver was collected. Data are means ± SEM ($n = 6$). Expression data were normalized by the geometric mean of *S. aurata* *18s*, *actb* and *ef1a* mRNA levels. Homogeneous subsets for the treatment are shown with different letters ($P < 0.05$).

5 DISCUSSION

5.1 Expression of fish codon-optimized *C. elegans* FAT-1 and FAT-2 in HepG2 cells

PUFA are essential for vertebrates due to the lack of $\Delta 12/n-6$ and $\Delta 15/n-3$ desaturases for *de novo* PUFA synthesis. Both enzyme activities have been preserved in plants and a few invertebrates such as *C. elegans* during evolutionary diversification of desaturases (Hashimoto et al., 2008). PUFA serve as fuel but they are also involved in physiological functions. In particular, *n-3* LC-PUFA such as EPA and DHA have beneficial effects on inflammation, CVD, and neural development. The present study was intended to boost the synthesis of *n-3* LC-PUFA in the liver of *Sparus aurata* by means of transient overexpression of foreign desaturases such as *C. elegans* FAT-1 and FAT-2. In addition, we addressed the effects of FAT-1 and FAT-2 overexpression on growth and intermediary metabolism, including hepatic lipogenesis and glycolysis, the latter of which is known to provide substrates for DNL. To this end, we hypothesized that chitosan-TPP nanoparticles complexed with FAT-1 and FAT-2 expression plasmids could efficiently increase *n-3* LC-PUFA and the *n-3/n-6* ratio in *S. aurata*.

In recent years, increasing studies reported applications of chitosan-TPP nanoparticles delivering foreign genes in fish for bacterial and viral infection, gonadal development and improved dietary nutrients utilization (Wu et al., 2020a). We have previously assayed chitosan-TPP nanoparticles to overexpress or silence target genes with major roles in controlling fish intermediary metabolism in order to improve the use of dietary carbohydrates in *S. aurata*. The results of these studies showed successful expression of exogenous protein such as hamster SREBF1a and shRNAs designed to downregulate the expression of cytosolic Alt and glutamate dehydrogenase in the liver 72-hour after intraperitoneal injection (Juan D. González et al., 2016; Silva-Marrero et al., 2019).

In the present study, fish codon-optimized *C. elegans* FAT-1 and FAT-2 were successfully ligated into pSG5 and functionality of both constructs (pSG5-FAT-1 and pSG5-FAT-2) to express FAT-1 and FAT-2 was validated by transient transfection of HepG2 cells. The pSG5 vector allows expression of transcripts in eukaryotic cells under the control of the SV40 promoter (Benoist and Chambon, 1981; Tabor and Richardson, 1985). In addition, pSG5 carries the gene regulatory element beta-globin intron II, which enhances the maturation process of cargo gene mRNA (Antoniou et al., 1998), a feature that may improve the expression levels of FAT-1 and FAT-2 in the present study. Our findings indicate that the constructed expression systems were able to generate functional FAT-1 and FAT-2 transcripts in HepG2 cells 48 h after transfection. Co-expression of FAT-1 and FAT-2 in HepG2 cells led to significantly higher proportions of PUFA, notably *n-3* LC-PUFA, and lower proportions of

SFA, especially PA. Separately, FAT-1 and FAT-2 affected similarly the fatty acid profile in HepG2 cells; in both cases the effects were in the same direction than FAT-1 + FAT-2 co-expression, but with lower intensity. In regard of *n*-3 LC-PUFA such as EPA and DHA, while both FAT-1 and FAT-2 showed a trend to increase DHA proportions, surprisingly none of the treatments assayed modified EPA values in the cells transfected for 48 hours. Possibly, the fact that HepG2 is an established human-derived cell line while FAT-1 and FAT-2 desaturases used in the present study are fish codon-optimized *C. elegans* sequences, may somewhat limit the catalytic activity of the foreign enzymes in human cells. Other factors, such as the limited time of action in the transfected cells (up to 48 hours) may also reduce the efficiency of FAT-1 and FAT-2 activity. Elevation of *n*-3 LC-PUFA by heterologous expression of FAT-1 was also observed in other eukaryotic cells, such as 3T3-L1 cells (An et al., 2012), cardiac myocytes (Kang et al., 2001) and goat ear skin-derived fibroblast cells (Fan et al., 2016). In any case, and taken together, our data indicate that the catalytic functions of the two desaturases were performed in HepG2 cells transfected with pSG5-FAT-1 and pSG5-FAT-2.

5.2 Delivery of chitosan-TPP complexed with fish codon-optimized FAT-1 and FAT-2 nanoparticles to *S. aurata*

Having concluded that pSG5-FAT-1 and pSG5-FAT-2 can be used as proper expression vectors for fish codon-optimized *C. elegans* FAT-1 and FAT-2 in eukaryotic cells, we addressed the use of chitosan-TPP nanoparticles to allow sustained expression of both desaturases in the liver of *S. aurata*, an animal model with limited LC-PUFA synthesis and low glucose tolerance. The main objective was to induce *n*-3 LC-PUFA synthesis by overexpressing FAT-1 and FAT-2 and evaluate acute and long-term effects on growth and intermediary metabolism in the *S. aurata* liver.

To this end, pSG5 (control), pSG5-FAT-1 and pSG5-FAT-2 were encapsulated into chitosan-TPP nanoparticles by the ionotropic gelation technique to facilitate hepatic delivery of the plasmid constructs after intraperitoneal injection. This delivery system is increasingly used as carrier for delivering nucleic acids *in vivo* due to its well-known low toxicity, mucoadhesion, biodegradability and biocompatibility (Wu et al., 2020a). Indeed, abundant transcripts of FAT-1 and FAT-2 were detected in *S. aurata* liver at 72-h post-injection, which is in line with our previous studies using chitosan-TPP nanoparticles to deliver plasmids expressing SREBP1a (sterol regulatory element binding protein 1a) and silencing endogenous cytosolic ALT and glutamate dehydrogenase (Gaspar et al., 2018b; Juan D. González et al., 2016; Silva-Marrero et al., 2019).

In contrast to rapid degradation of naked DNA, encapsulation with nanoparticles allows sustained expression of cargo gene and hepatic retention after administration (Intra and Salem, 2008; Bachir et al., 2018). In line with this, monthly intraperitoneal administration of 3 doses of the resulting nanoparticles allowed long-standing high expressional levels of the two exogenous proteins in the liver, mild expression in the intestine and barely detectable levels in the skeletal muscle and brain. Biodistribution of fish codon-optimized FAT-1 and FAT-2 expression shows that the particle size of chitosan-TPP-DNA complexes used in the present study favored liver retention in *S. aurata*, which confirms previous reports with hepatic delivery of exogenous *srebf1a* and shRNAs (Gaspar et al., 2018b; Juan D. González et al., 2016; Silva-Marrero et al., 2019). Possibly, discontinuous endothelia of the intestine enables chitosan-TPP-DNA nanoparticle absorption and transportation to the liver through portal circulation (Hagens et al., 2007a), while the tight morphology of capillary endothelium in the muscle and brain may limit the transfer of nanoparticles and result in scarce levels of transcripts (Kooij et al., 2005).

5.2.1 Effects of FAT-1 and FAT-2 expression on body composition and growth performance

Body fatty acid composition is affected by multiple factors, including DNL, physiological requirements and dietary fatty acid profile. Single-gene expression of either FAT-1 and FAT-2 enhanced fatty acid desaturation and, consequently, *n*-3 LC-PUFA synthesis in transgenic mice (Pai et al., 2014a), pig (Tang et al., 2019), zebrafish (Pang et al., 2014), and common carp (Zhang et al., 2019). Similarly, *S. aurata* long-term treated with chitosan-TPP-DNA nanoparticles expressing either FAT-1 or FAT-2 showed a general trend to increase liver and muscle EPA, DHA, and total *n*-3 fatty acids and PUFA, while decreased the *n*-6/*n*-3 ratio and SFA, conceivably by conversion into unsaturated fatty acids. Most of these effects were potentiated by hepatic co-expression of FAT-1 and FAT-2. Combined activities of FAT-1 and FAT-2 decreased SFA such as 14:0, 16:0 and 17:0, while increased unsaturated fatty acids, particularly *n*-3, and to a lesser extend *n*-9 and *n*-6. Thus, co-expression of FAT-1 and FAT-2 promoted a synergistic effect that favored *n*-3 LC-PUFA accumulation in the muscle, particularly EPA and DHA. Given that FAT-1 and FAT-2 mRNA levels were scarcely detected in the skeletal muscle of *S. aurata*, changes in the muscle fatty acid profile between treatments may ascribe to hepatic fat exportation of fatty acids forming part of VLDL.

Transgenesis of FAT-1, a gene that facilitates the conversion of *n*-6 to *n*-3 fatty acids, scarcely affected body growth in zebrafish, common carp, mice, pig and lamb (Bhattacharya et al., 2006a; Ji et

al., 2009a; X. Liu et al., 2016a; Sun et al., 2020a; Zhang et al., 2019; J. Zhang et al., 2018a). However, in the present study long-term hepatic expression of FAT-1 and FAT-1 + FAT-2 significantly increased weight gain but not lipid content in *S. aurata*. A trend to increase SGR values was also observed in fish co-expressing FAT-1 and FAT-2. Our findings suggest that increased levels of *n*-3 LC-PUFA and decreased *n*-6/*n*-3 fatty acid ratio resulting from expression of fish codon-optimized FAT-1 and FAT-2 may contribute to increased growth performance in *S. aurata*. In support of this hypothesis, substitution of fish oil by vegetable oil enhances the *n*-6/*n*-3 ratio and lowers *n*-3 LC-PUFA and weight gain in *S. aurata* (Houston et al., 2017), as well as in other marine fish such as cobia (Trushenski et al., 2012) and the anadromous Atlantic salmon (Qian et al., 2020a). However, dietary fish oil (rich in *n*-3 LC-PUFA) does not significantly affect growth in freshwater fish such as zebrafish (Meguro and Hasumura, 2018), common carp (Ljubojević et al., 2015), red hybrid tilapia (Al-Souti et al., 2012) and rainbow trout (Richard et al., 2006a). Greater capacity of freshwater fish than marine fish for converting *n*-3 and *n*-6 C₁₈ PUFA into highly unsaturated long-chain fatty acids (Castro et al., 2016), may explain different adaptative responses to dietary *n*-3 LC-PUFA. Better growth performance of *S. aurata* submitted to sustained expression of fish codon-optimized FAT-1 and FAT-1 + FAT-2 may also result from improved health condition due to increased *n*-3 LC-PUFA and decreased *n*-6/*n*-3 ratio. Consistently, FAT-1 transgenesis prevents liver steatosis and lipid deposition in the abdominal cavity of zebrafish by a mechanism involving hepatic downregulation of lipogenic-related genes and upregulation of steatolysis-related genes (Sun et al., 2020a). Moreover, FAT-1 transgenesis prevents glucose intolerance, insulin resistance, *non*-alcoholic fatty liver disease and allergic airway responses in mice (Bilal et al., 2011; Boyle et al., 2020; Kim et al., 2012; Romanatto et al., 2014a), and exerts protective vascular effects on pigs and cattle by reducing inflammatory factors and improving the immune system (X.-F. F. Liu et al., 2017; X. Liu et al., 2016a). The low HSI values observed in FAT-1 and FAT-1 + FAT-2 treated fish may be a trait reflecting low lipid deposition in the liver. In support of this hypothesis, *n*-3 fatty acids reduce circulating triglycerides, and supplementation with dietary fish oil correlates with lower HSI values in fish (Peng et al., 2008, 2016; Piedecausa et al., 2007).

5.2.2 Effects of FAT-1 and FAT-2 expression on serum metabolites

High levels of circulating triglycerides are considered as a cardiovascular risk factor, while *n*-3 LC-PUFA are well known for their role in decreasing plasma triglycerides. A number of studies revealed the serum triglycerides-lowering effect resulting from dietary supplementation with fish oil in humans. However, considering longer periods of fish oil supplementation, a meta-analysis found no

difference in serum triglyceride levels with longer trial durations from 6.58 to 199.9 weeks (Eslick et al., 2009). In this regard, in the present study we showed that both short- and long-term post-treatment with FAT-1 + FAT-2 reduced serum triglycerides, which may be at least partially attributed to the increase of *n*-3 LC-PUFA in the *S. aurata* liver. Consistently, among biochemical parameters improved by FAT-1 transgenesis, reduced triglycerides were reported in serum of mice (Romanatto et al., 2014a), pig (X. Liu et al., 2016a), cattle (X.-F. F. Liu et al., 2017) and the liver of zebrafish (Sun et al., 2020a). Decreased serum triglycerides may be attributed in part to the increase of *n*-3 LC-PUFA in the liver, where *n*-3 fatty acids are generally thought to reduce the production of VLDL and induce fatty acid β -oxidation (Shearer et al., 2012a). In addition, FAT-1 transgenesis is also associated with decreased levels of glucose and cholesterol in mice and cattle serum as well as in the zebrafish liver (X.-F. F. Liu et al., 2017; Romanatto et al., 2014a; Sun et al., 2020a).

The levels of *n*-3 LC-PUFA are known to decrease total and LDL-loaded cholesterol while increase HDL-loaded cholesterol (Lorente-Cebrián et al., 2013). Although no statistically significant at the short-term, a clear trend to decrease serum cholesterol was found in *S. aurata* long-term treated with FAT-1 + FAT-2, which was in line with results reported for FAT-1 transgenic zebrafish (Sun et al., 2020a).

In the present study, no significant effect on serum glucose was found by expressing FAT-1, FAT-2 and FAT-1 + FAT-2. Even though dietary intake of *n*-3 LC-PUFA was shown to decrease serum fasting glucose (T. T. Zhang et al., 2019), whether and how such effect is related to glucose tolerance remains obscure (Green et al., 2020).

5.2.3 Effects of FAT-1 and FAT-2 expression on hepatic and muscular fatty acid profiles in *S. aurata*

Fatty acid composition of fish is affected by multiple factors, such as physiological requirements and dietary fatty acid profiles. Generally, in the present study, short-term expression of FAT-1 alone elevated the proportion of EPA and total *n*-3 LC-PUFA, whereas co-expression of FAT-1 and FAT-2 induced hepatic DHA and total PUFA proportion in *S. aurata* liver. Consistently, sustained expression of FAT-1 + FAT-2 for 70 days elevated hepatic EPA and DHA proportions, which also increased *n*-3 PUFA and the *n*-6/*n*-3 ratio as a consequence. Consistently, transgenic expression of either FAT-1 or FAT-2 intensified *n*-3 LC-PUFA synthesis in previous reports (Lai et al., 2006a; X.-F. F. Liu et al., 2017; Pang et al., 2014; Romanatto et al., 2014a; Tang et al., 2019). In the present study,

21 fatty acids (from a total of 29 fatty acids identified) significantly altered their proportions in the muscle by the administration of chitosan-TPP-DNA nanoparticles expressing FAT-1 and FAT-2, while 3 fatty acids were significantly affected in the liver (out of 30 fatty acids identified). Together with the lessened SFA proportion by FAT-1 + FAT-2 in the skeletal muscle, elevation of the proportions of MUFA, *n*-9 PUFA and *n*-6 PUFA indicates a forward conversion of SFA into unsaturated fatty acids in *S. aurata* treated with FAT-1 + FAT-2. In transgenic models, single-gene expression of either FAT-1 or FAT-2 induced *n*-3 and *n*-6 LC-PUFA synthesis, respectively, in mice (Pai et al., 2014a), pig (Tang et al., 2019), zebrafish (Pang et al., 2014) and common carp (X. Zhang et al., 2018). A similar trend was observed in *S. aurata*, having maximal production in fish treated with nanoparticles expressing FAT-1 + FAT-2, which in turn favored *n*-3 LC PUFA production. Given that fish codon-optimized *C. elegans* FAT-1 and FAT-2 mRNA were scarcely detected in *S. aurata* muscle of fish administered with nanoparticles, apparent differences of fatty acid profiles between liver and muscle in treated fish may ascribe to lipid mobilization from the liver to the muscle. Moreover, co-presence of FAT-1 and FAT-2 may raise a synergistic effect for *n*-3 LC-PUFA synthesis in the liver, which may explain less intense effects observed in the liver and muscle fatty acid profile of fish treated with FAT-1 and FAT-2 alone. Conceivably, hepatic expression of FAT-1 may drain FAT-2 products and diminish allosteric inhibition of FAT-2 activity by its products (Shi et al., 2020), while concomitant products catalyzed by FAT-2 could satisfy substrates for FAT-1.

C. elegans FAT-1 is a *n*-3 desaturase with activity at $\Delta 15$ and $\Delta 17$ fatty acid substrates. Mutation of *C. elegans* FAT-1 leads to decreased levels of 18:3*n*-3, 20:4*n*-3 and 20:5*n*-3, and increased proportions of 18:2*n*-6, 20:3*n*-6 and 20:4*n*-6 (Kahn-Kirby et al., 2004; Watts and Browse, 2002). Transgenic expression of *C. elegans* FAT-1 in mammalian cells decreases *n*-6 LC-PUFA such as 18:2*n*-6, 20:2*n*-6, 20:3*n*-6, 20:4*n*-6, 22:4*n*-6 and 22:5*n*-6, while increases 18:3*n*-3, 20:4*n*-3, 20:5*n*-3, 22:5*n*-3 and 22:6*n*-3 (Kang et al., 2001). On the other hand, heterologous expression of FAT-2 reveals its ability to insert double bonds sequentially at the $\Delta 12$ and $\Delta 15$ positions in substrates with preexisting $\Delta 9$ double bond (Zhou et al., 2011). In the present study, a significant increase of 18:2*n*-6 was observed in the muscle by treatment with FAT-1 + FAT-2, which was not concomitant with decreased levels of fatty acids containing $\Delta 9$ double bond, *i.e.*, 18:1*n*-9, 20:1*n*-9, 22:1*n*-9 and 24:1*n*-9. Nevertheless, the decrease of muscular SFA, 14:0, 16:0 and 17:0, paralleled increased values of *n*-9, *n*-6 and *n*-3 fatty acids in fish treated with FAT-1 + FAT-2. Substrate recognition and the particular catalysis performed by fish codon-optimized *C. elegans* FAT-1 and FAT-2 desaturases in the *S. aurata* liver remains unclear and needs further investigation.

5.2.4 Effects of FAT-1 and FAT-2 expression on lipid metabolism

Concomitant to the alteration of hepatic fatty acid profile, DNL (*acaca*, *acacb*, *fasn* and *scd1a*) and LC-PUFA (*fads2*) synthesis related genes were downregulated at 72 h post-treatment with FAT-1, FAT-2 and FAT-1 + FAT-2 in *S. aurata*. In transgenic animals, the effect of FAT-1 seems to depend on a variety of factors including the species, environmental conditions and dietary lipid content. Previous reports on FAT-1 transgenic common carp (X. Zhang et al., 2018), zebrafish (Pang et al., 2014) and goat ear skin-derived fibroblast cells (Fan et al., 2016) showed elevated mRNA levels of fatty acid desaturases and elongases, which are also induced in FAT-2 and FAT-1 + FAT-2 transgenic models (Pang et al., 2014; Tang et al., 2019). Nonetheless, a recent study showed that the nutritional status had dramatic impacts on lipogenesis of zebrafish transfected with FAT-1: when compared to wild type, FAT-1 transgenic zebrafish fed low fat diet showed higher hepatic mRNA levels of *fasn*, *acaca* and *scd1*, which were reversed in transgenic fish fed with high fat diet (Sun et al., 2020a). Similarly, when treated with *n*-3 LC-PUFA, mice fed normal diets showed no differences of hepatic *Acac*, *Fasn* and *Scd1* mRNA levels, but they were decreased when mice were fed a high fat diet (Echeverriá et al., 2019). In line with our findings, FAT-1 transgenesis in mice decreased the levels of phosphorylated ACACA and FASN (Romanatto et al., 2014a). Consistently, a short-term supplement of *n*-3 PUFA also decreased the hepatic mRNA levels of *Acac* and *Fasn* in mice fed a high fat diet (Wang et al., 2017). Thus, LC-PUFA synthesis may be regulated in a feedback manner that combines sense of cellular LC-PUFA levels with regulation of the activity of lipogenic enzymes. Interestingly, in long-term treated *S. aurata* periodically administrated with nanoparticles, the combined action of FAT-1 + FAT-2 was the condition that exerted a stronger reduction of the expression of most key enzymes in fatty acid synthesis, desaturation and elongation, such as *acaca*, *acacb*, *fads2* and *elovl5*. Since that expression of lipogenic enzymes is known to be regulated by their downstream products, co-presence of FAT-1 and FAT-2 may raise a synergistic effect on the synthesis of downstream fatty acids in the liver, which in turn promote stronger negative feedback to the upstream enzymes. Less intense reduction of the expression of fatty acid synthesis-related genes was generally observed by long-term treatment of FAT-1 and FAT-2 alone. Therefore, unpaired expression of FAT-1 and FAT-2 may result in limited LC-PUFA synthesis and transcriptional suppression in the feedback loop. Additionally, decreased expression of *hmgcr*, a rate-limiting enzyme for cholesterol synthesis, in both short- and long-term periodically treated with FAT-1 and FAT-2 is in line with reduced serum cholesterol levels. Downregulation of *hmgcr* may be also due to elevated *n*-3 LC-PUFA in the liver. Consistently with our findings, previous reports in mice confirmed that EPA is able to suppress hepatic *Hmgcr* expression

(Chang et al., 2018).

The effect of *n*-3 LC-PUFA supplementation on hepatic *cpt1* expression is unclear. Increased hepatic mRNA levels of *Cpt1* were reported in mice fed fish oil (Bargut et al., 2014). However, substitution of fish oil by vegetable oil, which contains lower *n*-3 LC-PUFA, increased *cpt1* expression in *S. aurata* liver (Betancor et al., 2016). In addition, mice fed high fat diet + EPA showed no differences on hepatic *Cpt1* expression compared with the non-EPA diet (Du et al., 2013). Nevertheless, expression of *cpt1* in these studies, notably at short time, were synchronized to the expression of *ppara*. Indeed, hepatic PPARA was shown to direct regulate *cpt1* expression (discussed in section 4.2.5). In line with this, the present study showed a similar expression pattern between *cpt1a* and *ppara* in the liver of *S. aurata* 72 h post-treatment with nanoparticles. Nevertheless, the induction of hepatic *cpt1a* expression by FAT-2 was buried in long-term periodically treated fish. In fact, any of the treatments assayed affected the mRNA abundance of *cpt1a* at long-term. CPT1A is essential for the mitochondrial uptake of long-chain fatty acids and their subsequent β -oxidation in the mitochondrion. In mitochondria, ACACB catalyzes conversion of acetyl-CoA into malonyl-CoA, the latter of which is a potent allosteric inhibitor of CPT1A (Saggerson, 2008a). Thus, our data suggest that in addition to decrease DNL, sustained co-expression of FAT-1 and FAT-2 may do not reduce fatty acid oxidation in the liver of *S. aurata*. Hence, transgenesis of FAT-1 and double transgenesis of FAT-1 and FAT-2 increased expression of *cpt1a* in zebrafish (Pang et al., 2014; Sun et al., 2020a).

Similar to our findings indicating increased *nr1b3* expression in the liver of *S. aurata* treated with FAT-1 + FAT-2, supplementation with *n*-3 LC-PUFA also upregulated expression of *nr1b3* in Atlantic salmon (Huyben et al., 2021; Sprague et al., 2019). LXR α , encoded by *nr1b3*, is known to stimulate cholesterol efflux, lipogenesis, and triglycerides secretion in liver (Wang and Tontonoz, 2018). Consistent with the activation of LXR α to low cholesterol levels, in the present study, sustained expression of FAT-1 + FAT-2 exhibited low serum cholesterol levels concomitant with high hepatic *nr1b3* transcripts, while marginal effects were concomitantly observed for the serum and hepatic changes in the short-term fish. In support of this, studies in HepG2 cells showed that depletion of LXR α induced expression of HMGCR, the rate-limiting enzyme for cholesterol synthesis (Wang et al., 2008). Coincidentally, long-term periodical administration of nanoparticles to express FAT-1 + FAT-2 reduced *hmgcr* expression in the *S. aurata* liver. In addition, LXR is engaged in the activation of lipogenesis via transcriptional induction of *SREBF1c*, which is a potent factor in regulating lipogenesis.

In mammals, alternate promoters of the *Srebf1* gene generate Srebf1a and Srebf1c, which constitute transcription factors with a major role in activating DNL. Srebf1c primarily transactivates genes required for fatty acid and triglyceride synthesis while Srebf1a is a potent activator of all SREBF-responsive genes, including genes associated with cholesterol synthesis. Consistent with the role of *srebf1* in the transcription of lipogenic genes both in fish and mammals (Carmona-Antoñanzas et al., 2014; Silva-Marrero et al., 2019), downregulation of *srebf1* in the liver of *S. aurata* submitted to both short- and long-term periodically sustained expression of fish codon-optimized FAT-1 and FAT-1 + FAT-2 led to a trend to decrease the expression of genes involved in cholesterol synthesis (*hmgcr*) and fatty acid synthesis (*acaca*, *acacb* and *fasn*), desaturation (*scd1a* and *fads2*) and elongation (*elovl4a*, *elovl4b* and *elovl5*). In agreement with our findings, transgenic zebrafish expressing FAT-1, FAT-2 and FAT-1 + FAT-2 and double transgenic pigs for FAT-1 and FAT-2 also showed downregulated expression levels of *srebf1*. Since DHA suppresses *srebf1* expression and enhances its protein degradation (Jump, 2008), increased levels of DHA seem the main responsible for downregulating *srebf1* and DNL genes in the liver of *S. aurata* expressing FAT-1 and FAT-1 + FAT-2. Consistently, substitution of fish oil, rich in DHA, by vegetable oil leads to upregulation of *srebf1* and fatty acid synthesis-related genes in *S. aurata* (Ofori-Mensah et al., 2020a). A LXRE is present in the *SREBF1* promoter. However, the mechanism addressing *srebf1* downregulation in *S. aurata* treated with FAT-1 and FAT-2 may be an antagonistic action of LXR α , a transcription factor encoded by *nr1h3*, which expression levels were upregulated under this condition.

PPARA is a nuclear receptor activated by a wide range of ligands including fatty acids and fatty acid metabolites, such as eicosanoids. In the mammalian liver, PPARA controls the expression of genes involved in fatty acid uptake, intracellular transport, acyl-CoA formation and fatty acid mitochondrial and peroxisomal oxidation, ketogenesis and lipoprotein metabolism (Bougarne et al., 2018a). PPARA-mediated transcriptional regulation of lipid metabolism is achieved either indirectly via SREBP1 (Fernández-Alvarez et al., 2011), or through direct mediation on the expression of fatty acid transport proteins and transferases such as CPT1A (Bougarne et al., 2018a), as it may occur in the liver of *S. aurata* treated with FAT-2 at short time. In the present study, long-term sustained expression of FAT-1 and FAT-2 downregulated *ppara* in the liver of *S. aurata*. Supplementation of fish oil to rodents enhances *Ppara* expression in the liver (Hein et al., 2010a; Kamisako et al., 2012a), possibly as a result of increased availability of *n*-3 LC-PUFA. The effect of dietary fish oil on *ppara* expression in fish varies among the species. Similar to *S. aurata* expressing FAT-1 and FAT-2, fish oil supplementation was shown to decrease the hepatic mRNA levels of *ppara* in *S. aurata* and juvenile turbot (Ofori-

Mensah et al., 2020a; Peng et al., 2014), while the opposite effect was reported in large yellow croaker and lean, but not fat Atlantic salmon (Du et al., 2017a; Morais et al., 2011a). Similarly, LC-PUFA, especially *n*-3 LC-PUFA, are effective to activate Ppara and increase its gene expression as well (Echeverría et al., 2016; Tapia et al., 2014). However, as pointed out by Peng et al., (Peng et al., 2014) fatty acid-derived factors other than EPA-mediated activation may contribute to species-specific regulation of *ppara* expression in fishes. Additionally, in fish, two homologous *ppara1* and *ppara2* have been identified and their response to fatty acid supplement varies not only from fish species but also between the two homologs. For example, dietary replacement of fish oil with vegetable oil increased expression of *ppara2* in the liver of rainbow trout but decreased the expression in Japanese seabass (Dong et al., 2017), while diet-enriched ALA or fish oil inhibited hepatic *ppara1* and upregulated *ppara2* mRNA levels when compared with PA- or OA-rich diets in the same species (Dong et al., 2015).

Similar to *ppara*, activation of Pparg is also involved in regulating lipogenesis via elevating expression of genes such as *Acaca*, *Scd1* and *Fasn* in mice liver (Wang et al., 2020). Meanwhile SFA are unable to bind PPARG (Xu et al., 1999), PUFA including *n*-3 and *n*-6 fatty acids exhibit binding affinity with PPARG (Xu et al., 1999). In spite of this, increased dietary *n*-3/*n*-6 LC-PUFA ratio was associated with decreased hepatic *pparg* levels in juvenile grass carp and large yellow croaker (Tian et al., 2014; Wang et al., 2012). However, contradictory results were obtained about the effect of FAT-1 on PPARG expression: as in *S. aurata*, FAT-1 transgenic zebrafish showed decreased expression of hepatic *pparg* (Sun et al., 2020a), while goat cells transfected with FAT-1 showed increased expression (Fan et al., 2016). Supplementation of *n*-3 LC-PUFA or fish oil also shows controversial effects on *pparg* transcript levels between fish species (Tian et al., 2014; You et al., 2017), which may due to the existence of two isoforms encoded from same gene by different promoters (Lee et al., 2018).

5.2.5 Effects of FAT-1 and FAT-2 expression on glycolysis-gluconeogenesis, PPP, the Krebs cycle and amino acid metabolism

The effect of *C. elegans* FAT-1 and FAT-2 on glucose metabolism remains largely unknown. Nevertheless, the general knowledge of hepatic coordination between glycolysis and lipogenesis drove us to further evaluate the effects of FAT-1 and FAT-2 expression on glycolysis-gluconeogenesis, PPP, the Krebs cycle and amino acid metabolism in the *S. aurata* liver.

Glycolysis-gluconeogenesis. In the present study, FAT-2 and FAT-1 + FAT-2 activated hepatic glycolysis in both short- and long-term periodically treated *S. aurata*. By controlling the flux through

the fructose-6-phosphate (fru-6-P)/fructose-1,6-bisphosphate (fru-1,6-P₂) substrate cycle, *pfkl* and *fbp1* exert critical roles in hepatic glycolysis-gluconeogenesis. Although the mRNA levels of *pfkl* and *fbp1* were not significantly affected by any of the treatments, expression of FAT-2 and FAT-1 + FAT-2 promoted higher levels of PFKL/FBP1 activity ratio, possibly as a result of *pfkfb1* upregulation. The bifunctional enzyme *pfkfb1* catalyses the synthesis and degradation of fructose-2,6-bisphosphate (fru-2,6-P₂), which is a major regulator of glycolysis-gluconeogenesis through allosteric activation of PFKL and inhibition of FBP1 (Okar et al., 2004). We previously showed that refeeding and high carbohydrate diets upregulate *pfkfb1* and the kinase activity of the bifunctional enzyme in the liver of *S. aurata*, leading to concomitant increased fru-2,6-P₂ levels (I Metón et al., 1999a; Metón et al., 2000). As in mammals, fru-2,6-P₂ is an allosteric activator of *S. aurata* Pfkf (Mediavilla et al., 2008). Therefore, after long-term sustained expression of FAT-1 and FAT-2, the results obtained suggest that *pfkfb1* upregulation in the liver of fish expressing FAT-2 (and FAT-1 + FAT-2) may be a key step favouring the glycolytic flux through the fru-6-P/fru-1,6-P₂ substrate cycle, which in turn will increase the hepatic content of fru-1,6-P₂ (Jurica et al., 1998). Altogether led to higher levels of Pfkf/Fbp1 activity ratio and a concomitant activation of glycolysis. Pklr activity is known to be allosterically promoted by its upstream substrates such as PEP and fru-1,6-P₂. Indeed, in line with the elevated expression of *pfkfb1*, which may suggest enhanced production of fru-1,6-P₂, increased Pklr activity were observed in fish expressing FAT-2 and FAT-1 + FAT-2. On the other hand, G6Pase, the catalytic unit of which is encoded by *G6PC1*, hydrolyzes the phosphate of glu-6-P to produce glucose. In present study, fish expressing FAT-1 for 72 h decreased hepatic *g6pc1* expression, while long-term sustained expression of FAT-1 + FAT-2 showed marginal effects. The transcriptional changes of *g6pc1* may ascribe to the regulation by Hnf4a, which binding element was found in *S. aurata* *g6pc* promoter (Salgado et al., 2004). Nevertheless, hepatic expression of *pkc1* was scarcely affected, which may suggest negligible changes of the gluconeogenic flux in both short-term and long-term periodically treated fish.

PPP. To our knowledge, the effect of *C. elegans* FAT-1 and FAT-2 on PPP has not been previously addressed. In the present study, long-term expression of FAT-2 significantly promoted the expression and activity of G6pd, which encodes the rate-limiting enzyme in the oxidative phase of the PPP. Correspondingly, the activity of Pgd, which also belongs to the PPP, was elevated by FAT-2 in both the short- and long-term studies, suggesting stimulation of this pathway in the *S. aurata* liver. Activation of G6pd and Pgd produce NADPH, a reducing power necessary for fatty acid synthesis. Therefore, fish expressing FAT-2 (and co-expressing FAT-2 together with FAT-1) may favor hepatic lipogenesis through the activation of PPP. Our findings support that fatty acid composition,

particularly the *n-3/n-6* ratio, also seems to regulate the hepatic expression of *g6pd*. In agreement with *g6pd* upregulation by *n-3* LC-PUFA, fish oil stimulated G6PD activity in the rat liver (Yilmaz et al., 2004), and dietary supplementation with *n-3* PUFA increased *G6pd* mRNA levels in the pig muscle (Vitali et al., 2018). Furthermore, *n-6* PUFA, particularly LA, decreased *G6pd* mRNA levels in rat hepatocytes (Kohan et al., 2011). Additionally, certain fatty acid altered by the expression of FAT-1 and FAT-2 may also affect PPP activation via insulin signals, such as MUFA. Meanwhile lack of *n-3* PUFA effects on insulin signaling (Akinkuolie et al., 2011), MUFA was shown to improve insulin sensitivity (Johns et al., 2020), the improvement of which is evident in elevating hepatic G6pd expression and activity in mammals and fish (Enes et al., 2010; Polakof et al., 2010; F. Wang et al., 2012). Although not statistically significant, in the present study, the highest MUFA proportions were observed in fish expressing FAT-2. Species-specific regulation of *g6pd* expression by fatty acid composition may occur in other fishes. In this regard, total replacement of fish oil by vegetable oil did not affect G6pd activity but increased the mRNA levels in the liver of Nile tilapia (Ayisi et al., 2018), while enhanced G6pd activity in the liver of Atlantic salmon (Menoyo et al., 2005). Bearing in mind a general trend to downregulate *de novo* hepatic lipogenesis in *S. aurata* co-expressing FAT-1 and FAT-2, NADPH resulting from *g6pd* upregulation by *n-3* LC-PUFA may reinforce cellular protection from oxidative stress.

LXR promotes the expression of carbohydrate response element binding protein (*ChREBP*) (Wang and Tontonoz, 2018). Thus, regarding the elevated Pfk1/Fbp1 activity ratio and *pkfr* expression and enzyme activity by FAT-1 + FAT-2, the induced *nr1h3* may also contribute to the activation of glycolysis via Chrebp (Iizuka and Horikawa, 2008). Furthermore, LXR stimulating glycolysis was also shown via inducing *PFKFB* expression in human (Zhao et al., 2012). Additionally, the LXR α -*ChREBP* was also shown to promote *G6PD* expression (Zhu et al., 2021). In line with these findings, in the present study, hepatic *nr1h3*, *g6pd* and *pfkfb1* showed similar expression pattern by the treatments in both short- and long-term periodically treated fish.

The nuclear receptor *hnf4a* is a master regulator of liver metabolism through transcriptional regulation of target genes involved in glucose metabolism, lipid metabolism and hepatocyte differentiation (Meng et al., 2016). Early studies showed that DHA had 2.7-fold higher binding affinity for HNF4A than EPA (Hertz et al., 1998). Consistently, DHA supplement upregulated hepatic HNF4 mRNA in mice (Zhuang et al., 2021), while the effect of EPA was marginal (Zhuang et al., 2021). Similarly, dietary supplementation with dried marine algae, rich in *n-3* LC-PUFA (particularly DHA),

induced *hnf4a* expression in the pig liver (Meadus et al., 2011). In agreement, FAT-1 transgenic mice presented increased mRNA levels of *hnf4a* in the liver (Kim et al., 2012). The present study showed a trend to upregulate hepatic *hnf4a* expression in fish treated by FAT-2 and FAT-1 + FAT-2 both at short-term and after long-term sustained expression of the exogenous enzymes, while no effect was observed in fish treated with FAT-1 alone. Since DHA values were similarly increased by FAT-1 and FAT-2 in the liver of *S. aurata*, upregulation of *hnf4a* expression may be due to DHA levels but also can be affected by additional pathways associated with *hnf4a* expression. Consistent with enhancement of glycolysis in *S. aurata*, *hnf4a* expression was previously shown to increase in *S. aurata* under glycolytic conditions versus gluconeogenic conditions such as fasting and treatment with streptozotocin (Salgado et al., 2012). Furthermore, Hnf4a was shown to induce the expression of *nr1h3* (Theofilatos et al., 2016a), a nuclear receptor that is also involved in glucose and lipid metabolism (Iizuka and Horikawa, 2008).

The Krebs cycle. In present study, both at short-term and in long-term periodically treated fish, Ogdh activity decreased in *S. aurata* expressing FAT-2, while activity of Idh was not affected by any of the treatments assayed. Thus, the reduction of Ogdh activity may indicate accumulation of α -ketoglutarate, which may flow out from the Krebs cycle and be utilized for biosynthetic purposes (Metallo et al., 2012). Co-enzyme thiamine diphosphate, substrates, products, allosteric effectors and thioredoxin are known to affect OGDH activity (Bunik and Strumilo, 2009), which may be affected in turn by changes in the fatty acid profile. Mediation through NADH, the product and allosteric inhibitor of Ogdh, among other factors that can be affected by fatty acids, may favor reasoning the decreased activity by FAT-2. In this regard, induced glycolytic flux observed in fish expressing FAT-2 can contribute to NADH production and allosteric inhibition of Ogdh activity. Indeed, FAT-2-dependent inhibition of Ogdh activity was abrogated in fish co-expressing both FAT-1 and FAT-2. Further investigation is needed to unravel the molecular mechanism that mediates between the expression of fish codon-optimized FAT-1 and FAT-2 and the flux through the Krebs cycle in *S. aurata*.

Amino acid metabolism. In the present study, scarce differences of Alt and Ast activity were noticed among the treatments in *S. aurata* liver. In vertebrates, certain fatty acids were shown to affect Alt and Ast activities. For example, dietary *n*-3 LC-PUFA trends to decrease serum Alt and Ast activities in juvenile *Onychostoma macrolepis* (Gou et al., 2020), while dietary *n*-6 LC-PUFA increases the activities of the two enzymes in serum of Japanese eel (Shahkar et al., 2016). Other fatty acid such as

DISCUSSION

erucic acid, which is prevalent in rapeseed oil, has been shown to increase ALT and AST activities in rat serum (Hasan et al., 2018). Thus, lack of specific effects on hepatic Alt and Ast activity levels in the *S. aurata* periodically treated with FAT-1 and FAT-2 could result from compensatory effects of the contents of individual fatty acids.

6 CONCLUSIONS

1. Transient transfection of HepG2 cells showed that pSG5-FAT-1 and pSG5-FAT-2 are efficient constructs for driving the expression of fish codon-optimized *C. elegans* FAT-1 and FAT-2 in eukaryotic cells.
2. Co-expression of fish codon-optimized *C. elegans* FAT-1 and FAT-2 for 48 hours in HepG2 cells significantly increased fatty acid proportions of SA (18:0), OA (18:1*n*-9c), LA (18:2*n*-6c), ARA (20:4*n*-6), PUFA, *n*-3 fatty acids, *n*-6 fatty acids and *n*-9 fatty acids.
3. Seventy-two hours following intraperitoneal administration of a single dose of chitosan-TPP complexed with pSG5-FAT-1 and pSG5-FAT-2 (10 µg plasmid/g BW) allowed detection of high mRNA levels of fish codon-optimized *C. elegans* FAT-1 (16.5-fold increase) and FAT-2 (21.2-fold increase) in the liver of *S. aurata*.
4. Co-expression of fish codon-optimized *C. elegans* FAT-1 and FAT-2 in the liver of *S. aurata* for 72 hours decreased serum triglycerides to 53.4 % of control values.
5. Treatment with chitosan-TPP-DNA nanoparticles for 72 hours after a single dose also affected the fatty acid profile in the liver of *S. aurata*. Expression of FAT-1 increased 1.3-fold EPA (20:5*n*-3) and total *n*-3 fatty acids, while expression of FAT-2 decreased SA (18:0) to 69.7 % of control levels. Co-expression of FAT-1 + FAT-2 increased 1.4-fold DHA (22:6*n*-3) and 1.1-fold PUFA, while decreased heptadecenoic acid (17:1*n*-7), dihomo- γ -linolenic acid (20:3*n*-6) and nervonic acid (24:1*n*-9), to 9.5 %, 23 % and 25 % of control levels.
6. Seventy-two hours after nanoparticle administration, treatment with FAT-1 significantly decreased the expression of *g6pc1* (to 63.5 % of controls), while increased *fbp1* (1.4-fold) expression in the liver. FAT-2 increased the hepatic expression of *pfkl* (1.5-fold), *fbp1* (1.5-fold) and *pklr* (1.3-fold), while co-expression of FAT-1 and FAT-2 increased 1.8-fold the mRNA levels of *pfkl*. Fish expressing FAT-2 significantly increased the activity of key enzymes in both glycolysis (Pfk1, 1.8-fold; Pklr, 1.7-fold) and gluconeogenesis (Fbp1, 1.6-fold). Similarly, co-expression of FAT-1 + FAT-2 induced the activity of Pklr (1.4-fold) and Fbp1 (1.5-fold). Any treatment assayed affected significantly the Pfk1/Fbp1 enzyme activity ratio. In regard of other metabolic pathways, FAT-2 induced the PPP by increasing Pgd activity 1.4-fold, FAT-1 and FAT-2 caused opposite effects on Ogdh activity from the Krebs cycle (FAT-1 increased hepatic Ogdh activity 1.6-fold, while FAT-2 reduced Ogdh activity to 39.9 % of control values), and Alt and Ast transaminases were not significantly altered.

7. Short-term expression of FAT-2 induced hepatic *ppara* mRNA levels to 1.3-fold compared to control fish. FAT-2 and its co-expression with FAT-1, significantly decreased hepatic mRNA levels of *pparg* (to 48.6 % and 50.7 % of controls, respectively), while increased the expression of *bnf4a* (1.6-fold and 2.2-fold, respectively). Expression of FAT-1, FAT-2 and FAT-1 + FAT-2 significantly downregulated *srebfl* to 60.5 %, 42.1 % and 35.6 % of control values, respectively.

8. Seventy-two hours after nanoparticle administration, treatments with FAT-1, FAT-2 and FAT-1 + FAT-2 suppressed expression of genes *acaca* (to 5.9 %, 3.4 % and 4.4 % of control values, respectively), *acacb* (to 64.8 %, 72.3 % and 53.5 %), *fasn* (to 25.3 %, 23.3 % and 19.7 %), *scd1a* (to 18.2 %, 6.4 % and 8.5 %) and *fads2* (45.1 %, 12.2 % and 41.4 %). Expression of FAT-1 and FAT-2 decreased to 21.7 % and 27.3 % of the expression of *hmgcr* in control fish, respectively. Expression of FAT-2 increased 1.7-fold the expression of *cpt1a* in the liver.

9. The mRNA levels of fish codon-optimized *C. elegans* FAT-1 and FAT-2 lasts at high levels (74.8- and 70.2-fold increased, respectively) in the liver of *S. aurata* for at least 4 weeks after a single intraperitoneal injection of chitosan-TPP-pSG5-FAT-1 and chitosan-TPP-pSG5-FAT-2.

10. Periodical administration (every 4 weeks) of intraperitoneal doses of chitosan-TPP complexed with pSG5-FAT-1 and pSG5-FAT-2 (3 doses in a total period of 70 days, each dose with 10 µg plasmid/g BW) to *S. aurata*, significantly increased the mRNA levels of FAT-1 and FAT-2 in the liver (201.8- and 297.4-fold, respectively) and intestine (10.6- 24.7-fold, respectively), while no significant detection was observed in skeletal muscle and brain.

11. Seventy days following periodical administration of chitosan-TPP nanoparticles complexed with pSG5-FAT-1 and pSG5-FAT-2, expression of FAT-1 and FAT-1 + FAT-2 significantly increased weight gain (18 % and 26 % of increase, respectively) in *S. aurata*. In contrast, HSI significantly decreased in fish treated with FAT-1 and FAT-1 + FAT-2 to 72 % of control values. In regard of body composition, co-expression of FAT-1 + FAT-2 caused a 7.6 % decrease of whole-body crude protein.

12. Sustained co-expression of FAT-1 and FAT-2 for 70 days decreased serum triglycerides and cholesterol to 41.6 % and 67.7 % of control levels, respectively, in *S. aurata*.

13. In the liver of *S. aurata* periodically administered with chitosan-TPP-DNA, expression of FAT-1 significantly increased EPA (20:5n-3, 1.5-fold), DHA (22:6n-3, 2.4-fold) and total n-3 fatty acids (1.7-

fold), while decreased palmitoleic acid (16:1 n -7; to 58.4 % of control levels) and the n -6/ n -3 ratio (to 60.3 % of control values). Expression of FAT-2 decreased the n -6/ n -3 ratio (to 66.9 % of control values). Co-expression of FAT-1 + FAT-2 significantly increased EPA (20:5 n -3, 1.6-fold), DHA (22:6 n -3, 2.3-fold) and total n -3 fatty acids (1.7-fold), while reduced the n -6/ n -3 ratio (to 63.7 % of control values).

14. The fatty acid profile of the skeletal muscle of *S. aurata* was significantly affected by periodical administration of chitosan-TPP-DNA nanoparticles to express fish codon-optimized *C. elegans* FAT-1 and FAT-2. Co-expression of FAT-1 + FAT-2 significantly decreased total SFA (to 57.1 % of controls), myristic acid (14:0; to 34.4 %), PA (16:0; to 56.3 %) and margaric acid (17:0; to 50.0 %), while increased SA (18:0; 1.2-fold) and raised arachidic acid (20:0), behenic acid (22:0), tricosylic acid (23:0) and lignoceric acid (24:0) from non-detectable levels in control fish to low but detectable levels. Co-expression of FAT-1 + FAT-2 also increased MUFA (1.3-fold), PUFA (1.3-fold) and total n -9 (1.5-fold), n -6 (1.1-fold) and n -3 (2.2-fold) fatty acids, while decreased the n -6/ n -3 ratio to 52.0 % of control levels. In regard of unsaturated fatty acids, co-expression of FAT-1 + FAT-2 significantly increased EPA (20:5 n -3, 1.7-fold) and DHA (22:6 n -3, 3.0-fold) from the n -3 series, LA (18:2 n -6c; 1.1-fold), OA (18:1 n -9c; 1.5-fold), *cis*-10-heptadecenoic acid (17:1 n -7; 1.5-fold), gondoic acid (20:1 n -9; 3.2-fold), erucic acid (22:1 n -9; 5.2-fold), eicosadienoic acid (20:2 n -6; 6.2-fold) and ARA (20:4 n -6; 1.4-fold), while decreased palmitoleic acid (16:1 n -7) to 61.5 % of control levels. In contrast to co-expression of FAT-1 + FAT-2, FAT-1 and FAT-2 alone only affected significantly margaric acid (17:0), which decreased in both cases to 50 % of control values.

15. Seventy days of sustained expression of FAT-2 in the liver of *Sparus aurata* induced the hepatic expression of glycolytic genes such as *pkf1* (1.5-fold) and *pkfb1* (1.4-fold), and the activity of rate-limiting enzymes in glycolysis (Pfk1, 1.6-fold; Pk1r, 1.6-fold) and PPP (G6pd, 1.5-fold; Pgd, 1.6-fold), while decreased Ogdh (39 % of control values). Similarly, co-expression of FAT-1 + FAT-2 upregulated the mRNA levels of *pkf1* (1.9-fold) and *pkfb1* (1.4-fold), and PKL activity (1.9-fold).

16. Sustained co-expression of FAT-1 + FAT-2 for 70 days significantly downregulated the hepatic expression of key genes involved in cholesterol synthesis (*hmgr*, to 64.2 % of control values) and fatty acid synthesis (*acaca*, to 31.4 %; *acacb*, to 65.0 %), desaturation (*fads2*, to 69.4 %) and elongation (*elovl4b*, to 59.1 %; *elovl5*, to 41.8 %). Treatment with FAT-1 significantly decreased the mRNA levels of fatty acid elongases (*elovl4a*, to 43.3 %; *elovl4b*, 45.4 %; *elovl5*, to 62.3 %), while FAT-2 expression

downregulated *elov15* (to 43.6 %).

17. In regard of transcription factors involved in lipogenesis, sustained expression of FAT-1 downregulated the expression of *ppara* (to 46.0 % of control values) and *srebf1* (to 46.0 %). Treatment with FAT-2 also decreased *ppara* mRNA levels (to 56.3 %), while increased *hmf4a* expression (1.5-fold). Co-expression of FAT-1 + FAT-2 downregulated *pparg* (to 62.8 %) and *srebf1* (to 41.8 %), while upregulated *nr1h3* (1.6-fold).

7 REFERENCES

REFERENCES

- Abu-Elheiga, L., Brinkley, W.R., Zhong, L., Chirala, S.S., Woldegiorgis, G., Wakil, S.J., 2000. The subcellular localization of acetyl-CoA carboxylase 2. *Proc. Natl. Acad. Sci. U. S. A.* 97, 1444–1449. <https://doi.org/10.1073/pnas.97.4.1444>
- Abu-Elheiga, L., Matzuk, M.M., Abo-Hashema, K.A.H., Wakil, S.J., 2001. Continuous fatty acid oxidation and reduced fat storage in mice lacking acetyl-coa carboxylase 2. *Science (80-.)*. 291, 2613–2616. <https://doi.org/10.1126/science.1056843>
- Adamson, A.W., Suchankova, G., Rufo, C., Nakamura, M.T., Teran-Garcia, M., Clarke, S.D., Gettys, T.W., 2006. Hepatocyte nuclear factor-4 α contributes to carbohydrate-induced transcriptional activation of hepatic fatty acid synthase. *Biochem. J.* 399, 285–295. <https://doi.org/10.1042/BJ20060659>
- Ahmadian, M., Suh, J.M., Hah, N., Liddle, C., Atkins, A.R., Downes, M., Evans, R.M., 2013. Ppar γ signaling and metabolism: The good, the bad and the future. *Nat. Med.* 19, 557–566. <https://doi.org/10.1038/nm.3159>
- Akinkuolie, A.O., Ngwa, J.S., Meigs, J.B., Djoussé, L., 2011. Omega-3 polyunsaturated fatty acid and insulin sensitivity: A meta-analysis of randomized controlled trials. *Clin. Nutr.* 30, 702–707. <https://doi.org/10.1016/j.clnu.2011.08.013>
- Al-Souti, A., Al-Sabahi, J., Soussi, B., Goddard, S., 2012. The effects of fish oil-enriched diets on growth, feed conversion and fatty acid content of red hybrid tilapia, *Oreochromis* sp. *Food Chem.* 133, 723–727. <https://doi.org/10.1016/j.foodchem.2012.01.080>
- Alimuddin, Kiron, V., Satoh, S., Takeuchi, T., Yoshizaki, G., 2008. Cloning and over-expression of a masu salmon (*Oncorhynchus masou*) fatty acid elongase-like gene in zebrafish. *Aquaculture* 282, 13–18. <https://doi.org/10.1016/J.AQUACULTURE.2008.06.033>
- Alimuddin, Yoshizaki, G., Kiron, V., Satoh, S., Takeuchi, T., 2007. Expression of Masu Salmon $\Delta 5$ -Desaturase-Like Gene Elevated EPA and DHA Biosynthesis in Zebrafish. *Mar. Biotechnol.* 9, 92–100. <https://doi.org/10.1007/s10126-006-6003-y>
- An, L., Pang, Y.W., Gao, H.M., Tao, L., Miao, K., Wu, Z.H., Tian, J.H., 2012. Heterologous expression of *C. elegans* fat-1 decreases the n-6/n-3 fatty acid ratio and inhibits adipogenesis in 3T3-L1 cells. *Biochem. Biophys. Res. Commun.* 428, 405–410. <https://doi.org/10.1016/j.bbrc.2012.10.068>
- Antoniou, M., Geraghty, F., Hurst, J., Grosveld, F., 1998. Efficient 3'-end formation of human β -globin mRNA in vivo requires sequences within the last intron but occurs independently of the splicing reaction. *Nucleic Acids Res.* 26, 721–729. <https://doi.org/10.1093/nar/26.3.721>
- Ayisi, C.L., Zhao, J.L., Hua, X.M., Apraku, A., 2018. Replacing fish oil with palm oil: Effects on mRNA expression of fatty acid transport genes and signalling factors related to lipid metabolism in Nile tilapia (*Oreochromis niloticus*). *Aquac. Nutr.* 24, 1822–1833. <https://doi.org/10.1111/anu.12821>
- Bachir, Z.A., Huang, Y.K., He, M.Y., Huang, L., Hou, X.Y., Chen, R.J., Gao, F., 2018. Effects of PEG surface density and chain length on the pharmacokinetics and biodistribution of methotrexate-loaded chitosan nanoparticles. *Int. J. Nanomedicine* 13, 5657–5671. <https://doi.org/10.2147/IJN.S167443>
- Bargut, T.C.L., Frantz, E.D.C., Mandarim-De-Lacerda, C.A., Aguila, M.B., 2014. Effects of a diet rich in n-3 polyunsaturated fatty acids on hepatic lipogenesis and beta-oxidation in mice. *Lipids* 49, 431–444. <https://doi.org/10.1007/s11745-014-3892-9>
- Belayev, L., Khoutorova, L., Atkins, K.D., Bazan, N.G., 2009. Robust docosahexaenoic acid-mediated neuroprotection in a rat model of transient, focal cerebral ischemia. *Stroke*. 40, 3121–3126.

REFERENCES

- <https://doi.org/10.1161/STROKEAHA.109.555979>
- Benoist, C., Chambon, P., 1981. In vivo sequence requirements of the SV40 early promoter region. *Nature* 290, 304–310.
<https://doi.org/10.1038/290304a0>
- Bertrand, S., Brunet, F.G., Escriva, H., Parmentier, G., Laudet, V., Robinson-Rechavi, M., 2004. Evolutionary genomics of nuclear receptors: From twenty-five ancestral genes to derived endocrine systems. *Mol. Biol. Evol.* 21, 1923–1937.
<https://doi.org/10.1093/molbev/msh200>
- Betancor, M.B., Sprague, M., Montero, D., Usher, S., Sayanova, O., Campbell, P.J., Napier, J.A., Caballero, M.J., Izquierdo, M., Tocher, D.R., 2016. Replacement of Marine Fish Oil with de novo Omega-3 Oils from Transgenic Camelina sativa in Feeds for Gilthead Sea Bream (*Sparus aurata* L.). *Lipids* 51, 1171–1191. <https://doi.org/10.1007/s11745-016-4191-4>
- Bhatt, D.L., Steg, P.G., Miller, M., Brinton, E.A., Jacobson, T.A., Ketchum, S.B., Doyle, R.T., Juliano, R.A., Jiao, L., Granowitz, C., Tardif, J.-C., Ballantyne, C.M., 2019. Cardiovascular Risk Reduction with Icosapent Ethyl for Hypertriglyceridemia. *N. Engl. J. Med.* 380, 11–22. <https://doi.org/10.1056/nejmoa1812792>
- Bhattacharya, A., Chandrasekar, B., Rahman, M.M., Banu, J., Kang, J.X., Fernandes, G., 2006a. Inhibition of inflammatory response in transgenic fat-1 mice on a calorie-restricted diet. *Biochem. Biophys. Res. Commun.* 349, 925–930.
<https://doi.org/10.1016/j.bbrc.2006.08.093>
- Bhattacharya, A., Chandrasekar, B., Rahman, M.M., Banu, J., Kang, J.X., Fernandes, G., 2006b. Inhibition of inflammatory response in transgenic fat-1 mice on a calorie-restricted diet. *Biochem. Biophys. Res. Commun.* 349, 925–930.
<https://doi.org/10.1016/J.BBRC.2006.08.093>
- Bilal, S., Haworth, O., Wu, L., Weylandt, K.H., Levy, B.D., Kang, J.X., 2011. Fat-1 transgenic mice with elevated omega-3 fatty acids are protected from allergic airway responses. *Biochim. Biophys. Acta - Mol. Basis Dis.* 1812, 1164–1169.
<https://doi.org/10.1016/j.bbadis.2011.05.002>
- Bjørndal, B., Brattelid, T., Strand, E., Vigerust, N.F., Svungen, G.F.T., Svardal, A., Nygård, O., Berge, R.K., 2013. Fish Oil and the Pan-PPAR Agonist Tetradecylthioacetic Acid Affect the Amino Acid and Carnitine Metabolism in Rats. *PLoS One* 8. <https://doi.org/10.1371/journal.pone.0066926>
- Bligh, E.G., Dyer, W.J., 1959. A rapid method of total lipid extraction and purification. *Can. J. Biochem. Physiol.* 37, 911–917.
<https://doi.org/10.1139/o59-099>
- Bordoni, A., Di Nunzio, M., Danesi, F., Biagi, P.L., 2006. Polyunsaturated fatty acids: From diet to binding to ppars and other nuclear receptors. *Genes Nutr.* 1, 95–106. <https://doi.org/10.1007/bf02829951>
- Bougarne, N., Weyers, B., Desmet, S.J., Deckers, J., Ray, D.W., Staels, B., De Bosscher, K., 2018a. Molecular actions of PPAR α in lipid metabolism and inflammation. *Endocr. Rev.* 39, 760–802. <https://doi.org/10.1210/er.2018-00064>
- Bougarne, N., Weyers, B., Desmet, S.J., Deckers, J., Ray, D.W., Staels, B., De Bosscher, K., 2018b. Molecular Actions of PPAR α in Lipid Metabolism and Inflammation. *Endocr. Rev.* 39, 760–802. <https://doi.org/10.1210/ER.2018-00064>
- Bouraoui, L., Sánchez-Gurmaches, J., Cruz-García, L., Gutiérrez, J., Benedito-Palos, L., Pérez-Sánchez, J., Navarro, I., 2011. Effect of dietary fish meal and fish oil replacement on lipogenic and lipoprotein lipase activities and plasma insulin in gilthead sea bream (*Sparus aurata*). *Aquac. Nutr.* 17, 54–63. <https://doi.org/10.1111/j.1365-2095.2009.00706.x>
- Boyle, K.E., Magill-Collins, M.J., Newsom, S.A., Janssen, R.C., Friedman, J.E., 2020. Maternal Fat-1 Transgene Protects Offspring from Excess Weight Gain, Oxidative Stress, and Reduced Fatty Acid Oxidation in Response to High-Fat

REFERENCES

- Diet. *Nutrients* 12. <https://doi.org/10.3390/NU12030767>
- Bozkir, A., Saka, O.M., 2004. Chitosan Nanoparticles for Plasmid DNA Delivery: Effect of Chitosan Molecular Structure on Formulation and Release Characteristics. *Drug Deliv. J. Deliv. Target. Ther. Agents* 11, 107–112. <https://doi.org/10.1080/10717540490280705>
- Bunik, V.I., Strumilo, S., 2009. Regulation of Catalysis Within Cellular Network: Metabolic and Signaling Implications of the 2-Oxoglutarate Oxidative Decarboxylation. *Curr. Chem. Biol.* 3, 279–290. <https://doi.org/10.2174/187231309789054904>
- Burr, G.O., Burr, M.M., 1929. a New Deficiency Disease Produced By the Rigid Exclusion of Fat From the Diet. *J. Biol. Chem.* 82, 345–367. [https://doi.org/10.1016/s0021-9258\(20\)78281-5](https://doi.org/10.1016/s0021-9258(20)78281-5)
- Busacker, G.P., Adelman, I.R., Goolish, E.M., 1990. Growth, in: Schreck, C.B., Moyle, P.B. (Eds.), *Methods for Fish Biology*. American Fisheries Society, Bethesda, pp. 363–387. <https://doi.org/10.47886/9780913235584.CH11>
- Calder, P.C., 2017. Omega-3 fatty acids and inflammatory processes: From molecules to man. *Biochem. Soc. Trans.* 45, 1105–1115. <https://doi.org/10.1042/BST20160474>
- Carmona-Antoñanzas, G., Tocher, D.R., Martínez-Rubio, L., Leaver, M.J., 2014. Conservation of lipid metabolic gene transcriptional regulatory networks in fish and mammals. *Gene* 534, 1–9. <https://doi.org/10.1016/j.gene.2013.10.040>
- Carpenter, K.E., De Angelis, N., 2016. The living marine resources of the Eastern Central Atlantic. Volume 4: Bony fishes part 2 (Perciformes to Tetradontiformes) and Sea turtles, FAO Species Identification Guide for Fishery Purposes.
- Carrillo, C., Suñé, J.M., Pérez-Lozano, P., García-Montoya, E., Sarrate, R., Fàbregas, A., Miñarro, M., Tico, J.R., 2014. Chitosan nanoparticles as non-viral gene delivery systems: Determination of loading efficiency. *Biomed. Pharmacother.* 68, 775–783. <https://doi.org/10.1016/j.biopha.2014.07.009>
- Carvalho, M., Marotta, B., Xu, H., Geraert, P.-A., Kaushik, S., Montero, D., Izquierdo, M., 2022. Complete replacement of fish oil by three microalgal products rich in n-3 long-chain polyunsaturated fatty acids in early weaning microdiets for gilthead sea bream (*Sparus aurata*). *Aquaculture* 558, 738354. <https://doi.org/10.1016/J.AQUACULTURE.2022.738354>
- Caseras, A., Metón, I., Fernández, F., Baanante, I. V., 2000. Glucokinase gene expression is nutritionally regulated in liver of gilthead sea bream (*Sparus aurata*). *Biochim. Biophys. Acta - Gene Struct. Expr.* 1493, 135–141. [https://doi.org/10.1016/S0167-4781\(00\)00173-1](https://doi.org/10.1016/S0167-4781(00)00173-1)
- Castro, C., Couto, A., Diógenes, A.F., Corraze, G., Panserat, S., Serra, C.R., Oliva-Teles, A., 2019. Vegetable oil and carbohydrate-rich diets marginally affected intestine histomorphology, digestive enzymes activities, and gut microbiota of gilthead sea bream juveniles. *Fish Physiol. Biochem.* 45, 681–695. <https://doi.org/10.1007/s10695-018-0579-9>
- Castro, L.F.C., Tocher, D.R., Monroig, O., 2016. Long-chain polyunsaturated fatty acid biosynthesis in chordates: Insights into the evolution of Fads and Elovl gene repertoire. *Prog. Lipid Res.* 62, 25–40. <https://doi.org/10.1016/j.plipres.2016.01.001>
- Cha, J.Y., Repa, J.J., 2007. The liver X receptor (LXR) and hepatic lipogenesis. The carbohydrate-response element-binding protein is a target gene of LXR. *J. Biol. Chem.* 282, 743–751. <https://doi.org/10.1074/JBC.M605023200>
- Chakravarthy, M. V., Lodhi, I.J., Yin, L., Malapaka, R.R.V., Xu, H.E., Turk, J., Semenkovich, C.F., 2009. Identification of a Physiologically Relevant Endogenous Ligand for PPAR α in Liver. *Cell* 138, 476–488. <https://doi.org/10.1016/j.cell.2009.05.036>

REFERENCES

- Chang, M., Zhang, T., Han, X., Tang, Q., Yanagita, T., Xu, J., Xue, C., Wang, Y., 2018. Comparative Analysis of EPA/DHA-PL Forage and Liposomes in Orotic Acid-Induced Nonalcoholic Fatty Liver Rats and Their Related Mechanisms. *J. Agric. Food Chem.* 66, 1408–1418. <https://doi.org/10.1021/acs.jafc.7b05173>
- Chen, Y., Mei, M., Zhang, P., Ma, K., Song, G., Ma, X., Zhao, T., Tang, B., Ouyang, H., Li, G., Li, Z., 2013. The generation of transgenic mice with fat1 and fat2 genes that have their own Polyunsaturated Fatty Acid Biosynthetic Pathway. *Cell. Physiol. Biochem.* 32, 523–532. <https://doi.org/10.1159/000354456>
- Cheng, C.-L., Huang, S.-J., Wu, C.-L., Gong, H.-Y., Ken, C.-F., Hu, S.-Y., Wu, J.-L., 2015. Transgenic expression of omega-3 PUFA synthesis genes improves zebrafish survival during *Vibrio vulnificus* infection. *J. Biomed. Sci.* 22, 103. <https://doi.org/10.1186/s12929-015-0208-1>
- Chew, J.L., Wolfowicz, C.B., Mao, H.Q., Leong, K.W., Chua, K.Y., 2003. Chitosan nanoparticles containing plasmid DNA encoding house dust mite allergen, Der p 1 for oral vaccination in mice. *Vaccine* 21, 2720–2729. [https://doi.org/10.1016/S0264-410X\(03\)00228-7](https://doi.org/10.1016/S0264-410X(03)00228-7)
- Circular, A., 2022. Regional review on status and trends in aquaculture development in Europe – 2020, Regional review on status and trends in aquaculture development in Asia and the Pacific – 2020. FAO. <https://doi.org/10.4060/cb7809en>
- Colombo, S.M., Wacker, A., Parrish, C.C., Kainz, M.J., Arts, M.T., 2017. A fundamental dichotomy in long-chain polyunsaturated fatty acid abundance between and within marine and terrestrial ecosystems. *Environ. Rev.* 25, 163–174. <https://doi.org/10.1139/er-2016-0062>
- Costa, L.F.C., Monroig, Ó., Leaver, M.J., Wilson, J., Cunha, I., Tocher, D.R., 2012. Functional desaturase fads1 (δ5) and fads2 (δ6) orthologues evolved before the origin of jawed vertebrates. *PLoS One* 7, 1–9. <https://doi.org/10.1371/journal.pone.0031950>
- Cruz-García, L., Sánchez-Gurmaches, J., Bouraoui, L., Saera-Vila, A., Pérez-Sánchez, J., Gutiérrez, J., Navarro, I., 2011. Changes in adipocyte cell size, gene expression of lipid metabolism markers, and lipolytic responses induced by dietary fish oil replacement in gilthead sea bream (*Sparus aurata* L.). *Comp. Biochem. Physiol. Part A Mol. Integr. Physiol.* 158, 391–399. <https://doi.org/10.1016/J.CBPA.2010.11.024>
- Csaba, N., Köping-Höggård, M., Alonso, M.J., 2009. Ionically crosslinked chitosan/tripolyphosphate nanoparticles for oligonucleotide and plasmid DNA delivery. *Int. J. Pharm.* 382, 205–214. <https://doi.org/10.1016/j.ijpharm.2009.07.028>
- Dangardt, F., Osika, W., Chen, Y., Nilsson, U., Gan, L.M., Gronowitz, E., Strandvik, B., Friberg, P., 2010. Omega-3 fatty acid supplementation improves vascular function and reduces inflammation in obese adolescents. *Atherosclerosis* 212, 580–585. <https://doi.org/10.1016/j.atherosclerosis.2010.06.046>
- De Campos, A.M., Diebold, Y., Carvalho, E.L.S., Sánchez, A., Alonso, M.J., 2004. Chitosan nanoparticles as new ocular drug delivery systems: In vitro stability, in vivo fate, and cellular toxicity. *Pharm. Res.* 21, 803–810. <https://doi.org/10.1023/B:PHAM.0000026432.75781.cb>
- Djuricic, I., Calder, P.C., 2021. Beneficial Outcomes of Omega-6 and Omega-3 Polyunsaturated Fatty Acids on Human Health: An Update for 2021. *Nutrients* 13, 2421. <https://doi.org/10.3390/NU13072421>
- Domenichiello, A.F., Kitson, A.P., Bazinet, R.P., 2015. Is docosahexaenoic acid synthesis from α -linolenic acid sufficient to supply the adult brain? *Prog. Lipid Res.* 59, 54–66. <https://doi.org/10.1016/j.plipres.2015.04.002>

REFERENCES

- Dong, L., Zou, H., Yuan, C., Hong, Y.H., Kuklev, D. V., Smith, W.L., 2016. Different fatty acids compete with arachidonic acid for binding to the allosteric or catalytic subunits of cyclooxygenases to regulate prostanoid synthesis. *J. Biol. Chem.* 291, 4069–4078. <https://doi.org/10.1074/jbc.M115.698001>
- Dong, X., Tan, P., Cai, Z., Xu, Hanlin, Li, J., Ren, W., Xu, Houguo, Zuo, R., Zhou, J., Mai, K., Ai, Q., 2017. Regulation of FADS2 transcription by SREBP-1 and PPAR- α influences LC-PUFA biosynthesis in fish. *Sci. Rep.* 7, 1–11. <https://doi.org/10.1038/srep40024>
- Dong, X., Xu, H., Mai, K., Xu, W., Zhang, Y., Ai, Q., 2015. Cloning and characterization of SREBP-1 and PPAR- α in Japanese seabass *Lateolabrax japonicus*, and their gene expressions in response to different dietary fatty acid profiles. *Comp. Biochem. Physiol. Part - B Biochem. Mol. Biol.* 180, 48–56. <https://doi.org/10.1016/j.cbpb.2014.10.001>
- Dong, Y., Wang, S., Chen, J., Zhang, Q., Liu, Y., You, C., Monroig, Ó., Tocher, D.R., Li, Y., 2016. Hepatocyte nuclear factor 4 α (HNF4 α) is a transcription factor of vertebrate fatty acyl desaturase gene as identified in marine teleost *Siganus canaliculatus*. *PLoS One* 11, 1–19. <https://doi.org/10.1371/journal.pone.0160361>
- Dong, Y., Wang, S., You, C., Xie, D., Jiang, Q., Li, Y., 2020. Hepatocyte nuclear factor 4 α (Hnf4 α) is involved in transcriptional regulation of $\Delta 6/\Delta 5$ fatty acyl desaturase (Fad) gene expression in marine teleost *Siganus canaliculatus*. *Comp. Biochem. Physiol. Part - B Biochem. Mol. Biol.* 239, 110353. <https://doi.org/10.1016/j.cbpb.2019.110353>
- Du, J., Xu, H., Li, S., Cai, Z., Mai, K., Ai, Q., 2017a. Effects of dietary chenodeoxycholic acid on growth performance, body composition and related gene expression in large yellow croaker (*Larimichthys crocea*) fed diets with high replacement of fish oil with soybean oil. *Aquaculture* 479, 584–590. <https://doi.org/10.1016/j.aquaculture.2017.06.023>
- Du, J., Xu, H., Li, S., Cai, Z., Mai, K., Ai, Q., 2017b. Effects of dietary chenodeoxycholic acid on growth performance, body composition and related gene expression in large yellow croaker (*Larimichthys crocea*) fed diets with high replacement of fish oil with soybean oil. *Aquaculture* 479, 584–590. <https://doi.org/10.1016/J.AQUACULTURE.2017.06.023>
- Du, Z.Y., Clouet, P., Huang, L.M., Degrace, P., Zheng, W.H., He, J.G., Tian, L.X., Liu, Y.J., 2008. Utilization of different dietary lipid sources at high level in herbivorous grass carp (*Ctenopharyngodon idella*): Mechanism related to hepatic fatty acid oxidation. *Aquac. Nutr.* 14, 77–92. <https://doi.org/10.1111/j.1365-2095.2007.00507.x>
- Du, Z.Y., Ma, T., Liaset, B., Keenan, A.H., Araujo, P., Lock, E.J., Demizieux, L., Degrace, P., Froyland, L., Kristiansen, K., Madsen, L., 2013. Dietary eicosapentaenoic acid supplementation accentuates hepatic triglyceride accumulation in mice with impaired fatty acid oxidation capacity. *Biochim. Biophys. Acta - Mol. Cell Biol. Lipids* 1831, 291–299. <https://doi.org/10.1016/j.bbalip.2012.10.002>
- Echeverría, F., Ortiz, M., Valenzuela, R., Videla, L.A., 2016. Long-chain polyunsaturated fatty acids regulation of PPARs, signaling: Relationship to tissue development and aging. *Prostaglandins Leukot. Essent. Fat. Acids* 114, 28–34. <https://doi.org/10.1016/j.plefa.2016.10.001>
- Echeverría, F., Valenzuela, R., Bustamante, A., Álvarez, D., Ortiz, M., Espinosa, A., Illesca, P., Gonzalez-Manañ, D., Videla, L.A., 2019. High-fat diet induces mouse liver steatosis with a concomitant decline in energy metabolism: Attenuation by eicosapentaenoic acid (EPA) or hydroxytyrosol (HT) supplementation and the additive effects upon EPA and HT co-administration. *Food Funct.* 10, 6170–6183. <https://doi.org/10.1039/c9fo01373c>
- Egea, M., Metón, I., Córdoba, M., Fernández, F., Baanante, I. V., 2008. Role of Sp1 and SREBP-1a in the insulin-mediated regulation of glucokinase transcription in the liver of gilthead sea bream (*Sparus aurata*). *Gen. Comp. Endocrinol.* 155, 359–367. <https://doi.org/10.1016/j.ygcen.2007.06.018>

REFERENCES

- Enes, P., Sanchez-Gurmaches, J., Navarro, I., Gutiérrez, J., Oliva-Teles, A., 2010. Role of insulin and IGF-I on the regulation of glucose metabolism in European sea bass (*Dicentrarchus labrax*) fed with different dietary carbohydrate levels. *Comp. Biochem. Physiol. - A Mol. Integr. Physiol.* 157, 346–353. <https://doi.org/10.1016/j.cbpa.2010.08.006>
- Eslick, G.D., Howe, P.R.C., Smith, C., Priest, R., Bensoussan, A., 2009. Benefits of fish oil supplementation in hyperlipidemia: a systematic review and meta-analysis. *Int. J. Cardiol.* 136, 4–16. <https://doi.org/10.1016/j.ijcard.2008.03.092>
- Fàbregas, A., Miñarro, M., García-Montoya, E., Pérez-Lozano, P., Carrillo, C., Sarrate, R., Sánchez, N., Ticó, J.R., Suñé-Negre, J.M., 2013. Impact of physical parameters on particle size and reaction yield when using the ionic gelation method to obtain cationic polymeric chitosan-tripolyphosphate nanoparticles. *Int. J. Pharm.* 446, 199–204. <https://doi.org/10.1016/j.ijpharm.2013.02.015>
- Fan, Y., Ren, C., Wang, Z., Jia, R., Wang, D., Zhang, Y., Zhang, G., Wan, Y., Huang, M., Wang, F., 2016. Transgenesis of humanized fat1 promotes n – 3 polyunsaturated fatty acid synthesis and expression of genes involved in lipid metabolism in goat cells. *Gene* 576, 249–255. <https://doi.org/10.1016/j.gene.2015.10.013>
- Feldstein, A.E., Lopez, R., Tamimi, T.A.R., Yerian, L., Chung, Y.M., Berk, M., Zhang, R., McIntyre, T.M., Hazen, S.L., 2010. Mass spectrometric profiling of oxidized lipid products in human nonalcoholic fatty liver disease and nonalcoholic steatohepatitis. *J. Lipid Res.* 51, 3046–3054. <https://doi.org/10.1194/jlr.M007096>
- Fernández-Alvarez, A., Soledad Alvarez, M., Gonzalez, R., Cucarella, C., Muntané, J., Casado, M., 2011. Human SREBP1c expression in liver is directly regulated by Peroxisome Proliferator-activated Receptor α (PPAR α). *J. Biol. Chem.* 286, 21466–21477. <https://doi.org/10.1074/jbc.M110.209973>
- Ferraz, R.B., Machado, A.M., Navarro, J.C., Cunha, I., Ozório, R., Salaro, A.L., Castro, L.F.C., Monroig, Ó., 2020. The fatty acid elongation genes *elovl4a* and *elovl4b* are present and functional in the genome of tambaqui (*Colossoma macropomum*). *Comp. Biochem. Physiol. Part - B Biochem. Mol. Biol.* 245, 110447. <https://doi.org/10.1016/j.cbpb.2020.110447>
- Forman, B.M., Chen, J., Evans, R.M., 1997. Hypolipidemic drugs, polyunsaturated fatty acids, and eicosanoids are ligands for peroxisome proliferator-activated receptors α and δ . *Proc. Natl. Acad. Sci. U. S. A.* 94, 4312–4317. <https://doi.org/10.1073/pnas.94.9.4312>
- Forsyth, S., Gautier, S., Salem, N., 2016. Global estimates of dietary intake of docosahexaenoic acid and arachidonic acid in developing and developed countries. *Ann. Nutr. Metab.* 68, 258–267. <https://doi.org/10.1159/000446855>
- Gan, Q., Wang, T., Cochrane, C., McCarron, P., 2005. Modulation of surface charge, particle size and morphological properties of chitosan-TPP nanoparticles intended for gene delivery. *Colloids Surfaces B Biointerfaces* 44, 65–73. <https://doi.org/10.1016/j.colsurfb.2005.06.001>
- Ganjam, G.K., Dimova, E.Y., Unterman, T.G., Kietzmann, T., 2009. FoxO1 and HNF-4 are involved in regulation of hepatic glucokinase gene expression by resveratrol. *J. Biol. Chem.* 284, 30783–30797. <https://doi.org/10.1074/JBC.M109.045260>
- Gao, M., Bu, L., Ma, Y., Liu, D., 2013. Concurrent Activation of Liver X Receptor and Peroxisome Proliferator-Activated Receptor Alpha Exacerbates Hepatic Steatosis in High Fat Diet-Induced Obese Mice. *PLoS One* 8, 1–11. <https://doi.org/10.1371/journal.pone.0065641>
- Gaspar, C., Silva-Marrero, J.I., Fàbregas, A., Miñarro, M., Ticó, J.R., Baanante, I.V., Metón, I., 2018a. Administration of chitosan-tripolyphosphate-DNA nanoparticles to knockdown glutamate dehydrogenase expression impairs

REFERENCES

- transdeamination and gluconeogenesis in the liver. *J. Biotechnol.* 286, 5–13.
<https://doi.org/10.1016/j.jbiotec.2018.09.002>
- Gaspar, C., Silva-Marrero, J.I., Fàbregas, A., Miñarro, M., Ticó, J.R., Baanante, I. V., Metón, I., 2018b. Administration of chitosan-tripolyphosphate-DNA nanoparticles to knockdown glutamate dehydrogenase expression impairs transdeamination and gluconeogenesis in the liver. *J. Biotechnol.* 286, 5–13.
<https://doi.org/10.1016/j.jbiotec.2018.09.002>
- Gingras, A.-A., White, P.J., Chouinard, P.Y., Julien, P., Davis, T.A., Dombrowski, L., Couture, Y., Dubreuil, P., Myre, A., Bergeron, K., Marette, A., Thivierge, M.C., 2007. Long-chain omega-3 fatty acids regulate bovine whole-body protein metabolism by promoting muscle insulin signalling to the Akt-mTOR-S6K1 pathway and insulin sensitivity. *J. Physiol.* 579, 269–284. <https://doi.org/10.1113/jphysiol.2006.121079>
- Glencross, B., Blyth, D., Irvin, S., Bourne, N., Campet, M., Boisot, P., Wade, N.M., 2016. An evaluation of the complete replacement of both fishmeal and fish oil in diets for juvenile Asian seabass, *Lates calcarifer*. *Aquaculture* 451, 298–309. <https://doi.org/10.1016/j.aquaculture.2015.09.012>
- Gonzalez, F.J., 2008. Regulation of hepatocyte nuclear factor 4 α -mediated transcription. *Drug Metab. Pharmacokinet.* 23, 2–7. <https://doi.org/10.2133/dmpk.23.2>
- González, Juan D, Silva-Marrero, J.I., Metón, I., Caballero-Solares, A., Viegas, I., Fernández, F., Miñarro, M., Fàbregas, A., Ticó, J.R., Jones, J.G., Baanante, I.V., 2016. Chitosan-mediated shRNA knockdown of cytosolic alanine aminotransferase improves hepatic carbohydrate metabolism. *Mar. Biotechnol.* 18, 85–97.
<https://doi.org/10.1007/s10126-015-9670-8>
- González, Juan D., Silva-Marrero, J.I., Metón, I., Caballero-Solares, A., Viegas, I., Fernández, F., Miñarro, M., Fàbregas, A., Ticó, J.R., Jones, J.G., Baanante, I. V., 2016. Chitosan-Mediated shRNA Knockdown of Cytosolic Alanine Aminotransferase Improves Hepatic Carbohydrate Metabolism. *Mar. Biotechnol.* 18, 85–97.
<https://doi.org/10.1007/s10126-015-9670-8>
- Gou, N., Ji, H., Chang, Z., Zhong, M., Deng, W., 2020. Effects of dietary essential fatty acid requirements on growth performance, fatty acid composition, biochemical parameters, antioxidant response and lipid related genes expression in juvenile *Onychostoma macrolepis*. *Aquaculture* 528, 735590. <https://doi.org/10.1016/j.aquaculture.2020.735590>
- Green, C.J., Pramfalk, C., Charlton, C.A., Gunn, P.J., Cornfield, T., Pavlides, M., Karpe, F., Hodson, L., 2020. Hepatic de novo lipogenesis is suppressed and fat oxidation is increased by omega-3 fatty acids at the expense of glucose metabolism. *BMJ open diabetes Res. care* 8, 1–13. <https://doi.org/10.1136/bmjdc-2019-000871>
- Grigorakis, K., 2007. Compositional and organoleptic quality of farmed and wild gilthead sea bream (*Sparus aurata*) and sea bass (*Dicentrarchus labrax*) and factors affecting it: A review. *Aquaculture* 272, 55–75.
<https://doi.org/10.1016/j.aquaculture.2007.04.062>
- Gu, H., Kausch, C., Machicao, F., Rett, K., Stumvoll, M., 2002. Expression in Human Skeletal Muscle Cell Cultures 51.
- Guenard, R., 2020. The State of World Fisheries and Aquaculture 2020, Inform. FAO. <https://doi.org/10.4060/ca9229en>
- Guesnet, P., Alessandri, J.M., 2011. Docosahexaenoic acid (DHA) and the developing central nervous system (CNS) - Implications for dietary recommendations. *Biochimie* 93, 7–12. <https://doi.org/10.1016/j.biochi.2010.05.005>
- H.C.Bimboim and J.Doly, Laboratoire, 1979. A rapid alkaline extraction procedure for screening recombinant plasmid DNA. *Nucleic Acids Res.* 7.

REFERENCES

- Hadj Taieb, A., Sley, A., Ghorbel, M., Jarboui, O., 2013. Feeding habits of *Sparus aurata* (Sparidae) from the Gulf of Gabes (central Mediterranean). *Cah. Biol. Mar.* 54, 263–270.
- Hagens, W.I., Oomen, A.G., de Jong, W.H., Cassee, F.R., Sips, A.J.A.M., 2007a. What do we (need to) know about the kinetic properties of nanoparticles in the body? *Regul. Toxicol. Pharmacol.* 49, 217–229.
<https://doi.org/10.1016/j.yrtph.2007.07.006>
- Hagens, W.I., Oomen, A.G., de Jong, W.H., Cassee, F.R., Sips, A.J.A.M., 2007b. What do we (need to) know about the kinetic properties of nanoparticles in the body? *Regul. Toxicol. Pharmacol.* 49, 217–229.
<https://doi.org/10.1016/J.YRTPH.2007.07.006>
- Haghiaci, M., Yang, X.H., Presley, L., Smith, S., Dettelback, S., Minium, J., Belury, M.A., Catalano, P.M., Hauguel-De Mouzon, S., 2015. Dietary omega-3 fatty acid supplementation reduces inflammation in obese pregnant women: A randomized double-blind controlled clinical trial. *PLoS One* 10, 1–14. <https://doi.org/10.1371/journal.pone.0137309>
- Hamid, N.K.A., Carmona-Antoñanzas, G., Monroig, Ó., Tocher, D.R., Turchini, G.M., Donald, J.A., 2016. Isolation and functional characterisation of a *fads2* in rainbow trout (*oncorhynchus mykiss*) with $\delta 5$ desaturase activity. *PLoS One* 11. <https://doi.org/10.1371/journal.pone.0150770>
- Hasan, K.M.M., Tamanna, N., Haque, M.A., 2018. Biochemical and histopathological profiling of Wistar rat treated with *Brassica napus* as a supplementary feed. *Food Sci. Hum. Wellness* 7, 77–82.
<https://doi.org/10.1016/j.fshw.2017.12.002>
- Hashimoto, K., Yoshizawa, A.C., Okuda, S., Kuma, K., Goto, S., Kanehisa, M., 2008. The repertoire of desaturases and elongases reveals fatty acid variations in 56 eukaryotic genomes. *J. Lipid Res.* 49, 183–191.
<https://doi.org/10.1194/jlr.M700377-JLR200>
- Hattori, T., Obinata, H., Ogawa, A., Kishi, M., Tatei, K., Ishikawa, O., Izumi, T., 2008. G2A plays proinflammatory roles in human keratinocytes under oxidative stress as a receptor for 9-hydroxyoctadecadienoic acid. *J. Invest. Dermatol.* 128, 1123–1133. <https://doi.org/10.1038/sj.jid.5701172>
- HE, T., LF, L., GJ, D., WT, W., SC, C., ML, K., R, T., GS, L., MH, T., 2012. Pro-opiomelanocortin gene delivery suppresses the growth of established Lewis lung carcinoma through a melanocortin-1 receptor-independent pathway. *J. Gene Med.* 14, 44–53. <https://doi.org/10.1002/jgm>
- Hein, G.J., Bernasconi, A.M., Montanaro, M.A., Pellon-Maison, M., Finarelli, G., Chicco, A., Lombardo, Y.B., Brenner, R.R., 2010a. Nuclear receptors and hepatic lipidogenic enzyme response to a dyslipidemic sucrose-rich diet and its reversal by fish oil n-3 polyunsaturated fatty acids. *Am. J. Physiol. - Endocrinol. Metab.* 298, 429–439.
<https://doi.org/10.1152/ajpendo.00513.2009>
- Hein, G.J., Bernasconi, A.M., Montanaro, M.A., Pellon-Maison, M., Finarelli, G., Chicco, A., Lombardo, Y.B., Brenner, R.R., 2010b. Nuclear receptors and hepatic lipidogenic enzyme response to a dyslipidemic sucrose-rich diet and its reversal by fish oil n-3 polyunsaturated fatty acids. *Am. J. Physiol. Endocrinol. Metab.* 298.
<https://doi.org/10.1152/AJPENDO.00513.2009>
- Hertz, R., Magenheimer, J., Berman, I., Bar-Tana, J., 1998. Fatty acyl-CoA thioesters are ligands of hepatic nuclear factor-4 α . *Nature* 392, 512–516. <https://doi.org/10.1038/33185>
- Hidalgo, M., Urea, E., Sanz, A., 1999. Comparative study of digestive enzymes in fish with different nutritional habits. Proteolytic and amylase activities. *Aquaculture* 170, 267–283. [https://doi.org/10.1016/S0044-8486\(98\)00413-X](https://doi.org/10.1016/S0044-8486(98)00413-X)

REFERENCES

- Hirota, K., Sakamaki, J.I., Ishida, J., Shimamoto, Y., Nishihara, S., Kodama, N., Ohta, K., Yamamoto, M., Tanimoto, K., Fukamizu, A., 2008. A combination of HNF-4 and Foxo1 is required for reciprocal transcriptional regulation of glucokinase and glucose-6-phosphatase genes in response to fasting and feeding. *J. Biol. Chem.* 283, 32432–32441. <https://doi.org/10.1074/JBC.M806179200>
- Hishikawa, D., Yanagida, K., Nagata, K., Kanatani, A., Iizuka, Y., Hamano, F., Yasuda, M., Okamura, T., Shindou, H., Shimizu, T., 2020. Hepatic Levels of DHA-Containing Phospholipids Instruct SREBP1-Mediated Synthesis and Systemic Delivery of Polyunsaturated Fatty Acids. *iScience* 23, 101495. <https://doi.org/10.1016/j.isci.2020.101495>
- Horn, S.S., Sonesson, A.K., Krasnov, A., Moghadam, H., Hillestad, B., Meuwissen, T.H.E., Ruyter, B., 2019. Individual differences in EPA and DHA content of Atlantic salmon are associated with gene expression of key metabolic processes. *Sci. Rep.* 9, 1–13. <https://doi.org/10.1038/s41598-019-40391-2>
- Houston, S.J.S., Karalazos, V., Tinsley, J., Betancor, M.B., Martin, S.A.M., Tocher, D.R., Monroig, O., 2017. The compositional and metabolic responses of gilthead seabream (*Sparus aurata*) to a gradient of dietary fish oil and associated n-3 long-chain PUFA content. *Br. J. Nutr.* 118, 1010–1022. <https://doi.org/10.1017/S0007114517002975>
- Hu, Y.L., Qi, W., Han, F., Shao, J.Z., Gao, J.Q., 2011. Toxicity evaluation of biodegradable chitosan nanoparticles using a zebrafish embryo model. *Int. J. Nanomedicine* 6, 3351–3359. <https://doi.org/10.2147/ijn.s25853>
- Hunkeler, M., Haggmann, A., Stutfeld, E., Chami, M., Guri, Y., Stahlberg, H., Maier, T., 2018. Structural basis for regulation of human acetyl-CoA carboxylase. *Nature* 558, 470–474. <https://doi.org/10.1038/s41586-018-0201-4>
- Hussain, M.M., 2014. Intestinal lipid absorption and lipoprotein formation. *Curr. Opin. Lipidol.* 25, 200–206. <https://doi.org/10.1097/MOL.0000000000000084>
- Huyben, D., Grobler, T., Matthew, C., Bou, M., Ruyter, B., Glencross, B., 2021. Requirement for omega-3 long-chain polyunsaturated fatty acids by Atlantic salmon is relative to the dietary lipid level. *Aquaculture* 531, 735805. <https://doi.org/10.1016/j.aquaculture.2020.735805>
- Iizuka, K., Horikawa, Y., 2008. ChREBP: A glucose-activated transcription factor involved in the development of metabolic syndrome. *Endocr. J.* 55, 617–624. <https://doi.org/10.1507/endocrj.K07E-110>
- Intra, J., Salem, A.K., 2008. Characterization of the transgene expression generated by branched and linear polyethylenimine-plasmid DNA nanoparticles in vitro and after intraperitoneal injection in vivo. *J. Control. Release* 130, 129–138. <https://doi.org/10.1016/j.jconrel.2008.04.014>
- Islam, N., Dmour, I., Taha, M.O., 2019. Degradability of chitosan micro/nanoparticles for pulmonary drug delivery. *Heliyon* 5, e01684. <https://doi.org/10.1016/j.heliyon.2019.e01684>
- Jalil, A., Bourgeois, T., Ménégaut, L., Lagrost, L., Thomas, C., Masson, D., 2019. Revisiting the role of LXRs in PUFA metabolism and phospholipid homeostasis. *Int. J. Mol. Sci.* 20, 9–11. <https://doi.org/10.3390/ijms20153787>
- Jeevanandam, J., Barhoum, A., Chan, Y.S., Dufresne, A., Danquah, M.K., 2018. Review on nanoparticles and nanostructured materials: History, sources, toxicity and regulations. *Beilstein J. Nanotechnol.* 9, 1050–1074. <https://doi.org/10.3762/bjnano.9.98>
- Ji, S., Hardy, R.W., Wood, P.A., 2009a. Transgenic expression of n-3 fatty acid desaturase (fat-1) in C57/BL6 mice: Effects on glucose homeostasis and body weight. *J. Cell. Biochem.* 107, 809–817. <https://doi.org/10.1002/jcb.22179>
- Ji, S., Hardy, R.W., Wood, P.A., 2009b. Transgenic expression of n-3 fatty acid desaturase (fat-1) in C57/BL6 mice: Effects on glucose homeostasis and body weight. *J. Cell. Biochem.* 107, 809–817. <https://doi.org/10.1002/JCB.22179>

REFERENCES

- Jia, S., Li, X., Zheng, S., Wu, G., 2017. Amino acids are major energy substrates for tissues of hybrid striped bass and zebrafish. *Amino Acids* 49, 2053–2063. <https://doi.org/10.1007/s00726-017-2481-7>
- Johns, I., Frost, G., Dornhorst, A., 2020. Increasing the proportion of plasma MUFA, as a result of dietary intervention, is associated with a modest improvement in insulin sensitivity. *J. Nutr. Sci.* 9, 1–7. <https://doi.org/10.1017/jns.2019.29>
- Joon, N.L., Zhang, X., Feramisco, J.D., Gong, Y., Ye, J., 2008. Unsaturated fatty acids inhibit proteasomal degradation of insig-1 at a postubiquitination step. *J. Biol. Chem.* 283, 33772–33783. <https://doi.org/10.1074/jbc.M806108200>
- Jump, D.B., 2008. N-3 polyunsaturated fatty acid regulation of hepatic gene transcription. *Curr. Opin. Lipidol.* 19, 242–247. <https://doi.org/10.1097/MOL.0B013E3282FFAF6A>
- Jurica, M.S., Mesecar, A., Heath, P.J., Shi, W., Nowak, T., Stoddard, B.L., 1998. The allosteric regulation of pyruvate kinase by fructose-1,6-bisphosphate. *Structure* 6, 195–210. [https://doi.org/10.1016/S0969-2126\(98\)00021-5](https://doi.org/10.1016/S0969-2126(98)00021-5)
- Kahn-Kirby, A.H., Dantzer, J.L.M., Apicella, A.J., Schafer, W.R., Browse, J., Bargmann, C.I., Watts, J.L., 2004. Specific polyunsaturated fatty acids drive TRPV-dependent sensory signaling in vivo. *Cell* 119, 889–900. <https://doi.org/10.1016/j.cell.2004.11.005>
- Kamalam, B.S., Medale, F., Panserat, S., 2017. Utilisation of dietary carbohydrates in farmed fishes: New insights on influencing factors, biological limitations and future strategies. *Aquaculture* 467, 3–27. <https://doi.org/10.1016/j.aquaculture.2016.02.007>
- Kamisako, T., Tanaka, Y., Ikeda, T., Yamamoto, K., Ogawa, H., 2012a. Dietary fish oil regulates gene expression of cholesterol and bile acid transporters in mice. *Hepatol. Res.* 42, 321–326. <https://doi.org/10.1111/j.1872-034X.2011.00924.x>
- Kamisako, T., Tanaka, Y., Ikeda, T., Yamamoto, K., Ogawa, H., 2012b. Dietary fish oil regulates gene expression of cholesterol and bile acid transporters in mice. *Hepatol. Res.* 42, 321–326. <https://doi.org/10.1111/J.1872-034X.2011.00924.X>
- Kang, J.X., Wang, J., Wu, L., Kang, Z.B., 2004. Fat-1 mice convert n-6 to n-3 fatty acids. *Nature* 427, 504–504. <https://doi.org/10.1038/427504a>
- Kang, Z.B., Ge, Y., Chen, Z., Cluette-Brown, J., Laposata, M., Leaf, A., Kang, J.X., 2001. Adenoviral gene transfer of *Caenorhabditis elegans* n-3 fatty acid desaturase optimizes fatty acid composition in mammalian cells. *Proc. Natl. Acad. Sci. U. S. A.* 98, 4050–4054. <https://doi.org/10.1073/pnas.061040198>
- Katas, H., Alpar, H.O., 2006. Development and characterisation of chitosan nanoparticles for siRNA delivery. *J. Control. Release* 115, 216–225. <https://doi.org/10.1016/j.jconrel.2006.07.021>
- Kawakita, E., Hashimoto, M., Shido, O., 2006. Docosahexaenoic acid promotes neurogenesis in vitro and in vivo. *Neuroscience* 139, 991–997. <https://doi.org/10.1016/j.neuroscience.2006.01.021>
- Kersten, S., 2014. Physiological regulation of lipoprotein lipase. *Biochim. Biophys. Acta - Mol. Cell Biol. Lipids* 1841, 919–933. <https://doi.org/10.1016/j.bbali.2014.03.013>
- Kim, E.H., Bae, J.S., Hahn, K.B., Cha, J.Y., 2012. Endogenously synthesized n-3 polyunsaturated fatty acids in fat-1 mice ameliorate high-fat diet-induced non-alcoholic fatty liver disease. *Biochem. Pharmacol.* 84, 1359–1365. <https://doi.org/10.1016/J.BCP.2012.08.029>
- Kim, H., Zhang, H., Meng, D., Russell, G., Lee, J.N., Ye, J., 2013. UAS domain of Ubxd8 and FAF1 polymerizes upon interaction with long-chain unsaturated fatty acids. *J. Lipid Res.* 54, 2144–2152. <https://doi.org/10.1194/jlr.M037218>

REFERENCES

- Kır, M., 2020. Thermal tolerance and standard metabolic rate of juvenile gilthead seabream (*Sparus aurata*) acclimated to four temperatures. *J. Therm. Biol.* 93, 102739. <https://doi.org/10.1016/j.jtherbio.2020.102739>
- Knebel, B., Haas, J., Hartwig, S., Jacob, S., Köllmer, C., Nitzgen, U., Müller-Wieland, D., Kotzka, J., 2012. Liver-specific expression of transcriptionally active *srebp-1c* is associated with fatty liver and increased visceral fat mass. *PLoS One* 7, 1–15. <https://doi.org/10.1371/journal.pone.0031812>
- Kohan, A.B., Qing, Y., Cyphert, H.A., Tso, P., Salati, L.M., 2011. Chylomicron Remnants and Nonesterified Fatty Acids Differ in Their Ability to Inhibit Genes Involved in Lipogenesis in Rats. *J. Nutr.* 141, 171–176. <https://doi.org/10.3945/JN.110.129106>
- Kooij, G., van Horsen, J., de Vries, E., 2005. Tight Junctions of the Blood–Brain Barrier, in: de Vries, E., Prat, A. (Eds.), *The Blood-Brain Barrier and Its Microenvironment*. CRC Press, pp. 69–92. <https://doi.org/10.1201/B14290-7>
- Kruger, N.J., 1996. The Bradford Method for Protein Quantitation. *Protein Protoc. Handb.* 32, 15–20. https://doi.org/10.1007/978-1-60327-259-9_4
- Lai, L., Kang, J.X., Li, R., Wang, J., Witt, W.T., Hwan, Y.Y., Hao, Y., Wax, D.M., Murphy, C.N., Rieke, A., Samuel, M., Linville, M.L., Korte, S.W., Evans, R.W., Starzl, T.E., Prather, R.S., Dai, Y., 2006a. Generation of cloned transgenic pigs rich in omega-3 fatty acids. *Nat. Biotechnol.* 24, 435–436. <https://doi.org/10.1038/nbt1198>
- Lai, L., Kang, J.X., Li, R., Wang, J., Witt, W.T., Hwan, Y.Y., Hao, Y., Wax, D.M., Murphy, C.N., Rieke, A., Samuel, M., Linville, M.L., Korte, S.W., Evans, R.W., Starzl, T.E., Prather, R.S., Dai, Y., 2006b. Generation of cloned transgenic pigs rich in omega-3 fatty acids. *Nat. Biotechnol.* 24, 435–436. <https://doi.org/10.1038/NBT1198>
- Larsson, M., Allan, C.M., Jung, R.S., Heizer, P.J., Beigneux, A.P., Young, S.G., Fong, L.G., 2017. Apolipoprotein C-III inhibits triglyceride hydrolysis by GPIIIBP1-bound LPL. *J. Lipid Res.* 58, 1893–1902. <https://doi.org/10.1194/jlr.M078220>
- Lazado, C.C., Caipang, C.M.A., Kiron, V., 2012. Enzymes from the gut bacteria of Atlantic cod, *Gadus morhua* and their influence on intestinal enzyme activity. *Aquac. Nutr.* 18, 423–431. <https://doi.org/10.1111/j.1365-2095.2011.00928.x>
- Lee, Y.K., Park, J.E., Lee, M., Hardwick, J.P., 2018. Hepatic lipid homeostasis by peroxisome proliferator-activated receptor gamma 2. *Liver Res.* 2, 209–215. <https://doi.org/10.1016/j.livres.2018.12.001>
- Li, F.J., Lin, X., Lin, S.M., Chen, W.Y., Guan, Y., 2016. Effects of dietary fish oil substitution with linseed oil on growth, muscle fatty acid and metabolism of tilapia (*Oreochromis niloticus*). *Aquac. Nutr.* 22, 499–508. <https://doi.org/10.1111/anu.12270>
- Li, G., Sinclair, A.J., Li, D., 2011. Comparison of Lipid Content and Fatty Acid Composition in the Edible Meat of Wild and Cultured Freshwater and Marine Fish and Shrimps from China. *J. Agric. Food Chem.* 59, 1871–1881. <https://doi.org/10.1021/jf104154q>
- Li, M., Ouyang, H., Yuan, H., Li, J., Xie, Z., Wang, K., Yu, T., Liu, M., Chen, X., Tang, X., Jiao, H., Pang, D., 2018. Site-Specific Fat-1 Knock-In Enables Significant Decrease of n-6PUFAs/n-3PUFAs Ratio in Pigs. *G3 (Bethesda)*. 8, 1747–1754. <https://doi.org/10.1534/G3.118.200114>
- Li, Y., Zeng, X., Dong, Y., Chen, C., You, C., Tang, G., Chen, J., Wang, S., 2018. *Hnf4α* is involved in LC-PUFA biosynthesis by up-regulating gene transcription of elongase in marine teleost *Siganus canaliculatus*. *Int. J. Mol. Sci.* 19, 1–16. <https://doi.org/10.3390/ijms19103193>
- Li, Yang, Wen, Z., You, C., Xie, Z., Tocher, D.R., Zhang, Y., Wang, S., Li, Yuanyou, 2020. Genome wide identification and

REFERENCES

- functional characterization of two LC-PUFA biosynthesis elongase (elov18) genes in rabbitfish (*Siganus canaliculatus*). *Aquaculture* 522, 735127. <https://doi.org/10.1016/j.aquaculture.2020.735127>
- Liu, C., Wang, J., Ma, Z., Li, T., Xing, W., Jiang, N., Li, W., Li, C., Luo, L., 2018. Effects of totally replacing dietary fish oil by linseed oil or soybean oil on juvenile hybrid sturgeon, *Acipenser baeri* Brandt♀×*A. schrenckii* Brandt♂. *Aquac. Nutr.* 24, 184–194. <https://doi.org/10.1111/anu.12546>
- Liu, H., Guo, X., Gooneratne, R., Lai, R., Zeng, C., Zhan, F., Wang, W., 2016. The gut microbiome and degradation enzyme activity of wild freshwater fishes influenced by their trophic levels. *Sci. Rep.* 6, 1–12. <https://doi.org/10.1038/srep24340>
- Liu, X.-F., Wei, Z.-Y., Bai, C.-L., Ding, X.-B., Li, X., Su, G.-H., Cheng, L., Zhang, L., Guo, H., Li, G.-P., 2017. Insights into the function of n-3 PUFAs in fat-1 transgenic cattle. *J. Lipid Res.* 58, 1524–1535. <https://doi.org/10.1194/jlr.M072983>
- Liu, X.-F.F., Wei, Z.-Y.Y., Bai, C.-L.L., Ding, X.-B. Bin, Li, X., Su, G.-H.H., Cheng, L., Zhang, L., Guo, H., Li, G.-P.P., 2017. Insights into the function of n-3 PUFAs in fat-1 transgenic cattle. *J. Lipid Res.* 58, 1524–1535. <https://doi.org/10.1194/jlr.M072983>
- Liu, X., Pang, D., Yuan, T., Li, Zhuang, Li, Zhanjun, Zhang, M., Ren, W., Ouyang, H., Tang, X., 2016a. N-3 polyunsaturated fatty acids attenuates triglyceride and inflammatory factors level in hfat-1 transgenic pigs. *Lipids Health Dis.* 15, 1–7. <https://doi.org/10.1186/s12944-016-0259-7>
- Liu, X., Pang, D., Yuan, T., Li, Zhuang, Li, Zhanjun, Zhang, M., Ren, W., Ouyang, H., Tang, X., 2016b. N-3 polyunsaturated fatty acids attenuates triglyceride and inflammatory factors level in hfat-1 transgenic pigs. *Lipids Health Dis.* 15. <https://doi.org/10.1186/S12944-016-0259-7>
- Liu, X.F., Wei, Z.Y., Bai, C.L., Ding, X. Bin, Li, X., Su, G.H., Cheng, L., Zhang, L., Guo, H., Li, G.P., 2017. Insights into the function of n-3 PUFAs in fat-1 transgenic cattle. *J. Lipid Res.* 58, 1524–1535. <https://doi.org/10.1194/jlr.M072983>
- Livak, K.J., Schmittgen, T.D., 2001. Analysis of relative gene expression data using real-time quantitative PCR and the 2- $\Delta\Delta CT$ method. *Methods* 25, 402–408. <https://doi.org/10.1006/meth.2001.1262>
- Ljubojević, D., Radosavljević, V., Puvača, N., Živkov Baloš, M., Dordević, V., Jovanović, R., Čirković, M., 2015. Interactive effects of dietary protein level and oil source on proximate composition and fatty acid composition in common carp (*Cyprinus carpio* L.). *J. Food Compos. Anal.* 37, 44–50. <https://doi.org/10.1016/j.jfca.2014.09.005>
- López-Soldado, I., Avella, M., Botham, K.M., 2009. Suppression of VLDL secretion by cultured hepatocytes incubated with chylomicron remnants enriched in n-3 polyunsaturated fatty acids is regulated by hepatic nuclear factor-4 α . *Biochim. Biophys. Acta - Mol. Cell Biol. Lipids* 1791, 1181–1189. <https://doi.org/10.1016/j.bbali.2009.08.004>
- Lopez, S., Bermudez, B., Ortega, A., Varela, L.M., Pacheco, Y.M., Villar, J., Abia, R., Muriana, F.J.G., 2011. Effects of meals rich in either monounsaturated or saturated fat on lipid concentrations and on insulin secretion and action in subjects with high fasting triglyceride concentrations. *Am. J. Clin. Nutr.* 93, 494–499. <https://doi.org/10.3945/ajcn.110.003251>
- López, S., Bermúdez, B., Pacheco, Y.M., Villar, J., Abia, R., Muriana, F.J.G., 2008. Distinctive postprandial modulation of β cell function and insulin sensitivity by dietary fats: Monounsaturated compared with saturated fatty acids. *Am. J. Clin. Nutr.* 88, 638–644. <https://doi.org/10.1093/ajcn/88.3.638>
- Lorente-Cebrián, S., Costa, A.G.V., Navas-Carretero, S., Zabala, M., Martínez, J.A., Moreno-Aliaga, M.J., 2013. Role of

REFERENCES

- omega-3 fatty acids in obesity, metabolic syndrome, and cardiovascular diseases: A review of the evidence. *J. Physiol. Biochem.* 69, 633–651. <https://doi.org/10.1007/s13105-013-0265-4>
- Lucas, A. (Albert), 1996. Bioenergetics of Organisms: Methods, in: Priede, I.G. (Ed.), *Bioenergetics of Aquatic Animals*. Taylor & Francis, London, pp. 65–81.
- Lundebye, A.K., Lock, E.J., Rasinger, J.D., Nøstbakken, O.J., Hannisdal, R., Karlsbakk, E., Wennevik, V., Madhun, A.S., Madsen, L., Graff, I.E., Ørnsrud, R., 2017. Lower levels of Persistent Organic Pollutants, metals and the marine omega 3-fatty acid DHA in farmed compared to wild Atlantic salmon (*Salmo salar*). *Environ. Res.* 155, 49–59. <https://doi.org/10.1016/j.envres.2017.01.026>
- Luo, R., Zheng, Z., Yang, C., Zhang, X., Cheng, L., Su, G., Bai, C., Li, G., 2020. Comparative Transcriptome Analysis Provides Insights into the Polyunsaturated Fatty Acid Synthesis Regulation of Fat-1 Transgenic Sheep. *Int. J. Mol. Sci.* 21, 1121. <https://doi.org/10.3390/IJMS21031121>
- Ma, H. na, Jin, M., Zhu, T. ting, Li, C. chen, Lu, Y., Yuan, Y., Xiong, J., Zhou, Q. cun, 2018. Effect of dietary arachidonic acid levels on growth performance, fatty acid profiles and lipid metabolism of juvenile yellow catfish (*Pelteobagrus fulvidraco*). *Aquaculture* 486, 31–41. <https://doi.org/10.1016/j.aquaculture.2017.11.055>
- Ma, J., Wang, J., Zhang, D., Hao, T., Sun, J., Sun, Y., Zhang, L., 2014. Estimation of optimum docosahexaenoic to eicosapentaenoic acid ratio (DHA/EPA) for juvenile starry flounder, *Platichthys stellatus*. *Aquaculture* 433, 105–114. <https://doi.org/10.1016/j.aquaculture.2014.05.042>
- Magalhães, R., Guerreiro, I., Coutinho, F., Moutinho, S., Sousa, S., Delerue-Matos, C., Domingues, V.F., Olsen, R.E., Peres, H., Oliva-Teles, A., 2020. Effect of dietary ARA/EPA/DHA ratios on growth performance and intermediary metabolism of gilthead sea bream (*Sparus aurata*) juveniles. *Aquaculture* 516, 734644. <https://doi.org/10.1016/j.aquaculture.2019.734644>
- Magalhães, R., Martins, N., Fontinha, F., Moutinho, S., Olsen, R.E., Peres, H., Oliva-Teles, A., 2021. Effects of dietary arachidonic acid and docosahexaenoic acid at different carbohydrates levels on gilthead sea bream growth performance and intermediary metabolism. *Aquaculture* 545. <https://doi.org/10.1016/j.aquaculture.2021.737233>
- Marin, E., Briceño, M.I., Caballero-George, C., 2013. Critical evaluation of biodegradable polymers used in nanodrugs. *Int. J. Nanomedicine* 8, 3071–3091. <https://doi.org/10.2147/IJN.S47186>
- Marion-Letellier, R., Savoye, G., Ghosh, S., 2016. Fatty acids, eicosanoids and PPAR gamma. *Eur. J. Pharmacol.* 785, 44–49. <https://doi.org/10.1016/j.ejphar.2015.11.004>
- Marquardt, A., Stöhr, H., White, K., Weber, B.H.F., 2000. cDNA cloning, genomic structure, and chromosomal localization of three members of the human fatty acid desaturase family. *Genomics* 66, 175–183. <https://doi.org/10.1006/geno.2000.6196>
- Meadus, W.J., Duff, P., Rolland, D., Aalhus, J.L., Uttaro, B., Dugan, M.E.R., 2011. Feeding docosahexaenoic acid to pigs reduces blood triglycerides and induces gene expression for fat oxidation. *Can. J. Anim. Sci.* 91, 601–612. <https://doi.org/10.4141/cjas2011-055>
- Mediavilla, D., Metón, I., Baanante, I.V., 2008. Purification and kinetic characterization of 6-phosphofructo-1-kinase from the liver of gilthead sea bream (*Sparus aurata*). *J. Biochem.* 144, 235–244. <https://doi.org/mvn066> [pii] 10.1093/jb/mvn066
- Meguro, S., Hasumura, T., 2018. Fish Oil Suppresses Body Fat Accumulation in Zebrafish. *Zebrafish* 15, 27–32.

REFERENCES

- <https://doi.org/10.1089/zeb.2017.1475>
- Meng, J., Feng, M., Dong, W., Zhu, Y., Li, Y., Zhang, P., Wu, L., Li, M., Lu, Ying, Chen, H., Liu, X., Lu, Yan, Sun, H., Tong, X., 2016. Identification of HNF-4 α as a key transcription factor to promote ChREBP expression in response to glucose. *Sci. Rep.* 6. <https://doi.org/10.1038/SREP23944>
- Menoyo, D., Izquierdo, M.S., Robaina, L., Ginés, R., Lopez-Bote, C.J., Bautista, J.M., 2004. Adaptation of lipid metabolism, tissue composition and flesh quality in gilthead sea bream (*Sparus aurata*) to the replacement of dietary fish oil by linseed and soyabean oils. *Br. J. Nutr.* 92, 41–52. <https://doi.org/10.1079/bjn20041165>
- Menoyo, D., López-Bote, C.J., Obach, A., Bautista, J.M., 2005. Effect of dietary fish oil substitution with linseed oil on the performance, tissue fatty acid profile, metabolism, and oxidative stability of Atlantic salmon. *J. Anim. Sci.* 83, 2853–2862. <https://doi.org/10.2527/2005.83122853x>
- Metallo, C.M., Gameiro, P.A., Bell, E.L., Mattaini, K.R., Yang, J., Hiller, K., Jewell, C.M., Johnson, Z.R., Irvine, D.J., Guarente, L., Kelleher, J.K., Vander Heiden, M.G., Iliopoulos, O., Stephanopoulos, G., 2012. Reductive glutamine metabolism by IDH1 mediates lipogenesis under hypoxia. *Nature* 481, 380–384. <https://doi.org/10.1038/nature10602>
- Metón, I., Caseras, A., Fernández, F., Baanante, I.V., 2000. 6-Phosphofructo-2-kinase/fructose-2,6-bisphosphatase gene expression is regulated by diet composition and ration size in liver of gilthead sea bream, *Sparus aurata*. *Biochim. Biophys. Acta - Gene Struct. Expr.* 1491, 220–228.
- Metón, I., Caseras, A., Mediavilla, D., Fernández, F., Baanante, I.V., 1999a. Molecular cloning of a cDNA encoding 6-phosphofructo-2-kinase/fructose-2,6-bisphosphatase from liver of *Sparus aurata*: nutritional regulation of enzyme expression. *Biochim. Biophys. Acta* 1444, 153–165. [https://doi.org/S0167-4781\(98\)00270-X](https://doi.org/S0167-4781(98)00270-X) [pii]
- Metón, I., Egea, M., Anemaet, I.G., Fernández, F., Baanante, I. V., 2006. Sterol regulatory element binding protein-1a transactivates 6-phosphofructo-2-kinase/fructose-2,6-bisphosphatase gene promoter. *Endocrinology* 147, 3446–3456. <https://doi.org/10.1210/en.2005-1506>
- Metón, I., Mediavilla, D., Caseras, A., Cantó, E., Fernández, F., Baanante, I.V., 1999b. Effect of diet composition and ration size on key enzyme activities of glycolysis-gluconeogenesis, the pentose phosphate pathway and amino acid metabolism in liver of gilthead sea bream (*Sparus aurata*). *Br. J. Nutr.* 82, 223–232.
- Metón, I., Mediavilla, D., Caseras, A., Cantó, E., Fernández, F., Baanante, I. V., 1999. Effect of diet composition and ration size on key enzyme activities of glycolysis-gluconeogenesis, the pentose phosphate pathway and amino acid metabolism in liver of gilthead sea bream (*Sparus aurata*). *Br. J. Nutr.* 82, 223–232. <https://doi.org/10.1017/s0007114599001403>
- Minghetti, M., Leaver, M.J., Tocher, D.R., 2011. Transcriptional control mechanisms of genes of lipid and fatty acid metabolism in the Atlantic salmon (*Salmo salar* L.) established cell line, SHK-1. *Biochim. Biophys. Acta - Mol. Cell Biol. Lipids* 1811, 194–202. <https://doi.org/10.1016/j.bbalip.2010.12.008>
- Mock, T.S., Francis, D.S., Jago, M.K., Glencross, B.D., Smullen, R.P., Turchini, G.M., 2019. Endogenous biosynthesis of n-3 long-chain PUFA in Atlantic salmon. *Br. J. Nutr.* 121, 1108–1123. <https://doi.org/10.1017/S0007114519000473>
- Monroig, Ó., Wang, S., Zhang, L., You, C., Tocher, D.R., Li, Y., 2012. Elongation of long-chain fatty acids in rabbitfish *Siganus canaliculatus*: Cloning, functional characterisation and tissue distribution of Elovl5- and Elovl4-like elongases. *Aquaculture* 350–353, 63–70. <https://doi.org/10.1016/j.aquaculture.2012.04.017>

REFERENCES

- Monteiro, M., Matos, E., Ramos, R., Campos, I., Valente, L.M.P., 2018. A blend of land animal fats can replace up to 75% fish oil without affecting growth and nutrient utilization of European seabass. *Aquaculture* 487, 22–31. <https://doi.org/10.1016/j.aquaculture.2017.12.043>
- Morais, S., Pratoomyot, J., Taggart, J.B., Bron, J.E., Guy, D.R., Bell, J.G., Tocher, D.R., 2011a. Genotype-specific responses in Atlantic salmon (*Salmo salar*) subject to dietary fish oil replacement by vegetable oil: A liver transcriptomic analysis. *BMC Genomics* 12. <https://doi.org/10.1186/1471-2164-12-255>
- Morais, S., Pratoomyot, J., Taggart, J.B., Bron, J.E., Guy, D.R., Bell, J.G., Tocher, D.R., 2011b. Genotype-specific responses in Atlantic salmon (*Salmo salar*) subject to dietary fish oil replacement by vegetable oil: A liver transcriptomic analysis. *BMC Genomics* 12, 1–17. <https://doi.org/10.1186/1471-2164-12-255/TABLES/5>
- Moxness Reksten, A., Ho, Q.T., Nøstbakken, O.J., Wik Markhus, M., Kjelleevold, M., Bokevoll, A., Hannisdal, R., Frøyland, L., Madsen, L., Dahl, L., 2022. Temporal variations in the nutrient content of Norwegian farmed Atlantic salmon (*Salmo salar*), 2005–2020. *Food Chem.* 373. <https://doi.org/10.1016/j.foodchem.2021.131445>
- Mozanzadeh, M.T., Marammazi, J.G., Yavari, V., Agh, N., Mohammadian, T., Gisbert, E., 2015. Dietary n-3 LC-PUFA requirements in silvery-black porgy juveniles (*Sparidentex hasta*). *Aquaculture* 448, 151–161. <https://doi.org/10.1016/j.aquaculture.2015.06.007>
- Muhlhauser, B.S., Cook-Johnson, R., James, M., Miljkovic, D., Duthoit, E., Gibson, R., 2010. Opposing effects of omega-3 and omega-6 long chain polyunsaturated fatty acids on the expression of lipogenic genes in omental and retroperitoneal adipose depots in the rat. *J. Nutr. Metab.* 2010. <https://doi.org/10.1155/2010/927836>
- Napier, J.A., Usher, S., Haslam, R.P., Ruiz-Lopez, N., Sayanova, O., 2015. Transgenic plants as a sustainable, terrestrial source of fish oils. *Eur. J. Lipid Sci. Technol.* 117, 1317–1324. <https://doi.org/10.1002/ejlt.201400452>
- Nasti, A., Zaki, N.M., De Leonardis, P., Ungphaiboon, S., Sansongsak, P., Rimoli, M.G., Tirelli, N., 2009. Chitosan/TPP and chitosan/TPP-hyaluronic acid nanoparticles: Systematic optimisation of the preparative process and preliminary biological evaluation. *Pharm. Res.* 26, 1918–1930. <https://doi.org/10.1007/s11095-009-9908-0>
- Nayerossadat, N., Ali, P., Maedeh, T., 2012. Viral and nonviral delivery systems for gene delivery. *Adv. Biomed. Res.* 1, 27. <https://doi.org/10.4103/2277-9175.98152>
- Nicholls, S.J., Lincoff, A.M., Garcia, M., Bash, D., Ballantyne, C.M., Barter, P.J., Davidson, M.H., Kastelein, J.J.P., Koenig, W., McGuire, D.K., Mozaffarian, D., Ridker, P.M., Ray, K.K., Katona, B.G., Himmelmann, A., Loss, L.E., Rensfeldt, M., Lundström, T., Agrawal, R., Menon, V., Wolski, K., Nissen, S.E., 2020. Effect of High-Dose Omega-3 Fatty Acids vs Corn Oil on Major Adverse Cardiovascular Events in Patients at High Cardiovascular Risk: The STRENGTH Randomized Clinical Trial. *JAMA - J. Am. Med. Assoc.* 324, 2268–2280. <https://doi.org/10.1001/jama.2020.22258>
- Niki, E., 2009. Lipid peroxidation: Physiological levels and dual biological effects. *Free Radic. Biol. Med.* 47, 469–484. <https://doi.org/10.1016/j.freeradbiomed.2009.05.032>
- Ofori-Mensah, S., Yıldız, M., Arslan, M., Eldem, V., 2020a. Fish oil replacement with different vegetable oils in gilthead seabream, *Sparus aurata* diets: Effects on fatty acid metabolism based on whole-body fatty acid balance method and genes expression. *Aquaculture* 529. <https://doi.org/10.1016/j.aquaculture.2020.735609>
- Ofori-Mensah, S., Yıldız, M., Arslan, M., Eldem, V., 2020b. Fish oil replacement with different vegetable oils in gilthead seabream, *Sparus aurata* diets: Effects on fatty acid metabolism based on whole-body fatty acid balance method and genes expression. *Aquaculture* 529, 735609. <https://doi.org/10.1016/J.AQUACULTURE.2020.735609>

REFERENCES

- Ohno, Y., Suto, S., Yamanaka, M., Mizutani, Y., Mitsutake, S., Igarashi, Y., Sassa, T., Kihara, A., 2010. ELOVL1 production of C24 acyl-CoAs is linked to C24 sphingolipid synthesis. *Proc. Natl. Acad. Sci. U. S. A.* 107, 18439–18444. <https://doi.org/10.1073/pnas.1005572107>
- Okar, D.A., Wu, C., Lange, A.J., 2004. Regulation of the regulatory enzyme, 6-phosphofructo-2-kinase/fructose-2,6-bisphosphatase. *Adv. Enzyme Regul.* 44, 123–154.
- Oliva-Teles, A., Enes, P., Peres, H., 2015. Replacing fishmeal and fish oil in industrial aquafeeds for carnivorous fish, *Feed and Feeding Practices in Aquaculture*. Elsevier Ltd. <https://doi.org/10.1016/B978-0-08-100506-4.00008-8>
- Osmond, A.T.Y., Colombo, S.M., 2019. The future of genetic engineering to provide essential dietary nutrients and improve growth performance in aquaculture: Advantages and challenges. *J. World Aquac. Soc.* 50, 490–509. <https://doi.org/10.1111/jwas.12595>
- Özogul, Y., Özogul, F., Alagoz, S., 2007. Fatty acid profiles and fat contents of commercially important seawater and freshwater fish species of Turkey: A comparative study. *Food Chem.* 103, 217–223. <https://doi.org/10.1016/J.FOODCHEM.2006.08.009>
- Pai, V.J., Wang, B., Li, X., Wu, L., Kang, J.X., 2014a. Transgenic mice convert carbohydrates to essential fatty acids. *PLoS One* 9, 1–6. <https://doi.org/10.1371/journal.pone.0097637>
- Pai, V.J., Wang, B., Li, X., Wu, L., Kang, J.X., 2014b. Transgenic mice convert carbohydrates to essential fatty acids. *PLoS One* 9. <https://doi.org/10.1371/JOURNAL.PONE.0097637>
- Pang, S.-C., Wang, H.-P., Li, K.-Y., Zhu, Z.-Y., Kang, J.X., Sun, Y.-H., 2014. Double Transgenesis of Humanized fat1 and fat2 Genes Promotes Omega-3 Polyunsaturated Fatty Acids Synthesis in a Zebrafish Model. *Mar. Biotechnol.* 16, 580–593. <https://doi.org/10.1007/s10126-014-9577-9>
- Panserat, S., Plagnes-Juan, E., Kaushik, S., 2002. Gluconeogenic enzyme gene expression is decreased by dietary carbohydrates in common carp (*Cyprinus carpio*) and gilthead seabream (*Sparus aurata*). *Biochim. Biophys. Acta - Gene Struct. Expr.* 1579, 35–42. [https://doi.org/10.1016/S0167-4781\(02\)00501-8](https://doi.org/10.1016/S0167-4781(02)00501-8)
- Park, Y., Harris, W.S., 2003. Omega-3 fatty acid supplementation accelerates chylomicron triglyceride clearance. *J. Lipid Res.* 44, 455–463. <https://doi.org/10.1194/jlr.M200282-JLR200>
- Parrizas, M., Planas, J., Plisetskaya, E.M., Gutierrez, J., 1994. Insulin binding and receptor tyrosine kinase activity in skeletal muscle of carnivorous and omnivorous fish. *Am. J. Physiol. - Regul. Integr. Comp. Physiol.* 266. <https://doi.org/10.1152/ajpregu.1994.266.6.r1944>
- Peng, M., Xu, W., Mai, K., Zhou, H., Zhang, Y., Liufu, Z., Zhang, K., Ai, Q., 2014. Growth performance, lipid deposition and hepatic lipid metabolism related gene expression in juvenile turbot (*Scophthalmus maximus* L.) fed diets with various fish oil substitution levels by soybean oil. *Aquaculture* 433, 442–449. <https://doi.org/10.1016/j.aquaculture.2014.07.005>
- Peng, S., Chen, L., Qin, J.G., Hou, J., Yu, N., Long, Z., Ye, J., Sun, X., 2008. Effects of replacement of dietary fish oil by soybean oil on growth performance and liver biochemical composition in juvenile black seabream, *Acanthopagrus schlegelii*. *Aquaculture* 276, 154–161. <https://doi.org/10.1016/j.aquaculture.2008.01.035>
- Peng, X., Li, F., Lin, S., Chen, Y., 2016. Effects of total replacement of fish oil on growth performance, lipid metabolism and antioxidant capacity in tilapia (*Oreochromis niloticus*). *Aquac. Int.* 24, 145–156. <https://doi.org/10.1007/s10499-015-9914-7>

REFERENCES

- Peters, C.J., Picardy, J.A., Darrouzet-Nardi, A., Griffin, T.S., 2014. Feed conversions, ration compositions, and land use efficiencies of major livestock products in U.S. agricultural systems. *Agric. Syst.* 130, 35–43. <https://doi.org/10.1016/j.agsy.2014.06.005>
- Pfaffl, M.W., 2001. A new mathematical model for relative quantification in real-time RT-PCR. *Nucleic Acids Res.* 29, e45.
- Piedecausa, M.A., Mazón, M.J., García García, B., Hernández, M.D., 2007. Effects of total replacement of fish oil by vegetable oils in the diets of sharpnose seabream (*Diplodus puntazzo*). *Aquaculture* 263, 211–219. <https://doi.org/10.1016/j.aquaculture.2006.09.039>
- Polakof, S., Médale, F., Skiba-Cassy, S., Corraze, G., Panserat, S., 2010. Molecular regulation of lipid metabolism in liver and muscle of rainbow trout subjected to acute and chronic insulin treatments. *Domest. Anim. Endocrinol.* 39, 26–33. <https://doi.org/10.1016/j.domaniend.2010.01.003>
- Prato, E., Biandolino, F., 2012. Total lipid content and fatty acid composition of commercially important fish species from the Mediterranean, Mar Grande Sea. *Food Chem.* 131, 1233–1239. <https://doi.org/10.1016/j.foodchem.2011.09.110>
- Qi, K., Fan, C., Jiang, J., Zhu, H., Jiao, H., Meng, Q., Deckelbaum, R.J., 2008. Omega-3 fatty acid containing diets decrease plasma triglyceride concentrations in mice by reducing endogenous triglyceride synthesis and enhancing the blood clearance of triglyceride-rich particles. *Clin. Nutr.* 27, 424–430. <https://doi.org/10.1016/j.clnu.2008.02.001>
- Qian, C., Hart, B., Colombo, S.M., 2020a. Re-evaluating the dietary requirement of EPA and DHA for Atlantic salmon in freshwater. *Aquaculture* 518, 734870. <https://doi.org/10.1016/j.aquaculture.2019.734870>
- Qian, C., Hart, B., Colombo, S.M., 2020b. Re-evaluating the dietary requirement of EPA and DHA for Atlantic salmon in freshwater. *Aquaculture* 518, 734870. <https://doi.org/10.1016/J.AQUACULTURE.2019.734870>
- Qin, G., Xu, D., Lou, B., Chen, R., Wang, L., Tan, P., 2020. iTRAQ-based quantitative phosphoproteomics provides insights into the metabolic and physiological responses of a carnivorous marine fish (*Nibealabiflora*) fed a linseed oil-rich diet. *J. Proteomics* 228, 103917. <https://doi.org/10.1016/j.jprot.2020.103917>
- Rajas, F., Gautier, A., Bady, I., Montano, S., Mithieux, G., 2002. Polyunsaturated fatty acyl coenzyme a suppress the glucose-6-phosphatase promoter activity by modulating the DNA binding of hepatocyte nuclear factor 4 α . *J. Biol. Chem.* 277, 15736–15744. <https://doi.org/10.1074/jbc.M200971200>
- Rampino, A., Borgogna, M., Blasi, P., Bellich, B., Cesàro, A., 2013. Chitosan nanoparticles: Preparation, size evolution and stability. *Int. J. Pharm.* 455, 219–228. <https://doi.org/10.1016/j.ijpharm.2013.07.034>
- Repa, J.J., Liang, G., Ou, J., Bashmakov, Y., Lobaccaro, J.M.A., Shimomura, I., Shan, B., Brown, M.S., Goldstein, J.L., Mangelsdorf, D.J., 2000. Regulation of mouse sterol regulatory element-binding protein-1c gene (SREBP-1c) by oxysterol receptors, LXR α and LXR β . *Genes Dev.* 14, 2819–2830. <https://doi.org/10.1101/gad.844900>
- Ricciotti, E., Fitzgerald, G.A., 2011. Prostaglandins and inflammation. *Arterioscler. Thromb. Vasc. Biol.* 31, 986–1000. <https://doi.org/10.1161/ATVBAHA.110.207449>
- Richard, N., Kaushik, S., Larroquet, L., Panserat, S., Corraze, G., 2006a. Replacing dietary fish oil by vegetable oils has little effect on lipogenesis, lipid transport and tissue lipid uptake in rainbow trout (*Oncorhynchus mykiss*). *Br. J. Nutr.* 96, 299–309. <https://doi.org/10.1079/bjn20061821>
- Richard, N., Kaushik, S., Larroquet, L., Panserat, S., Corraze, G., 2006b. Replacing dietary fish oil by vegetable oils has little effect on lipogenesis, lipid transport and tissue lipid uptake in rainbow trout (*Oncorhynchus mykiss*). *Br. J. Nutr.* 96, 299–309. <https://doi.org/10.1079/BJN20061821>

REFERENCES

- Rinaudo, M., 2006. Chitin and chitosan: Properties and applications. *Prog. Polym. Sci.* 31, 603–632.
<https://doi.org/10.1016/j.progpolymsci.2006.06.001>
- Romanatto, T., Fiamoncini, J., Wang, B., Curi, R., Kang, J.X., 2014a. Elevated tissue omega-3 fatty acid status prevents age-related glucose intolerance in fat-1 transgenic mice. *Biochim. Biophys. Acta - Mol. Basis Dis.* 1842, 186–191.
<https://doi.org/10.1016/j.bbadis.2013.10.017>
- Romanatto, T., Fiamoncini, J., Wang, B., Curi, R., Kang, J.X., 2014b. Elevated tissue omega-3 fatty acid status prevents age-related glucose intolerance in fat-1 transgenic mice. *Biochim. Biophys. Acta* 1842, 186–191.
<https://doi.org/10.1016/J.BBADIS.2013.10.017>
- Saggerson, D., 2008a. Malonyl-CoA, a key signaling molecule in mammalian cells. *Annu. Rev. Nutr.* 28, 253–272.
<https://doi.org/10.1146/annurev.nutr.28.061807.155434>
- Saggerson, D., 2008b. Malonyl-CoA, a key signaling molecule in mammalian cells. *Annu. Rev. Nutr.* 28, 253–272.
<https://doi.org/10.1146/ANNUREV.NUTR.28.061807.155434>
- Sahebkar, A., Simental-Mendía, L.E., Mikhailidis, D.P., Pirro, M., Banach, M., Sirtori, C.R., Reiner, Ž., 2018. Effect of omega-3 supplements on plasma apolipoprotein C-III concentrations: a systematic review and meta-analysis of randomized controlled trials. *Ann. Med.* 50, 565–575. <https://doi.org/10.1080/07853890.2018.1511919>
- Sales, R., Galafat, A., Vizcaíno, A.J., Sáez, M.I., Martínez, T.F., Cerón-García, M.C., Navarro-López, E., Tsuzuki, M.Y., Acien-Fernández, F.G., Molina-Grima, E., Alarcón, F.J., 2021. Effects of dietary use of two lipid extracts from the microalga *Nannochloropsis gaditana* (Lubián, 1982) alone and in combination on growth and muscle composition in juvenile gilthead seabream, *Sparus aurata*. *Algal Res.* 53, 102162. <https://doi.org/10.1016/J.ALGAL.2020.102162>
- Salgado, M.C., Metón, I., Anemaet, I.G., González, J.D., Fernández, F., Baanante, I.V., 2012. Hepatocyte nuclear factor 4alpha transactivates the mitochondrial alanine aminotransferase gene in the kidney of *Sparus aurata*. *Mar. Biotechnol.* 14, 46–62. <https://doi.org/10.1007/s10126-011-9386-3>
- Salgado, M.C., Metón, I., Egea, M., Baanante, I. V., 2004. Transcriptional regulation of glucose-6-phosphatase catalytic subunit promoter by insulin and glucose in the carnivorous fish, *Sparus aurata* 783–795.
<https://doi.org/10.1677/jme.1.01552>
- Santos-Carballal, B., Fernández, E.F., Goycoolea, F.M., 2018. Chitosan in non-viral gene delivery: Role of structure, characterization methods, and insights in cancer and rare diseases therapies. *Polymers (Basel)*. 10, 1–51.
<https://doi.org/10.3390/polym10040444>
- Semenkovich, C.F., Coleman, T., Fiedorek, F.T., 1995. Human fatty acid synthase mRNA: Tissue distribution, genetic mapping, and kinetics of decay after glucose deprivation. *J. Lipid Res.* 36, 1507–1521. [https://doi.org/10.1016/s0022-2275\(20\)39738-8](https://doi.org/10.1016/s0022-2275(20)39738-8)
- Serhan, C.N., Petasis, N.A., 2011. Resolvins and protectins in inflammation resolution. *Chem. Rev.* 111, 5922–5943.
<https://doi.org/10.1021/cr100396c>
- Sertoglu, E., Kayadibi, H., Uyanik, M., 2015. A biochemical view: Increase in polyunsaturated fatty acid ω -6/ ω -3 ratio in relation to hepatic steatosis in patients with non-alcoholic fatty liver disease. *J. Diabetes Complications* 29, 157.
<https://doi.org/10.1016/j.jdiacomp.2014.10.005>
- Shahkar, E., Yun, H., Lee, S., Kim, D.J., Kim, S.K., Lee, B.I., Bai, S.C., 2016. Evaluation of the optimum dietary arachidonic acid level and its essentiality based on growth and non-specific immune responses in Japanese eel, *Anguilla japonica*.

REFERENCES

- Aquaculture 452, 209–216. <https://doi.org/10.1016/j.aquaculture.2015.10.034>
- Shearer, G.C., Savinova, O. V., Harris, W.S., 2012a. Fish oil - How does it reduce plasma triglycerides? *Biochim. Biophys. Acta - Mol. Cell Biol. Lipids* 1821, 843–851. <https://doi.org/10.1016/j.bbailip.2011.10.011>
- Shearer, G.C., Savinova, O. V., Harris, W.S., 2012b. Fish oil -- how does it reduce plasma triglycerides? *Biochim. Biophys. Acta* 1821, 843–851. <https://doi.org/10.1016/J.BBALIP.2011.10.011>
- Shi, H., Tian, J., Wu, C., Li, M., An, F., Wu, R., Shao, J., Zheng, Y., Luo, X., Tao, D., Chen, X., Pi, Y., Zhao, C., Yue, X., Wu, J., 2020. Determination of allosteric and active sites responsible for catalytic activity of delta 12 fatty acid desaturase from *Geotrichum candidum* and *Mortierella alpina* by domain swapping. *Enzyme Microb. Technol.* 138. <https://doi.org/10.1016/j.enzmictec.2020.109563>
- Shoji, T., Kakiya, R., Hayashi, T., Tsujimoto, Y., Sonoda, M., Shima, H., Mori, K., Fukumoto, S., Tahara, H., Shioi, A., Tabata, T., Emoto, M., Nishizawa, Y., Inaba, M., 2013. Serum n-3 and n-6 polyunsaturated fatty acid profile as an independent predictor of cardiovascular events in hemodialysis patients. *Am. J. Kidney Dis.* 62, 568–576. <https://doi.org/10.1053/j.ajkd.2013.02.362>
- Silva-Marrero, J.I., Sáez, A., Caballero-Solares, A., Viegas, I., Almajano, M.P., Fernández, F., Baanante, I.V., Metón, I., 2017. A transcriptomic approach to study the effect of long-term starvation and diet composition on the expression of mitochondrial oxidative phosphorylation genes in gilthead sea bream (*Sparus aurata*). *BMC Genomics* 18, 768. <https://doi.org/10.1186/s12864-017-4148-x>
- Silva-Marrero, J.I., Villasante, J., Rashidpour, A., Palma, M., Fábregas, A., Almajano, M.P., Viegas, I., Jones, J.G., Miñarro, M., Ticó, J.R., Baanante, I. V., Metón, I., 2019. The administration of chitosan-tripolyphosphate-DNA nanoparticles to express exogenous SREBP1a enhances conversion of dietary carbohydrates into lipids in the liver of *Sparus aurata*. *Biomolecules* 9. <https://doi.org/10.3390/biom9080297>
- Simopoulos, A.P., 2016. An increase in the Omega-6/Omega-3 fatty acid ratio increases the risk for obesity. *Nutrients* 8, 1–17. <https://doi.org/10.3390/nu8030128>
- Soyal, S.M., Nofziger, C., Dossena, S., Paulmichl, M., Patsch, W., 2015. Targeting SREBPs for treatment of the metabolic syndrome. *Trends Pharmacol. Sci.* 36, 406–416. <https://doi.org/10.1016/j.tips.2015.04.010>
- Sprague, M., Xu, G., Betancor, M.B., Olsen, R.E., Torrissen, O., Glencross, B.D., Tocher, D.R., 2019. Endogenous production of n-3 long-chain PUFA from first feeding and the influence of dietary linoleic acid and the α -linolenic:linoleic ratio in Atlantic salmon (*Salmo salar*). *Br. J. Nutr.* 122, 1091–1102. <https://doi.org/10.1017/S0007114519001946>
- Spychalla, J.P., Kinney, A.J., Browse, J., 1997. Identification of an animal ω -3 fatty acid desaturase by heterologous expression in *Arabidopsis*. *Proc. Natl. Acad. Sci. U. S. A.* 94, 1142–1147. <https://doi.org/10.1073/pnas.94.4.1142>
- Strand, S.P., Tømmeraas, T., Vårum, K.M., Østgaard, K., 2001. Electrophoretic light scattering studies of chitosans with different degrees of N-acetylation. *Biomacromolecules* 2, 1310–1314. <https://doi.org/10.1021/bm015598x>
- Su, J., Gong, Y., Mei, L., Xi, L., Chi, S., Yang, Y., Jin, J., Liu, H., Zhu, X., Xie, S., Han, D., 2020. The characteristics of glucose homeostasis in grass carp and Chinese longsnout catfish after oral starch administration: A comparative study between herbivorous and carnivorous species of fish. *Br. J. Nutr.* 123, 627–641. <https://doi.org/10.1017/S0007114519003234>
- Sun, S., Castro, F., Monroig, Ó., Cao, X., Gao, J., 2020a. Fat-1 Transgenic Zebrafish Are Protected From Abnormal Lipid

REFERENCES

- Deposition Induced By High-Vegetable Oil Feeding. *Appl. Microbiol. Biotechnol.* 104, 7355–7365.
<https://doi.org/10.1007/s00253-020-10774-x>
- Sun, S., Castro, F., Monroig, Ó., Cao, X., Gao, J., 2020b. fat-1 transgenic zebrafish are protected from abnormal lipid deposition induced by high-vegetable oil feeding. *Appl. Microbiol. Biotechnol.* 104, 7355–7365.
<https://doi.org/10.1007/S00253-020-10774-X>
- Svennerholm, L., 1968. Distribution and fatty acid composition of phosphoglycerides in normal human brain. *J. Lipid Res.* 9, 570–579. [https://doi.org/10.1016/s0022-2275\(20\)42702-6](https://doi.org/10.1016/s0022-2275(20)42702-6)
- Tabor, S., Richardson, C.C., 1985. A bacteriophage T7 RNA polymerase/promoter system for controlled exclusive expression of specific genes. *Proc. Natl. Acad. Sci. U. S. A.* 82, 1074–1078. <https://doi.org/10.1073/pnas.82.4.1074>
- Tang, F., Yang, X., Liu, D., Zhang, X., Huang, X., He, X., Shi, J., Li, Z., Wu, Z., 2019. Co-expression of fat1 and fat2 in transgenic pigs promotes synthesis of polyunsaturated fatty acids. *Transgenic Res.* 28, 369–379.
<https://doi.org/10.1007/s11248-019-00127-4>
- Tapia, G., Valenzuela, R., Espinosa, A., Romanque, P., Dossi, C., Gonzalez-Mañán, D., Videla, L.A., D'Espessailles, A., 2014. N-3 long-chain PUFA supplementation prevents high fat diet induced mouse liver steatosis and inflammation in relation to PPAR- α upregulation and NF- κ B DNA binding abrogation. *Mol. Nutr. Food Res.* 58, 1333–1341.
<https://doi.org/10.1002/mnfr.201300458>
- Teles, A.O., Couto, A., Enes, P., Peres, H., 2020. Dietary protein requirements of fish – a meta-analysis. *Rev. Aquac.* 12, 1445–1477. <https://doi.org/10.1111/raq.12391>
- Theofilatos, D., Anestis, A., Hashimoto, K., Kardassis, D., 2016a. Transcriptional regulation of the human Liver X Receptor α gene by Hepatocyte Nuclear Factor 4 α . *Biochem. Biophys. Res. Commun.* 469, 573–579.
<https://doi.org/10.1016/j.bbrc.2015.12.031>
- Theofilatos, D., Anestis, A., Hashimoto, K., Kardassis, D., 2016b. Transcriptional regulation of the human Liver X Receptor α gene by Hepatocyte Nuclear Factor 4 α . *Biochem. Biophys. Res. Commun.* 469, 573–579.
<https://doi.org/10.1016/J.BBRC.2015.12.031>
- Tian, J., Ji, H., Oku, H., Zhou, J., 2014. Effects of dietary arachidonic acid (ARA) on lipid metabolism and health status of juvenile grass carp, *Ctenopharyngodon idellus*. *Aquaculture* 430, 57–65.
<https://doi.org/10.1016/j.aquaculture.2014.03.020>
- Timmis, A., Townsend, N., Gale, C.P., Torbica, A., Lettino, M., Petersen, S.E., Mossialos, E.A., Maggioni, A.P., Kazakiewicz, D., May, H.T., De Smedt, D., Flather, M., Zuhlke, L., Beltrame, J.F., Huculeci, R., Tavazzi, L., Hindricks, G., Bax, J., Casadei, B., Achenbach, S., Wright, L., Vardas, P., Mimosza, L., Artan, G., Aurel, D., Chettibi, M., Hammoudi, N., Sisakian, H., Pepoyan, S., Metzler, B., Siostrzonek, P., Weidinger, F., Jahangirov, T., Aliyev, F., Rustamova, Y., Mrochak, N.M.A., Lancellotti, P., Pasquet, A., Claeys, M., Kusljagic, Z., Hudic, L.D., Smajic, E., Tokmakova, M.P., Gatzov, P.M., Milicic, D., Bergovec, M., Christou, C., Moustra, H.H., Christodoulides, T., Linhart, A., Taborsky, M., Abdelhamid, M., Shokry, K., Kampus, P., Viigimaa, M., Ryödi, E., Niemela, M., Rissanen, T.T., Le Heuzey, J.Y., Gilard, M., Aladashvili, A., Gamkrelidze, A., Kereselidze, M., Zeiher, A., Katus, H., Bestehorn, K., Tsioufis, C., Goudevenos, J., Csanádi, Z., Becker, D., Tóth, K., Hrafnkelsdóttir, P.J., Crowley, J., Kearney, P., Dalton, B., Zahger, D., Wolak, A., Gabrielli, D., Indolfi, C., Urbinati, S., Imantayeva, G., Berkinbayev, S., Bajraktari, G., Ahmeti, A., Berisha, G., Erkin, M., Saamay, A., Erglis, A., Bajare, I., Jegere, S., Mohammed, M., Sarkis, A., Saadeh, G., Zvirblyte,

REFERENCES

- R., Sakalyte, G., Slapikas, R., Ellafi, K., El Ghamari, F., Banu, C., Beissel, J., Felice, T., Buttigieg, S.C., Xuereb, R.G., Popovici, M., Boskovic, A., Rabrenovic, M., Ztot, S., Abir-Khalil, S., Van Rossum, A.C., Mulder, B.J.M., Elsendoorn, M.W., Srinovska-Kostovska, E., Kostov, J., Marjan, B., Steigen, T., Mjølstad, O.C., Ponikowski, P., Witkowski, A., Jankowski, P., Gil, V.M., Mimoso, J., Baptista, S., Vinereanu, D., Chioncel, O., Popescu, B.A., Shlyakhto, E., Oganov, R., Foscoli, M., Zavatta, M., Dikic, A.D., Beleslin, B., Radovanovic, M.R., Hlivak, P., Hatala, R., Kaliska, G., Kenda, M., Frascas, Z., Anguita, M., Cequier, A., Muniz, J., James, S., Johansson, B., Platonov, P., Zellweger, M.J., Pedrazzini, G.B., Carballo, D., Shebli, H.E., Kabbani, S., Abid, L., Addad, F., Bozkurt, E., Kayıkçıoğlu, M., Erol, M.K., Kovalenko, V., Nesukay, E., Wragg, A., Ludman, P., Ray, S., Kurbanov, R., Boateng, D., Daval, G., De Benito Rubio, V., Sebastiao, D., De Courtelary, P.T., Bardin, I., 2020. European society of cardiology: Cardiovascular disease statistics 2019. *Eur. Heart J.* 41, 12–85. <https://doi.org/10.1093/eurheartj/ehz859>
- Tocher, D.R., 2010. Fatty acid requirements in ontogeny of marine and freshwater fish. *Aquac. Res.* 41, 717–732. <https://doi.org/10.1111/j.1365-2109.2008.02150.x>
- Tocher, D.R., Betancor, M.B., Sprague, M., Olsen, R.E., Napier, J.A., 2019. Omega-3 Long-Chain Polyunsaturated Fatty Acids, EPA and DHA: Bridging the Gap between Supply and Demand. *Nutrients* 11, 89. <https://doi.org/10.3390/nu11010089>
- Trushenski, J., Schwarz, M., Bergman, A., Rombenso, A., Delbos, B., 2012. DHA is essential, EPA appears largely expendable, in meeting the n-3 long-chain polyunsaturated fatty acid requirements of juvenile coho salmon *Oncorhynchus kisutch*. *Aquaculture* 326–329, 81–89. <https://doi.org/10.1016/j.aquaculture.2011.11.033>
- Tu, W.C., Cook-Johnson, R.J., James, M.J., Mühlhäusler, B.S., Gibson, R.A., 2010. Omega-3 long chain fatty acid synthesis is regulated more by substrate levels than gene expression. *Prostaglandins Leukot. Essent. Fat. Acids* 83, 61–68. <https://doi.org/10.1016/j.plefa.2010.04.001>
- Turchini, G.M., Hermon, K.M., Francis, D.S., 2018. Fatty acids and beyond: Fillet nutritional characterisation of rainbow trout (*Oncorhynchus mykiss*) fed different dietary oil sources. *Aquaculture* 491, 391–397. <https://doi.org/10.1016/j.aquaculture.2017.11.056>
- Uhe, A.M., Collier, G.R., O’Dea, K., 1992. A comparison of the effects of beef, chicken and fish protein on satiety and amino acid profiles in lean male subjects. *J. Nutr.* 122, 467–472. <https://doi.org/10.1093/jn/122.3.467>
- Vagner, M., Santigosa, E., 2011. Characterization and modulation of gene expression and enzymatic activity of delta-6 desaturase in teleosts: A review. *Aquaculture* 315, 131–143. <https://doi.org/10.1016/j.aquaculture.2010.11.031>
- Vasconi, M., Caprino, F., Bellagamba, F., Moretti, V.M., 2017. Fatty Acid Composition of Gilthead Sea Bream (*Sparus aurata*) Fillets as Affected by Current Changes in Aquafeed Formulation. *Turkish J. Fish. Aquat. Sci.* 17, 51–60. https://doi.org/10.4194/1303-2712-v17_3_01
- Vitali, M., Dimauro, C., Sirri, R., Zappaterra, M., Zambonelli, P., Manca, E., Sami, D., Fiego, D.P. Lo, Davoli, R., 2018. Effect of dietary polyunsaturated fatty acid and antioxidant supplementation on the transcriptional level of genes involved in lipid and energy metabolism in swine. *PLoS One* 13, e0204869. <https://doi.org/10.1371/JOURNAL.PONE.0204869>
- Vusse, G.J. van der, 2009. Albumin as Fatty Acid Transporter. *Drug Metab. Pharmacokinet.* 24, 300–307.
- Wang, B., Tontonoz, P., 2018. Liver X receptors in lipid signalling and membrane homeostasis. *Nat. Rev. Endocrinol.* 14, 452–463. <https://doi.org/10.1038/s41574-018-0037-x>

REFERENCES

- Wang, C., Liu, W., Yao, L., Zhang, X., Zhang, X., Ye, C., Jiang, H., He, J., Zhu, Y., Ai, D., 2017. Hydroxyeicosapentaenoic acids and epoxyeicosatetraenoic acids attenuate early occurrence of nonalcoholic fatty liver disease. *Br. J. Pharmacol.* 174, 2358–2372. <https://doi.org/10.1111/bph.13844>
- Wang, F., Zhao, Y., Niu, Y., Wang, C., Wang, M., Li, Y., Sun, C., 2012. Activated glucose-6-phosphate dehydrogenase is associated with insulin resistance by upregulating pentose and pentosidine in diet-induced obesity of rats. *Horm. Metab. Res.* 44, 938–942. <https://doi.org/10.1055/s-0032-1323727>
- Wang, J., Yu, L., Schmidt, R.E., Su, C., Huang, X., Gould, K., Cao, G., 2005. Characterization of HSCD5, a novel human stearoyl-CoA desaturase unique to primates. *Biochem. Biophys. Res. Commun.* 332, 735–742. <https://doi.org/10.1016/J.BBRC.2005.05.013>
- Wang, Li, Y.J., Hou, C.L., Gao, Y., Wang, Y.Z., 2012. Influence of different dietary lipid sources on the growth, tissue fatty acid composition, histological changes and peroxisome proliferator-activated receptor γ gene expression in large yellow croaker (*Pseudosciaena crocea* R.). *Aquac. Res.* 43, 281–291. <https://doi.org/10.1111/j.1365-2109.2011.02826.x>
- Wang, S., Liu, X., Xu, S., Wu, Q., You, C., Monroig, Ó., Tocher, D.R., Li, Y., 2018. Total Replacement of Dietary Fish Oil with a Blend of Vegetable Oils in the Marine Herbivorous Teleost, *Siganus canaliculatus*. *J. World Aquac. Soc.* 49, 692–702. <https://doi.org/10.1111/jwas.12434>
- Wang, X.X., Li, Y.J., Hou, C.L., Gao, Y., Wang, Y.Z., 2012. Influence of different dietary lipid sources on the growth, tissue fatty acid composition, histological changes and peroxisome proliferator-activated receptor γ gene expression in large yellow croaker (*Pseudosciaena crocea* R.). *Aquac. Res.* 43, 281–291. <https://doi.org/10.1111/j.1365-2109.2011.02826.x>
- Wang, Y., Nakajima, T., Gonzalez, F.J., Tanaka, N., 2020. PPARs as metabolic regulators in the liver: Lessons from liver-specific PPAR-null mice. *Int. J. Mol. Sci.* 21. <https://doi.org/10.3390/ijms21062061>
- Wang, Y., Rogers, P.M., Su, C., Varga, G., Stayrook, K.R., Burris, T.P., 2008. Regulation of cholesterologenesis by the oxysterol receptor, LXR α . *J. Biol. Chem.* 283, 26332–26339. <https://doi.org/10.1074/jbc.M804808200>
- Watts, J.L., Browse, J., 2002. Genetic dissection of polyunsaturated fatty acid synthesis in *Caenorhabditis elegans*. *Proc. Natl. Acad. Sci. U. S. A.* 99, 5854–5859. <https://doi.org/10.1073/pnas.092064799>
- Wilkie, M.P., 2002. Ammonia excretion and urea handling by fish gills: Present understanding and future research challenges. *J. Exp. Zool.* 293, 284–301. <https://doi.org/10.1002/jez.10123>
- Williams, C.D., Whitley, B.M., Hoyo, C., Grant, D.J., Iraggi, J.D., Newman, K.A., Gerber, L., Taylor, L.A., McKeever, M.G., Freedland, S.J., 2011. A high ratio of dietary n-6/n-3 polyunsaturated fatty acids is associated with increased risk of prostate cancer. *Nutr. Res.* 31, 1–8. <https://doi.org/10.1016/j.nutres.2011.01.002>
- Wu, Y., Rashidpour, A., Almajano, M.P., Metón, I., 2020a. Chitosan-Based drug delivery system: Applications in fish biotechnology. *Polymers (Basel).* 12. <https://doi.org/10.3390/POLYM12051177>
- Wu, Y., Rashidpour, A., Almajano, M.P., Metón, I., 2020b. Chitosan-based drug delivery system: Applications in fish biotechnology. *Polymers (Basel).* 12, 1177. <https://doi.org/10.3390/polym12051177>
- Xie, D., Chen, C., Dong, Y., You, C., Wang, S., Monroig, Ó., Tocher, D.R., Li, Y., 2021. Regulation of long-chain polyunsaturated fatty acid biosynthesis in teleost fish. *Prog. Lipid Res.* 82. <https://doi.org/10.1016/j.plipres.2021.101095>

REFERENCES

- Xie, D., Guan, J., Huang, X., Xu, C., Pan, Q., Li, Y., 2022. Tilapia can be a Beneficial n-3 LC-PUFA Source due to Its High Biosynthetic Capacity in the Liver and Intestine. *J. Agric. Food Chem.* 70, 2701–2711.
<https://doi.org/10.1021/acs.jafc.1c05755>
- Xu, H.E., Lambert, M.H., Montana, V.G., Parks, D.J., Blanchard, S.G., Brown, P.J., Sternbach, D.D., Rgen, J., Lehmann, M., Wisely, G.B., Willson, T.M., Kliewer, S.A., Milburn, M. V, 1999. Molecular Recognition of Fatty Acids by Peroxisome Proliferator–Activated Receptors that activate the PPARs in vitro have pharmacological effects similar to those reported for the synthetic PPAR. *Mol. Cell* 3, 397–403.
- Yang, L.G., Song, Z.X., Yin, H., Wang, Y.Y., Shu, G.F., Lu, H.X., Wang, S.K., Sun, G.J., 2016. Low n-6/n-3 PUFA Ratio Improves Lipid Metabolism, Inflammation, Oxidative Stress and Endothelial Function in Rats Using Plant Oils as n-3 Fatty Acid Source. *Lipids* 51, 49–59. <https://doi.org/10.1007/s11745-015-4091-z>
- Yildiz, M., Şener, E., Timur, M., 2008. Effects of differences in diet and seasonal changes on the fatty acid composition in fillets from farmed and wild sea bream (*Sparus aurata* L.) and sea bass (*Dicentrarchus labrax* L.). *Int. J. Food Sci. Technol.* 43, 853–858. <https://doi.org/10.1111/j.1365-2621.2007.01526.x>
- Yilmaz, H.R., Songur, A., Özyurt, B., Zararsiz, I., Sarsilmaz, M., 2004. The effects of n-3 polyunsaturated fatty acids by gavage on some metabolic enzymes of rat liver. *Prostaglandins. Leukot. Essent. Fatty Acids* 71, 131–135.
<https://doi.org/10.1016/J.PLEFA.2004.03.002>
- Yin, L., Ma, H., Ge, X., Edwards, P.A., Zhang, Y., 2011. Hepatic hepatocyte nuclear factor 4 α is essential for maintaining triglyceride and cholesterol homeostasis. *Arterioscler. Thromb. Vasc. Biol.* 31, 328–336.
<https://doi.org/10.1161/ATVBAHA.110.217828>
- Yokoyama, C., Wang, X., Briggs, M.R., Admon, A., Wu, J., Hua, X., Goldstein, J.L., Brown, M.S., 1993. SREBP-1, a basic-helix-loop-helix-leucine zipper protein that controls transcription of the low density lipoprotein receptor gene. *Cell* 75, 187–197. [https://doi.org/10.1016/S0092-8674\(05\)80095-9](https://doi.org/10.1016/S0092-8674(05)80095-9)
- You, C., Jiang, D., Zhang, Q., Xie, D., Wang, S., Dong, Y., Li, Y., 2017. Cloning and expression characterization of peroxisome proliferator-activated receptors (PPARs) with their agonists, dietary lipids, and ambient salinity in rabbitfish *Siganus canalicularis*. *Comp. Biochem. Physiol. Part - B Biochem. Mol. Biol.* 206, 54–64.
<https://doi.org/10.1016/j.cbpb.2017.01.005>
- You, W., Li, M., Qi, Y., Wang, Y., Chen, Y., Liu, Y., Li, L., Ouyang, H., Pang, D., 2021. CRISPR/Cas9-Mediated Specific Integration of Fat-1 and IGF-1 at the p Rosa26 Locus. *Genes (Basel)*. 12, 1027.
<https://doi.org/10.3390/GENES12071027>
- Yu, H., Shan, L., Li, L., Zhang, Q., Liu, D., 2022. Effect of dietary lipid levels on the anti-oxidant responses, initial immunity, and mTOR signaling in the liver of coho salmon (*Oncorhynchus kisutch*). *Aquac. Reports* 23, 101090.
<https://doi.org/10.1016/j.aqrep.2022.101090>
- Yúfera, M., Conceição, L.E.C., Battaglene, S., Fushimi, H., Kotani, T., 2011. Early Development and Metabolism, in: *Sparidae*. Wiley-Blackwell, Oxford, UK, pp. 133–168. <https://doi.org/10.1002/9781444392210.ch5>
- Zhang, J., Cui, M.L., Nie, Y.W., Dai, B., Li, F.R., Liu, D.J., Liang, H., Cang, M., 2018a. CRISPR/Cas9-mediated specific integration of fat-1 at the goat MSTN locus. *FEBS J.* 285, 2828–2839. <https://doi.org/10.1111/febs.14520>
- Zhang, J., Cui, M.L., Nie, Y.W., Dai, B., Li, F.R., Liu, D.J., Liang, H., Cang, M., 2018b. CRISPR/Cas9-mediated specific integration of fat-1 at the goat MSTN locus. *FEBS J.* 285, 2828–2839. <https://doi.org/10.1111/FEBS.14520>

REFERENCES

- Zhang, J.Y., Kothapalli, K.S.D., Brenna, J.T., 2016. Desaturase and elongase-limiting endogenous long-chain polyunsaturated fatty acid biosynthesis. *Curr. Opin. Clin. Nutr. Metab. Care* 19, 103–10.
<https://doi.org/10.1097/MCO.0000000000000254>
- Zhang, Pang, S., Liu, C., Wang, H., Ye, D., Zhu, Z., Sun, Y., 2019. A Novel Dietary Source of EPA and DHA: Metabolic Engineering of an Important Freshwater Species—Common Carp by fat1-Transgenesis. *Mar. Biotechnol.* 21, 171–185. <https://doi.org/10.1007/s10126-018-9868-7>
- Zhang, T.T., Xu, J., Wang, Y.M., Xue, C.H., 2019. Health benefits of dietary marine DHA/EPA-enriched glycerophospholipids. *Prog. Lipid Res.* 75, 100997. <https://doi.org/10.1016/j.plipres.2019.100997>
- Zhang, X., Pang, S., Liu, C., Wang, H., Ye, D., Zhu, Z., Sun, Y., 2019. A Novel Dietary Source of EPA and DHA: Metabolic Engineering of an Important Freshwater Species—Common Carp by fat1-Transgenesis. *Mar. Biotechnol.* 21, 171–185. <https://doi.org/10.1007/s10126-018-9868-7>
- Zhang, X., Pang, S., Liu, C., Wang, H., Ye, D., Zhu, Z., Sun, Y., 2018. A Novel Dietary Source of EPA and DHA: Metabolic Engineering of an Important Freshwater Species-Common Carp by fat1-Transgenesis. *Mar. Biotechnol.* (NY).
<https://doi.org/10.1007/s10126-018-9868-7>
- Zhao, L.F., Iwasaki, Y., Nishiyama, M., Taguchi, T., Tsugita, M., Okazaki, M., Nakayama, S., Kambayashi, M., Fujimoto, S., Hashimoto, K., Murao, K., Terada, Y., 2012. Liver X receptor α is involved in the transcriptional regulation of the 6-phosphofructo-2-kinase/fructose-2,6-bisphosphatase gene. *Diabetes* 61, 1062–1071. <https://doi.org/10.2337/DB11-1255>
- Zhao, Y., Calon, F., Julien, C., Winkler, J.W., Petasis, N.A., Lukiw, W.J., Bazan, N.G., 2011. Docosahexaenoic acid-derived neuroprotectin D1 induces neuronal survival via secretase- and PPAR γ -mediated mechanisms in Alzheimer's disease models. *PLoS One* 6. <https://doi.org/10.1371/journal.pone.0015816>
- Zhou, X.R., Green, A.G., Singh, S.P., 2011. *Caenorhabditis elegans* $\Delta 12$ -desaturase FAT-2 is a bifunctional desaturase able to desaturate a diverse range of fatty acid substrates at the $\Delta 12$ and $\Delta 15$ positions. *J. Biol. Chem.* 286, 43644–43650.
<https://doi.org/10.1074/jbc.M111.266114>
- Zhu, C., Huang, M., Kim, H.G., Chowdhury, K., Gao, J., Liu, S., Wan, J., Wei, L., Dong, X.C., 2021. SIRT6 controls hepatic lipogenesis by suppressing LXR, ChREBP, and SREBP1. *Biochim. Biophys. Acta - Mol. Basis Dis.* 1867, 166249.
<https://doi.org/10.1016/j.bbadis.2021.166249>
- Zhuang, P., Li, H., Jia, W., Shou, Q., Zhu, Y., Mao, L., Wang, W., Wu, F., Chen, X., Wan, X., Wu, Y., Liu, X., Li, Y., Zhu, F., He, L., Chen, J., Zhang, Y., Jiao, J., 2021. Eicosapentaenoic and docosahexaenoic acids attenuate hyperglycemia through the microbiome-gut-organs axis in db/db mice. *Microbiome* 9, 1–21. <https://doi.org/10.1186/s40168-021-01126-6>
- Zhuo, M.Q., Luo, Z., Pan, Y.X., Wu, K., Fan, Y.F., Zhang, L.H., Song, Y.F., 2015. Effects of insulin and its related signaling pathways on lipid metabolism in the yellow catfish *Pelteobagrus fulvidraco*. *J. Exp. Biol.* 218, 3083–3090.
<https://doi.org/10.1242/jeb.124271>
- Zohar, Y., Abraham, M., Gordin, H., 1978. The gonadal cycle of the captivity-reared hermaphroditic teleost *Sparus aurata* (L.) during the first two years of life. *Ann. Biol. Anim. Biochim. Biophys.* 18, 877–882.
<https://doi.org/10.1051/rnd:19780519>

8 APPENDIX

Publications




Wu, Yuanbing, Ania Rashidpour, María Pilar Almajano, and Isidoro Metón. "Chitosan-based drug delivery system: Applications in fish biotechnology." *Polymers* 12, no. 5 (2020): 1177.

Sáez-Arteaga, Alberto, **Yuanbing Wu**, Jonás I. Silva-Marrero, Ania Rashidpour, María Pilar Almajano, Felipe Fernández, Isabel V. Baanante, and Isidoro Metón. "Gene markers of dietary macronutrient composition and growth in the skeletal muscle of gilthead sea bream (*Sparus aurata*)." *Aquaculture* 555 (2022): 738221.

Yuanbing Wu, Ania Rashidpour, Anna Fàbregas, María Pilar Almajano, Isidoro Metón. "Chitosan-mediated expression of fish codon-optimised *Caenorhabditis elegans* FAT-1 and FAT-2 boosts EPA and DHA biosynthesis in *Sparus aurata*" (manuscript under review)

Review

Chitosan-Based Drug Delivery System: Applications in Fish Biotechnology

Yuanbing Wu ^{1,†} , Ania Rashidpour ^{1,†}, María Pilar Almajano ²  and Isidoro Metón ^{1,*} 

¹ Secció de Bioquímica i Biologia Molecular, Departament de Bioquímica i Fisiologia, Facultat de Farmàcia i Ciències de l'Alimentació, Universitat de Barcelona, Joan XXIII 27–31, 08028 Barcelona, Spain; wuuanbing@gmail.com (Y.W.); aniyarashidpour2017@gmail.com (A.R.)

² Departament d'Enginyeria Química, Universitat Politècnica de Catalunya, Diagonal 647, 08028 Barcelona, Spain; m.pilar.almajano@upc.edu

* Correspondence: imeton@ub.edu; Tel.: +34-93-4024521

† Both authors contributed equally to this work.

Received: 29 April 2020; Accepted: 19 May 2020; Published: 21 May 2020



Abstract: Chitosan is increasingly used for safe nucleic acid delivery in gene therapy studies, due to well-known properties such as bioadhesion, low toxicity, biodegradability and biocompatibility. Furthermore, chitosan derivatization can be easily performed to improve the solubility and stability of chitosan–nucleic acid polyplexes, and enhance efficient target cell drug delivery, cell uptake, intracellular endosomal escape, unpacking and nuclear import of expression plasmids. As in other fields, chitosan is a promising drug delivery vector with great potential for the fish farming industry. This review highlights state-of-the-art assays using chitosan-based methodologies for delivering nucleic acids into cells, and focuses attention on recent advances in chitosan-mediated gene delivery for fish biotechnology applications. The efficiency of chitosan for gene therapy studies in fish biotechnology is discussed in fields such as fish vaccination against bacterial and viral infection, control of gonadal development and gene overexpression and silencing for overcoming metabolic limitations, such as dependence on protein-rich diets and the low glucose tolerance of farmed fish. Finally, challenges and perspectives on the future developments of chitosan-based gene delivery in fish are also discussed.

Keywords: chitosan; gene delivery; gene overexpression; gene silencing; fish biotechnology

1. Introduction

Chitosan is a cationic polymer of β (1-4)-linked 2-amino-2-deoxy-D-glucose interspersed by residual 2-acetamido-2-deoxy- β -D-glucose, derived from chitin by deacetylation under alkaline conditions. Chitin is the second most abundant polysaccharide in nature, after cellulose, and it is obtained from the external skeleton and skin of arthropods and insects. Chitin is also found in some microorganisms, yeast and fungi. Mucoadhesion, low toxicity, biodegradability and biocompatibility, as well as antioxidant, antibacterial, antifungal, antitumor and anti-inflammatory properties led, in recent years, to the increasing use of chitosan in a wide variety of pharmaceutical, biomedical and biotechnological fields, including wound healing, tissue engineering, bone regeneration, gene therapy, food industry and agriculture [1–6].

Chitosan has many desirable biological properties that make it a highly suitable carrier to deliver nucleic acids for the development of gene therapy assays. The goal of gene therapy is to introduce exogenous genetic material into target cells, with the aim of modifying the expression of specific genes. The efficient delivery of plasmid DNA to express exogenous genes or siRNA to knockdown the expression of target genes must overcome systemic and cell barriers, depending on the target tissue

and nature of the molecular mechanism triggered by the gene therapy. Ideally, for safe nucleic acid delivery, the vector must establish a stable interaction with the cargo, protect it from the action of nucleases, reach target cells, enable crossing the cell membrane and, once inside the cell, facilitate escape from endosomes and lysosomes. Decomplexation from the carrier must allow plasmid DNA to cross the nuclear membrane and become transcribed, or in the case of siRNA, render the cargo in the cytosol [7–9].

Nucleic acid delivery into cells is facilitated by viral and non-viral vectors. The choice of the vector for gene therapy is a key step to properly reach target cells, confer protection from nucleases, cross the cell membrane, nucleic acid escape from endosomal vesicles, determine transient or permanent effects, allow transcription of delivered plasmid DNA and knockdown the expression of target genes by RNA interference (RNAi) [7,10].

Due to its high transfection efficiency, viral vectors are still used in most gene therapy assays. However, immunogenicity, acute inflammation and other unwanted effects, such as reversal of the wild-type phenotype associated with the use of viral vectors, have focused attention on the development of safer alternative gene delivery systems [9,11,12]. Non-viral vectors include lipid-based vectors and cationic polymers. Low transfection efficiency in vivo, reduced half-life of lipoplex circulation, cytotoxicity and other non-desired effects, such as complement activation, limit in vivo use of cationic lipids and lipid-based vectors [10,13–16]. Unlike viral vectors, cationic polymers, such as chitosan and its derivatives, exhibit increased ability to select target tissues, easy large-scale production, low toxicity and immunogenicity in vivo and biocompatibility [4,9,10]. In this review, we will summarize recent advances in chitosan-based formulations for delivering nucleic acids, and address current progress of the use of chitosan for fish biotechnology applications and gene therapy.

2. Chitosan as a Nucleic Acid Delivery Vector

The use of chitosan as a vector for nucleic acid delivery was proposed in 1995 [17]. A few years later, in 1998, in vivo administration of chitosan complexed with plasmid DNA to express a reporter gene in the upper small intestine and colon of rabbits was published [18]. It was in 2006 when chitosan nanoparticles encapsulating small interfering RNA (siRNA) were shown to be also effective for silencing the expression of target genes [19]. Since pioneering studies, much progress has been made in this area, and chitosan is considered, at present, one of the most effective non-viral gene delivery systems. Figure 1 shows Web of Science (Clarivate Analytics) citations, with the topics chitosan, fish and gene delivery until 2019.

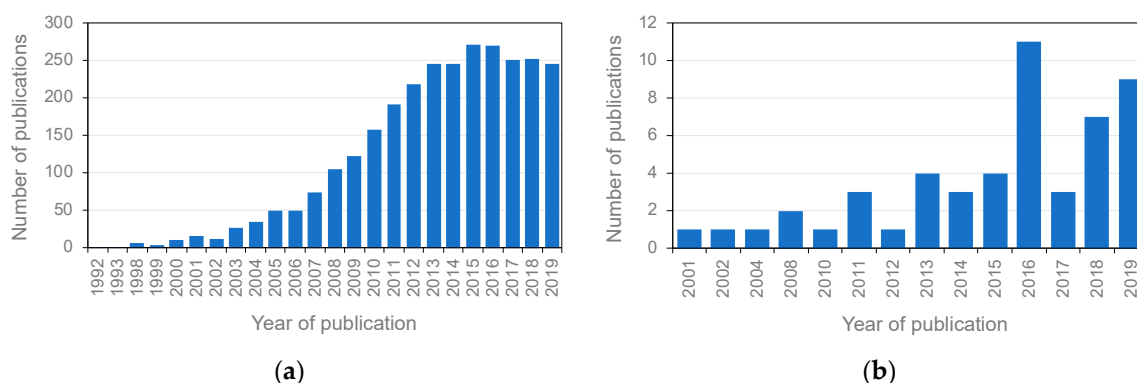


Figure 1. Web of Science (Clarivate Analytics) citations published until 2019 with the topics: (a) chitosan and gene therapy; (b) chitosan, fish and gene therapy.

The presence of numerous primary amine groups that are protonated at slightly acidic pH in chitosan allows electrostatic interaction with negatively charged nucleic acids. The stability of the complex formed between chitosan and nucleic acids allows oral, nasal, intravenous and intraperitoneal

administration of chitosan–DNA complexes, and prevents dissociation before reaching the intracellular compartment [20–22]. Oral delivery would mainly result in intestinal absorption of the product [22]. Biodistribution of radioiodinated chitosan fractions with different molecular mass, intravenously injected to rats, showed rapid plasma clearance (<15% in the blood 5 min following treatment) and localization in the liver of most of the chitosan with diameter size >10 kDa (>50% at 5 min following intravenous administration and >80% at 60 min post-treatment). However, low molecular weight chitosan (<5 kDa) was cleared more slowly from the circulation and significantly less retained in the liver at the short- and long-term [20].

2.1. Chitosan Derivatization

Derivatization can greatly influence biodistribution of chitosan complexes. An illustrative example was developed by Kang et al. to down-regulate Akt2 expression for treatment of colorectal liver metastases in mice [23]. To protect siRNA from gastrointestinal degradation, facilitate active transport into enterocytes and enhance transportation to the liver through the enterohepatic circulation, the authors first obtained gold nanoparticles conjugated with thiolated siRNA (AR). The resulting complex was subsequently complexed with glycol chitosan–taurocholic acid (GT) through electrostatic interaction to generate AR-GT nanoparticles. Derivatization with taurocholic acid successfully protected Akt2-siRNA from gastrointestinal degradation and favored targeting to the liver through the enterohepatic circulation. Chitosan derivatization with hydrophilic ethylene glycol (glycol chitosan) increases solubility in water at a neutral/acidic pH. In addition, the reactive functional groups of glycol chitosan facilitate chemical modifications and formation of different derivatives useful for targeting gene delivery [24]. In addition to the properties of chitosan derivatives, the efficient delivery of the cargo greatly depends on chitosan polyplex properties, such as pH, molecular weight, deacetylation degree and N/P ratio [7,9].

The molecular weight of chitosan is a major factor affecting polyplex formation, the stability of the chitosan/DNA complex, cell entry, DNA unpacking after endosomal escape and transfection efficiency. Furthermore, the average particle size is highly dependent on the molecular weight of chitosan [7,9,25]. Chitosan between ~20–150 kDa forms chitosan–plasmid DNA complexes with diameter size of ~155–200 nm. High molecular weight chitosan >150 kDa losses solubility and favors aggregate formation, whereas chitosan of molecular weight <20 kDa tends to form polyplexes with diameter size >200 nm [26]. The optimal molecular weight range for stable chitosan–siRNA nanoparticle formation and efficient transfection and silencing effect is considered to be ~65–170 kDa [27].

Chemical modification of chitosan can greatly improve desirable properties for gene delivery. Functional groups of chitosan include C₃-OH, C₆-OH, C₂-NH₂, acetyl amino and glycoside bonds [6,28]. Two of the functional groups, C₆-OH and C₂-NH₂, have chemical properties that make them of particular interest for derivatization (Figure 2).

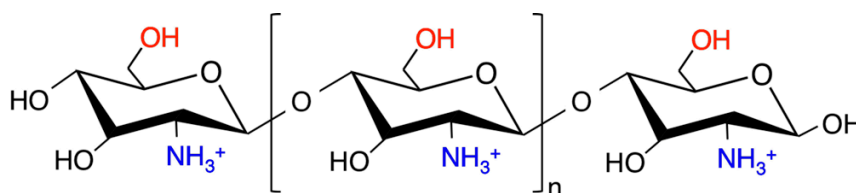


Figure 2. Schematic representation of chitosan. Functional groups C₂-NH₂ and C₆-OH and are represented in blue and red color, respectively.

2.2. Chitosan Solubility

The water solubility of chitosan is low due to the presence of highly crystalline intermolecular and intramolecular hydrogen bonds, and can be greatly influenced by the pH, molecular weight and deacetylation degree [6,9,29]. The solubility of chitosan has been improved by introducing a hydrophilic

group on amino or hydroxyl groups. Examples include: N-acylated chitosan derivatives, which exhibit enhanced biocompatibility, anticoagulability, blood compatibility and sustained drug release [6,30]; chitosan conjugation with saccharides through N-alkylation, such as glycosylation [3,31,32]; and the introduction of a quaternary ammonium salt group, which increases chargeability, mucoadhesion, crossing of mucus layers and binding to epithelial surfaces [6,33,34].

2.3. Stability of Chitosan Polyplexes

To increase the stability of chitosan-based formulations, a number of chitosan derivatives have been developed. Among them, PEGylation [35–37], glycosylation [3,38,39] and quaternization [39–42]. The choice of the method for preparing chitosan–nucleic acid complexes can also significantly affect stability of the complex and transfection efficiency. Katas and Alpar showed that for efficient siRNA-mediated silencing of the expression of target genes in CHO K1 and HEK 293 cells, nanoparticles produced by ionic gelation of tripolyphosphate (TPP) with chitosan were more efficient in delivering siRNA than chitosan–siRNA complexes and siRNA adsorbed onto chitosan–TPP nanoparticles. Chitosan–TPP–siRNA nanoparticles generated by ionic gelation presented higher binding capacity and loading efficiency [19]. During ionic gelation, TPP is a polyanion that crosslinks with positively charged chitosan through electrostatic interaction, avoiding the use of toxic reagents for chemical crosslinking, and allowing for the easy modulation of size and surface charge of the nanoparticles (Figure 3). The addition of TPP was shown to reduce the particle size and increase the stability of complexes in biological fluids [19,43–47]. The inclusion of hyaluronic acid in chitosan–siRNA polyplexes can be also a promising strategy to increase stability and targeting capacity, while lowering aggregation in the presence of serum proteins [48].

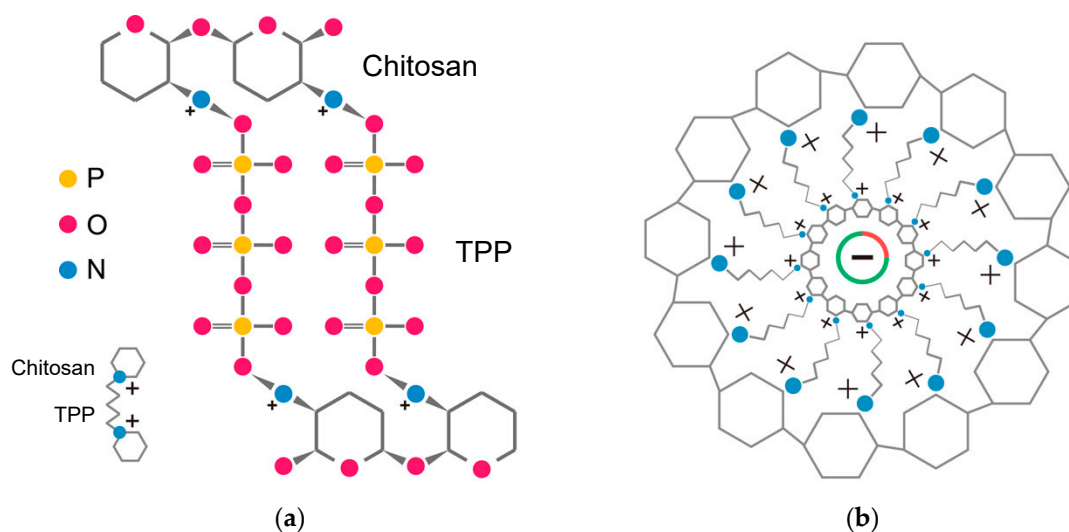


Figure 3. Molecular structure and electrostatic interactions of chitosan–tripolyphosphate (TPP) (a), and chitosan–TPP–plasmid DNA nanoparticles (b).

One major advantage of chitosan is that chitosan–DNA complexation protects DNA from DNase-mediated degradation, possibly as a result of modification of the DNA tertiary structure [20,49]. Cell penetration of chitosan-based gene delivery systems involves interaction between positively charged chitosan–nucleic acid polyplexes and negatively charged cell membrane components, such as heparan sulfate proteoglycans, enabling ATP-driven crossing of the cell membrane, or receptor-mediated endocytosis. In any case, chitosan polyplexes are internalized following the endocytic-lysosomal pathway [7].

2.4. Targeting Drug Delivery, Cellular Uptake and Intracellular Trafficking

Safe and effective therapies can be performed by using chitosan derivatives to improve target drug delivery. To this end, a variety of molecules can be conjugated to chitosan, such as proteins and peptides, polysaccharides, oligonucleotides and other molecules [4].

2.4.1. Targeting Drug Delivery with Chitosan Derivatives

A common strategy to target drug delivery is based on ligand-receptor specificity. Cell-target delivery drugs can be thus enhanced by conjugation of chitosan–nucleic acid complexes with ligands that enable binding to receptors specifically found in the target cell membrane. Examples of ligands conjugated to chitosan formulations include transferrin, galactose and mannose. For instance, transferrin can be used as a targeting ligand for delivery into tumor cells through binding to the transferrin receptor, whose expression is enhanced in tumor cells to provide iron as a necessary cofactor for DNA synthesis and rapid cell proliferation [50–52]. The presence of asialoglycoprotein receptors on the hepatocyte surface and selective binding of asialoglycoprotein receptors to galactose allow galactosylated chitosan to target hepatocytes [53,54]. Mannosylated chitosan takes advantage of mannose recognition by mannose receptors to target dendritic cells [55].

Chitosan derivatives generally achieve mucosal adhesion through hydrogen bonding or non-specific, non-covalent, electrostatic interactions. Thiolated chitosan increases mucoadhesion and enhances crossing capability through the cell membrane and ophthalmic drug delivery [56–60]. The mucoadhesive properties of chitosan derivatives allow oral administration and nasal immunization to treat respiratory diseases [61]. Other examples include O-carboxymethyl chitosan, which can be used for intestine-targeted drug delivery [62], and acetylated low molecular weight chitosan, for targeting the kidneys [63].

2.4.2. Endosomal Escape, Unpacking and Nuclear Import of DNA

The proton sponge effect of chitosan gene delivery formulations allows endosomal escape before the maturation of early endosomes into late endosomes, and the ultimate fusion with lysosomes. The increasing acidification in early endosomes generated by the V-type ATPase proton pump results in progressive protonation of the amine groups of chitosan (pKa value of ~6.5), leading to the influx of water and chloride ions into the endosomes, increased osmotic swelling, endosome lysis and cytosolic release of the endosomal content [9,64]. The endosomal release of chitosan polyplexes can be enhanced by fusogenic peptides [65,66] and pH-sensitive neutral lipids [67]. Efficient transfection and endosomal escape of chitosan polyplexes can be also enhanced by chitosan–polyethylenimine (PEI) copolymeric delivery systems. PEI is a cationic polymer non-viral vector with high transfection efficiency and a strong buffering capacity, which may enhance the influx of chloride anions, osmotic swelling and endosomal lysis. However, PEI-dependent cytotoxic effects constitute a major concern when using PEI for gene delivery [7,68–70]. In contrast, chitosan–PEI complexes exhibit efficient uptake by target cells, high transfection efficiency and negligible toxicity [36,71–75].

Following endosomal escape into the cytosol, chitosan polyplexes carrying DNA must be unpacked, and the entrance of loaded DNA into the nucleus is needed for transfection. The molecular events that mediate DNA unpacking after endosomal release and translocation to the nucleus remain not fully understood. It is generally accepted that, in non-dividing cells, molecules smaller than ~40 kDa can passively diffuse through the nuclear pores, while larger molecules must carry nuclear localization signals for active transportation [68]. Sun et al. largely improved DNA unpacking from chitosan and transfection efficiency upon the conjugation of chitosan with small peptides that can be phosphorylated [76]. The phosphorylation of conjugated peptides mimics the process leading to genomic DNA release and the activation of transcription, mediated by histone phosphorylation. In addition, the introduction of negatively charged phosphate groups may result in electric repulsion between DNA and chitosan conjugated with phosphorylated peptides. Hence, further enhancement of

transfection was obtained by conjugating chitosan with small peptides carrying a nuclear localization signal, in addition to a potentially phosphorylatable serine residue [77]. Exogenous gene expression was improved through a mechanism that enabled DNA import into the nucleus, and enhanced unpacking by the action of nuclear histone kinases. Miao et al. improved endosomal escape and intracellular drug release in HepG2.2.15 cells by loading DNA into a redox-responsive chitosan oligosaccharide-SS-octadecylamine (CSSO) polymer. Intracellular reduction and cleavage of CSSO disulfide bonds ‘-SS-’ by glutathione allowed rapid DNA release [78].

For strategies aiming RNAi on target genes, chitosan has been mostly complexed with siRNA, microRNA (miRNA) and plasmids expressing short hairpin RNA (shRNA). After unpacking, siRNA/miRNA associates with RNA-induced silencing complex (RISC) in the cytosol. The RNAi-guided complex hybridizes with target mRNA, leading to mRNA cleavage and/or translation repression, and subsequent inhibition of protein synthesis [9,10,48,79]. The use of shRNA expression plasmids allowing long lasting expression of siRNA may improve RNAi in vivo. Following plasmid DNA transcription in the nucleus, the transcribed shRNA is processed by Drosha, exported to the cytosol and processed by Dicer, leading to cleavage of double-stranded shRNA and the formation of specific siRNA [75,80–85].

Sequential events associated with three illustrative examples using chitosan to deliver nucleic acids are represented in Figure 4 (chitosan–TPP complexed with a plasmid construct, to express an exogenous protein), Figure 5 (chitosan–TPP complexed with a plasmid construct, to express a shRNA designed for target gene silencing) and Figure 6 (chitosan loading siRNA for target gene silencing).

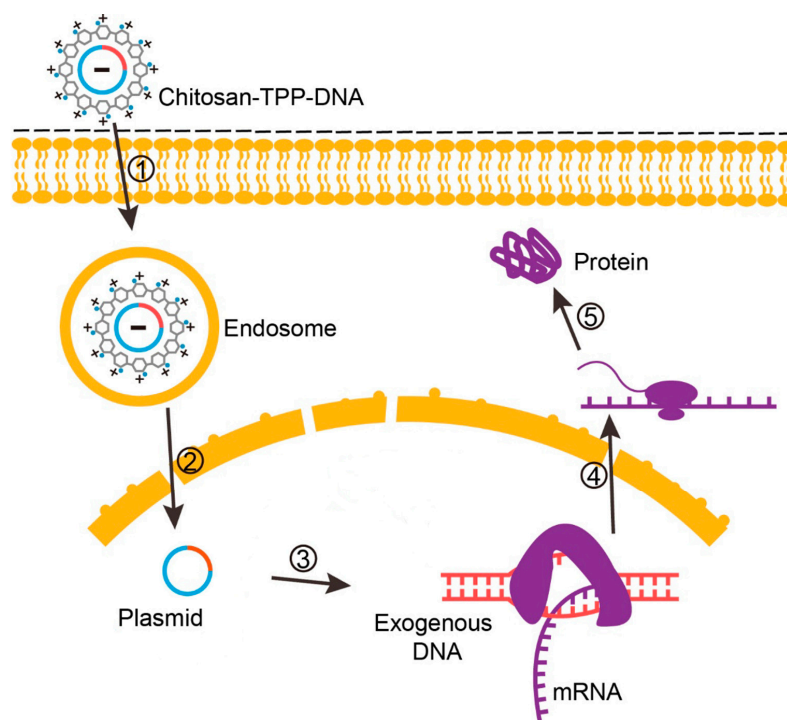


Figure 4. Cellular events associated with chitosan-based plasmid delivery for exogenous gene expression. 1, Cellular uptake of chitosan–DNA by endocytosis. 2, Endosomal escape of the chitosan–DNA complex, plasmid dissociation from chitosan and translocation to the nucleus. 3, Transcription of plasmid (exogenous DNA) in the nucleus and mRNA generation. 4, Translation of newly transcribed mRNA in the cytosol. 5, Exogenous protein assembly.

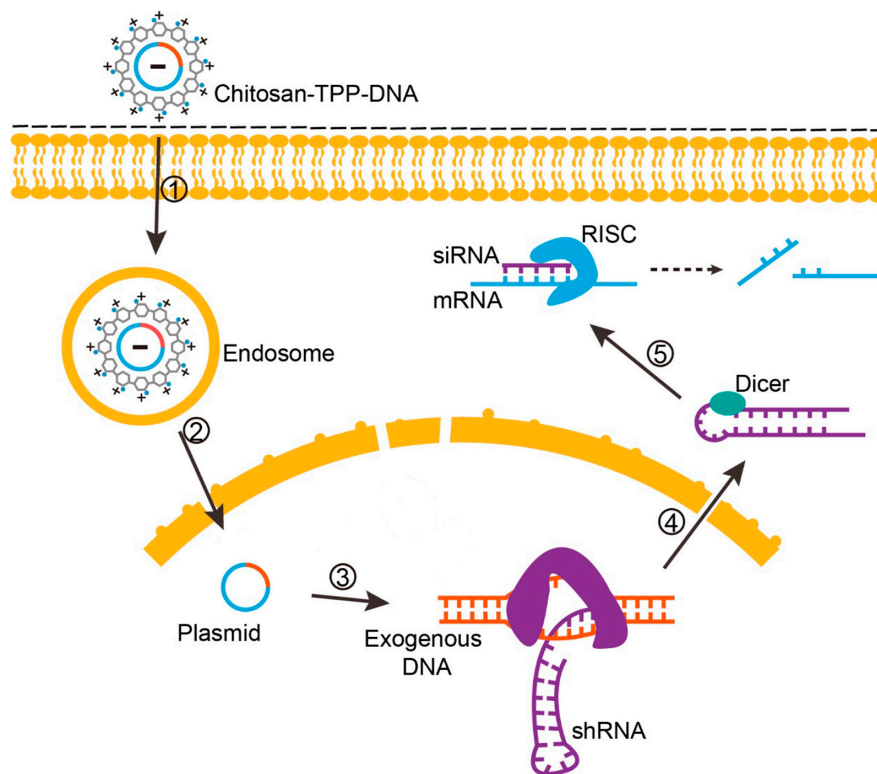


Figure 5. Cellular events associated with chitosan-based plasmid delivery for short hairpin RNA (shRNA) expression, siRNA formation and target gene silencing. 1, Cellular uptake of chitosan–DNA by endocytosis. 2, Endosomal escape of chitosan–DNA complex, plasmid dissociation from chitosan and translocation to the nucleus. 3, Transcription of plasmid (exogenous DNA) in the nucleus and generation of shRNA. 4, Transportation of shRNA to the cytosol and association with Dicer to generate siRNA. 5, siRNA association with RNA-induced silencing complex (RISC) and target mRNA by base pairing, resulting in mRNA cleavage and/or translation repression, and subsequent inhibition of protein synthesis.

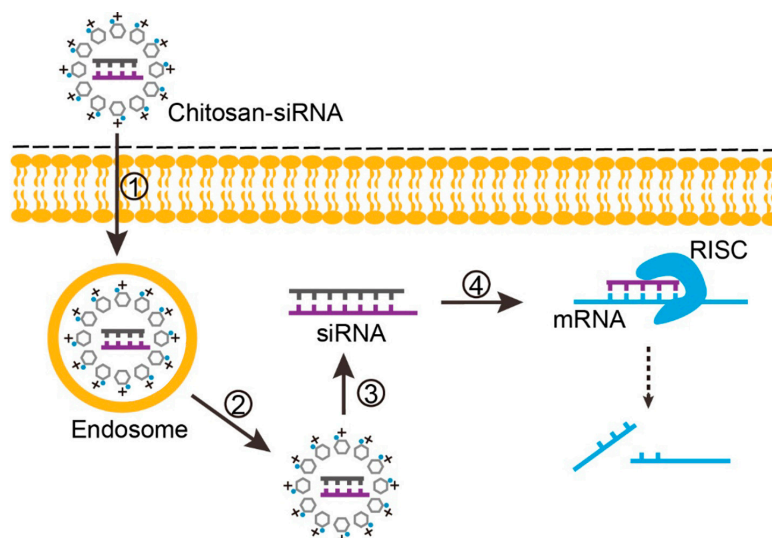


Figure 6. Cellular events associated with chitosan-based siRNA delivery for target gene silencing. 1, Cellular uptake of chitosan–siRNA by endocytosis. 2, Endosomal escape of chitosan–siRNA. 3, Dissociation of siRNA from chitosan. 4, siRNA association with RISC and target mRNA by base pairing, resulting in target mRNA cleavage and/or translation repression, and subsequent inhibition of protein synthesis.

3. Use of Chitosan in Fish Biotechnology

Chitosan and its derivatives are widely used in aquaculture. Low toxicity, biodegradability, biocompatibility, bioadhesion and immunomodulatory properties make chitosan and its derivatives of increasing interest for the fish farming industry as dietary additives, non-viral vectors enabling fish vaccination and protection against diseases, control of gonadal development and for the gene therapy-based modulation of fish metabolism.

3.1. Chitosan and Its Derivatives as Dietary Additives

Dietary supplementation with chitosan and its derivatives has been shown to improve fish growth performance, non-specific immunity and antioxidant effects [86,87]. However, the strategy for chitosan dietary supplementation in fish requires extensive investigation, according to the species and the growth stage of fish.

3.1.1. Dietary Supplementation with Chitosan

The inclusion of chitosan as feed additive for fish has been receiving attention since the 1980s [88]. Shiao et al. reported that inclusion of dietary levels of chitosan from 2% to 10% for 28 days decreases the weight gain and increases the feed conversion ratio (FCR) in hybrid tilapia (*Oreochromis niloticus* × *Oreochromis aureus*) [89]. However, other studies performed in *Oreochromis niloticus* showed positive effects of chitosan on fish growth. Feed supplementation of tilapia with chitosan (0–8 g/kg dry diet) for 56 days led to the conclusion that 4 g/kg of chitosan was the optimal dose to promote the highest body weight gain (BWG) rate and specific growth rate (SGR) [90]. Similarly, chitosan supplementation at 5 g/kg diet for 60 days improved growth performance, BWG, SGR and FCR in tilapia [91]. The contradictory effects reported for chitosan on tilapia growth could be attributed to the fact that the studies were performed using different fish growth stages. Indeed, the initial weight of fish in the study by Shiao et al. was of 0.99 ± 0.01 g, while the latter two reports used a significantly higher initial body weight (50.1 ± 4.1 g and 39.3 ± 0.3 g, respectively).

In addition to the developmental stage and amount of dietary chitosan supplied, chitosan effects exerted on fish growth performance also seem to depend on the species [87]. According to the effect observed on SGR, the apparent digestibility coefficient of dry matter and the apparent digestibility coefficient of protein, 75 days of feeding on diets supplemented with 10–20 g chitosan/kg significantly reduced the growth performance of gibel carp (*Carassius gibelio*) (initial body weight, 4.80 ± 0.01 g) [92]. However, the supply of 0–0.2 g chitosan/kg diet caused a dose dependent increase of the average daily weight and SGR in post-larvae sea bass (*Dicentrarchus labrax*) [93]. Yan et al. also reported that dietary supplementation of 0%–5% chitosan improved growth performance by inducing dose dependent increases of BWG and SGR, while FCR decreased [94]. Similarly, 70 days of supplementation with 1–5 g chitosan/kg diet of loach fish (*Misgurnus anguillicadatus*) with an average body weight of 3.14 ± 0.05 g, significantly increased BWG, SGR and condition factor (CF), whereas it decreased FCR [95]. In contrast, Najafabad et al. found that Caspian kutum (*Rutilus kutum*) fingerlings (1.7 ± 0.15 g) supplied with 0–2 g chitosan/kg diet for 60 days showed no effect of final weight, SGR and condition factor [96].

The positive effect of chitosan on the growth performance of some fish species might result from its role in nonspecific immunity. Chitosan acts as an immunostimulatory drug through induction of nonspecific immunity in fish. In loach fish, the dietary supplement of chitosan increased the serum levels of factors considered as immune boosters, such as the content of immunoglobulin M (IgM), complement component 3 (C3) levels, the activity of lysozyme, acid phosphatase and alkaline phosphatase, as well as increased the survival rate after being challenged by *Aeromonas hydrophila* [95]. In accordance with the immune boost, other investigations also showed immune reinforcement by chitosan, when fish were challenged by bacteria in regard to immunoglobulin content, serum lysozyme, bactericidal activity, immune-related gene expression, phagocytosis and respiratory burst activity [90,92,94,97]. Consistently, chitosan was shown to modify hematological parameters of fish,

which are also considered important indicators of immunostimulation. In Asian seabass (*Lates calcarifer*), chitosan supplement during 60 days at 5–20 g/kg diet increased red blood cells (RBC), white blood cells (WBC), total serum protein, albumin and globulin [98]. Supplementation with chitosan was reported also to increase RBC, WBC, haemoglobin, lymphocytes, monocytes, neutrophils and thrombocytes in mrigal carp (*Cirrhinus mrigala*) and kelp grouper (*Epinephelus bruneus*) [99–101].

Concomitant to the effects on immunity, chitosan also elevates antioxidant responses in fish. In loach fish, the activity of phenoloxidase, superoxide dismutase (SOD) and glutathione peroxidase (GPx) increased after 12 weeks of chitosan supplementation [95]. Similarly, chitosan induced the activity of SOD and catalase (CAT) after 56 days of dietary supplementation in tilapia [90], and the mRNA levels of SOD, CAT, GPx and nuclear factor erythroid 2-related factor 2 [94]. The protective effect of chitosan from oxidative stress was also reported in olive flounder (*Paralichthys olivaceus*) challenged with H₂O₂ [97]. The authors observed that chitosan-coated diets significantly narrowed the increase of protein carbonyl formation and DNA damage in the plasma.

3.1.2. Dietary Supplementation with Chitosan Nanoparticles

Wang et al. reported that BWG significantly increased in tilapia (initial body weight, 23.6 ± 1.2 g) fed with chitosan nanoparticles (5 g/kg dry diet) [102]. Similar results were described by other authors. Chitosan nanoparticle intake increased final weight, weight gain, SGR and FCR in tilapia supplied for 45 days with 0–2 g/kg (initial body weight, 19.8 ± 0.6 g) and 70 days for 1–5 g/kg (initial body weight, 5.66 ± 0.02 g). In these reports, innate immunity was also enhanced and fish exhibited increased respiratory burst activity, lysozyme malondialdehyde, CAT and SOD activity, and hematological parameters such as RBC, hematocrit, hemoglobin, mean corpuscular volume, WBC and platelets [103,104]. Remarkably, optimal supplement of dietary chitosan nanoparticles to improve growth and immunity against pathogens may vary, according to parameters such as developmental growth stage and species.

Dietary supplementation of chitosan nanoparticles complexed with vitamin C and thymol is more effective in enhancing immunity than supplementation with the single additives. Dietary chitosan–vitamin C nanoparticles slightly improved growth performance of tilapia, while inducing the viscerosomatic index, therefore decreasing economic performance. However, when fish fed chitosan–vitamin C nanoparticles were challenged by imidacloprid-polluted water, chitosan–vitamin C supplementation significantly strengthened immunity and antioxidant activity, including the activity of lysozyme, glutathione reductase and CAT, C3 and immunoglobulins [105]. Growth effects of dietary supplementation with chitosan nanoparticles mixed with thymol, the most important phenolic compound in *Thymus vulgaris* essential oil, were evaluated on hematological parameters, and the liver and kidney function in tilapia [106]. The results showed that chitosan–thymol nanoparticle supplementation increased feed efficiency and protein efficiency ratio, while it had moderated effects on final weight, weight gain and SGR. Nevertheless, chitosan–thymol produced a synergistic effect on lymphocytes and monocyte leukocytes. The use of chitosan nanoparticles as feed additive is limited by the fact that it can exhibit toxic effects at high levels. In this regard, chitosan nanoparticles significantly decreased hatching rate and survival rate of zebrafish (*Danio rerio*) when the immersion concentration reached 20 and 30 µg/mL or higher [107,108].

3.1.3. Dietary Supplementation with Chitin and Chitooligosaccharide

Meanwhile the inclusion of chitin in the diet has no significant effects on fish growth performance [109–111], chitooligosaccharide (COS) enhances growth performance parameters such as BWG, hepatosomatic and intestosomatic index, SGR and FCR in a number of fish species, including juvenile largemouth bass (*Micropterus salmoides*) [112], striped catfish (*Pangasianodon hypophthalmus*) [113], Nile tilapia (*Oreochromis niloticus*) [114], tiger puffer (*Takifugu rubripes*) [115], koi (*Cyprinus carpio koi*) [116], and silverfish (*Trachinotus ovatus*) [117]. Similarly as in most fish species, dietary supplementation with low molecular weight and highly deacetylated COS

enhances growth performance, innate immunity and digestive enzyme activity in Pacific white shrimp (*Litopenaeus vannamei*) [118]. However, the effect of dietary COS may depend on the species. In this regard, dietary COS supplementation was reported to cause not significant effects on weight gain, FCR and the survival rate in hybrid tilapia (*Oreochromis niloticus* × *O. aureus*) [109]. Similar results were reported for rainbow trout (*Oncorhynchus mykiss*) [119]. Incomplete intestinal development in early developmental stages may contribute to the lack of COS effect on growth performance observed in several fish species.

A number of studies showed that both chitin and COS can be potentially utilized as immunostimulants in fish. Respiratory burst activity, phagocytic activity and lysozyme activity, which are considered indicators of non-specific immunity, have been shown to be significantly stimulated by chitin and COS in a number of fish species, including juvenile largemouth bass (*Micropterus salmoides*) [112], Nile tilapia (*Oreochromis niloticus*) [114], striped catfish (*Pangasianodon hypophthalmus*) [113] and mrigal carp (*Cirrhina mrigala*) [99]. Chitin and COS also induce other immunity parameters, such as nitric oxide production, inducible nitric oxide synthase (iNOS) activity and gene expression [112,120], leukocyte count [99,112,116] and complement activity [99,100].

3.2. Chitosan as a Carrier for Drug Delivery in Fish

Chitosan is nanoscale, biodegradable, biocompatible, hemocompatible, simple and mild for preparation conditions, and is highly efficient for drug loading. Therefore, chitosan has been used for loading a variety of bioactive compounds, such as vitamins, metal ions, inactivated pathogens for vaccines, proteins and nucleic acids in a variety of applications in fish farming. In addition, loading into chitosan can significantly boost the bioeffects of these compounds.

3.2.1. Chitosan Loading Chemical Compounds

The sustained release of compounds complexed with chitosan nanoparticles fulfills the requirements of artificial breeding in fish farming and enable delivery and cell uptake of compounds with low toxicity [121,122]. Chitosan nanoparticles loaded with vitamin C, an important but labile antioxidant, were proven to enhance sustained vitamin C release in the stomach, the intestine and in serum after oral administration in rainbow trout (*Oncorhynchus mykiss*) [123]. Chitosan–vitamin C nanoparticles exhibited a markedly high antioxidant activity and no toxicity up to 2.5 mg/mL in the culture medium of ZFL cells, a zebrafish liver-derived cell line. In addition, chitosan–vitamin C nanoparticles showed the capability to penetrate the intestinal epithelium of *Solea senegalensis* [124]. Several studies evaluated chitosan nanoparticles loading aromatase inhibitors and eurycomanone, compounds that promote gonadal development. Chitosan-mediated delivery of aromatase inhibitors and eurycomanone prolonged serum presence, improved testicular development with lack of testicular toxicity, and led to higher serum concentrations of reproductive hormones [125–128].

3.2.2. Chitosan Loading Metal Ions

Loading with chitosan facilitates delivery of metal ions that are micronutrients and antibacterial factors, such as selenium and silver, to fish in culture. Barakat et al. showed that chitosan–silver nanoparticles successfully treated European sea bass larvae infected with *Vibrio anguillarum*. Chitosan–silver nanoparticles significantly decreased the bacterial number and improved fish survival [129]. In addition, dietary supplementation with chitosan–silver nanoparticles were shown to altering gut morphometry and microbiota in zebrafish. Feeding with chitosan–silver nanoparticles increased *Fusobacteria* and *Bacteroidetes* phyla, goblet cell density and villi height, while upregulated the expression of immune-related genes [130]. Similarly, chitosan–selenium nanoparticles had immunostimulatory roles and increased disease resistance in zebrafish and *Paramisgurnus dabryanus* by improving the activity of lysozyme, acid phosphatase and alkaline phosphatase, phagocytic respiratory burst and splenocyte-responses towards concanavalin A [131,132].

3.2.3. Chitosan Loading Inactivated Pathogens

Vaccines against pathogens is a major challenge in aquaculture. In this regard, chitosan can be used as proper carrier and adjuvant to enhance effectiveness of vaccination. A number of inactivated bacteria and virus have been evaluated with chitosan or its derivatives as adjuvant against infections in fish. Vaccines, such as inactivated *Edwardsiella ictaluri* and infectious spleen and kidney necrosis virus, have been tested with chitosan in yellow catfish (*Pelteobagrus fulvidraco*) and Chinese perch (*Siniperca chuatsi*), respectively. Chitosan enhanced incorporation into the host cells and improved fish survival rate and immune response, increasing IgM content, lysozyme activity and mRNA levels of interleukin (IL)-1 β , IL-2 and interferon (IFN)- γ 2 [133,134]. A mixture of COS and inactivated *Vibrio anguillarum* vaccine significantly reduced zebrafish mortality against *Vibrio anguillarum* [135], while COS combined with inactivated *Vibrio harveyi* also markedly increased survival rate, IgM and the expression of immune-related genes, such as IL-1 β , IL-16, tumor necrosis factor-alpha (TNF- α) and major histocompatibility complex class I alpha (MHC-I α), in the grouper ♀*Epinephelus fuscoguttatus* × ♂ *Epinephelus lanceolatus* [136]. Similarly, rainbow trout (*Oncorhynchus mykiss*) immunized against bacterial infection (*Lactococcus garvieae* and *Streptococcus iniae*) through chitosan–alginate coated vaccination exhibited a higher survival rate, immune-related gene expression, and antibody titer than fish submitted to non-coated vaccination [137].

Olive flounder (*Paralichthys olivaceus*) vaccinated against inactivated viral haemorrhagic septicaemia virus encapsulated with chitosan through oral and immersion routes showed effective immunization in the head kidney, which is considered as the primary organ responsible for the initiation of adaptive immunity in fish, skin and intestine, which are regarded as the main sites for antigen uptake and mucosal immunity. Additionally to upregulation of IgM, immunoglobulin T (IgT), polymeric Ig receptor (pIgR), MHC-I, major histocompatibility complex class II (MHC-II) and IFN- γ in the three tissues, caspase 3 was also highly induced 48 h post-challenge, suggesting cytotoxicity due to rapid T-cell response and impairment of viral proliferation [138].

Coating chitosan with membrane vesicles from pathogens such as *Piscirickettsia salmonis* was also shown to be an effective strategy to induce immune response in zebrafish (*Danio rerio*) and upregulation of CD 4, CD 8, MHC-I, macrophage-expressed 1, tandem duplicate 1 (Mpeg1.1), TNF α , IL-1 β , IL-10, and IL-6 [139].

3.2.4. Chitosan Loading Proteins

Effectiveness of fish vaccination against infections can be also improved with antigenic proteins derived from bacteria and virus. For example, chitosan nanoparticles encapsulated with the recombinant outer membrane protein A of *Edwardsiella tarda* was used for oral vaccination of fringed-lipped peninsula carp (*Labeo fimbriatus*). Treated fish showed significant higher levels of post-vaccination antibody in circulation and survival rate against *Edwardsiella tarda* [140]. In another study, oral vaccination with alginate-chitosan microspheres encapsulating the recombinant protein serine-rich repeat (rSrr) of *Streptococcus iniae* were evaluated and the results showed that lysozyme activity and immune-related genes were induced, leading to a 60% increased survival rate of channel catfish (*Ictalurus punctatus*) against *Streptococcus iniae* infection [141]. In grass carp (*Ctenopharyngodon idella*), chitosan was also used for carrying the immunomodulatory factor IFN- γ 2. Treatment with chitosan–*Ctenopharyngodon idella* IFN- γ 2 highly upregulated inflammatory factors, leading to severe inflammatory damage in the intestine, hepatopancreas and decreased survival rate [142].

3.2.5. Chitosan Loading Nucleic Acids

Compared to chitosan-based gene delivery in other organisms, gene therapy methodologies using chitosan for improving desirable traits in farmed fish have great potential for development (Figure 1b). A number of studies addressed the characterization of factors that can influence the efficiency of chitosan loading and nucleic acid release, such as the average diameter, zeta potential

and encapsulation efficiency of chitosan–DNA microspheres or nanospheres. Table 1 summarizes chitosan–plasmid DNA encapsulation efficiency and changes in particle diameter and zeta potential before and after encapsulation for fish biotechnology studies. Existing data show that the diameter of chitosan nanospheres before loading DNA mostly ranged from ~30 to ~230 nm, while encapsulation with plasmid DNA led to ~40–190 nm diameter increase. The zeta potential indicates the surface charge on the particles. A higher positive zeta potential suggests higher stability of nanoparticles in the suspension [143]. The zeta potential before loading plasmid DNA were ~25–33 mV, which mostly tended to decrease to ~14–18 mV. The exception was reported by Rather et al., who found that zeta potential of chitosan nanospheres increased ~6 mV following DNA encapsulation [144]. DNA encapsulation efficiency was generally higher than 80%, which indicates that chitosan is capable to load a high mass of DNA, which in turn may benefit many applications in aquaculture.

Table 1. Characteristics of chitosan–plasmid DNA polyplexes for studies performed in fish.

Preloading Diameter (nm)	Postloading Diameter (nm)	Preloading Zeta Potential (mV)	Postloading Zeta Potential (mV)	Encapsulation Efficiency	References
-	<10,000	-	-	94.5%	[145]
30–60	-	-	-	-	[146]
-	200	-	-	91.5%	[147]
-	-	-	-	83.6%	[148]
193 ± 53 ¹	246 ± 74 ¹	32.0 ± 1.0 ¹	14.4 ± 1.3 ¹	-	[80]
-	146 ± 2 ²	-	24.3 ± 0.5 ²	92.8% ± 1.4% ²	[149]
-	133	-	34.3	63%	[150]
-	50–200	-	-	97.5%	[151]
87	156	30.3	36.5	60%	[144]
-	743	-	-	98.6%	[152]
135	-	26.7	-	86%	[153]
-	-	-	-	84.2%	[154]
224 ± 62 ¹	Similar to preloading diameter	33.0 ± 1.2 ¹	14.4 ± 1.3 ¹	-	[81]
-	750–950	-	-	98.6%	[155]
116	306	24.7	18.0	-	[156]
231 ± 18 ²	272 ± 36 ²	31.2 ± 1.5 ²	14.1 ± 2.3 ²	-	[157]
-	267	-	27.1	87.4%	[158]

¹ Mean ± SD; ² mean ± SEM.

Chitosan-encapsulated DNA is more stable in vivo, exhibit sustained-release and increased cell uptake than naked DNA. Taken together, these factors confer chitosan-delivered DNA a particular expression profile regarding tissue distribution, persistence of expression and abundance in fish. Sáez et al. found that intramuscular injection led to a restricted expression to adjacent tissues of both chitosan-encapsulated DNA and naked DNA, while the oral administration of chitosan-encapsulated DNA, largely used for fish vaccination studies, showed enhanced expression not only in the intestine, but also in the liver of gilthead sea bream (*Sparus aurata*) [152,155]. Furthermore, oral administration of chitosan nanoparticles loaded with pCMV β , a plasmid encoding for *Escherichia coli* β -galactosidase, enabled sustained detection of the exogenous plasmid and bacterial β -galactosidase activity in the liver and the intestine of *Sparus aurata* juveniles up to 60 days posttreatment [152].

Through the immersion route, Rao et al. showed that chitosan-coated DNA was confined to the surface area of rohu (*Labeo rohita*), i.e., gill, intestine and skin-muscle, while no detection was observed in the kidney and the liver. Naked DNA was undetectable due to degradation [158]. Oral delivery seems to have a wider distribution of chitosan-encapsulated DNA, being found in the stomach, spleen, intestine, gill, muscle, liver, heart and kidney [148,154,159]. Chitosan-encapsulated DNA has longer and more abundant presence than naked DNA after administration. For example, Rajesh Kumar et al. showed that antibody in serum from fish immunized with a chitosan–DNA vaccine was 30% higher

than naked DNA after 21 days of oral immunity [160]. The presence of DNA vaccine was reported more than 90 days after oral administration of chitosan–DNA [145]. Additionally, Rather et al. reported that chitosan–DNA induced 2-fold longer and higher peak abundant expression of downstream genes than naked DNA [144].

3.3. Chitosan-Based Applications in Fish Biotechnology and Gene Therapy

In recent years, chitosan has been increasingly used for drug and gene delivery in fish biotechnology. Most of the studies used chitosan-based systems to improve oral vaccination, control of gonadal development, and the modification of fish intermediary metabolism.

3.3.1. Fish Vaccination

DNA vaccines delivered by chitosan significantly increase relative percent survival of fish at a range of 45%–82% against bacterial and viral infection [151,156]. Higher doses of chitosan–DNA vaccines resulted in concomitant increase of fish relative percent survival from ~47% to ~70% [154]. In addition, DNA vaccination with chitosan stimulated expression of immune-related genes. Zheng et al. reported upregulation of the expression of immune-related genes, such as interferon-induced GTP-binding protein Mx2 (MX2), IFN, chemokine receptor (CXCR), T-cell receptor (TCR), MHC-I α and MHC-II α , 7 days after oral vaccination against reddish body iridovirus in turbot (*Scophthalmus maximus*). A 10-fold higher expression of TNF- α gene expression was found in the hindgut [149].

In addition to the short-term modification of the expression levels of immune-related genes, the administration of chitosan–DNA vaccines also promote a sustained effect after treatment. Valero et al. found that European sea bass (*Dicentrarchus labrax*) orally vaccinated with chitosan-encapsulated DNA against nodavirus failed to induce circulating IgM. However, the expression of genes involved in cell-mediated cytotoxicity (TCR β and CD8 α) and the interferon pathway (IFN, MX and IFN- γ) were upregulated. Three months following vaccination, challenged fish exhibited partial protection with retarded onset of fish death and lower cumulative mortality [151]. Kole et al. immunized rohu (*Labeo rohita*) with chitosan nanoparticles complexed with a bicistronic DNA plasmid encoding the antigen *Edwardsiella tarda* glyceraldehyde 3-phosphate dehydrogenase and the immune adjuvant gene *Labeo rohita* IFN- γ [156]. Follow-up of the expression of immune-related genes in the kidney, liver and spleen showed maximal upregulation of IgHC (IgM heavy chain), iNOS, toll like receptor 22 (TLR22), nucleotide binding and oligomerization domain-1 (NOD1) and IL-1 β at 14 days post immunization. The authors also confirmed that oral and immersion vaccination with chitosan–DNA nanoparticles enhances the fish immune response to a greater extent than intramuscular injection of naked DNA. In another study, the oral vaccination of rainbow trout fry with chitosan–TPP nanoparticles complexed with pcDNA3.1-VP2, showed that the expression of genes related with innate immune response, IFN-1 and MX, reached maximal values at 3 days postvaccination and 7 days after boosting (22 days postvaccination), while, with regard to genes involved in the adaptive immune response, CD4 peaked at 15 days postvaccination and IgM and IgT at 30 days postvaccination [154].

3.3.2. Control of Gonadal Development

Chitosan nanoparticles have been used for drug delivery in studies aiming proper gonadal development in fish farming. Bhat et al. administered chitosan conjugated with salmon luteinizing hormone-releasing hormone (sLHRH) into walking catfish (*Clarias batrachus*) to promote gonadal development. Chitosan-conjugated sLHRH and naked sLHRH exerted similar effects: upregulation of Sox9 expression in the gonads and increase of circulating steroid hormonal levels, testosterone and 11-ketotestosterone in males and testosterone and 17 β -estradiol in females. However, sLHRH conjugation with chitosan induced sustained and controlled release of the hormones with maximal levels observed in the last sampling point of the experiment (36 h posttreatment), while naked sLHRH peaked circulating steroid hormones at 12 h posttreatment [150]. Similarly, compared to the administration of naked kisspeptin-10, intramuscular injection of chitosan-encapsulated kisspeptin-10

in immature female *Catla catla* caused a delayed but greater increase of gonadotropin-releasing hormone, luteinizing hormone and follicle-stimulating hormone expression, as well as circulating levels of 11-ketotestosterone and 17 β -estradiol [144].

With the ultimate goal of controlling gonadal development in fish, chitosan was also assayed for gene delivery. In walking catfish (*Clarias batrachus*), intramuscular administration of chitosan nanoparticles conjugated with an expression plasmid encoding steroidogenic acute regulatory protein (StAR), a major regulator of steroidogenesis, also resulted in long-lasting stimulatory effects than administration of the naked plasmid construct on the expression of key genes in reproduction, cytochrome P450 (CYP) 11A1, CYP17A1, CYP19A1, 3 β -hydroxysteroid dehydrogenase and 17 β -hydroxysteroid dehydrogenase [153].

3.3.3. Control of Fish Metabolism

Chitosan has been used for enhancing fish digestibility, the absorption of food constituents and increasing the utilization of dietary carbohydrate in carnivorous fish. To supplement exogenous proteolytic enzymes and thus facilitate protein digestion and amino acid absorption, Kumari et al. orally administered chitosan–TPP nanoparticles encapsulating trypsin to *Labeo rohita* over 45 days. Treatment with chitosan–TPP–trypsin enhanced nutrient digestibility, intestinal protease activity and transamination activity, alanine aminotransferase (ALT) and aspartate aminotransferase (AST), in the liver and the muscle [161].

The substitution of dietary protein by cheaper nutrients with reduced environmental impact in farmed fish is a challenging trend for sustainable aquaculture [162]. However, the metabolic features of fish, particularly carnivorous fish, constrain the replacement of dietary protein by other nutrients in aquafeeds. Carnivorous fish exhibit a preferential use of amino acids as fuel and gluconeogenic substrates, and thus require high levels of dietary protein for optimal growth. Instead, carbohydrates are metabolized markedly slower than in mammals, and give rise to prolonged hyperglycemia [163,164]. The essential role of the liver in controlling the intermediary metabolism makes this organ an ideal target for investigating and modifying the glucose tolerance of farmed fish.

To overcome metabolic limitations of carnivorous fish, in recent years we synthesized chitosan–TPP nanoparticles, complexed with plasmid DNA, to induce in vivo transient overexpression and the silencing of target genes in the liver of gilthead sea bream (*Sparus aurata*). With the aim of decreasing the use of amino acids for gluconeogenic purposes and improving carbohydrate metabolism in the liver, chitosan–TPP nanoparticles complexed with a plasmid overexpressing a shRNA designed to silence the expression of cytosolic ALT (cALT) were intraperitoneally administered to *Sparus aurata* juveniles. Seventy-two hours posttreatment, a significant decrease in cALT1 mRNA levels, immunodetectable ALT and ALT activity was observed in the liver of treated fish. Knockdown of cALT expression to ~63%–70% of the values observed in control fish significantly increased the hepatic activity of key enzymes in glycolysis, 6-phosphofructo 1-kinase (PFK1) and pyruvate kinase, and protein metabolism, glutamate dehydrogenase (GDH). In addition to showing efficient gene silencing after administration of chitosan–TPP–DNA nanoparticles, the findings supported evidence that the downregulation of liver transamination increased the use of dietary carbohydrates to obtain energy, and thus made it possible to spare protein in carnivorous fish [80].

Following the same methodology, we showed that the shRNA-mediated knockdown of GDH significantly decreased GDH mRNA and immunodetectable levels in the liver, which, in turn, reduced GDH activity to ~53%. Downregulation of GDH decreased liver glutamate, glutamine and 2-oxoglutarate, as well as the hepatic activity of AST, while it increased 2-oxoglutarate dehydrogenase activity and the PFK1/fructose-1,6-bisphosphatase (FBP1) activity ratio. Therefore, by reducing hepatic transamination and gluconeogenesis, the knockdown of GDH could impair the use of amino acids as gluconeogenic substrates and facilitate the metabolic use of dietary carbohydrates [81].

With the aim of inducing a multigenic action leading to a stronger protein-sparing effect, *Sparus aurata* were intraperitoneally injected with chitosan–TPP nanoparticles complexed with a

plasmid expressing the N-terminal nuclear fragment of hamster SREBP1a, a transcription factor that—in addition to exhibiting strong transactivating capacity of genes required for fatty acid, triglycerides and cholesterol synthesis—previous reports showed can also transactivate the promoter of genes encoding key enzymes in hepatic glycolysis, glucokinase (GK) and 6-phosphofructo 2-kinase/fructose 2,6-bisphosphatase (PFKFB1) in fish [165,166]. Overexpression of exogenous SREBP1a in the liver of *Sparus aurata* enhanced the expression of glycolytic enzymes GK and PFKFB1, decreased the activity of the gluconeogenic enzyme FBP1 and increased the mRNA levels of key enzymes in fatty acid synthesis, elongation and desaturation (acetyl-CoA carboxylase 1, acetyl-CoA carboxylase 2, elongation of very long chain fatty acids protein 5, fatty acid desaturase 2), as well as induced NADPH formation (glucose 6-phosphate dehydrogenase) and cholesterol synthesis (3-hydroxy-3-methylglutaryl-coenzyme A reductase). As a result, chitosan-mediated SREBP1a overexpression caused a multigenic action that enabled the conversion of dietary carbohydrates into lipids (Figure 7), leading to increased circulating levels of triglycerides and cholesterol in carnivorous fish [157].

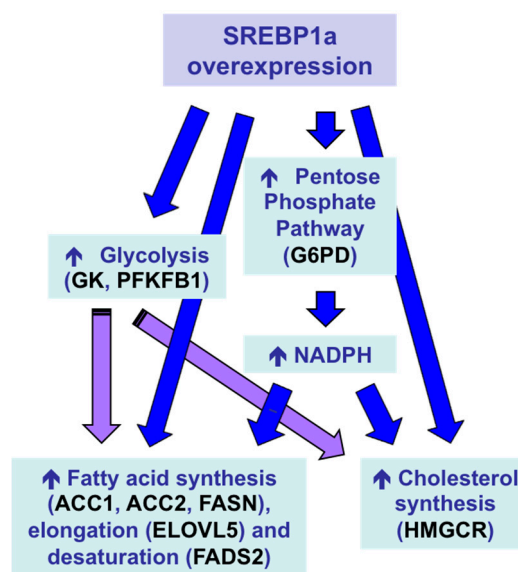


Figure 7. Multigenic action and metabolic effects in the liver of *Sparus aurata* after intraperitoneal administration of chitosan–TPP–DNA nanoparticles to overexpress exogenous SREBP1a [157]. ACC1, acetyl-CoA carboxylase 1; ACC2, acetyl-CoA carboxylase 2; ELOVL5, elongation of very long chain fatty acids protein 5; FADS2, fatty acid desaturase 2; G6PD, glucose 6-phosphate dehydrogenase; GK, glucokinase; HMGCR, 3-hydroxy-3-methylglutaryl-coenzyme A reductase; PFKFB1, 6-phosphofructo 2-kinase/fructose 2,6-bisphosphatase.

4. Conclusions

Characteristics such as nanoscale, low-toxicity, biodegradability, biocompatibility, derivatization, immunomodulatory effects, and easily affordable preparation conditions make chitosan a strong candidate for drug delivery into fish. Therefore, the use of chitosan in fish biotechnology has received growing attention in recent years. However, applications based on novel chitosan-based gene therapy methodologies to improve desirable traits in farmed fish have enormous potential for development. Most remarkable advances in the field addressed fish immunization, the control of reproduction for broodstock management and the modulation of gene expression to spare protein and overcome metabolic limitations of farmed fish. Further studies are needed for a better understanding of the extracellular and intracellular process, following chitosan-mediated gene delivery into fish. In addition, future trends in fish farming may greatly benefit from improved and more efficient chitosan formulations for enhancing gene delivery targeting and intracellular traffic in farmed fish.

Author Contributions: Conceptualization, I.M. and M.P.A.; writing—Original draft preparation, Y.W., A.R., M.P.A. and I.M.; writing—Review and editing, M.P.A. and I.M.; supervision, I.M.; project administration, I.M.; funding acquisition, I.M. All authors have read and agreed to the published version of the manuscript.

Funding: This research was funded by Ministerio de Economía, Industria y Competitividad (Spain), grant number AGL2016-78124-R, co-funded by the European Regional Development Fund (EC).

Conflicts of Interest: The authors declare no conflict of interest.

References

1. Mahdy Samar, M.; El-Kalyoubi, M.H.; Khalaf, M.M.; Abd El-Razik, M.M. Physicochemical, functional, antioxidant and antibacterial properties of chitosan extracted from shrimp wastes by microwave technique. *Ann. Agric. Sci.* **2013**, *58*, 33–41. [[CrossRef](#)]
2. Sun, M.; Wang, T.; Pang, J.; Chen, X.; Liu, Y. Hydroxybutyl chitosan centered biocomposites for potential curative applications: A critical review. *Biomacromolecules* **2020**, *21*, 1351–1367. [[CrossRef](#)] [[PubMed](#)]
3. Sacco, P.; Cok, M.; Scognamiglio, F.; Pizzolitto, C.; Vecchies, F.; Marfoggia, A.; Marsich, E.; Donati, I. Glycosylated-chitosan derivatives: A systematic review. *Molecules* **2020**, *25*, 1534. [[CrossRef](#)] [[PubMed](#)]
4. Chuan, D.; Jin, T.; Fan, R.; Zhou, L.; Guo, G. Chitosan for gene delivery: Methods for improvement and applications. *Adv. Colloid Interface Sci.* **2019**, *268*, 25–38. [[CrossRef](#)]
5. Ivanova, D.G.; Yaneva, Z.L. Antioxidant properties and redox-modulating activity of chitosan and its derivatives: Biomaterials with application in cancer therapy. *Biores. Open Access* **2020**, *9*, 64–72. [[CrossRef](#)]
6. Wang, W.; Meng, Q.; Li, Q.; Liu, J.; Zhou, M.; Jin, Z.; Zhao, K. Chitosan derivatives and their application in biomedicine. *Int. J. Mol. Sci.* **2020**, *21*, 487. [[CrossRef](#)]
7. Raftery, R.; O'Brien, F.J.; Cryan, S.-A. Chitosan for gene delivery and orthopedic tissue engineering applications. *Molecules* **2013**, *18*, 5611–5647. [[CrossRef](#)]
8. Lostalé-Seijo, I.; Montenegro, J. Synthetic materials at the forefront of gene delivery. *Nat. Rev. Chem.* **2018**, *2*, 258–277. [[CrossRef](#)]
9. Cao, Y.; Tan, Y.F.; Wong, Y.S.; Liew, M.W.J.; Venkatraman, S. Recent Advances in Chitosan-Based Carriers for Gene Delivery. *Mar. Drugs* **2019**, *17*, 381. [[CrossRef](#)]
10. Santos-Carballal, B.; Fernández Fernández, E.; Goycoolea, F. Chitosan in non-viral gene delivery: Role of structure, characterization methods, and insights in cancer and rare diseases therapies. *Polymers* **2018**, *10*, 444. [[CrossRef](#)]
11. Ginn, S.L.; Amaya, A.K.; Alexander, I.E.; Edelstein, M.; Abedi, M.R. Gene therapy clinical trials worldwide to 2017: An update. *J. Gene Med.* **2018**, *20*, e3015. [[CrossRef](#)] [[PubMed](#)]
12. Picanço-Castro, V.; Pereira, C.G.; Covas, D.T.; Porto, G.S.; Athanassiadou, A.; Figueiredo, M.L. Emerging patent landscape for non-viral vectors used for gene therapy. *Nat. Biotechnol.* **2020**, *38*, 151–157. [[CrossRef](#)] [[PubMed](#)]
13. Simões, S.; Filipe, A.; Faneca, H.; Mano, M.; Penacho, N.; Düzgünes, N.; de Lima, M.P. Cationic liposomes for gene delivery. *Expert Opin. Drug Deliv.* **2005**, *2*, 237–254. [[CrossRef](#)] [[PubMed](#)]
14. Saffari, M.; Moghimi, H.; Dass, C. Barriers to liposomal gene delivery: From application site to the target. *Iran. J. Pharm. Res.* **2016**, *15*, 3–17.
15. Ramamoorth, M.; Narvekar, A. Non viral vectors in gene therapy- an overview. *J. Clin. Diagn. Res.* **2015**, *9*, GE01–GE06. [[CrossRef](#)]
16. Patil, S.; Gao, Y.G.; Lin, X.; Li, Y.; Dang, K.; Tian, Y.; Zhang, W.J.; Jiang, S.F.; Qadir, A.; Qian, A.R. The development of functional non-viral vectors for gene delivery. *Int. J. Mol. Sci.* **2019**, *20*, 5491. [[CrossRef](#)]
17. Mumper, R.; Wang, J.; Claspell, J.; Rolland, A. Novel polymeric condensing carriers for gene delivery. *Proc. Int. Symp. Control. Release Bioact. Mater.* **1995**, *22*, 178–179.
18. MacLaughlin, F.C.; Mumper, R.J.; Wang, J.; Tagliaferri, J.M.; Gill, I.; Hinchcliffe, M.; Rolland, A.P. Chitosan and depolymerized chitosan oligomers as condensing carriers for in vivo plasmid delivery. *J. Control. Release* **1998**, *56*, 259–272. [[CrossRef](#)]
19. Katas, H.; Alpar, H.O. Development and characterisation of chitosan nanoparticles for siRNA delivery. *J. Control. Release* **2006**, *115*, 216–225. [[CrossRef](#)]

20. Richardson, S.C.; Kolbe, H.V.; Duncan, R. Potential of low molecular mass chitosan as a DNA delivery system: Biocompatibility, body distribution and ability to complex and protect DNA. *Int. J. Pharm.* **1999**, *178*, 231–243. [[CrossRef](#)]
21. Xu, W.; Shen, Y.; Jiang, Z.; Wang, Y.; Chu, Y.; Xiong, S. Intranasal delivery of chitosan-DNA vaccine generates mucosal SIgA and anti-CVB3 protection. *Vaccine* **2004**, *22*, 3603–3612. [[CrossRef](#)] [[PubMed](#)]
22. Sun, C.-J.; Pan, S.-P.; Xie, Q.-X.; Xiao, L.-J. Preparation of chitosan-plasmid DNA nanoparticles encoding zona pellucida glycoprotein-3alpha and its expression in mouse. *Mol. Reprod. Dev.* **2004**, *68*, 182–188. [[CrossRef](#)] [[PubMed](#)]
23. Kang, S.H.; Revuri, V.; Lee, S.-J.; Cho, S.; Park, I.-K.; Cho, K.J.; Bae, W.K.; Lee, Y. Oral siRNA delivery to treat colorectal liver metastases. *ACS Nano* **2017**, *11*, 10417–10429. [[CrossRef](#)] [[PubMed](#)]
24. Lin, F.; Jia, H.-R.; Wu, F.-G. Glycol chitosan: A water-soluble polymer for cell imaging and drug delivery. *Molecules* **2019**, *24*, 4371. [[CrossRef](#)] [[PubMed](#)]
25. Huang, M.; Fong, C.-W.; Khor, E.; Lim, L.-Y. Transfection efficiency of chitosan vectors: Effect of polymer molecular weight and degree of deacetylation. *J. Control. Release* **2005**, *106*, 391–406. [[CrossRef](#)] [[PubMed](#)]
26. Huang, M.; Khor, E.; Lim, L.-Y. Uptake and cytotoxicity of chitosan molecules and nanoparticles: Effects of molecular weight and degree of deacetylation. *Pharm. Res.* **2004**, *21*, 344–353. [[CrossRef](#)] [[PubMed](#)]
27. Liu, X.; Howard, K.A.; Dong, M.; Andersen, M.Ø.; Rahbek, U.L.; Johnsen, M.G.; Hansen, O.C.; Besenbacher, F.; Kjems, J. The influence of polymeric properties on chitosan/siRNA nanoparticle formulation and gene silencing. *Biomaterials* **2007**, *28*, 1280–1288. [[CrossRef](#)]
28. Razmi, F.A.; Ngadi, N.; Wong, S.; Inuwa, I.M.; Opotu, L.A. Kinetics, thermodynamics, isotherm and regeneration analysis of chitosan modified pandan adsorbent. *J. Clean. Prod.* **2019**, *231*, 98–109. [[CrossRef](#)]
29. Alameh, M.; Lavertu, M.; Tran-Khanh, N.; Chang, C.-Y.; Lesage, F.; Bail, M.; Darras, V.; Chevrier, A.; Buschmann, M.D. siRNA delivery with chitosan: Influence of chitosan molecular weight, degree of deacetylation, and amine to phosphate ratio on in vitro silencing efficiency, hemocompatibility, biodistribution, and in vivo efficacy. *Biomacromolecules* **2018**, *19*, 112–131. [[CrossRef](#)]
30. Al-Remawi, M. Application of N-hexoyl chitosan derivatives with high degree of substitution in the preparation of super-disintegrating pharmaceutical matrices. *J. Drug Deliv. Sci. Technol.* **2015**, *29*, 31–41. [[CrossRef](#)]
31. Chung, Y.-C.; Kuo, C.-L.; Chen, C.-C. Preparation and important functional properties of water-soluble chitosan produced through Maillard reaction. *Bioresour. Technol.* **2005**, *96*, 1473–1482. [[CrossRef](#)] [[PubMed](#)]
32. Gullón, B.; Montenegro, M.I.; Ruiz-Matute, A.I.; Cardelle-Cobas, A.; Corzo, N.; Pintado, M.E. Synthesis, optimization and structural characterization of a chitosan-glucose derivative obtained by the Maillard reaction. *Carbohydr. Polym.* **2016**, *137*, 382–389. [[CrossRef](#)] [[PubMed](#)]
33. Uccello-Barretta, G.; Balzano, F.; Aiello, F.; Senatore, A.; Fabiano, A.; Zambito, Y. Mucoadhesivity and release properties of quaternary ammonium-chitosan conjugates and their nanoparticulate supramolecular aggregates: An NMR investigation. *Int. J. Pharm.* **2014**, *461*, 489–494. [[CrossRef](#)] [[PubMed](#)]
34. Li, H.; Zhang, Z.; Bao, X.; Xu, G.; Yao, P. Fatty acid and quaternary ammonium modified chitosan nanoparticles for insulin delivery. *Colloids Surf. B. Biointerfaces* **2018**, *170*, 136–143. [[CrossRef](#)]
35. Jiang, X.; Dai, H.; Leong, K.W.; Goh, S.-H.; Mao, H.-Q.; Yang, Y.-Y. Chitosan-g-PEG/DNA complexes deliver gene to the rat liver via intrabiliary and intraportal infusions. *J. Gene Med.* **2006**, *8*, 477–487. [[CrossRef](#)]
36. Ping, Y.; Liu, C.; Zhang, Z.; Liu, K.L.; Chen, J.; Li, J. Chitosan-graft-(PEI-β-cyclodextrin) copolymers and their supramolecular PEGylation for DNA and siRNA delivery. *Biomaterials* **2011**, *32*, 8328–8341. [[CrossRef](#)]
37. Lee, H.; Jeong, J.H.; Park, T.G. PEG grafted polylysine with fusogenic peptide for gene delivery: High transfection efficiency with low cytotoxicity. *J. Control. Release* **2002**, *79*, 283–291. [[CrossRef](#)]
38. Strand, S.P.; Issa, M.M.; Christensen, B.E.; Vårnum, K.M.; Artursson, P. Tailoring of chitosans for gene delivery: Novel self-branched glycosylated chitosan oligomers with improved functional properties. *Biomacromolecules* **2008**, *9*, 3268–3276. [[CrossRef](#)]
39. Thanou, M.; Florea, B.I.; Geldof, M.; Junginger, H.E.; Borchard, G. Quaternized chitosan oligomers as novel gene delivery vectors in epithelial cell lines. *Biomaterials* **2002**, *23*, 153–159. [[CrossRef](#)]
40. Kean, T.; Roth, S.; Thanou, M. Trimethylated chitosans as non-viral gene delivery vectors: Cytotoxicity and transfection efficiency. *J. Control. Release* **2005**, *103*, 643–653. [[CrossRef](#)]

41. Ren, Y.; Zhao, X.; Liang, X.; Ma, P.X.; Guo, B. Injectable hydrogel based on quaternized chitosan, gelatin and dopamine as localized drug delivery system to treat Parkinson's disease. *Int. J. Biol. Macromol.* **2017**, *105*, 1079–1087. [[CrossRef](#)]
42. Raik, S.V.; Andranoviš, S.; Petrova, V.A.; Xu, Y.; Lam, J.K.-W.; Morris, G.A.; Brodskaia, A.V.; Casettari, L.; Kritchenkov, A.S.; Skorik, Y.A. Comparative study of diethylaminoethyl-chitosan and methylglycol-chitosan as potential non-viral vectors for gene therapy. *Polymers* **2018**, *10*, 442. [[CrossRef](#)] [[PubMed](#)]
43. Calvo, P.; Remuñán-López, C.; Vila-Jato, J.L.; Alonso, M.J. Novel hydrophilic chitosan-polyethylene oxide nanoparticles as protein carriers. *J. Appl. Polym. Sci.* **1997**, *63*, 125–132. [[CrossRef](#)]
44. Gan, Q.; Wang, T.; Cochrane, C.; McCarron, P. Modulation of surface charge, particle size and morphological properties of chitosan-TPP nanoparticles intended for gene delivery. *Colloids Surf. B Biointerfaces* **2005**, *44*, 65–73. [[CrossRef](#)] [[PubMed](#)]
45. Raja, M.A.G.; Katas, H.; Jing Wen, T. Stability, intracellular delivery, and release of siRNA from chitosan nanoparticles using different cross-linkers. *PLoS ONE* **2015**, *10*, e0128963.
46. Vimal, S.; Abdul Majeed, S.; Taju, G.; Nambi, K.S.N.; Sundar Raj, N.; Madan, N.; Farook, M.A.; Rajkumar, T.; Gopinath, D.; Sahul Hameed, A.S. Chitosan tripolyphosphate (CS/TPP) nanoparticles: Preparation, characterization and application for gene delivery in shrimp. *Acta Trop.* **2013**, *128*, 486–493. [[CrossRef](#)]
47. Fàbregas, A.; Miñarro, M.; García-Montoya, E.; Pérez-Lozano, P.; Carrillo, C.; Sarrate, R.; Sánchez, N.; Ticó, J.R.; Suñé-Negre, J.M. Impact of physical parameters on particle size and reaction yield when using the ionic gelation method to obtain cationic polymeric chitosan-tripolyphosphate nanoparticles. *Int. J. Pharm.* **2013**, *446*, 199–204. [[CrossRef](#)]
48. Serrano-Sevilla, I.; Artiga, Á.; Mitchell, S.G.; De Matteis, L.; de la Fuente, J.M. Natural polysaccharides for siRNA delivery: Nanocarriers based on chitosan, hyaluronic acid, and their derivatives. *Molecules* **2019**, *24*, 2570. [[CrossRef](#)]
49. Köping-Höggård, M.; Tubulekas, I.; Guan, H.; Edwards, K.; Nilsson, M.; Vårum, K.; Artursson, P. Chitosan as a nonviral gene delivery system. Structure–property relationships and characteristics compared with polyethylenimine in vitro and after lung administration in vivo. *Gene Ther.* **2001**, *8*, 1108–1121. [[CrossRef](#)]
50. Mao, H.Q.; Roy, K.; Troung-Le, V.L.; Janes, K.A.; Lin, K.Y.; Wang, Y.; August, J.T.; Leong, K.W. Chitosan-DNA nanoparticles as gene carriers: Synthesis, characterization and transfection efficiency. *J. Control. Release* **2001**, *70*, 399–421. [[CrossRef](#)]
51. Chan, P.; Kurisawa, M.; Chung, J.E.; Yang, Y.-Y. Synthesis and characterization of chitosan-g-poly(ethylene glycol)-folate as a non-viral carrier for tumor-targeted gene delivery. *Biomaterials* **2007**, *28*, 540–549. [[CrossRef](#)] [[PubMed](#)]
52. Jhaveri, A.; Deshpande, P.; Pattni, B.; Torchilin, V. Transferrin-targeted, resveratrol-loaded liposomes for the treatment of glioblastoma. *J. Control. Release* **2018**, *277*, 89–101. [[CrossRef](#)] [[PubMed](#)]
53. Gao, S.; Chen, J.; Xu, X.; Ding, Z.; Yang, Y.-H.; Hua, Z.; Zhang, J. Galactosylated low molecular weight chitosan as DNA carrier for hepatocyte-targeting. *Int. J. Pharm.* **2003**, *255*, 57–68. [[CrossRef](#)]
54. Park, I.-K.; Yang, J.; Jeong, H.-J.; Bom, H.-S.; Harada, I.; Akaike, T.; Kim, S.-I.; Cho, C.-S. Galactosylated chitosan as a synthetic extracellular matrix for hepatocytes attachment. *Biomaterials* **2003**, *24*, 2331–2337. [[CrossRef](#)]
55. Kim, T.H.; Nah, J.W.; Cho, M.-H.; Park, T.G.; Cho, C.S. Receptor-mediated gene delivery into antigen presenting cells using mannosylated chitosan/DNA nanoparticles. *J. Nanosci. Nanotechnol.* **2006**, *6*, 2796–2803. [[CrossRef](#)] [[PubMed](#)]
56. Negm, N.A.; Hefni, H.H.H.; Abd-Elaal, A.A.A.; Badr, E.A.; Abou Kana, M.T.H. Advancement on modification of chitosan biopolymer and its potential applications. *Int. J. Biol. Macromol.* **2020**, *152*, 681–702. [[CrossRef](#)] [[PubMed](#)]
57. Shastri, D.H. Thiolated chitosan: A boon to ocular delivery of therapeutics. *MOJ Bioequivalence Bioavailab.* **2017**, *3*, 34–37. [[CrossRef](#)]
58. Mahmood, A.; Lanthaler, M.; Laffleur, F.; Huck, C.W.; Bernkop-Schnürch, A. Thiolated chitosan micelles: Highly mucoadhesive drug carriers. *Carbohydr. Polym.* **2017**, *167*, 250–258. [[CrossRef](#)]
59. Boateng, J.S.; Ayensu, I. Preparation and characterization of laminated thiolated chitosan-based freeze-dried wafers for potential buccal delivery of macromolecules. *Drug Dev. Ind. Pharm.* **2014**, *40*, 611–618. [[CrossRef](#)]
60. Boateng, J.; Mitchell, J.; Pawar, H.; Ayensu, I. Functional characterisation and permeation studies of lyophilised thiolated chitosan xerogels for buccal delivery of insulin. *Protein Pept. Lett.* **2014**, *21*, 1163–1175. [[CrossRef](#)]

61. Liu, Q.; Zhang, C.; Zheng, X.; Shao, X.; Zhang, X.; Zhang, Q.; Jiang, X. Preparation and evaluation of antigen/N-trimethylaminoethylmethacrylate chitosan conjugates for nasal immunization. *Vaccine* **2014**, *32*, 2582–2590. [[CrossRef](#)] [[PubMed](#)]
62. Huang, G.-Q.; Zhang, Z.-K.; Cheng, L.-Y.; Xiao, J.-X. Intestine-targeted delivery potency of O-carboxymethyl chitosan-coated layer-by-layer microcapsules: An in vitro and in vivo evaluation. *Mater. Sci. Eng. C Mater. Biol. Appl.* **2019**, *105*, 110129. [[CrossRef](#)] [[PubMed](#)]
63. Zhou, P.; Sun, X.; Zhang, Z. Kidney-targeted drug delivery systems. *Acta Pharm. Sin. B* **2014**, *4*, 37–42. [[CrossRef](#)] [[PubMed](#)]
64. Vasanthakumar, T.; Rubinstein, J.L. Structure and roles of V-type ATPases. *Trends Biochem. Sci.* **2020**, *45*, 295–307. [[CrossRef](#)]
65. Li, W.; Nicol, F.; Szoka, F.C. GALA: A designed synthetic pH-responsive amphipathic peptide with applications in drug and gene delivery. *Adv. Drug Deliv. Rev.* **2004**, *56*, 967–985. [[CrossRef](#)]
66. El Ouahabi, A.; Thiry, M.; Pector, V.; Fuks, R.; Ruyschaert, J.M.; Vandenbranden, M. The role of endosome destabilizing activity in the gene transfer process mediated by cationic lipids. *FEBS Lett.* **1997**, *414*, 187–192.
67. Ma, Z.; Yang, C.; Song, W.; Wang, Q.; Kjems, J.; Gao, S. Chitosan Hydrogel as siRNA vector for prolonged gene silencing. *J. Nanobiotechnol.* **2014**, *12*, 23. [[CrossRef](#)]
68. Shi, B.; Zheng, M.; Tao, W.; Chung, R.; Jin, D.; Ghaffari, D.; Farokhzad, O.C. Challenges in DNA delivery and recent advances in multifunctional polymeric DNA delivery systems. *Biomacromolecules* **2017**, *18*, 2231–2246. [[CrossRef](#)]
69. Molinaro, R.; Wolfram, J.; Federico, C.; Cilurzo, F.; Di Marzio, L.; Ventura, C.A.; Carafa, M.; Celia, C.; Fresta, M. Polyethylenimine and chitosan carriers for the delivery of RNA interference effectors. *Expert Opin. Drug Deliv.* **2013**, *10*, 1653–1668. [[CrossRef](#)]
70. Boussif, O.; Lezoualc'h, F.; Zanta, M.A.; Mergny, M.D.; Scherman, D.; Demeneix, B.; Behr, J.P. A versatile vector for gene and oligonucleotide transfer into cells in culture and in vivo: Polyethylenimine. *Proc. Natl. Acad. Sci. USA* **1995**, *92*, 7297–7301. [[CrossRef](#)]
71. Bae, Y.; Lee, Y.H.; Lee, S.; Han, J.; Ko, K.S.; Choi, J.S. Characterization of glycol chitosan grafted with low molecular weight polyethylenimine as a gene carrier for human adipose-derived mesenchymal stem cells. *Carbohydr. Polym.* **2016**, *153*, 379–390. [[CrossRef](#)] [[PubMed](#)]
72. Chen, H.; Cui, S.; Zhao, Y.; Zhang, C.; Zhang, S.; Peng, X. Grafting chitosan with polyethylenimine in an ionic liquid for efficient gene delivery. *PLoS ONE* **2015**, *10*, e0121817. [[CrossRef](#)] [[PubMed](#)]
73. Liu, Q.; Jin, Z.; Huang, W.; Sheng, Y.; Wang, Z.; Guo, S. Tailor-made ternary nanopolyplexes of thiolated trimethylated chitosan with pDNA and folate conjugated cis-aconitic amide-polyethylenimine for efficient gene delivery. *Int. J. Biol. Macromol.* **2020**, *152*, 948–956. [[CrossRef](#)]
74. Lee, Y.H.; Park, H.I.; Choi, J.S. Novel glycol chitosan-based polymeric gene carrier synthesized by a Michael addition reaction with low molecular weight polyethylenimine. *Carbohydr. Polym.* **2016**, *137*, 669–677. [[CrossRef](#)]
75. Javan, B.; Atyabi, F.; Shahbazi, M. Hypoxia-inducible bidirectional shRNA expression vector delivery using PEI/chitosan-TBA copolymers for colorectal Cancer gene therapy. *Life Sci.* **2018**, *202*, 140–151. [[CrossRef](#)]
76. Sun, B.; Zhao, R.; Kong, F.; Ren, Y.; Zuo, A.; Liang, D.; Zhang, J. Phosphorylatable short peptide conjugation for facilitating transfection efficacy of CS/DNA complex. *Int. J. Pharm.* **2010**, *397*, 206–210. [[CrossRef](#)]
77. Zhao, R.; Sun, B.; Liu, T.; Liu, Y.; Zhou, S.; Zuo, A.; Liang, D. Optimize nuclear localization and intra-nucleus disassociation of the exogene for facilitating transfection efficacy of the chitosan. *Int. J. Pharm.* **2011**, *413*, 254–259. [[CrossRef](#)]
78. Miao, J.; Yang, X.; Gao, Z.; Li, Q.; Meng, T.; Wu, J.; Yuan, H.; Hu, F. Redox-responsive chitosan oligosaccharide-SS-Octadecylamine polymeric carrier for efficient anti-Hepatitis B Virus gene therapy. *Carbohydr. Polym.* **2019**, *212*, 215–221. [[CrossRef](#)]
79. Cryan, S.-A.; McKiernan, P.; Cunningham, C.M.; Greene, C. Targeting miRNA-based medicines to cystic fibrosis airway epithelial cells using nanotechnology. *Int. J. Nanomed.* **2013**, *8*, 3907. [[CrossRef](#)]
80. González, J.D.; Silva-Marrero, J.I.; Metón, I.; Caballero-Solares, A.; Viegas, I.; Fernández, F.; Miñarro, M.; Fàbregas, A.; Ticó, J.R.; Jones, J.G.; et al. Chitosan-mediated shRNA knockdown of cytosolic alanine aminotransferase improves hepatic carbohydrate metabolism. *Mar. Biotechnol.* **2016**, *18*, 85–97. [[CrossRef](#)]

81. Gaspar, C.; Silva-Marrero, J.I.; Fàbregas, A.; Miñarro, M.; Ticó, J.R.; Baanante, I.V.; Metón, I. Administration of chitosan-tripolyphosphate-DNA nanoparticles to knockdown glutamate dehydrogenase expression impairs transdeamination and gluconeogenesis in the liver. *J. Biotechnol.* **2018**, *286*, 5–13. [[CrossRef](#)] [[PubMed](#)]
82. Acharya, R. The recent progresses in shRNA-nanoparticle conjugate as a therapeutic approach. *Mater. Sci. Eng. C* **2019**, *104*, 109928. [[CrossRef](#)] [[PubMed](#)]
83. Zheng, H.; Tang, C.; Yin, C. Oral delivery of shRNA based on amino acid modified chitosan for improved antitumor efficacy. *Biomaterials* **2015**, *70*, 126–137. [[CrossRef](#)] [[PubMed](#)]
84. Wang, S.-L.; Yao, H.-H.; Guo, L.-L.; Dong, L.; Li, S.-G.; Gu, Y.-P.; Qin, Z.-H. Selection of optimal sites for TGFB1 gene silencing by chitosan-TPP nanoparticle-mediated delivery of shRNA. *Cancer Genet. Cytogenet.* **2009**, *190*, 8–14. [[CrossRef](#)] [[PubMed](#)]
85. Karimi, M.; Avci, P.; Ahi, M.; Gazori, T.; Hamblin, M.R.; Naderi-Manesh, H. Evaluation of chitosan-tripolyphosphate nanoparticles as a p-shRNA delivery vector: Formulation, optimization and cellular uptake study. *J. Nanopharm. Drug Deliv.* **2013**, *1*, 266–278. [[CrossRef](#)] [[PubMed](#)]
86. Ahmed, F.; Soliman, F.M.; Adly, M.A.; Soliman, H.A.M.; El-Matbouli, M.; Saleh, M. Recent progress in biomedical applications of chitosan and its nanocomposites in aquaculture: A review. *Res. Vet. Sci.* **2019**, *126*, 68–82. [[CrossRef](#)]
87. Abdel-Ghany, H.M.; Salem, M.E. Effects of dietary chitosan supplementation on farmed fish; a review. *Rev. Aquac.* **2020**, *12*, 438–452. [[CrossRef](#)]
88. Kono, M.; Matsui, T.; Shimizu, C. Effect of chitin, chitosan, and cellulose as diet supplements on the growth of cultured fish. *Bull. Jpn. Soc. Sci. Fish.* **1987**, *53*, 125–129. [[CrossRef](#)]
89. Shiau, S.-Y.; Yu, Y.-P. Dietary supplementation of chitin and chitosan depresses growth in tilapia, *Oreochromis niloticus* × *O. aureus*. *Aquaculture* **1999**, *179*, 439–446. [[CrossRef](#)]
90. Wu, S. The growth performance, body composition and nonspecific immunity of Tilapia (*Oreochromis niloticus*) affected by chitosan. *Int. J. Biol. Macromol.* **2020**, *145*, 682–685. [[CrossRef](#)]
91. Fadl, S.E.; El-Gammal, G.A.; Abdo, W.S.; Barakat, M.; Sakr, O.A.; Nassef, E.; Gad, D.M.; El-Sheshtawy, H.S. Evaluation of dietary chitosan effects on growth performance, immunity, body composition and histopathology of Nile tilapia (*Oreochromis niloticus*) as well as the resistance to *Streptococcus agalactiae* infection. *Aquac. Res.* **2020**, *51*, 1120–1132. [[CrossRef](#)]
92. Chen, Y.; Zhu, X.; Yang, Y.; Han, D.; Jin, J.; Xie, S. Effect of dietary chitosan on growth performance, haematology, immune response, intestine morphology, intestine microbiota and disease resistance in gibel carp (*Carassius auratus gibelio*). *Aquac. Nutr.* **2014**, *20*, 532–546. [[CrossRef](#)]
93. El-Sayed, H.S.; Barakat, K.M. Effect of dietary chitosan on challenged *Dicentrarchus labrax* post larvae with *Aeromonas hydrophila*. *Russ. J. Mar. Biol.* **2016**, *42*, 501–508. [[CrossRef](#)]
94. Yan, J.; Guo, C.; Dawood, M.A.O.; Gao, J. Effects of dietary chitosan on growth, lipid metabolism, immune response and antioxidant-related gene expression in *Misgurnus anguillicaudatus*. *Benef. Microbes* **2017**, *8*, 439–449. [[CrossRef](#)] [[PubMed](#)]
95. Chen, J.; Chen, L. Effects of chitosan-supplemented diets on the growth performance, nonspecific immunity and health of loach fish (*Misgurnus anguillicaudatus*). *Carbohydr. Polym.* **2019**, *225*, 115227. [[CrossRef](#)] [[PubMed](#)]
96. Kamali Najafabad, M.; Imanpoor, M.R.; Taghizadeh, V.; Alishahi, A. Effect of dietary chitosan on growth performance, hematological parameters, intestinal histology and stress resistance of Caspian kutum (*Rutilus frisii kutum* Kamenskii, 1901) fingerlings. *Fish Physiol. Biochem.* **2016**, *42*, 1063–1071. [[CrossRef](#)] [[PubMed](#)]
97. Samarakoon, K.W.; Cha, S.-H.; Lee, J.-H.; Jeon, Y.-J. The growth, innate immunity and protection against H₂O₂-induced oxidative damage of a chitosan-coated diet in the olive flounder *Paralichthys olivaceus*. *Fish. Aquat. Sci.* **2013**, *16*, 149–158. [[CrossRef](#)]
98. Ranjan, R.; Prasad, K.P.; Vani, T.; Kumar, R. Effect of dietary chitosan on haematology, innate immunity and disease resistance of Asian seabass *Lates calcarifer* (Bloch). *Aquac. Res.* **2014**, *45*, 983–993. [[CrossRef](#)]
99. Shanthi Mari, L.S.; Jagruthi, C.; Anbazahan, S.M.; Yogeshwari, G.; Thirumurugan, R.; Arockiaraj, J.; Mariappan, P.; Balasundaram, C.; Harikrishnan, R. Protective effect of chitin and chitosan enriched diets on immunity and disease resistance in *Cirrhina mrigala* against *Aphanomyces invadans*. *Fish Shellfish Immunol.* **2014**, *39*, 378–385. [[CrossRef](#)]

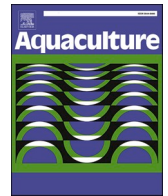
100. Harikrishnan, R.; Kim, J.-S.; Balasundaram, C.; Heo, M.-S. Immunomodulatory effects of chitin and chitosan enriched diets in *Epinephelus bruneus* against *Vibrio alginolyticus* infection. *Aquaculture* **2012**, *326–329*, 46–52. [[CrossRef](#)]
101. Harikrishnan, R.; Kim, J.-S.; Balasundaram, C.; Heo, M.-S. Dietary supplementation with chitin and chitosan on haematology and innate immune response in *Epinephelus bruneus* against *Philasterides dicentrarchi*. *Exp. Parasitol.* **2012**, *131*, 116–124. [[CrossRef](#)] [[PubMed](#)]
102. Wang, Y.; Li, J. Effects of chitosan nanoparticles on survival, growth and meat quality of tilapia, *Oreochromis nilotica*. *Nanotoxicology* **2011**, *5*, 425–431. [[CrossRef](#)] [[PubMed](#)]
103. Abdel-Tawwab, M.; Razeq, N.A.; Abdel-Rahman, A.M. Immunostimulatory effect of dietary chitosan nanoparticles on the performance of Nile tilapia, *Oreochromis niloticus* (L.). *Fish Shellfish Immunol.* **2019**, *88*, 254–258. [[CrossRef](#)] [[PubMed](#)]
104. Abd El-Naby, F.S.; Naiel, M.A.E.; Al-Sagheer, A.A.; Negm, S.S. Dietary chitosan nanoparticles enhance the growth, production performance, and immunity in *Oreochromis niloticus*. *Aquaculture* **2019**, *501*, 82–89. [[CrossRef](#)]
105. Naiel, M.A.E.; Ismael, N.E.M.; Abd El-hameed, S.A.A.; Amer, M.S. The antioxidative and immunity roles of chitosan nanoparticle and vitamin C-supplemented diets against imidacloprid toxicity on *Oreochromis niloticus*. *Aquaculture* **2020**, *523*, 735219. [[CrossRef](#)]
106. Abd El-Naby, A.S.; Al-Sagheer, A.A.; Negm, S.S.; Naiel, M.A.E. Dietary combination of chitosan nanoparticle and thymol affects feed utilization, digestive enzymes, antioxidant status, and intestinal morphology of *Oreochromis niloticus*. *Aquaculture* **2020**, *515*, 734577. [[CrossRef](#)]
107. Gao, J.-Q.; Hu, Y.L.; Wang, Q.; Han, F.; Shao, J.Z. Toxicity evaluation of biodegradable chitosan nanoparticles using a zebrafish embryo model. *Int. J. Nanomed.* **2011**, *6*, 3351–3359. [[CrossRef](#)]
108. Nikapitiya, C.; Dananjaya, S.H.S.; De Silva, B.C.J.; Heo, G.-J.; Oh, C.; De Zoysa, M.; Lee, J. Chitosan nanoparticles: A positive immune response modulator as display in zebrafish larvae against *Aeromonas hydrophila* infection. *Fish Shellfish Immunol.* **2018**, *76*, 240–246. [[CrossRef](#)]
109. Qin, C.; Zhang, Y.; Liu, W.; Xu, L.; Yang, Y.; Zhou, Z. Effects of chito-oligosaccharides supplementation on growth performance, intestinal cytokine expression, autochthonous gut bacteria and disease resistance in hybrid tilapia *Oreochromis niloticus* ♀ × *Oreochromis aureus* ♂. *Fish Shellfish Immunol.* **2014**, *40*, 267–274. [[CrossRef](#)]
110. Gopalakannan, A.; Arul, V. Immunomodulatory effects of dietary intake of chitin, chitosan and levamisole on the immune system of *Cyprinus carpio* and control of *Aeromonas hydrophila* infection in ponds. *Aquaculture* **2006**, *255*, 179–187. [[CrossRef](#)]
111. Karlsen, Ø.; Amlund, H.; Berg, A.; Olsen, R.E. The effect of dietary chitin on growth and nutrient digestibility in farmed Atlantic cod, Atlantic salmon and Atlantic halibut. *Aquac. Res.* **2017**, *48*, 123–133. [[CrossRef](#)]
112. Lin, S.-M.; Jiang, Y.; Chen, Y.-J.; Luo, L.; Doolgindachbaporn, S.; Yuangsoi, B. Effects of Astragalus polysaccharides (APS) and chito-oligosaccharides (COS) on growth, immune response and disease resistance of juvenile largemouth bass, *Micropterus salmoides*. *Fish Shellfish Immunol.* **2017**, *70*, 40–47. [[CrossRef](#)] [[PubMed](#)]
113. Nguyen, N.D.; Van Dang, P.; Le, A.Q.; Nguyen, T.K.L.; Pham, D.H.; Van Nguyen, N.; Nguyen, Q.H. Effect of oligochitosan and oligo-β-glucan supplementation on growth, innate immunity, and disease resistance of striped catfish (*Pangasianodon hypophthalmus*). *Biotechnol. Appl. Biochem.* **2017**, *64*, 564–571. [[CrossRef](#)]
114. Meng, X.; Wang, J.; Wan, W.; Xu, M.; Wang, T. Influence of low molecular weight chito-oligosaccharides on growth performance and non-specific immune response in Nile tilapia *Oreochromis niloticus*. *Aquac. Int.* **2017**, *25*, 1265–1277. [[CrossRef](#)]
115. Su, P.; Han, Y.; Jiang, C.; Ma, Y.; Pan, J.; Liu, S.; Zhang, T. Effects of chitosan-oligosaccharides on growth performance, digestive enzyme and intestinal bacterial flora of tiger puffer (*Takifugu rubripes* Temminck et Schlegel, 1850). *J. Appl. Ichthyol.* **2017**, *33*, 458–467. [[CrossRef](#)]
116. Lin, S.; Mao, S.; Guan, Y.; Luo, L.; Luo, L.; Pan, Y. Effects of dietary chitosan oligosaccharides and *Bacillus coagulans* on the growth, innate immunity and resistance of koi (*Cyprinus carpio koi*). *Aquaculture* **2012**, *342–343*, 36–41.
117. Lin, S.; Mao, S.; Guan, Y.; Lin, X.; Luo, L. Dietary administration of chito-oligosaccharides to enhance growth, innate immune response and disease resistance of *Trachinotus ovatus*. *Fish Shellfish Immunol.* **2012**, *32*, 909–913. [[CrossRef](#)]

118. Liu, Y.; Xing, R.; Liu, S.; Qin, Y.; Li, K.; Yu, H.; Li, P. Effects of chitoooligosaccharides supplementation with different dosages, molecular weights and degrees of deacetylation on growth performance, innate immunity and hepatopancreas morphology in Pacific white shrimp (*Litopenaeus vannamei*). *Carbohydr. Polym.* **2019**, *226*, 115254. [[CrossRef](#)]
119. Luo, L.; Cai, X.; He, C.; Xue, M.; Wu, X.; Cao, H. Immune response, stress resistance and bacterial challenge in juvenile rainbow trouts *Oncorhynchus mykiss* fed diets containing chitosan-oligosaccharides. *Curr. Zool.* **2009**, *55*, 416–422. [[CrossRef](#)]
120. Liu, L.; Zhou, Y.; Zhao, X.; Wang, H.; Wang, L.; Yuan, G.; Asim, M.; Wang, W.; Zeng, L.; Liu, X.; et al. Oligochitosan stimulated phagocytic activity of macrophages from blunt snout bream (*Megalobrama amblycephala*) associated with respiratory burst coupled with nitric oxide production. *Dev. Comp. Immunol.* **2014**, *47*, 17–24. [[CrossRef](#)]
121. Fernández-Díaz, C.; Coste, O.; Malta, E. Polymer chitosan nanoparticles functionalized with *Ulva ohnoi* extracts boost in vitro ulvan immunostimulant effect in *Solea senegalensis* macrophages. *Algal Res.* **2017**, *26*, 135–142. [[CrossRef](#)]
122. Wisdom, K.S.; Bhat, I.A.; Chanu, T.I.; Kumar, P.; Pathakota, G.-B.; Nayak, S.K.; Walke, P.; Sharma, R. Chitosan grafting onto single-walled carbon nanotubes increased their stability and reduced the toxicity in vivo (catfish) model. *Int. J. Biol. Macromol.* **2020**, *155*, 697–707. [[CrossRef](#)] [[PubMed](#)]
123. Alishahi, A.; Mirvaghefi, A.; Tehrani, M.R.; Farahmand, H.; Koshio, S.; Dorkoosh, F.A.; Elsabee, M.Z. Chitosan nanoparticle to carry vitamin C through the gastrointestinal tract and induce the non-specific immunity system of rainbow trout (*Oncorhynchus mykiss*). *Carbohydr. Polym.* **2011**, *86*, 142–146. [[CrossRef](#)]
124. Jiménez-Fernández, E.; Ruyra, A.; Roher, N.; Zuasti, E.; Infante, C.; Fernández-Díaz, C. Nanoparticles as a novel delivery system for vitamin C administration in aquaculture. *Aquaculture* **2014**, *432*, 426–433. [[CrossRef](#)]
125. Bhat, I.A.; Nazir, M.I.; Ahmad, I.; Pathakota, G.-B.; Chanu, T.I.; Goswami, M.; Sundaray, J.K.; Sharma, R. Fabrication and characterization of chitosan conjugated eurycomanone nanoparticles: In vivo evaluation of the biodistribution and toxicity in fish. *Int. J. Biol. Macromol.* **2018**, *112*, 1093–1103. [[CrossRef](#)]
126. Wisdom, K.S.; Bhat, I.A.; Kumar, P.; Pathan, M.K.; Chanu, T.I.; Walke, P.; Sharma, R. Fabrication of chitosan nanoparticles loaded with aromatase inhibitors for the advancement of gonadal development in *Clarias magur* (Hamilton, 1822). *Aquaculture* **2018**, *497*, 125–133. [[CrossRef](#)]
127. Bhat, I.A.; Ahmad, I.; Mir, I.N.; Yousf, D.J.; Ganie, P.A.; Bhat, R.A.H.; Gireesh-Babu, P.; Sharma, R. Evaluation of the in vivo effect of chitosan conjugated eurycomanone nanoparticles on the reproductive response in female fish model. *Aquaculture* **2019**, *510*, 392–399. [[CrossRef](#)]
128. Bhat, I.A.; Ahmad, I.; Mir, I.N.; Bhat, R.A.H.; P, G.-B.; Goswami, M.; Sundaray, J.K.; Sharma, R. Chitosan-eurycomanone nanoformulation acts on steroidogenesis pathway genes to increase the reproduction rate in fish. *J. Steroid Biochem. Mol. Biol.* **2019**, *185*, 237–247. [[CrossRef](#)]
129. Barakat, K.M.; El-Sayed, H.S.; Gohar, Y.M. Protective effect of squilla chitosan–silver nanoparticles for *Dicentrarchus labrax* larvae infected with *Vibrio anguillarum*. *Int. Aquat. Res.* **2016**, *8*, 179–189. [[CrossRef](#)]
130. Udayangani, R.M.C.; Dananjaya, S.H.S.; Nikapitiya, C.; Heo, G.-J.; Lee, J.; De Zoysa, M. Metagenomics analysis of gut microbiota and immune modulation in zebrafish (*Danio rerio*) fed chitosan silver nanocomposites. *Fish Shellfish Immunol.* **2017**, *66*, 173–184. [[CrossRef](#)]
131. Xia, I.F.; Cheung, J.S.; Wu, M.; Wong, K.-S.; Kong, H.-K.; Zheng, X.-T.; Wong, K.-H.; Kwok, K.W. Dietary chitosan-selenium nanoparticle (CTS-SeNP) enhance immunity and disease resistance in zebrafish. *Fish Shellfish Immunol.* **2019**, *87*, 449–459. [[CrossRef](#)] [[PubMed](#)]
132. Victor, H.; Zhao, B.; Mu, Y.; Dai, X.; Wen, Z.; Gao, Y.; Chu, Z. Effects of Se-chitosan on the growth performance and intestinal health of the loach *Paramisgurnus dabryanus* (Sauvage). *Aquaculture* **2019**, *498*, 263–270. [[CrossRef](#)]
133. Zhang, J.; Fu, X.; Zhang, Y.; Zhu, W.; Zhou, Y.; Yuan, G.; Liu, X.; Ai, T.; Zeng, L.; Su, J. Chitosan and anisodamine improve the immune efficacy of inactivated infectious spleen and kidney necrosis virus vaccine in *Siniperca chuatsi*. *Fish Shellfish Immunol.* **2019**, *89*, 52–60. [[CrossRef](#)]
134. Zhu, W.; Zhang, Y.; Zhang, J.; Yuan, G.; Liu, X.; Ai, T.; Su, J. Astragalus polysaccharides, chitosan and poly(I:C) obviously enhance inactivated *Edwardsiella ictaluri* vaccine potency in yellow catfish *Pelteobagrus fulvidraco*. *Fish Shellfish Immunol.* **2019**, *87*, 379–385. [[CrossRef](#)]

135. Liu, X.; Zhang, H.; Gao, Y.; Zhang, Y.; Wu, H.; Zhang, Y. Efficacy of chitosan oligosaccharide as aquatic adjuvant administered with a formalin-inactivated *Vibrio anguillarum* vaccine. *Fish Shellfish Immunol.* **2015**, *47*, 855–860. [[CrossRef](#)]
136. Wei, G.; Cai, S.; Wu, Y.; Ma, S.; Huang, Y. Immune effect of *Vibrio harveyi* formalin-killed cells vaccine combined with chitosan oligosaccharide and astragalus polysaccharides in ♀*Epinephelus fuscoguttatus* × ♂ *Epinephelus lanceolatus*. *Fish Shellfish Immunol.* **2020**, *98*, 186–192. [[CrossRef](#)]
137. Halimi, M.; Alishahi, M.; Abbaspour, M.R.; Ghorbanpoor, M.; Tabandeh, M.R. Valuable method for production of oral vaccine by using alginate and chitosan against *Lactococcus garvieae*/*Streptococcus iniae* in rainbow trout (*Oncorhynchus mykiss*). *Fish Shellfish Immunol.* **2019**, *90*, 431–439. [[CrossRef](#)]
138. Kole, S.; Qadiri, S.S.N.; Shin, S.-M.; Kim, W.-S.; Lee, J.; Jung, S.-J. Nanoencapsulation of inactivated-viral vaccine using chitosan nanoparticles: Evaluation of its protective efficacy and immune modulatory effects in olive flounder (*Paralichthys olivaceus*) against viral haemorrhagic septicaemia virus (VHSV) infection. *Fish Shellfish Immunol.* **2019**, *91*, 136–147. [[CrossRef](#)]
139. Tandberg, J.; Lagos, L.; Ropstad, E.; Smistad, G.; Hiorth, M.; Winther-Larsen, H.C. The use of chitosan-coated membrane vesicles for immunization against salmonid rickettsial septicemia in an adult zebrafish model. *Zebrafish* **2018**, *15*, 372–381. [[CrossRef](#)]
140. Dubey, S.; Avadhani, K.; Mutalik, S.; Sivadasan, S.; Maiti, B.; Girisha, S.; Venugopal, M.; Mutoloki, S.; Evensen, Ø.; Karunasagar, I.; et al. Edwardsiella tarda OmpA encapsulated in chitosan nanoparticles shows superior protection over inactivated whole cell vaccine in orally vaccinated fringed-lipped peninsula carp (*Labeo fimbriatus*). *Vaccines* **2016**, *4*, 40. [[CrossRef](#)]
141. Wang, E.; Wang, X.; Wang, K.; He, J.; Zhu, L.; He, Y.; Chen, D.; Ouyang, P.; Geng, Y.; Huang, X.; et al. Preparation, characterization and evaluation of the immune effect of alginate/chitosan composite microspheres encapsulating recombinant protein of *Streptococcus iniae* designed for fish oral vaccination. *Fish Shellfish Immunol.* **2018**, *73*, 262–271. [[CrossRef](#)] [[PubMed](#)]
142. Chen, T.; Hu, Y.; Zhou, J.; Hu, S.; Xiao, X.; Liu, X.; Su, J.; Yuan, G. Chitosan reduces the protective effects of IFN- γ 2 on grass carp (*Ctenopharyngodon idella*) against *Flavobacterium columnare* infection due to excessive inflammation. *Fish Shellfish Immunol.* **2019**, *95*, 305–313. [[CrossRef](#)] [[PubMed](#)]
143. Sharma, D.; Maheshwari, D.; Philip, G.; Rana, R.; Bhatia, S.; Singh, M.; Gabrani, R.; Sharma, S.K.; Ali, J.; Sharma, R.K.; et al. Formulation and optimization of polymeric nanoparticles for intranasal delivery of lorazepam using Box-Behnken design: In vitro and in vivo evaluation. *Biomed Res. Int.* **2014**, *2014*, 156010. [[CrossRef](#)]
144. Rather, M.A.; Bhat, I.A.; Gireesh-Babu, P.; Chaudhari, A.; Sundaray, J.K.; Sharma, R. Molecular characterization of kisspeptin gene and effect of nano-encapsulated kisspeptin-10 on reproductive maturation in *Catla catla*. *Domest. Anim. Endocrinol.* **2016**, *56*, 36–47. [[CrossRef](#)] [[PubMed](#)]
145. Tian, J.; Yu, J.; Sun, X. Chitosan microspheres as candidate plasmid vaccine carrier for oral immunisation of Japanese flounder (*Paralichthys olivaceus*). *Vet. Immunol. Immunopathol.* **2008**, *126*, 220–229. [[CrossRef](#)]
146. Vimal, S.; Taju, G.; Nambi, K.S.N.; Abdul Majeed, S.; Sarath Babu, V.; Ravi, M.; Sahul Hameed, A.S. Synthesis and characterization of CS/TPP nanoparticles for oral delivery of gene in fish. *Aquaculture* **2012**, *358–359*, 14–22. [[CrossRef](#)]
147. Li, L.; Lin, S.-L.; Deng, L.; Liu, Z.-G. Potential use of chitosan nanoparticles for oral delivery of DNA vaccine in black seabream *Acanthopagrus schlegelii* Bleeker to protect from *Vibrio parahaemolyticus*. *J. Fish Dis.* **2013**, *36*, 987–995. [[CrossRef](#)]
148. Vimal, S.; Abdul Majeed, S.; Nambi, K.S.N.; Madan, N.; Farook, M.A.; Venkatesan, C.; Taju, G.; Venu, S.; Subburaj, R.; Thirunavukkarasu, A.R.; et al. Delivery of DNA vaccine using chitosan–tripolyphosphate (CS/TPP) nanoparticles in Asian sea bass, *Lates calcarifer* (Bloch, 1790) for protection against nodavirus infection. *Aquaculture* **2014**, *420–421*, 240–246. [[CrossRef](#)]
149. Zheng, F.; Liu, H.; Sun, X.; Zhang, Y.; Zhang, B.; Teng, Z.; Hou, Y.; Wang, B. Development of oral DNA vaccine based on chitosan nanoparticles for the immunization against reddish body iridovirus in turbot (*Scophthalmus maximus*). *Aquaculture* **2016**, *452*, 263–271. [[CrossRef](#)]
150. Bhat, I.A.; Rather, M.A.; Saha, R.; Pathakota, G.-B.; Pavan-Kumar, A.; Sharma, R. Expression analysis of Sox9 genes during annual reproductive cycles in gonads and after nanodelivery of LHRH in *Clarias batrachus*. *Res. Vet. Sci.* **2016**, *106*, 100–106. [[CrossRef](#)]
151. Valero, Y.; Awad, E.; Buonocore, F.; Arizcun, M.; Esteban, M.Á.; Meseguer, J.; Chaves-Pozo, E.; Cuesta, A. An oral chitosan DNA vaccine against nodavirus improves transcription of cell-mediated cytotoxicity and

- interferon genes in the European sea bass juveniles gut and survival upon infection. *Dev. Comp. Immunol.* **2016**, *65*, 64–72. [[CrossRef](#)] [[PubMed](#)]
152. Sáez, M.I.; Vizcaíno, A.J.; Alarcón, F.J.; Martínez, T.F. Comparison of lacZ reporter gene expression in gilthead sea bream (*Sparus aurata*) following oral or intramuscular administration of plasmid DNA in chitosan nanoparticles. *Aquaculture* **2017**, *474*, 1–10. [[CrossRef](#)]
153. Rathor, P.K.; Bhat, I.A.; Rather, M.A.; Gireesh-Babu, P.; Kumar, K.; Purayil, S.B.P.; Sharma, R. Steroidogenic acute regulatory protein (StAR) gene expression construct: Development, nanodelivery and effect on reproduction in air-breathing catfish, *Clarias batrachus*. *Int. J. Biol. Macromol.* **2017**, *104*, 1082–1090. [[CrossRef](#)] [[PubMed](#)]
154. Ahmadvand, S.; Soltani, M.; Behdani, M.; Evensen, Ø.; Alirahimi, E.; Hassanzadeh, R.; Soltani, E. Oral DNA vaccines based on CS-TPP nanoparticles and alginate microparticles confer high protection against infectious pancreatic necrosis virus (IPNV) infection in trout. *Dev. Comp. Immunol.* **2017**, *74*, 178–189. [[CrossRef](#)] [[PubMed](#)]
155. Sáez, M.I.; Vizcaíno, A.J.; Alarcón, F.J.; Martínez, T.F. Feed pellets containing chitosan nanoparticles as plasmid DNA oral delivery system for fish: In vivo assessment in gilthead sea bream (*Sparus aurata*) juveniles. *Fish Shellfish Immunol.* **2018**, *80*, 458–466. [[CrossRef](#)]
156. Kole, S.; Kumari, R.; Anand, D.; Kumar, S.; Sharma, R.; Tripathi, G.; Makesh, M.; Rajendran, K.V.; Bedekar, M.K. Nanoconjugation of bicistronic DNA vaccine against *Edwardsiella tarda* using chitosan nanoparticles: Evaluation of its protective efficacy and immune modulatory effects in *Labeo rohita* vaccinated by different delivery routes. *Vaccine* **2018**, *36*, 2155–2165. [[CrossRef](#)]
157. Silva-Marrero, J.I.; Villasante, J.; Rashidpour, A.; Palma, M.; Fàbregas, A.; Almajano, M.P.; Viegas, I.; Jones, J.G.; Miñarro, M.; Ticó, J.R.; et al. The administration of chitosan-tripolyphosphate-DNA nanoparticles to express exogenous SREBP1a enhances conversion of dietary carbohydrates into lipids in the liver of *Sparus aurata*. *Biomolecules* **2019**, *9*, 297. [[CrossRef](#)]
158. Rao, B.M.; Kole, S.; Gireesh-Babu, P.; Sharma, R.; Tripathi, G.; Bedekar, M.K. Evaluation of persistence, bio-distribution and environmental transmission of chitosan/PLGA/pDNA vaccine complex against *Edwardsiella tarda* in *Labeo rohita*. *Aquaculture* **2019**, *500*, 385–392. [[CrossRef](#)]
159. Ramos, E.A.; Relucio, J.L.V.; Torres-Villanueva, C.A.T. Gene expression in tilapia following oral delivery of chitosan-encapsulated plasmid DNA incorporated into fish feeds. *Mar. Biotechnol.* **2005**, *7*, 89–94. [[CrossRef](#)]
160. Rajesh Kumar, S.; Ishaq Ahmed, V.P.; Parameswaran, V.; Sudhakaran, R.; Sarath Babu, V.; Sahul Hameed, A.S. Potential use of chitosan nanoparticles for oral delivery of DNA vaccine in Asian sea bass (*Lates calcarifer*) to protect from *Vibrio* (*Listonella*) *anguillarum*. *Fish Shellfish Immunol.* **2008**, *25*, 47–56. [[CrossRef](#)]
161. Kumari, R.; Gupta, S.; Singh, A.R.; Ferosekhan, S.; Kothari, D.C.; Pal, A.K.; Jadhao, S.B. Chitosan nanoencapsulated exogenous trypsin biomimics zymogen-like enzyme in fish gastrointestinal tract. *PLoS ONE* **2013**, *8*, e74743. [[CrossRef](#)] [[PubMed](#)]
162. Naylor, R.L.; Hardy, R.W.; Bureau, D.P.; Chiu, A.; Elliott, M.; Farrell, A.P.; Forster, I.; Gatlin, D.M.; Goldburg, R.J.; Hua, K.; et al. Feeding aquaculture in an era of finite resources. *Proc. Natl. Acad. Sci. USA* **2009**, *106*, 15103–15110. [[CrossRef](#)] [[PubMed](#)]
163. Polakof, S.; Panserat, S.; Soengas, J.L.; Moon, T.W. Glucose metabolism in fish: A review. *J. Comp. Physiol. B.* **2012**, *182*, 1015–1045. [[CrossRef](#)]
164. Rashidpour, A.; Silva-Marrero, J.I.; Seguí, L.; Baanante, I.V.; Metón, I. Metformin counteracts glucose-dependent lipogenesis and impairs transdeamination in the liver of gilthead sea bream (*Sparus aurata*). *Am. J. Physiol. Integr. Comp. Physiol.* **2019**, *316*, R265–R273. [[CrossRef](#)]
165. Metón, I.; Egea, M.; Anemaet, I.G.; Fernández, F.; Baanante, I.V. Sterol regulatory element binding protein-1a transactivates 6-phosphofructo-2-kinase/fructose-2,6-bisphosphatase gene promoter. *Endocrinology* **2006**, *147*, 3446–3456. [[CrossRef](#)]
166. Egea, M.; Metón, I.; Córdoba, M.; Fernández, F.; Baanante, I.V. Role of Sp1 and SREBP-1a in the insulin-mediated regulation of glucokinase transcription in the liver of gilthead sea bream (*Sparus aurata*). *Gen. Comp. Endocrinol.* **2008**, *155*, 359–367. [[CrossRef](#)]





Gene markers of dietary macronutrient composition and growth in the skeletal muscle of gilthead sea bream (*Sparus aurata*)

Alberto Sáez-Arteaga^a, Yuanbing Wu^b, Jonás I. Silva-Marrero^b, Ania Rashidpour^b, María Pilar Almajano^c, Felipe Fernández^d, Isabel V. Baanante^b, Isidoro Metón^{b,*}

^a Instituto de Ciencias Biomédicas, Facultad de Ciencias de la Salud, Universidad Autónoma de Chile, Temuco, Chile

^b Secció de Bioquímica i Biologia Molecular, Departament de Bioquímica i Fisiologia, Facultat de Farmàcia i Ciències de l'Alimentació, Universitat de Barcelona, Joan XXIII 27-31, 08028 Barcelona, Spain

^c Departament d'Enginyeria Química, Universitat Politècnica de Catalunya, Diagonal 647, 08028 Barcelona, Spain

^d Secció d'Ecologia, Departament de Biologia Evolutiva, Ecologia i Ciències Ambientals, Facultat de Biologia, Universitat de Barcelona, Diagonal 645, 08028 Barcelona, Spain

ARTICLE INFO

Keywords:

Dietary macronutrients
Gene expression
Gene markers
Growth
Muscle
Sparus aurata

ABSTRACT

To increase our current knowledge on the nutritional regulation of growth and gene expression pattern in fish skeletal muscle, the effect of dietary macronutrient composition was assessed on digestibility, nutrient retention, growth performance, and the mRNA levels of key genes involved in functionality, growth and development of the skeletal muscle in gilthead sea bream (*Sparus aurata*). Long-term starvation decreased the expression of myogenic regulatory factors such as Myod2, Myf5, myogenin (Myog) and Myf6 in the skeletal muscle of *S. aurata*. The supply of high or medium protein, low carbohydrate diets enhanced growth parameters, feed efficiency ratio, feed conversion ratio and significantly upregulated *myod2*. However, the supply of low protein, high carbohydrate diets restricted growth and stimulated the mRNA levels of *myostatin*, while downregulated *follistatin* (*fst*), *igf1*, *mtor* and *rps6*. Microarray analysis revealed *igfals*, *tnni2*, and *gadd45a* as gene markers upregulated by diets enriched with protein, lipids and carbohydrates, respectively. The results of the present study show that in addition to *myod2*, *fst*, *igf1*, *mtor* and *rps6*, the expression levels of *igfals*, *tnni2* and remarkably *gadd45a* in the skeletal muscle can be used as markers to evaluate the effect of dietary macronutrient changes on fish growth and muscle development in *S. aurata*.

1. Introduction

The development of the skeletal muscle follows a well-ordered structure that is highly adaptable to changing conditions. The process of myogenesis has a marked plasticity, which constitutes a fundamental event for proliferation, differentiation, migration and fusion of new myoblasts (Johnston, 2006). This complex and dynamic process leads to fusion of myocytes with existing myofibers (hypertrophy) and increasing proliferation of myocytes (hyperplasia) (Zhu et al., 2014). Myogenesis is primarily controlled by myogenic regulatory factors (MRFs) which include Myod, Myf5, myogenin (Myog) and Myf6, among others (Braun and Gautel, 2011; Rescan, 2001; Alami-Durante et al., 2019). MRFs are highly conserved proteins from teleosts to mammals that belong to a larger group of transcription factors containing a basic DNA-binding motif and a helix-loop-helix dimerisation domain (Olson

and Klein, 1994; Rossi and Messina, 2014). Myod and Myf5 are essential for initiation of the myogenic program, while Myog and Myf6 are expressed later, during myofibre differentiation (Holterman and Rudnicki, 2005; Rescan, 2001; Tan and Du, 2002). Additional factors, such as myostatin (Mstn) and follistatin (Fst), which belong to the transforming growth factor beta (Tgfb) superfamily, were also shown to have a major role in skeletal muscle growth and development. Mstn is a potent negative regulator of skeletal muscle growth (McPherron et al., 1997). Knockout mice for Mstn present 2 to 3-fold greater skeletal muscle mass than wild-type animals. Fst is an activin-binding protein essential for muscle fibre formation (Medeiros et al., 2009), and a potent antagonist of several members of the Tgfb superfamily, including Mstn (Amthor et al., 2004). Overexpression of Fst in mice and rainbow trout (*Oncorhynchus mykiss*) evidences the capacity of Fst to increase muscle mass (Lee and McPherron, 2001; Medeiros et al., 2009).

* Corresponding author.

E-mail address: imeton@ub.edu (I. Metón).

<https://doi.org/10.1016/j.aquaculture.2022.738221>

Received 11 November 2021; Received in revised form 22 February 2022; Accepted 1 April 2022

Available online 7 April 2022

0044-8486/© 2022 The Authors. Published by Elsevier B.V. This is an open access article under the CC BY license (<http://creativecommons.org/licenses/by/4.0/>).

Somatotropic compounds such as insulin-like growth factor 1 (Igf1) exert an important role in nutritional regulation of metabolism. Igf1 expression increases muscle mass and decreases muscle atrophy (Christoffolete et al., 2015; Glass, 2003a, 2003b; Vélez et al., 2014). Protein synthesis and glucose and amino acid uptake is stimulated by Igf1 in rainbow trout (*O. mykiss*) and gilthead sea bream (*S. aurata*) myocytes (Castillo et al., 2004; Montserrat et al., 2012). Igf1 and amino acids activate the phosphatidylinositol 3-kinase (Pi3k)-Akt pathway, which leads to phosphorylation of the serine/threonine protein kinase mechanistic target of rapamycin (Mtor) and activation of a critical pathway involved in cellular processes such as apoptosis, protein synthesis, gene transcription and cell proliferation (Vélez et al., 2016). Indeed, Mtor is an essential sensor of nutrient and amino acid availability through phosphorylation of 40S ribosomal protein S6 (Rps6) (Glass, 2005; Schiaffino and Mammucari, 2011).

Despite the fact that carnivorous fish are considered glucose intolerant (Panserat et al., 2019; Rashidpour et al., 2019), we previously showed that partial replacement of dietary protein by carbohydrates stimulates glucose oxidation via glycolysis and pentose phosphate pathway in the liver of *S. aurata* (Fernández et al., 2007; Metón et al., 1999). Indeed, the administration of chitosan-tripolyphosphate-DNA to overexpress *srebp1a* stimulates conversion of dietary carbohydrates into lipids in *S. aurata* through enhanced hepatic glycolysis, pentose phosphate pathway and lipogenesis (Silva-Marrero et al., 2019; Wu et al., 2020). Dietary carbohydrates upregulate the expression of glycolytic genes in the muscle of rainbow trout (Song et al., 2018), while it was claimed that glucose regulates protein synthesis and growth-related mechanisms in myogenic precursor cells from this species (Latimer et al., 2019). Although the fundamental events in muscle growth and development were well conserved during vertebrate evolution, fishes have unique features such as continuous growth and different proportion of white and red muscle fibres than mammals. Indeed, the molecular events that mediate the effect of dietary nutrients on signaling pathways that control growth of fish skeletal muscle remain unclear. With the aim to increase our current knowledge about the nutritional regulation of skeletal muscle growth and development in fish, we addressed the effect of dietary macronutrient composition on nutrient retention, growth performance and the gene expression pattern in the skeletal muscle of *S. aurata*, and identified novel gene markers for nutritional studies in cultured fish.

2. Materials and methods

2.1. Animals, feeding trial and sampling

S. aurata juveniles were obtained from Piscicultura Marina Mediterranea (Burriana, Castellón, Spain). A total of 330 fish (8.22 g ± 0.26 body weight) were transported to the laboratory, and distributed in 12 aquaria of 260 l supplied with running seawater at 21 °C in a closed system with active pump filter and UV lamps. The photoperiod was adjusted to a 12 h: 12 h dark-light cycle. Fish maintenance conditions were as previously described (Fernández et al., 2007). Three diets were formulated with gross energy at 20–22 kJ/g and macronutrient composition at levels above and below those in commercially available aquafeeds: HLL (high protein, low lipid, low carbohydrate), MHL (medium protein, high lipid, low carbohydrate) and LLH (low protein, low lipid, high carbohydrate) (Table 1). Following acclimation to our facilities, three groups of fish were fed twice a day (9:30 a.m. and 15:30 p.m.) with 25 g/kg body weight of the corresponding experimental diet for 23 days for microarray analysis and 37 days for evaluating growth, digestibility and gene expression (Fig. 1). Sampling points were selected according to previous studies showing that a period of 18–20 days is long enough for producing significant changes due to diet composition in the intermediary metabolism and gene expression profile of *S. aurata* juveniles (Metón et al., 1999; Silva-Marrero et al., 2017), while longer periods are necessary to obtain significant changes in growth and

Table 1
Composition of the diets supplied in this study to *S. aurata*.

	HLL	MHL	LLH
Formulation (%)			
Fish meal ^a	81.6	67.5	54.3
Fish oil ^b	0.8	13.1	6.0
Starch ^c	15.0	16.7	37.1
Carrageenan ^d	1.5	1.5	1.5
Mineral mixture ^e	0.9	0.9	0.9
Vitamin mixture ^f	0.2	0.2	0.2
Proximate Composition (%)			
Crude protein	59.5	50.1	40.6
Crude lipid	7.2	17.5	8.2
Carbohydrates ^g	18.4	20.9	40.9
Ash	14.9	11.5	10.3
Gross energy (kJ/g) ^h	20.2	22.4	19.9

^a Corpesca S.A. Super-Prime fish meal (Santiago de Chile, Chile).

^b Fish oil from A.F.A.M.S.A. (Vigo, Spain).

^c Pregelatinised corn starch from Brenntag Química S.A. (St. Andreu de la Barca, Barcelona, Spain).

^d Iota carrageenan (Sigma-Aldrich).

^e Mineral mixture provided (mg/kg): CaHPO₄·2 H₂O, 7340; MgO, 800; KCl, 750; FeSO₄·7 H₂O, 60; ZnO, 30; MnO₂, 15; CuSO₄·5 H₂O, 1.7; CoCl₂·6 H₂O, 1.5; KI, 1.5; Na₂SeO₃, 0.3.

^f Vitamin mixture provided (mg/kg): choline chloride, 1200; myo-inositol, 400; ascorbic acid, 200; nicotinic acid, 70; all-rac-tocopherol acetate, 60; calcium pantothenate, 30; riboflavin, 15; pyridoxin, 10; folic acid, 10; menadione, 10; thiamin-HCl, 8; all-trans retinol, 2; biotin, 0.7; cholecalciferol, 0.05; cyanocobalamin, 0.05.

^g Carbohydrates were calculated by difference.

^h Calculated from gross composition (protein 24 kJ/g, lipids 39 kJ/g, carbohydrates 17 kJ/g).

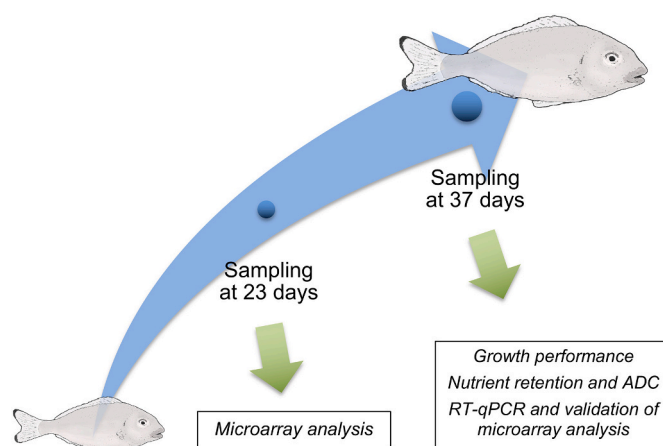


Fig. 1. Schematic workflow of sampling points and analysis carried out in the present study. ADC: apparent digestibility coefficient. RT-qPCR: reverse transcription coupled to quantitative real-time PCR.

nutrient retention parameters (Fernández et al., 2007). A fourth group of fish was submitted to starvation during the same period of time. Each dietary condition was assayed in 3 aquaria. All fish were weighed at the beginning of the experiment and every 12 days during the experiment. To calculate apparent digestibility coefficient (ADC), 0.1% yttrium oxide (Y₂O₃) was included in each experimental diet and used as inert marker the last week of the experiment. To determine body composition, 30 fish from the initial stock and 5 fish per aquarium at the end of the experiment were sampled and stored at -20 °C for subsequent analysis. Prior to sampling, fish were starved for 24 h and sacrificed by anaesthesia overdose with 1:12,500 tricaine methanesulfonate (MS-222) diluted in seawater followed by cervical section. Samples of skeletal

muscle extracted from the middle/dorsal region were dissected out, immediately frozen in liquid nitrogen and kept at -80 °C until analysis. For fecal collection, the posterior intestine was dissected out and the intestinal content was obtained by stripping. Posterior intestine samples were pooled (pools of 5 fish per aquarium), dried at 70 °C and kept at -20 °C. Experimental procedures involving fish complied with the guidelines of the University of Barcelona's Animal Welfare Committee and EU Directive 2010/63/EU for animal experiments.

2.2. Diet and body composition

To determine moisture, samples were dried at 70 °C until constant weight was obtained (Busacker et al., 1990; Lucas, 1996). Samples were analysed for carbon (C) and nitrogen (N) with a Carlo Erba NA 2100 elemental analyser (CE Instruments, Wigan, UK). Lipid content was extracted with petroleum ether using a Foss Tecator Soxtec HT 1043 extraction system (Hillerød, Denmark). Ash content was determined after incineration of samples in muffle furnace at 450 °C for 12 h (Busacker et al., 1990; Lucas, 1996). Protein was calculated from N content, using a factor of 6.25. Gross energy was calculated on the basis of dietary protein (24 kJ/g), lipid (39 kJ/g) and carbohydrate (17 kJ/g) (Bradfield and Llewellyn, 1982). For assaying Ca, P and Y, samples were digested and analysed with an inductively coupled plasma spectrometer (Polyscan 61E, Thermo Jarrell Ash Corporation, Waltham, MA, USA).

2.3. Apparent digestibility and growth parameters

Specific growth rate (SGR) was calculated as $(\ln W_f - \ln W_i) \cdot 100 / T$, where $\ln W_f$ and $\ln W_i$ are the natural logarithms of the final and initial mean fish weight in grams per aquarium, respectively, and T is time in days. Feed conversion ratio (FCR) was calculated as dry feed intake/wet weight gain. ADC of a given nutrient was calculated from the following equation (De Silva and Anderson, 1995):

$$ADC = 100 - [100 \cdot (\text{Nutrient}_{\text{Feces}} / \text{Nutrient}_{\text{Diet}}) \cdot (\text{Y}_{\text{Diet}} / \text{Y}_{\text{Feces}})]$$

For dry matter, the equation became:

$$ADC = 100 - [100 \cdot (\text{Y}_{\text{Diet}} / \text{Y}_{\text{Feces}})]$$

Other parameters calculated for each aquarium included: protein efficiency ratio (PER = g weight gain/g feed protein); protein retention (PR = g protein gain*100/g feed protein); lipid retention (LR = g lipid gain*100/g feed lipid) and hepatosomatic index (HSI = liver fresh weight*100/ fish body weight).

2.4. RNA isolation

Total RNA was extracted from the skeletal muscle using the RNeasy fibrous tissue Mini Kit (Qiagen, Sussex, UK) according to the manufacturer's recommendations. Concentration and purity were determined

spectrophotometrically at 260/280 nm using Nanodrop ND-1000 (Thermo Fischer Scientific, Waltham, MA, USA). RNA integrity was determined with an Agilent 2100 bioanalyser (Agilent Technologies, Santa Clara, CA, USA). Only samples with RNA Integrity Number (RIN) > 9.2 were used for subsequent studies.

2.5. Quantitative real-time PCR

The mRNA levels of key genes involved in skeletal muscle growth and development, and differentially expressed genes selected from the microarray analysis were assayed by reverse transcription coupled to quantitative real-time PCR (RT-qPCR). One microgram of total RNA isolated from white skeletal muscle of *S. aurata* was reverse-transcribed to cDNA with Moloney murine leukemia virus RT (Life Technologies, Carlsbad, CA, USA) for 1 h at 37 °C in the presence of random hexamer primers. The cDNA product was used for subsequent qPCR. The mRNA levels of *S. aurata* genes listed in Table 2 were determined in a StepOnePlus Real-Time PCR System (Applied Biosystems, Foster City, CA, USA) using 0.4 μM of each specific primer (Table 2), 10 μl of SYBR Green (Applied Biosystems Foster City, CA, USA), and 1.6 μl of the diluted cDNA product in a final volume of 18 μl. The temperature cycle protocol for amplification was: 1 cycle of initial activation at 95 °C for 10 min and 40 cycles of 15 s at 95 °C, 1 min at 62 °C. To validate the amplification efficiency of primers, standard curves with serial dilutions of a control cDNA were generated, and PCR amplicons were separated electrophoretically on 2% agarose gel for band size confirmation. 18S ribosomal RNA (18 s) and elongation factor 1 alpha (ef1α) were selected to normalise the amount of mRNA for the genes of interest in each sample. Variations in gene expression were calculated by the standard ΔΔCt method (Pfaffl, 2001). Results are presented as mean ± SD (n = 4–6 fish).

2.6. Microarray hybridisation and data analysis

A microarray analysis was performed to detect differentially expressed genes with potential interest for nutritional and diet formulation studies in *S. aurata*. To this end, labelling, hybridisation and scanning of an Agilent custom high-density oligonucleotide microarray (8 × 60 k; ID 079501; Agilent Technologies, Santa Clara, CA, USA), previously described to contain 2 60-mer probes for each of 25,392 assembled unique sequences of *S. aurata* transcriptome (Silva-Marrero et al., 2017), were performed with the Two-Color Microarray-Based Gene Expression Analysis v. 6.5 kit (Agilent Technologies, Santa Clara, CA, USA). Total RNA isolated from the skeletal muscle of four fish was analysed for each condition (starved fish and fish fed diets HLL, MHL and LLH for 23 days). For each sample, 200 ng of total RNA was labelled with Cy3 or Cy5 using Low Input Quick Amp Labeling Kit (Agilent Technologies, Santa Clara, CA, USA), and microarray workflow for linearity, sensitivity and accuracy was monitored using The Two-Color and RNA

Table 2 Primers used to analyse gene expression by qPCR.

Gene	Forward (5' to 3')	Reverse (5' to 3')	GenBank accession nos.
18 s	TTACGCCCATGTGTCTGAG	AGGATTCTGCATGATGGTCACC	AM490061
ef1a	CCGCCTCTGTGTCCTTCG	CAGCAGTGTGGTCCGTTAGC	AF184170
fst	GGAACGACGGGATCATCTATGC	CGACTTGGCCCTTGATGATTTTCC	AY544167
gadd45a	AGCGGGTCTGTTTTTATTTCTTC	AGGAAGTGTGGTGTGTACCC	XM_030401611
igf1	ACTGCTGTGCGTCTCACCTGA	GTGCATTGGGGCCGTAGCCA	AY996779
igfals	TGTGGTGAACGCCAGAGCTTTG	GAGGCCAGAGAATGATGGGTTGTGAG	XM_030407223
mstn	GGATGCAGGAACACACACAC	AGACGACGAAGGACGAGAAA	AF258448.1
mtor	GGAGACTGTTTGGAGTCCGCC	ACCTCATCACCGTGTGGCA	MH594580
myf5	CGACGGCATGGTTGACAGCA	TCCGGCTGTCTTATCGCCA	JN034420
myf6	TCATCCCACAGCTTTAAAGGCA	AGTGAATCTTCGGCGTCTCTC	JN034421
myod2	CACTACAGCGGGATTCAGAC	CCGTTTGTCTTCTCTGGACT	AF478569
myog	TTCCCTGACACGCGCTCCTA	TCTGTTCTGTCAACCCCAAC	EF462191.1
rps6	CAGCAAGATCCGCAAGTCTT	CTTCTGGGTGCGCTGTCTCT	MN172174
tni2	GCCCTGAAGAAAGTACGTATGTCTGC	CTCCCTCTCTTGTACCTCTCTC	XM_030426857

Spike-In Kit, Two-Color. The *RNeasy Mini Kit* (Qiagen, Hilden, Germany) was used to purify labelled cRNA. Microarray hybridisation was performed using 2.5 µg of each labelled sample at 65 °C for 17 h following the *Gene Expression Hybridization Kit* instructions. A double loop hybridisation with dye swap experimental design was followed (Kerr and Churchill, 2001), and included eight hybridisations to maximise discovery of significant changes among assayed conditions (starvation and feeding with diets HLL, MHL and LLH; $n = 4$ per condition). Scanning was performed using an Agilent Microarray Scanner G2565BA, and outlier spots and spot intensity for Cy3 and Cy5 channels were extracted with Agilent Feature Extraction software v. 10.7. Loess and Aquantile normalisation for within-and inter-array normalisation, respectively, was performed with R-Bioconductor package (Gentleman et al., 2004). Data analysis was only considered for unique sequences involved in growth and development with E -value $< 1e-10$ and HSP/hit > 30 .

2.7. Statistics

Data concerning growth performance, nutrient retention, apparent digestibility and qPCR were analysed using SPSS Version 25 (IBM, Armonk, NY, USA). One-way analysis of variance (ANOVA) followed by the Duncan post-hoc test was performed to identify significant differences between treatments. Statistical significance was considered when $P < 0.05$. For microarray data, a linear model analysis using Limma (Smyth, 2004) was conducted to determine differentially expressed genes with adjusted $P < 0.05$. Correlation coefficient values were calculated to assess relationships between growth, nutrient retention, ADC and gene expression variables, considering statistical significance when $P < 0.05$.

3. Results

3.1. Growth performance, nutrient retention and digestibility

The effect of dietary macronutrient composition on growth parameters and nutrient retention was studied in *S. aurata* juveniles fed 37 days with diets HLL (macronutrient composition similar to the diet of wild *S. aurata*), MHL (composition similar to commercial diets) and LLH (composition similar to HLL but with partial substitution of protein by carbohydrates). Fish fed the high protein, low lipid, low carbohydrate diet (HLL) and the medium protein, high lipid, low carbohydrate diet (MHL) presented significantly higher values of final body weight and SGR than fish fed the low protein, low lipid, high carbohydrate diet (LLH; Table 3). The highest FCR value was found in fish fed the LLH diet, while no significant difference was found between diets HLL and MHL. Fish fed the LLH diet also presented the highest LR value. The lowest PER levels were found for fish fed diet HLL, which were significantly different than in fish fed the MHL diet (Table 3). Diet composition did not significantly affect HSI or PR.

No significant differences were found in ADC values for calcium, carbon and dry matter in the posterior intestine of fish fed 37 days with

Table 3
Growth performance and nutrient retention of *S. aurata* fed diets HLL, MHL and LLH for 37 days.

	HLL	MHL	LLH
Initial BW (g)	8.20 ± 0.04	8.52 ± 0.06	8.11 ± 0.21
Final BW (g)	17.69 ± 0.22 ^b	18.36 ± 0.18 ^b	14.76 ± 0.71 ^a
SGR	2.08 ± 0.04 ^b	2.08 ± 0.02 ^b	1.61 ± 0.10 ^a
FCR	1.58 ± 0.01 ^a	1.44 ± 0.04 ^a	1.96 ± 0.16 ^b
HSI	1.22 ± 0.08	1.11 ± 0.05	1.33 ± 0.11
PR (% intake)	17.92 ± 0.72	20.52 ± 1.05	20.34 ± 1.79
LR (% intake)	24.90 ± 4.14 ^a	33.21 ± 2.15 ^{ab}	41.95 ± 4.30 ^b
PER	1.06 ± 0.01 ^a	1.39 ± 0.04 ^b	1.27 ± 0.10 ^{ab}

Data are means ± SEM ($n = 3$ tanks). Different superscript letters indicate significant differences among dietary conditions ($P < 0.05$). BW: body weight.

different diets. However, fish fed LLH revealed a trend to present lower values than fish fed diets HLL and MHL (Table 4). ADC levels for protein were not affected by diet composition, while the highest values for phosphorus, calcium, carbon and dry matter were found in fish fed MHL. No significant correlation was found between ADC values and growth and nutrient retention parameters (Table 5).

3.2. Effect of diet composition and starvation on the expression of MRFs, *mstn* and *fst* in the skeletal muscle

Dietary macronutrient composition and food deprivation significantly affected the expression of MRFs in the white skeletal muscle of *S. aurata*. Starvation for 37 days significantly downregulated the mRNA levels of all MRFs assayed. Concerning fed animals, the supply of HLL and MHL significantly enhanced 1.7–1.9 fold the expression levels of *myod2* compared to fish fed with diet LLH (Fig. 2a). In a significant manner but to a lesser extent than *myod2*, feeding fish with the diet containing the lowest protein/carbohydrate ratio (LLH) decreased *myf5* and *myog* mRNA levels when compared to fish fed with medium protein, high lipid, low carbohydrate (MHL) and high protein, low lipid, low carbohydrate (HLL) diets, respectively (Fig. 2b-c). The only MRF assayed whose mRNA levels did not significantly differ as a result of diet composition was *Myf6* (Fig. 2d). The mRNA levels of *myod2* and *myog* correlated positively with final body weight and SGR, and negatively with FCR (Table 5).

In regard of genes with a major role in regulation of skeletal muscle growth, we also analysed the expression of *mstn* and *fst*. Feeding with LLH significantly upregulated *mstn* 2.1–2.9 fold over the values observed in starved fish and *S. aurata* fed with HLL and MHL (Fig. 3a). A different expressional pattern was observed for *fst*. The expression levels of *fst* were 1.8–2.0-fold significantly higher in fish fed HLL and MHL than in fish fed LLH and submitted to starvation (Fig. 3b). The expression levels of *mstn* and *fst* exhibited significant but opposite correlation with final body weight, SGR, FCR, HSI and LR (Table 5).

3.3. Effect of diet composition and starvation on the expression of *igf1*, *mtor* and *rps6* in the skeletal muscle

The effect of diet composition and starvation on *igf1* mRNA levels in the skeletal muscle of *S. aurata* was also addressed. Starvation for 37 days significantly downregulated 2.9–6.0 fold *igf1* expression depending on the diet supplied. Among fed fish, significant upregulation of *igf1* (1.8–2.0 fold) was found in fish fed diets with improved growth parameters (MHL and HLL) (Fig. 4a).

Previous studies indicated that in addition to posttranslational regulation, the nutritional status regulates Mtor and downstream proteins at the mRNA level in fish (Lavajoo et al., 2020; Qin et al., 2019). We therefore investigated the effects of starvation and feeding diets differing in macronutrient composition on *mtor* and *rps6* expression in the skeletal muscle of *S. aurata*. Among fed fish, the mRNA levels of *mtor* and *rps6* showed a significant dependence on the protein/carbohydrate ratio in the diet. For *mtor*, diet HLL promoted the highest expression values, which were 1.7-fold and 2.4-fold greater than in fish fed diets MHL and LLH, respectively. Likewise, fish fed HLL presented 1.3-fold

Table 4
Apparent digestibility coefficient (ADC) values obtained for *S. aurata* fed HLL, MHL and LLH diets.

	HLL	MHL	LLH
Phosphorus	39.96 ± 1.11	50.97 ± 3.48	44.74 ± 6.27
Calcium	54.71 ± 1.98	59.25 ± 5.34	45.07 ± 6.72
Carbon	70.53 ± 6.78	79.94 ± 3.44	65.08 ± 8.17
Protein	79.24 ± 2.38	78.08 ± 3.45	77.46 ± 0.73
Dry matter	64.76 ± 1.54	67.21 ± 4.30	57.18 ± 5.24

Data are means ± SEM ($n = 3$ tanks).

Table 5
Correlation coefficient values for growth and nutrient retention parameters versus ADC and gene expression values.

	Final BW	SGR	FCR	HSI	PR	LR	PER
Phosphorus	0.151	0.091	-0.202	-0.342	0.520	0.254	0.590
Calcium	0.628	0.639	-0.634	-0.621	-0.091	-0.430	0.103
Carbon	0.490	0.639	-0.512	-0.552	0.119	-0.210	0.278
Protein	0.134	0.000	-0.120	-0.072	-0.190	-0.204	-0.156
Dry matter	0.600	0.548	-0.601	-0.577	-0.134	-0.442	0.048
<i>myod2</i>	0.744**	0.822**	-0.746**	-0.715**	-0.167	-0.548	0.059
<i>myf5</i>	0.494	0.513	-0.508	-0.524	0.027	-0.273	0.183
<i>myog</i>	0.613*	0.616*	-0.578*	-0.442	-0.569	-0.703*	-0.428
<i>myf6</i>	-0.308	-0.140	0.318	0.336	-0.034	0.162	-0.137
<i>mstn</i>	-0.858**	-0.768**	0.857**	0.815**	0.220	0.650*	-0.040
<i>fst</i>	0.785**	0.804**	-0.766**	-0.688**	-0.385	-0.756**	-0.108
<i>igf1</i>	0.767**	0.837**	-0.768**	-0.735**	-0.244	-0.591	-0.017
<i>mtor</i>	0.662**	0.841**	-0.615*	-0.449	-0.725**	-0.857**	-0.544*
<i>rps6</i>	0.612*	0.737**	-0.565*	-0.400	-0.667**	-0.800**	-0.503
<i>tnni2</i>	0.519	0.462	-0.565	-0.676*	0.384	-0.052	0.562
<i>igfals</i>	0.249	0.444	-0.249	-0.249	-0.440	-0.552	-0.440
<i>gadd45a</i>	-0.645*	-0.539*	0.623*	0.528	0.435	0.649*	0.259

* Correlation is significant at the 0.05 level (2-tailed). ** Correlation is significant at the 0.01 level (2-tailed).

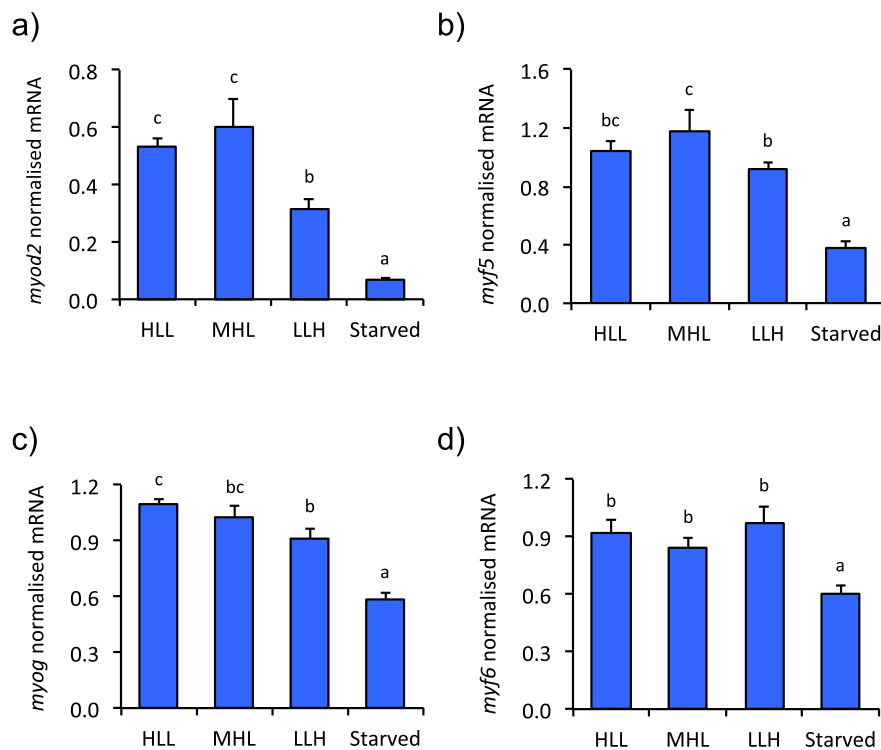


Fig. 2. Effect of diet composition and starvation on the expression of MRFs in the skeletal muscle of *S. aurata*. During 37 days, *S. aurata* juveniles were starved or fed with HLL, MHL and LLH diets. RT-qPCR analysis of *myod2* (a), *myf5* (b), *myog* (c) and *myf6* (d) expression in the skeletal muscle is shown. The mRNA levels for each gene were normalised with the geometrical mean of *S. aurata* 18 s and *ef1a*, which were used as housekeeping genes. Results are presented as mean \pm SEM ($n = 4-6$ fish). Different letters above deviation bars indicate significant differences ($P < 0.05$) among conditions.

and 1.6-fold higher *rps6* mRNA levels than fish supplied with MHL and LLH, respectively. The expression levels of *mtor* and *rps6* in starved fish were similar to those observed in the skeletal muscle of fish fed diet LLH (Fig. 4b-c). The mRNA levels of *igf1*, *mtor* and *rps6* positively correlated with final body weight and SGR, while negatively correlated with FCR (Table 5).

3.4. Microarray analysis

From a total of 247 genes involved in growth and development, the expression of 21 genes (included in the heat map hierarchical cluster shown in Fig. 5a) exhibited differential expression with an adjusted P value < 0.05 and at least 2-fold difference in the normalised intensity ratio (Cy5/Cy3 or Cy3/Cy5) between 2 or more dietary conditions (starvation and feeding for 23 days with diets HLL, MHL and LLH) in the

skeletal muscle of *S. aurata*. Starvation deeply affected the expression of most filtered genes. From the total of 21 genes selected, 3-6 genes (depending on the diet supplied) were significantly upregulated more than 2-fold in the skeletal muscle of starved fish, while food restriction downregulated 6-11 genes. Feeding upregulated genes associated with muscle contraction (*tnni2*, *tnnc2*, *stac3*, *ttn*, *actc1*, *calm*, *mpsf* and *cav3*), muscle development (*frg1*, *fgfr1* and *tagln*), as well as growth regulation and the growth hormone-Igf axis (*mstn*, *ghr1* and *igfals*), while downregulated genes were mostly involved in growth arrest and regulation (*gas6*, *ing3*, *gadd45a* and *naca*). Among upregulated genes by feeding with fold change > 2 , the greater values were found for *tnni2* (16.1, 39.1 and 29.0 fold change for fish fed HLL, MHL and LLH, respectively), followed by *stac3* (3.2, 3.5 and 2.8 fold change for fish supplied with HLL, MHL and LLH, respectively). The expression of *igfals* also increased in the skeletal muscle of fish fed diets HLL and MHL, but showed more

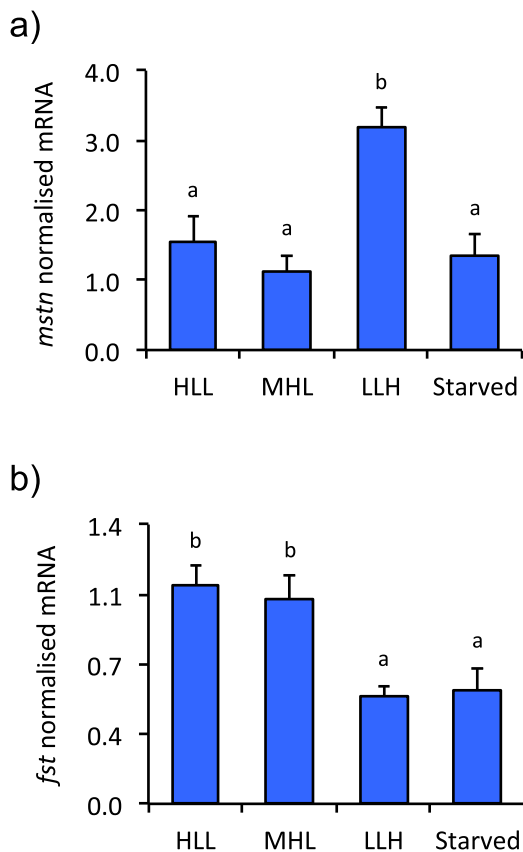


Fig. 3. Effect of diet composition and starvation on the expression of members of the Tgfb superfamily in the skeletal muscle of *S. aurata*. During 37 days, *S. aurata* juveniles were starved or fed with HLL, MHL and LLH diets. RT-qPCR analysis of *mstn* (a) and *fst* (b) expression in the skeletal muscle is shown. The mRNA levels for each gene were normalised with the geometrical mean of *S. aurata* *18 s* and *ef1a*, which were used as housekeeping genes. Results are presented as mean \pm SEM ($n = 4-6$ fish). Different letters above deviation bars indicate significant differences ($P < 0.05$) among conditions.

dependence on diet composition (5.3, 3.1 and 1.0 fold change for fish supplied with diet HLL, MHL and LLH, respectively). Similar expression patterns were found for *fgfr1* and *igfals*. In regard of downregulated genes by feeding, the greater fold changes were observed for *ing3* (4.6–6.7 fold change, depending on the diet supplied) and *gas6* (4.0–4.2 fold change, depending on the diet supplied), while *gadd45a* exhibited a higher dependence on diet composition (2.6, 2.3 and 1.6 fold change for fish supplied with HLL, MHL and LLH, respectively).

With the aim to identify gene markers regulated by dietary macronutrient composition, the mRNA levels of *gadd45a*, *igfals* and *tnni2* were assayed by RT-qPCR in the skeletal muscle of fish starved or fed diets HLL, MHL and LLH for 37 days (Fig. 5b). Starvation significantly upregulated *gadd45a* over the expression values observed in fish fed diets HLL, MHL and LLH (2.4, 1.7 and 1.4 fold, respectively). The mRNA levels of *gadd45a* negatively correlated with final body weight and SGR, while positively correlated with FCR and LR (Table 5). Similarly as *igf1*, the lowest *igfals* mRNA levels were promoted by starvation, while feeding with HLL significantly upregulated *igfals* 1.9 fold. In regard of *tnni2*, the lowest mRNA abundance was found in food-deprived animals. Among fed fish the highest *tnni2* expression was observed in the skeletal muscle of *S. aurata* fed diet MHL (2.0-, 4.2- and 45.3-fold increased levels than in fish fed diets HLL, LLH and under starvation, respectively). Significant negative correlation was found between *tnni2* expression and HSI (Table 5).

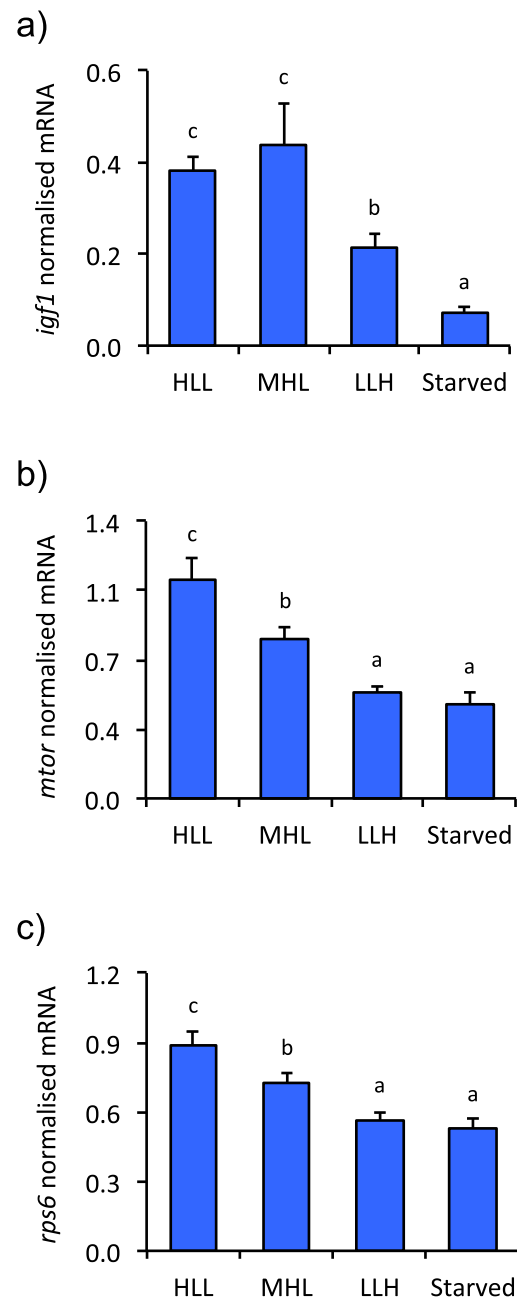


Fig. 4. Effect of diet composition and starvation on the expression of *igf1*, *mtor* and *rps6* in the skeletal muscle of *S. aurata*. During 37 days, *S. aurata* juveniles were starved or fed with HLL, MHL and LLH diets. RT-qPCR analysis of *igf1* (a), *mtor* (b) and *rps6* (c) expression in the skeletal muscle is shown. The mRNA levels for each gene were normalised with the geometrical mean of *S. aurata* *18 s* and *ef1a*, which were used as housekeeping genes. Results are presented as mean \pm SEM ($n = 4-6$ fish). Different letters above deviation bars indicate significant differences ($P < 0.05$) among conditions.

4. Discussion

Substitution of dietary protein by cheaper and sustainable nutrients is a challenging question in fish nutrition (Panserat et al., 2019). The results of this study showed that partial substitution of fish meal by carbohydrates had a strong negative impact on growth performance of *S. aurata* and nutrient retention parameters such as body weight, SGR and FCR. On the contrary, the supply of medium protein, high lipid, low carbohydrate diets (MHL) improved growth performance, although at

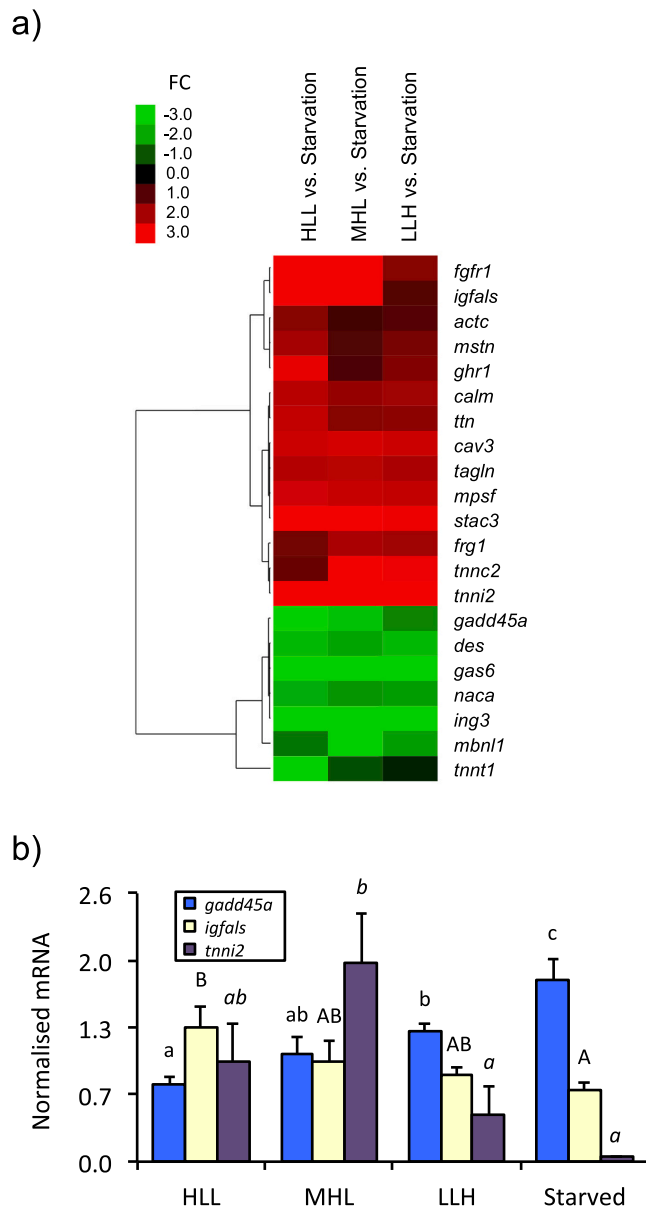


Fig. 5. Effect of diet composition and starvation on the expressional pattern of genes involved in skeletal muscle function, differentiation and growth, and validation of the expression of *gadd45a*, *igfals* and *tnni2*. (a) Heat map image of differentially transcribed genes involved in skeletal muscle function, differentiation and growth regulation. Three groups of fish were fed 23 days at a daily ration of 25 g/kg body weight with diets HLL, MHL and LLH, respectively. A fourth group of animals was submitted to starvation for the same period. Hierarchical clustering of differentially expressed genes in the skeletal muscle is represented from microarray data obtained from *S. aurata* fed with diets HLL, MHL and LLH versus starved fish, with an adjusted *P* value <0.05 and a difference of at least 2-fold in the normalised intensity ratio (Cy5/Cy3 or Cy3/Cy5) between two or more conditions. Results are presented as fold change (FC) mean value (*n* = 4 fish). Green color denotes downregulated genes and red color upregulated genes in fed animals. (b) RT-qPCR analysis of *gadd45a*, *igfals* and *tnni2* mRNA levels in the skeletal muscle of *S. aurata* following 37 days of starvation or feeding with diets HLL, MHL and LLH at a daily ration of 25 g/kg body weight. The mRNA levels for each gene were normalised with the geometrical mean of *S. aurata* 18 s and *ef1α*, which were used as housekeeping genes. Results are presented as mean ± SEM (*n* = 4–5 fish). Different letters above deviation bars indicate significant differences (*P* < 0.05) among conditions for a given gene. (For interpretation of the references to color in this figure legend, the reader is referred to the web version of this article.)

levels not far from those observed in fish fed high protein, low lipid, low carbohydrate diets (HLL). Increased PER values in fish fed MHL are in agreement with the increased weight gain exhibited by this group of fish. Consistent with our findings, diets with 54% of protein and 18% of carbohydrate, and therefore with macronutrient composition similar to MHL, are considered optimal to improve growth and nutritional parameters such as body weight and SGR in *S. aurata* (Fernández et al., 2007). A similar behaviour was observed in other fish species such as *Pagrus pagrus* (Schuchardt et al., 2008) and *O. mykiss* (Kamalam et al., 2012; Alami-Durante et al., 2019). A trend to present lower values for Ca, C and dry matter was observed in the group of fish fed LLH. Indeed, ADC levels for Ca, C and dry matter in turn showed a trend to correlate positively with final weight and negatively with FCR. Low tolerance of carnivorous fish to glucose (Polakof et al., 2012; Rashidpour et al., 2019), may determine the poor growth performance observed in fish fed the LLH diet.

Our observations also agree with the fact that long-term starvation and the supply of low protein, high carbohydrate diets in *S. aurata* affect similarly the expression of appetite-regulating peptides, leading to opposite effects than high protein, low carbohydrate diets on the expression of orexigenic and anorexigenic peptides (Babaei et al., 2017). Indeed, transcriptomic analysis revealed that both food deprivation and the supply of low protein, high carbohydrate diets also promoted similar effects on the expression levels of genes involved in mitochondrial oxidative phosphorylation in the skeletal muscle of *S. aurata* (Silva-Marrero et al., 2017).

In teleost fish, myoblast proliferation and hyperplasia occur mainly during the swim-up fry stage and through juvenile growth with a large increase in the number of white muscle fibres (Rowlerson and Veggetti, 2001). Herein, MRFs were measured to analyse myoblast proliferation and differentiation in *S. aurata* juveniles. Starvation downregulated *myod2*, *myf5*, *myog* and *myf6* in the skeletal muscle of *S. aurata*, which confirms previous observations in this species (García De La Serrana et al., 2014; Lavajoo et al., 2020). The strong reduction observed in the expression of *myod2* and *myf5* suggests that long-term starvation may promote muscular atrophy. Among fish fed different diets, the mRNA levels of *myod2* and to a lesser extent *myog* were more sensitive to the dietary protein to carbohydrate ratio than *myf5* and *myf6*. Therefore, *myod2* and *myog* mRNA levels significantly increased in fish that exhibited better growth performance (fish fed high or medium protein, low carbohydrate diets, MHL and HLL). However, low *myod2* mRNA levels in the skeletal muscle of fish fed LLH indicate that *myod2* can be used as sensitive marker of growth performance in *S. aurata* juveniles. In this regard, Igf-dependent expression of MRFs seems to play an important role in muscle differentiation and proliferation (Vélez et al., 2016). Indeed, in the present study, the expression of *igf1* positively correlated with growth rate and was highly dependent on nutritional status and diet composition. Consistent with our findings and the key role exerted in muscle growth, *igf1* was shown to stimulate growth and proliferation of *S. aurata* cultured myocytes (Vélez et al., 2014), while starvation markedly decreases *igf1* expression and Igf1 circulating levels in this species (Lavajoo et al., 2020; Metón et al., 2000; Pérez-Sánchez et al., 1995).

Upregulation of *mstn* expression inhibits cell growth and differentiation in the skeletal muscle of rainbow trout (Seilliez et al., 2012). Furthermore, high glucose supplementation inhibits protein synthesis in primary cultured muscle cells of olive flounder (*Paralichthys olivaceus*) by a mechanism involving downregulation of MRFs such as *myod* and *myog*, inhibition of Mtor signaling pathway and upregulation of *mstn1* (Liu et al., 2021). Similarly, *mstn* mRNA levels among fed fish were herein markedly higher in the skeletal muscle of *S. aurata* fed LLH, which was the diet that promoted the lowest growth performance. On the contrary, the lowest *mstn* expression was found in fish fed diet MHL, which in turn promoted better growth parameters. Therefore, downregulation of *mstn* in fish with enhanced growth performance may prevent *mstn*-dependent negative regulation of growth and induction of

muscle tissue hypertrophy. Consistent with this hypothesis, downregulation of *mstn* strongly enhances hyperplasia, hypertrophy and body size in zebrafish (*Danio rerio*) (Fuentes et al., 2013; Rossi and Messina, 2014). The *mstn* mRNA levels in *S. aurata* submitted to long-term starvation were even significantly lower than those presented by fish fed LLH. In this regard, *mstn* expression in food-deprived fish seems to depend on the species and the starvation period. For instance, 30 days of starvation upregulates *mstn* in the muscle of *S. aurata* (García De La Serrana et al., 2014), while 28 days and 10 weeks of starvation did not significantly affect *mstn* expression in the muscle of adult tilapia and rainbow trout, respectively (Chauvigné et al., 2003; Rodgers et al., 2003). Specific adaptations and dietary conditions previous to starvation may explain variations in *mstn* expression. Fst is a potent antagonist of Mstn (Amthor et al., 2004). Overexpression of *fst* increases muscle mass in rainbow trout through enhanced muscle hypertrophy and hyperplasia (Medeiros et al., 2009). Our findings support that *fst* may have a major role in regulating muscle growth in *S. aurata*. Accordingly, *fst* expression showed strong dependence on dietary macronutrient composition and was significantly downregulated by supplying low protein, high carbohydrate diets (LLH).

In agreement with previous results in *S. aurata* (Lavajoo et al., 2020), muscle mRNA levels of *mtor* and *rps6* decreased upon starvation. The results of the present study indicate that the Mtor signaling pathway may be activated in fish fed high or medium protein, low carbohydrate diets. Our findings are supported by the fact that Mtor activation triggers biological responses such as cell proliferation and contribution to muscle hypertrophy (Glass, 2003a, 2003b). In agreement with this hypothesis, fish fed MHL and HLL exhibited better growth performance. Given that Akt phosphorylation is induced by growth factors, such as Igf1 (Glass, 2005; Vélez et al., 2016), upregulation of *igf1* in fish fed MHL and HLL would facilitate Pi3k phosphorylation and induction of the Igf1/Pi3k/Akt signaling cascade, whose components are considered key mediators in muscle mass increase (Stitt et al., 2004). Consistently, the combined action of Igf1 and amino acids stimulated Mtor and Akt activity in *S. aurata* myocytes (Vélez et al., 2014), and low protein diets diminished growth performance and Mtor signaling pathway in yellow catfish (*Pelteobagrus fulvidraco*) by downregulating the mRNA levels of key genes such as *igf1*, *mtor* and *akt* (Qin et al., 2019).

A microarray analysis performed on RNA isolated from skeletal muscle of *S. aurata* allowed us to address the effect of nutritional status and diet composition on muscle expression pattern and identify novel gene markers of interest for nutritional studies and diet formulation. In general, feeding stimulated the expression of genes involved in growth, development and muscle function, while starvation upregulated genes implicated in growth regulation and arrest. Some of the differentially expressed genes were also dependent on dietary macronutrient composition. Remarkably, dietary carbohydrates, protein and lipids specifically upregulated the mRNA levels of *gadd45a*, *igfals* and *tnni2*, respectively, in the skeletal muscle of *S. aurata*, suggesting that their expression level can be used as marker for monitoring the effect of changes in dietary macronutrient composition and feeding regime in cultured fish. Indeed, the expression of *gadd45a* negatively correlated with final body weight and SGR, which suggests that *gadd45a* can be also used as sensitive marker of growth performance.

Gadd45a is a ubiquitously expressed protein belonging to the growth arrest and DNA damage 45 stress sensor gene family and is involved in cell response to DNA-damaging agents and growth cessation signals, such as starvation, by mediating cell cycle arrest and inhibition of cell entry into S phase (Salvador et al., 2013). Downregulation of *gadd45a* in the skeletal muscle of fed fish, particularly those supplied with high or medium protein diets (HLL and MHL) agrees with reports indicating increased *gadd45a* mRNA levels in human and rat muscle under starvation (Bongers et al., 2013; Ibrahim et al., 2020; Wijngaarden et al., 2014). Regulation of *gadd45a* expression by dietary macronutrients in fish remains largely unknown. However, a number of evidences point to *gadd45a* as sensitive stress sensor gene also in fish. Exposition to

cyanobacterial extracts, cadmium and DNA damage by acute exposure to hydrogen peroxide upregulate *gadd45* in zebrafish (Chen et al., 2014; Falfushynska et al., 2021; Reinardy et al., 2013). Moreover, the expression of *gadd45* increases in response to low temperature in rainbow trout, kelp grouper (*Epinephelus moara*) and large yellow croaker (*Larimichthys crocea*) (Borchel et al., 2017; Chen et al., 2020; Qian et al., 2020). Furthermore, the pattern of expression of *gadd45a* in tilapia (*Oreochromis* spp.) after infection with *Streptococcus agalactiae* and in grass carp (*Ctenopharyngodon idella*) following challenge with *Aeromonas hydrophila* suggests involvement of *gadd45a* in fish immunity against bacterial infection (Fang et al., 2018; Shen et al., 2016). In the present study, restricted-protein feeding (LLH diet) upregulated *gadd45a* to values not far from those observed in starved fish. Since *gadd45a* is critical mediator of muscle atrophy (Bongers et al., 2013; Ebert et al., 2012), the results of the present study suggest that protein restriction may shrink muscle growth in *S. aurata*.

Igfals encodes the insulin-like growth factor-binding protein complex acid labile subunit, which stabilises blood levels of Igf1, Igf2 and Igfbp proteins by binding binary complexes formed by Igf1 or Igf2 with Igfbp-3 or Igfbp-5 (Domené and Domené, 2020; Hwa et al., 2021). In the present study, changes in nutritional status and diet composition caused similar effects on *igfals* and *igf1* mRNA levels. Starvation downregulated *igfals*, while among fed fish the highest *igfals* expression was observed in *S. aurata* fed HLL. Our findings are consistent with reports in mammals showing that food deprivation reduces *igfals* expression and serum levels (Frystyk et al., 1999; Kong et al., 2002), while the supply of high protein diets and overfeeding increases Igfals circulating level (Khan et al., 2014; Rubio-Aliaga et al., 2011). Given that Igfals is well-established for its role in binding to Igf-Igfbp complexes and prolonge their half-life in serum (Boisclair et al., 2001), downregulation of *igfals* in fish fed low protein, high carbohydrate diets (LLH) would promote insulin insensitivity and growth impairment. Hence, Igfals deficiency decreases circulating levels of Igf and Igfbp proteins, leading to insulin insensitivity, growth impairment and puberty delay in humans (Domené and Domené, 2020; Hwa et al., 2021).

Tnni2 encodes the fast skeletal isoform of troponin I, which acts as the inhibitory subunit of the troponin complex during muscle contraction (Fu et al., 2009; Sheng and Jin, 2016). Knowledge of the effect of nutritional status and diet composition on *tnni2* expression in fish is scarce. However, our findings are consistent with previous observations that indicate downregulation of troponin in skeletal muscle of mandarin fish (*Siniperca chuatsi*) submitted to starvation (Liu et al., 2020). Accordingly, Lu et al. reported downregulation of troponin I in muscle of slow-growing grass carp (*C. idella*) (Lu et al., 2020). Conceivably, given that *S. aurata* is a carnivorous fish, starvation would promote the use of muscle protein as the major source of energy, while impairing muscle synthesis of proteins and contraction. However, the supply of dietary protein would avoid muscle breakdown, cessation of muscle contraction and facilitate muscle growth. Moreover, the fact that the highest *tnni2* expression was found in fish fed MHL suggests that dietary lipids could contribute to *tnni2* upregulation. In this regard, maternal dietary linoleic acid supplementation promotes muscle fibre transformation to type I fibre in a process that involves troponin I upregulation in the muscle of suckling piglets (Lu et al., 2017). Further studies are required to explore the hypothesis that the fatty acid profile of the diet can affect *tnni2* expression in fish.

5. Conclusions

The results of the present study show that the expression of MRFs and key genes in muscle growth and differentiation was markedly affected by nutritional status and dietary macronutrient composition in the skeletal muscle of *S. aurata*. In addition to the skeletal muscle mRNA levels of *myod2*, *fst*, *igf1*, *mtor* and *rps6*, our findings let us to report for the first time *gadd45a* and *igfals* as useful markers to study the effect of changes in feeding regime and diet composition on growth performance in fish.

Author contributions

Conception and design: Isidoro Metón, Isabel V. Baanante and Felipe Fernández. Material preparation, data collection and analysis were performed by Alberto Sáez-Arteaga, Yuanbing Wu, Jonás I. Silva-Marrero, Ania Rashidpour and María Pilar Almajano. Writing and original draft preparation: Isidoro Metón and Alberto Sáez-Arteaga. All authors read and approved the final manuscript.

CRedit authorship contribution statement

Alberto Sáez-Arteaga: Investigation, Formal analysis, Writing – original draft, Writing – review & editing. **Yuanbing Wu:** Investigation, Formal analysis, Writing – review & editing. **Jonás I. Silva-Marrero:** Investigation, Formal analysis, Writing – review & editing. **Ania Rashidpour:** Investigation, Formal analysis, Writing – review & editing. **María Pilar Almajano:** Investigation, Formal analysis, Writing – review & editing. **Felipe Fernández:** Conceptualization, Methodology, Writing – review & editing. **Isabel V. Baanante:** Conceptualization, Methodology, Writing – review & editing. **Isidoro Metón:** Conceptualization, Methodology, Supervision, Writing – original draft, Writing – review & editing, Funding acquisition.

Declaration of Competing Interest

The authors declare that they have no known competing financial interests or personal relationships that could have appeared to influence the work reported in this paper.

Acknowledgements

This work was supported by the Ministerio de Economía, Industria y Competitividad, Spain (grant no. AGL2016-78124-R; cofunded by the European Regional Development Fund, European Commission) and the Agencia Nacional de Investigación y Desarrollo, Chile (Becas Chile/2011–72111506). The authors thank Piscicultura Marina Mediterranea (Burriana, Castellón, Spain) for providing *S. aurata* juveniles.

References

- Alami-Durante, H., Cluzeaud, M., Bazin, D., Schrama, J., Saravanan, S., Geurden, I., 2019. Muscle growth mechanisms in response to isoenergetic changes in dietary non-protein energy source at low and high protein levels in juvenile rainbow trout. *Comp. Biochem. Physiol. A. Mol. Integr. Physiol.* 230, 91–99.
- Amthor, H., Nicholas, G., McKinnell, I., Kemp, C.F., Sharma, M., Kambadur, R., Patel, K., 2004. Follistatin complex Myostatin and antagonises Myostatin-mediated inhibition of myogenesis. *Dev. Biol.* 270, 19–30.
- Babaei, S., Sáez, A., Caballero-Solares, A., Fernández, F., Baanante, I.V., Metón, I., 2017. Effect of dietary macronutrients on the expression of cholecytokinin, leptin, ghrelin and neuropeptide Y in gilthead sea bream (*Sparus aurata*). *Gen. Comp. Endocrinol.* 240, 121–128.
- Boisclair, Y., Rhoads, R., Ueki, I., Wang, J., Ooi, G., 2001. The acid-labile subunit (ALS) of the 150 kDa IGF-binding protein complex: an important but forgotten component of the circulating IGF system. *J. Endocrinol.* 170, 63–70.
- Bongers, K., Fox, D., Ebert, S., Kunkel, S., Dyle, M., Bullard, S., Adams, C., 2013. Skeletal muscle denervation causes skeletal muscle atrophy through a pathway that involves both Gadd45a and HDAC4. *Am. J. Physiol. Endocrinol. Metab.* 305, E907–E915.
- Borchel, A., Verleih, M., Rebl, A., Goldammer, T., 2017. Identification of genes involved in cold-shock response in rainbow trout (*Oncorhynchus mykiss*). *J. Genet.* 96, 701–706.
- Bradclair, A.E., Llewellyn, M.J., 1982. *Animal Energetics*. Blackie and Son, Glasgow.
- Braun, T., Gautel, M., 2011. Transcriptional mechanisms regulating skeletal muscle differentiation, growth and homeostasis. *Nat. Rev. Mol. Cell Biol.* 12, 349–361.
- Busacker, G.P., Adelman, I.R., Goolish, E.M., 1990. Growth. In: Schreck, C.B., Moyle, P.B. (Eds.), *Methods for Fish Biology*. American Fisheries Society, Bethesda, pp. 363–387.
- Castillo, J., Codina, M., Martínez, M.L., Navarro, I., Gutiérrez, J., 2004. Metabolic and mitogenic effects of IGF-I and insulin on muscle cells of rainbow trout. *Am. J. Physiol. Regul. Integr. Comp. Physiol.* 286, R935–R941.
- Chauvigné, F., Gabillard, J.C., Weil, C., Rescan, P.Y., 2003. Effect of refeeding on IGF1, IGFII, IGF receptors, FGF2, FGF6, and myostatin mRNA expression in rainbow trout myotomal muscle. *Gen. Comp. Endocrinol.* 132, 209–215.
- Chen, Y.Y., Zhu, J.Y., Chan, K.M., 2014. Effects of cadmium on cell proliferation, apoptosis, and proto-oncogene expression in zebrafish liver cells. *Aquat. Toxicol.* 157, 196–206.
- Chen, Z., Tian, Y., Ma, W., Zhai, J., 2020. Gene expression changes in response to low temperatures in embryos of the kelp grouper, *Epinephelus moara*. *Cryobiology* 97, 159–167.
- Christoffolete, M.A., Silva, W.J., Ramos, G.V., Bento, M.R., Costa, M.O., Ribeiro, M.O., Moriscot, A.S., 2015. Muscle IGF-1-induced skeletal muscle hypertrophy evokes higher insulin sensitivity and carbohydrate use as preferential energy substrate. *Biomed. Res. Int.* 2015, 282984.
- De Silva, S., Anderson, T.A., 1995. *Fish Nutrition in Aquaculture*. Chapman and Hall, London.
- Domené, S., Domené, H., 2020. The role of acid-labile subunit (ALS) in the modulation of GH-IGF-I action. *Mol. Cell. Endocrinol.* 518, 111006.
- Ebert, S., Dyle, M., Kunkel, S., Bullard, S., Bongers, K., Fox, D., Adams, C., 2012. Stress-induced skeletal muscle Gadd45a expression reprograms myonuclei and causes muscle atrophy. *J. Biol. Chem.* 287, 27290–27301.
- Falfushynska, H., Horyn, O., Osypenko, I., Rzymiski, P., Wejnerowski, L., Dziuba, M., Sokolova, I., 2021. Multibiomarker-based assessment of toxicity of central European strains of filamentous cyanobacteria *Aphanizomenon gracile* and *Raphidiopsis raciborskii* to zebrafish *Danio rerio*. *Water Res.* 194, 116923.
- Fang, Y., Xu, X., Shen, Y., Li, J., 2018. Molecular cloning and functional analysis of growth arrest and DNA damage-inducible 45 aa and ab (Gadd45aa and Gadd45 ab) in *Ctenopharyngodon idella*. *Fish Shellfish Immunol.* 77, 187–193.
- Fernández, F., Miquel, A.G., Córdoba, M., Varas, M., Metón, I., Caseras, A., Baanante, I. V., 2007. Effects of diets with distinct protein-to-carbohydrate ratios on nutrient digestibility, growth performance, body composition and liver intermediary enzyme activities in gilthead sea bream (*Sparus aurata*, L.) fingerlings. *J. Exp. Mar. Biol. Ecol.* 343, 1–10.
- Frystyk, J., Delhanty, P., Skjaerbaek, C., Baxter, R., 1999. Changes in the circulating IGF system during short-term fasting and refeeding in rats. *Am. J. Phys.* 277, E245–E252.
- Fu, C., Lee, H., Tsai, H., 2009. The molecular structures and expression patterns of zebrafish troponin I genes. *Gene Expr. Patterns* 9, 348–356.
- Fuentes, E.N., Pino, K., Navarro, C., Delgado, I., Valdés, J.A., Molina, A., 2013. Transient inactivation of myostatin induces muscle hypertrophy and overcompensatory growth in zebrafish via inactivation of the SMAD signaling pathway. *J. Biotechnol.* 168, 295–302.
- García De La Serrana, D., Codina, M., Capilla, E., Jiménez-Amilburu, V., Navarro, I., Du, S.-J., Gutiérrez, J., 2014. Characterisation and expression of myogenesis regulatory factors during in vitro myoblast development and in vivo fasting in the gilthead sea bream (*Sparus aurata*). *Comp. Biochem. Physiol. A. Mol. Integr. Physiol.* 167, 90–99.
- Gentleman, R.C., Carey, V.J., Bates, D.M., Bolstad, B., Dettling, M., Dudoit, S., Zhang, J., 2004. Bioconductor: open software development for computational biology and bioinformatics. *Genome Biol.* 5, R80.
- Glass, D., 2003a. Signalling pathways that mediate skeletal muscle hypertrophy and atrophy. *Nat. Cell Biol.* 5, 87–90.
- Glass, D.J., 2003b. Molecular mechanisms modulating muscle mass. *Trends Mol. Med.* 9, 344–350.
- Glass, D.J., 2005. Skeletal muscle hypertrophy and atrophy signaling pathways. *Int. J. Biochem. Cell Biol.* 37, 1974–1984.
- Holterman, C.E., Rudnicki, M.A., 2005. Molecular regulation of satellite cell function. *Semin. Cell Dev. Biol.* 16, 575–584.
- Hwa, V., Fujimoto, M., Zhu, G., Gao, W., Foley, C., Kumbaji, M., Rosenfeld, R., 2021. Genetic causes of growth hormone insensitivity beyond GHR. *Rev. Endocr. Metab. Disord.* 22, 43–58.
- Ibrahim, M., Wasselín, T., Challet, E., Van Dorselaer, A., Le Maho, Y., Raclot, T., Bertile, F., 2020. Transcriptional changes involved in atrophying muscles during prolonged fasting in rats. *Int. J. Mol. Sci.* 21, 1–28.
- Johnston, I.A., 2006. Environment and plasticity of myogenesis in teleost fish. *J. Exp. Biol.* 209, 2249–2264.
- Kamalam, B.S., Medale, F., Kaushik, S., Polakof, S., Skiba-Cassy, S., Panserat, S., 2012. Regulation of metabolism by dietary carbohydrates in two lines of rainbow trout divergently selected for muscle fat content. *J. Exp. Biol.* 215, 2567–2578.
- Kerr, M.K., Churchill, G.A., 2001. Experimental design for gene expression microarrays. *Biostatistics* 2, 183–201.
- Khan, M.J., Jacometo, C.B., Graugnard, D.E., Corrêa, M.N., Schmitt, E., Cardoso, F., Loor, J.J., 2014. Overfeeding dairy cattle during late-pregnancy alters hepatic PPAR α -regulated pathways including hepatokines: impact on metabolism and peripheral insulin sensitivity. *Gene Regul. Syst. Bio.* 8, 97.
- Kong, S., Baxter, R., Delhanty, P., 2002. Age-dependent regulation of the acid-labile subunit in response to fasting-refeeding in rats. *Endocrinology* 143, 4505–4512.
- Latimer, M.N., Reid, R.M., Biga, P.R., Cleveland, B.M., 2019. Glucose regulates protein turnover and growth-related mechanisms in rainbow trout myogenic precursor cells. *Comp. Biochem. Physiol. Part A Mol. Integr. Physiol.* 232, 91–97.
- Lavajoo, F., Perelló-Amorós, M., Vélez, E., Sánchez-Moya, A., Balbuena-Pecino, S., Riera-Heredia, N., Gutiérrez, J., 2020. Regulatory mechanisms involved in muscle and bone remodeling during refeeding in gilthead sea bream. *Sci. Rep.* 10, 184.
- Lee, S.J., McPherron, A.C., 2001. Regulation of myostatin activity and muscle growth. *Proc. Natl. Acad. Sci. U. S. A.* 98, 9306–9311.
- Liu, X., Zeng, S., Liu, S., Wang, G., Lai, H., Zhao, X., Li, G., 2020. Identifying the related genes of muscle growth and exploring the functions by compensatory growth in mandarin fish (*Siniperca chuatsi*). *Front. Physiol.* 11, 553563.
- Liu, J., Pan, M., Huang, D., Wu, J., Liu, Y., Guo, Y., Mai, K., 2021. High glucose induces apoptosis, glycogen accumulation and suppresses protein synthesis in muscle cells of olive flounder *Paralichthys olivaceus*. *Br. J. Nutr.* <https://doi.org/10.1017/S0007114521002634>.

- Lu, Z., Ren, Y., Zhou, X., Yu, X., Huang, J., Yu, D., Wang, Y., 2017. Maternal dietary linoleic acid supplementation promotes muscle fibre type transformation in suckling piglets. *J. Anim. Physiol. Anim. Nutr. (Berl.)* 101, 1130–1136.
- Lu, X., Chen, H., Qian, X., Gui, J., 2020. Transcriptome analysis of grass carp (*Ctenopharyngodon idella*) between fast- and slow-growing fish. *Comp. Biochem. Physiol. Part D. Genomics Proteomics* 35, 100688.
- Lucas, A., 1996. Bioenergetics of organisms: Methods. In: Priede, I.G. (Ed.), *Bioenergetics of Aquatic Animals*. Taylor & Francis, London, pp. 65–81.
- McPherron, A., Lawler, A., Lee, S., 1997. Regulation of skeletal muscle mass in mice by a new TGF-beta superfamily member. *Nature* 387, 83–90.
- Medeiros, E.F., Phelps, M.P., Fuentes, F.D., Bradley, T.M., 2009. Overexpression of follistatin in trout stimulates increased muscling. *Am. J. Physiol. Regul. Integr. Comp. Physiol.* 297, R235–R242.
- Metón, I., Mediavilla, D., Caseras, A., Cantó, E., Fernández, F., Baanante, I.V., 1999. Effect of diet composition and ration size on key enzyme activities of glycolysis-gluconeogenesis, the pentose phosphate pathway and amino acid metabolism in liver of gilthead sea bream (*Sparus aurata*). *Br. J. Nutr.* 82, 223–232.
- Metón, I., Caseras, A., Cantó, E., Fernández, F., Baanante, I.V., 2000. Liver insulin-like growth factor-I mRNA is not affected by diet composition or ration size but shows diurnal variations in regularly-fed gilthead sea bream (*Sparus aurata*). *J. Nutr.* 130, 757–760.
- Montserrat, N., Capilla, E., Navarro, I., Gutiérrez, J., 2012. Metabolic effects of insulin and IGFs on gilthead sea bream (*Sparus aurata*) muscle cells. *Front. Endocrinol. (Lausanne)* 3, 55.
- Olson, E., Klein, W., 1994. bHLH factors in muscle development: dead lines and commitments, what to leave in and what to leave out. *Genes Dev.* 8, 1–8.
- Panserat, S., Marandel, L., Seiliez, I., Skiba-Cassy, S., 2019. New insights on intermediary metabolism for a better understanding of nutrition in teleosts. *Annu. Rev. Anim. Biosci.* 7, 195–220.
- Pérez-Sánchez, J., Martí-Palanca, H., Kaushik, S.J., 1995. Ration size and protein intake affect circulating growth hormone concentration, hepatic growth hormone binding and plasma insulin-like growth factor-I immunoreactivity in a marine teleost, the gilthead sea bream (*Sparus aurata*). *J. Nutr.* 125, 546–552.
- Pfaffl, M.W., 2001. A new mathematical model for relative quantification in real-time RT-PCR. *Nucleic Acids Res.* 29, e45.
- Polakof, S., Panserat, S., Soengas, J.L., Moon, T.W., 2012. Glucose metabolism in fish: a review. *J. Comp. Physiol. B.* 182, 1015–1045.
- Qian, B., Qi, X., Bai, Y., Wu, Y., 2020. The p53 signaling pathway of the large yellow croaker (*Larimichthys crocea*) responds to acute cold stress: evidence via spatiotemporal expression analysis of p53, p21, MDM2, IGF-1, Gadd45, Fas, and Akt. *PeerJ* 8, e10532.
- Qin, Q., Cao, X., Dai, Y., Wang, L., Zhang, D., Jiang, G., Liu, W., 2019. Effects of dietary protein level on growth performance, digestive enzyme activity, and gene expressions of the TOR signaling pathway in fingerling *Pelteobagrus fulvidraco*. *Fish Physiol. Biochem.* 45, 1747–1757.
- Rashidpour, A., Silva-Marrero, J.I., Seguí, L., Baanante, I.V., Metón, I., 2019. Metformin counteracts glucose-dependent lipogenesis and impairs transamination in the liver of gilthead sea bream (*Sparus aurata*). *Am. J. Physiol. Integr. Comp. Physiol.* 316, R265–R273.
- Reinardy, H., Dharamshi, J., Jha, A., Henry, T., 2013. Changes in expression profiles of genes associated with DNA repair following induction of DNA damage in larval zebrafish *Danio rerio*. *Mutagenesis* 28, 601–608.
- Rescan, P.Y., 2001. Regulation and functions of myogenic regulatory factors in lower vertebrates. *Comp. Biochem. Physiol. Part B Biochem. Mol. Biol.* 130, 1–12.
- Rodgers, B.D., Weber, G.M., Kelley, K.M., Levine, M.A., 2003. Prolonged fasting and cortisol reduce myostatin mRNA levels in tilapia larvae; short-term fasting elevates. *Am. J. Physiol. Integr. Comp. Physiol.* 284, R1277–R1286.
- Rossi, G., Messina, G., 2014. Comparative myogenesis in teleosts and mammals. *Cell. Mol. Life Sci.* 71, 3081–3099.
- Rowlerson, A.M., Veggetti, A., 2001. Cellular mechanisms of post-embryonic muscle growth in aquaculture species. *Fish Physiol.* 18, 103–140.
- Rubio-Aliaga, I., Marvin-Guy, L., Wang, P., Wagniere, S., Mansourian, R., Fuerholz, A., Kussmann, M., 2011. Mechanisms of weight maintenance under high- and low-protein, low-glycaemic index diets. *Mol. Nutr. Food Res.* 55, 1603–1612.
- Salvador, J.M., Brown-Clay, J.D., Fornace, A.J., 2013. Gadd45 in stress signaling, cell cycle control, and apoptosis. In: Liebermann, D., Hoffman, B. (Eds.), *Gadd45 Stress Sensor Genes*. Springer, New York LLC, New York, pp. 1–19.
- Schiaffino, S., Mammucari, C., 2011. Regulation of skeletal muscle growth by the IGF1-Akt/PKB pathway: insights from genetic models. *Skelet. Muscle* 1, 4.
- Schuchardt, D., Vergara, J.M., Fernández-Palacios, H., Kalinowski, C.T., Hernández-Cruz, C.M., Izquierdo, M.S., Robaina, L., 2008. Effects of different dietary protein and lipid levels on growth, feed utilization and body composition of red porgy (*Pagrus pagrus*) fingerlings. *Aquac. Nutr.* 14, 1–9.
- Seiliez, I., Sabin, N., Gabillard, J.-C., 2012. Myostatin inhibits proliferation but not differentiation of trout myoblasts. *Mol. Cell. Endocrinol.* 351, 220–226.
- Shen, Y., Ma, K., Liu, F., Yue, G., 2016. Characterization of two novel gadd45a genes in hybrid tilapia and their responses to the infection of *Streptococcus agalactiae*. *Fish Shellfish Immunol.* 54, 276–281.
- Sheng, J., Jin, J., 2016. TNNI1, TNNI2 and TNNI3: evolution, regulation, and protein structure-function relationships. *Gene* 576, 385–394.
- Silva-Marrero, J.I., Sáez, A., Caballero-Solares, A., Viegas, I., Almajano, M.P., Fernández, F., Metón, I., 2017. A transcriptomic approach to study the effect of long-term starvation and diet composition on the expression of mitochondrial oxidative phosphorylation genes in gilthead sea bream (*Sparus aurata*). *BMC Genomics* 18, 768.
- Silva-Marrero, J.I., Villasante, J., Rashidpour, A., Palma, M., Fàbregas, A., Almajano, M.P., Metón, I., 2019. The administration of chitosan-tripolyphosphate-DNA nanoparticles to express exogenous SREBP1a enhances conversion of dietary carbohydrates into lipids in the liver of *Sparus aurata*. *Biomolecules* 9, 297.
- Smyth, G.K., 2004. Linear models and empirical Bayes methods for assessing differential expression in microarray experiments. *Stat. Appl. Genet. Mol. Biol.* 3, 1–25.
- Song, X., Marandel, L., Skiba-Cassy, S., Corraze, G., Dupont-Nivet, M., Quillet, E., Panserat, S., 2018. Regulation by dietary carbohydrates of intermediary metabolism in liver and muscle of two isogenic lines of rainbow trout. *Front. Physiol.* 9, 1579.
- Stitt, T.N., Drujan, D., Clarke, B.A., Panaro, F., Timofeyeva, Y., Kline, W.O., Glass, D.J., 2004. The IGF-1/PI3K/Akt pathway prevents expression of muscle atrophy-induced ubiquitin ligases by inhibiting FOXO transcription factors. *Mol. Cell* 14, 395–403.
- Tan, X., Du, S.J., 2002. Differential expression of two MyoD genes in fast and slow muscles of gilthead seabream (*Sparus aurata*). *Dev. Genes Evol.* 212, 207–217.
- Vélez, E.J., Lutfi, E., Jiménez-Amilburu, V., Riera-Codina, M., Capilla, E., Navarro, I., Gutiérrez, J., 2014. IGF-I and amino acids effects through TOR signaling on proliferation and differentiation of gilthead sea bream cultured myocytes. *Gen. Comp. Endocrinol.* 205, 296–304.
- Vélez, E.J., Lutfi, E., Azizi, S., Montserrat, N., Riera-Codina, M., Capilla, E., Gutiérrez, J., 2016. Contribution of in vitro myocytes studies to understanding fish muscle physiology. *Comp. Biochem. Physiol. Part B Biochem. Mol. Biol.* 199, 67–73.
- Wijngaarden, M., Bakker, L., van der Zon, G., t Hoen, P., van Dijk, K., Jazet, I., Guigas, B., 2014. Regulation of skeletal muscle energy/nutrient-sensing pathways during metabolic adaptation to fasting in healthy humans. *Am. J. Physiol. Endocrinol. Metab.* 307, E885–E895.
- Wu, Y., Rashidpour, A., Almajano, M.P., Metón, I., 2020. Chitosan-based drug delivery system: applications in fish biotechnology. *Polymers (Basel)* 12, 1177.
- Zhu, K., Wang, H., Wang, H., Gul, Y., Yang, M., Zeng, C., Wang, W., 2014. Characterization of muscle morphology and satellite cells, and expression of muscle-related genes in skeletal muscle of juvenile and adult *Megalobrama amblycephala*. *Micron* 64, 66–75.

Chitosan-mediated expression of fish codon-optimised *Caenorhabditis elegans* FAT-1 and FAT-2 boosts EPA and DHA biosynthesis in *Sparus aurata*

Yuanbing Wu ^a, Ania Rashidpour ^a, Anna Fàbregas ^b, María Pilar Almajano ^c,
Isidoro Metón ^{a,*}

^a *Secció de Bioquímica i Biologia Molecular, Departament de Bioquímica i Fisiologia, Facultat de Farmàcia i Ciències de l'Alimentació, Universitat de Barcelona, Joan XXIII 27-31, 08028 Barcelona, Spain*

^b *Mimark Diagnostics S.L., Passeig Vall d'Hebron, 119-129, 08035 Barcelona, Spain*

^c *Departament d'Enginyeria Química, Universitat Politècnica de Catalunya, Diagonal 647, 08028 Barcelona, Spain*

*Corresponding author: Isidoro Metón, Secció de Bioquímica i Biologia Molecular, Departament de Bioquímica i Fisiologia, Facultat de Farmàcia i Ciències de l'Alimentació, Universitat de Barcelona, Joan XXIII 27-31, 08028 Barcelona, Spain. Tel.: +34 934024521; Fax: +34 934024520; E-mail: imeton@ub.edu; ORCID: 0000-0003-2301-2365

ABSTRACT

Omega-3 long-chain polyunsaturated fatty acids (*n*-3 LC-PUFA) are essential fatty acids required in healthy balanced diets for humans. To induce sustained production of *n*-3 LC-PUFA in gilthead seabream (*Sparus aurata*), chitosan-tripolyphosphate (TPP) nanoparticles encapsulating plasmids expressing fish codon-optimised *Caenorhabditis elegans* FAT-1 and FAT-2 were intraperitoneally administered every 4 weeks (3 doses in total, each of 10 µg plasmid per g of body weight). Growth performance and metabolic effects of chitosan-TPP complexed with pSG5 (empty plasmid), pSG5-FAT-1, pSG5-FAT-2 and pSG5-FAT-1 + pSG5-FAT-2 were assessed 70 days post-treatment. Tissue distribution analysis showed high expression levels of fish codon-optimised FAT-1 and FAT-2 in the liver (>200-fold). Expression of FAT-1 and FAT-1 + FAT-2 increased weight gain. Fatty acid methyl esters assay revealed that co-expression of FAT-1 and FAT-2 increased liver production and muscle accumulation of eicosapentaenoic acid (EPA), docosahexaenoic acid (DHA) and total *n*-3 LC-PUFA, while decreased the *n*-6/*n*-3 ratio. Co-expression of FAT-1 and FAT-2 downregulated *srebf1* and genes encoding rate-limiting enzymes for *de novo* lipogenesis in the liver, leading to decreased circulating triglycerides and cholesterol. In contrast, FAT-2 and FAT-1 + FAT-2 upregulated hepatic *hnf4a*, *nr1h3* and key enzymes in glycolysis and the pentose phosphate pathway. Our findings demonstrate for the first time efficient and sustained production of EPA and DHA in animals after long-term treatment with chitosan-TPP-DNA nanoparticles expressing FAT-1 and FAT-2, which enabled the production of functional fish rich in *n*-3 LC-PUFA for human consumption.

Keywords: Gene therapy, Chitosan, FAT-1, FAT-2, Omega 3 long-chain polyunsaturated fatty acids, *Sparus aurata*

1. Introduction

All organisms can synthesise saturated and monounsaturated fatty acids. However, the biosynthetic rate of long-chain polyunsaturated fatty acids (LC-PUFA) in vertebrates is markedly low and cannot cover physiological demands. Linoleic acid (18:2 n -6, LA) and α -linolenic acid (18:3 n -3, ALA) are precursors for the synthesis of omega-6 (n -6) and omega-3 (n -3) LC-PUFA series, respectively, and essential fatty acids for vertebrates, which lack Δ 12/ n -6 and Δ 15/ n -3 desaturases required to synthesise LA from oleic acid (18:1 n -9c, OA) and ALA from LA (Castro et al., 2016; Tocher et al., 2019). LC-PUFA are critical components for growth and development, acting as bioactive components of membrane phospholipids, precursors of signalling molecules and modulators of gene expression. Furthermore, n -3 LC-PUFA such as eicosapentaenoic acid (20:5 n -3, EPA) and docosahexaenoic acid (22:6 n -3, DHA) exert protective roles preventing atherosclerosis, stroke, obesity, type-2 diabetes, inflammation and autoimmune diseases, among others. In contrast, n -6 LC-PUFA, particularly arachidonic acid (20:4 n -6, ARA), are precursors of local hormones promoting acute and chronic inflammation (Djuricic and Calder, 2021). Apart from plants, fungi and some aquatic microorganisms, few other organisms such as the nematode *Caenorhabditis elegans* and some invertebrates can synthesise *de novo* n -3 and n -6 LC-PUFA in significant amounts. Vegetable oils are rich in LA and ALA, and often contain high levels of n -6 LC-PUFA, but are devoid of significant amounts of n -3 LC-PUFA, particularly EPA and DHA. Therefore, trophic transfer from microalgae and plankton to marine fish and seafood are major sources of LC-PUFA, notably n -3 LC-PUFA, in the human diet (Osmond and Colombo, 2019; Tocher et al., 2019).

Shortage of n -3 LC-PUFA and increased n -6/ n -3 ratio in fish fillets due to progressive replacement of fish oil with vegetable oils in aquafeeds is nowadays a major challenge for the aquaculture sector. To face this problem and increasing demands of functional food with high nutritional value, intense research is being conducted in order to improve the n -3 LC-PUFA content in farmed fish, including dietary incorporation of microalgae, genetically modified organisms (GMOs) such as yeast and algae, and plant GMO-derived oils, such as oil from false flax expressing microalgal genes (Betancor et al., 2016; Carvalho et al., 2022; Osmond and Colombo, 2019; Sales et al., 2021; Tocher et al., 2019). Production in large-scale fermenters and the supply of balanced amounts of EPA and DHA constrains the use of microalgae biomass in aquafeeds (Tocher et al., 2019). Transgenesis of fish fatty acid desaturases and elongases aiming to increase EPA and DHA levels was assayed in zebrafish (Alimuddin et al., 2008, 2007; Cheng et al., 2015).

However, fish desaturases and elongases act on both *n*-3 and *n*-6 fatty acid series and generally do not substantially change the *n*-6/*n*-3 ratio (Pang et al., 2014). Efficient conversion of *n*-6 PUFA into *n*-3 PUFA in transgenic mice expressing *Caenorhabditis elegans* *n*-3 fatty acid desaturase fat-1 (FAT-1), an *n*-3 fatty acid desaturase absent in vertebrates (Kang et al., 2004), led to use synthetically humanised and fish codon-optimised *C. elegans* FAT-1 to generate transgenic zebrafish (Pang et al., 2014), common carp (Zhang et al., 2019) and other vertebrates, including mice, cattle, pigs and sheep (Chen et al., 2013; Ji et al., 2009; Lai et al., 2006; Li et al., 2018; Liu et al., 2016, 2017; Luo et al., 2020; Sun et al., 2020; Tang et al., 2019; You et al., 2021). Transgenesis of *C. elegans* FAT-1 efficiently increases EPA and DHA, while decreases the *n*-6/*n*-3 ratio. The effect is potentiated in zebrafish and pigs by double transgenesis with codon-optimised *C. elegans* Δ 12 fatty acid desaturase fat-2 (FAT-2), a Δ 12 desaturase that converts OA into LA and which is also absent in vertebrates (Pang et al., 2014; Tang et al., 2019).

Given that there are major concerns on environmental risk, sustainability, fish welfare, food safety as well as consumer perception and acceptance of GMOs (Osmond and Colombo, 2019; Tocher et al., 2019), in recent years we developed an alternative methodology to GMO generation based on the production of chitosan-tripolyphosphate (TPP)-DNA nanoparticles for transient modification of the expression of target genes in the liver of gilthead seabream (*Sparus aurata*) (Gaspar et al., 2018; González et al., 2016; Silva-Marrero et al., 2019). Chitosan is a cationic polymer of glucosamine and N-acetylglucosamine derived from chitin by deacetylation. Chitosan is increasingly used as carrier for delivering nucleic acids *in vivo* due to its well-known mucoadhesion, low toxicity, biodegradability and biocompatibility (Wu et al., 2020).

With the aim to promote sustained production of *n*-3 LC-PUFA in *S. aurata*, in the present study chitosan-TPP nanoparticles encapsulating plasmids expressing fish codon-optimised *Caenorhabditis elegans* FAT-1 and FAT-2 were intraperitoneally administered every 4 weeks to *S. aurata* (3 doses in total). Seventy days post-treatment, the effect of chitosan-TPP-DNA nanoparticles was assessed on growth parameters, intermediary metabolism and fatty acid content in the liver and skeletal muscle of *S. aurata*.

2. Materials and methods

2.1. Animals

S. aurata juveniles ($7.7 \text{ g} \pm 0.2$, mean weight \pm SEM) were obtained from Piscicultura Marina Mediterranea (AVRAMAR Group, Burriana, Spain) and maintained at 20 °C in 250-L aquaria supplied

with running seawater in the aquatic animals facility of the Scientific and Technological Centers of the Universitat de Barcelona (CCiTUB) as described (Silva-Marrero et al., 2017). Fish were fed with commercial diet (Dibaq Microbaq 165, Dibaq, Segovia Spain), containing 52 % protein, 18 % lipids, 12 % carbohydrates, 10 % ash, 8 % moisture and 21.3 kJ/g gross energy. For the acclimation regime, fish were fed twice daily (9:00 and 17:00) at a ration of 5 % body weight (BW). Two weeks before experimental treatments, the ration was adjusted and kept to 3 % BW until the end of the experiment. To study the long-term effect of fish codon-optimised *C. elegans* FAT-1 and FAT-2 expression, 4 groups of fish were intraperitoneally injected up to 3 times (once every 4 weeks) with chitosan-TPP nanoparticles complexed with pSG5 (empty plasmid, control), pSG5-FAT-1, pSG5-FAT-2 and pSG5-FAT-1 + pSG5-FAT-2. Every single administration consisted of 10 µg plasmid per gram BW. Fourteen days after the last injection and 24 h following the last meal, fish were sacrificed by cervical section, blood was collected and the liver, intestine, skeletal muscle and brain were dissected out, frozen in liquid nitrogen and kept at -80 °C until use. To prevent stress, fish were anaesthetised by tricaine methanesulfonate (MS-222; 1:12,500) before handling. Experimental procedures involving fish were performed in accordance with the guidelines of the University of Barcelona's Animal Welfare Committee (proceeding #10811, Generalitat de Catalunya), in compliance with local legislation and EU Directive 2010/63/EU on the protection of animals used for scientific purposes.

2.2. Preparation and characterisation of chitosan-TPP-DNA nanoparticles

Fish codon-optimised FAT-1 and FAT-2 cDNA sequences (GenBank accession nos. ON374024 and ON374025, respectively) were synthesised based on *C. elegans* FAT-1 and FAT-2 using GeneArt Instant Designer (Thermo Fisher Scientific, Waltham, MA, USA) and ligated into pSG5 (Agilent Technologies, Palo Alto, CA, USA). The resulting constructs (pSG5-FAT-1 and pSG5-FAT-2) were verified by cycle sequencing on both sides. Chitosan-TPP nanoparticles encapsulating pSG5 (control), pSG5-FAT-1, pSG5-FAT-2 and pSG5-FAT-1 + pSG5-FAT-2 were prepared by ionic gelation (González et al., 2016). For each experimental condition, 1 mg of plasmid was mixed with 4 mL of 0.84 mg/mL TPP (Sigma-Aldrich, St. Louis, MO, USA). Chitosan-TPP-DNA nanoparticles were formed upon dropwise addition of the TPP-DNA solution into 10 mL of 2 mg/mL low molecular weight chitosan (Sigma-Aldrich, St. Louis, MO, USA)-acetate buffer (pH 4.4) solution. Nanoparticles were sedimented by centrifugation at 36,000 g for 20

min at 15 °C and resuspended in 2 mL of 2 % w/v mannitol, which acted as cryoprotector during lyophilisation. Nanoparticles were subjected to a freeze–drying process at –47 °C. Particle size and Z potential were determined by dynamic light scattering and laser Doppler electrophoresis, respectively, using Zetasizer Nano ZS fitted with a 633 nm laser (Malvern Instruments, Malvern, UK). Chitosan-TPP-DNA nanoparticles were resuspended in 0.9 % NaCl before intraperitoneal administration to *S. aurata*.

2.3. Body composition

For moisture determination, fish were dried at 85 °C until constant weight was reached (Busacker et al., 1990; Lucas, 1996). Moisture was calculated as (wet weight (g) – dry weight (g))*100 / wet weight (g). Dried samples were further used for assaying nitrogen (N), lipid and ash. N content was determined with FlashEA 1112 analyser (Thermo Fisher Scientific, Waltham, MA, USA) and was subsequently used to estimate crude protein by multiplying N content by a factor of 6.25. Crude lipid was extracted with petroleum ether using a Soxhlet extractor. For ash determination, samples were incinerated in a Hobersal 12PR/300 muffle furnace (Hobersal, Caldes de Montbui, Spain) at 550 °C for 12 h (Busacker et al., 1990; Lucas, 1996). Crude protein, lipid and ash are expressed as percentage of dry weight.

2.4. Growth parameters

Specific growth rate (SGR), feed conversion ratio (FCR), hepatosomatic index (HSI), protein retention (PR), lipid retention (LR) and protein efficiency ratio (PER) were calculated according to the following equations:

$SGR = (\ln W_f - \ln W_i) * 100 / T$; where W_f and W_i are mean final and initial body fresh weight (g) and T is time (days)

$FCR = \text{dry feed intake (g)} / \text{wet weight gain (g)}$

$HSI = \text{liver fresh weight (g)} * 100 / \text{fish body weight (g)}$

$PR = \text{body protein gain (g)} * 100 / \text{protein intake (g)}$

$LR = \text{body lipid gain (g)} * 100 / \text{lipid intake (g)}$

$PER = \text{weight gain (g)} / \text{feed protein provided (g)}$

2.5. Enzyme activity assays and metabolites

Enzyme activity assays and metabolites were spectrophotometrically determined at 30 °C in a Varioskan LUX multimode microplate reader (Thermo Fisher Scientific, Waltham, MA, USA). Liver crude extracts were obtained by homogenisation of powdered frozen tissue (1:5, *w/v*) in 50 mM Tris-HCl (pH 7.5), 4 mM, EDTA, 50 mM NaF, 0.5 mM phenylmethylsulfonyl fluoride, 1 mM dithiothreitol and 250 mM sucrose, 30 sec at 4 °C using PTA-7 Polytron (Kinematica GmbH, Littau-Luzern, Switzerland). Following centrifugation at 10,000 *g* for 30 min at 4 °C, the supernatant was collected for enzyme activity assays. Reaction mixtures for 6-phosphofructo-1-kinase (PFKL), fructose-1,6-bisphosphatase (FBP1) and total protein were as previously described (Metón et al., 1999b). Enzyme activities were expressed as specific activity (U/g protein). One unit of PFKL activity was considered the amount of enzyme needed to oxidise 2 µmol of NADH per min. One unit of FBP1 activity of was defined as the amount of enzyme necessary for transforming 1 µmol of substrate per min. Serum glucose, triglycerides and cholesterol were measured with commercial kits (Linear Chemicals, Montgat, Spain).

2.6. Reverse transcription coupled to quantitative real-time PCR (RT-qPCR)

Total RNA from *S. aurata* tissues was isolated using HigherPurity Tissue Total RNA Purification Kit (Canvax, Cordoba, Spain) and reverse-transcribed with Moloney murine leukaemia virus reverse transcriptase (Life Technologies, Carlsbad, CA, USA) according to manufacturer's instructions. The mRNA expression levels of genes listed in Table 1 were determined using QuantStudio 3 Real-Time PCR System (Thermo Fisher Scientific, Waltham, MA, USA). The reaction mixture contained 0.4 µM of each primer (Table 1), 5 µL of SYBR Green (Thermo Fisher Scientific, Foster City, CA, USA), 0.8 µL of diluted cDNA and sterilized milli-Q water to final volume of 10 µL. The amplification cycle was 95 °C for 10 min, followed by 40 cycles at 95 °C for 15 s and 62 °C for 1 min. For each gene, standard curves for determining efficiency of the amplification reaction were generated with serial dilutions of control cDNA. Amplification of single products was confirmed by checking dissociation curves after each experiment. Amplicon size was checked by agarose gel electrophoresis. *S. aurata* ribosomal subunit 18S (*18s*), β-actin (*actb*) and elongation factor 1 alpha (*ef1a*) were used as endogenous controls to normalise the mRNA levels for genes of interest in liver samples. For tissue distribution, normalisation was performed against *S. aurata 18s* expression. The standard $\Delta\Delta C_T$ method was used to calculate variations in gene expression (Pfaffl, 2001).

Table 1

Primer sequences used for RT-qPCR in the present study.

Gene	Forward Sequences (5' to 3')	Reverse Sequences (5' to 3')	GenBank Accession
<i>acaca</i>	CCCAACTTCTTCTACCACAG	GAACTGGAACTCTACTACAC	JX073712
<i>acacb</i>	TGACATGAGTCCTGTGCTGG	GCCTCAGTTCGTATGATGGT	JX073714
<i>actb</i>	CTGGCATCACACCTTCTACAACGAG	GCGGGGGTGTGAAGGTCTC	X89920
<i>cpt1a</i>	GAAGGGCAGATAAAGAGGGGC	GCATCGATCGCTGCATTCAGC	JQ308822
<i>eef1a</i>	CCCGCCTCTGTTGCCTTCG	CAGCAGTGTGGTTCCGTTAGC	AF184170
<i>elovl4a</i>	AAGAACAGAGAGCCCTTCCAG	TGCCACCCTGACTTCATTG	MK610320
<i>elovl4b</i>	TCTACACAGGCTGCCCATTC	CGAAGAGGATGATGAAGGTGAC	MK610321
<i>elovl5</i>	GGGATGGCTACTGCTCGACA	CAGGAGAGTGAGGCCAGAT	AY660879
<i>fads2</i>	CACTATGCTGGAGAGGATGCC	TATTCGGTCCTGGCTGGGC	AY055749
<i>fasn</i>	GTAGAGGACACGCCCATCGAT	TGCGTATGACCTCTGGTGTGCT	JQ277708
<i>fat-1</i>	TTCAACCCCATTCCTTTCAGCG	TAGGCGCACACGCAGCAGCA	ON374024
<i>fat-2</i>	AAGAGGACTACAACAACAGAACCGCCA	CGAACAGTCTGCTCCAAGGCCAA	ON374025
<i>fbp1</i>	CAGATGGTGAGCCGTGTGAGAAGGATG	GCCGTACAGAGCGTAACCAGCTGCC	AF427867
<i>gck</i>	TGTGTCAGCTCTCAACTCGACC	AGGATCTGCTCTACCATGTGGAT	AF169368
<i>g6pc1</i>	GCGTATTGGTGGCTGAGGTCG	AAGGAGAGGGTGGTGTGGAAG	AF151718
<i>g6pd</i>	TGATGATCCAACAGTTCCTA	GCTCGTTCCTGACACACTGA	JX073711
<i>hmgcr</i>	ACTGATGGCTGCTCTGGCTG	GGGACTGAGGGATGACGCAC	MN047456
<i>hnf4a</i>	GTGGACAAAGACAAGCGAAATC	GCATTGATGGATGGTAAACTGC	FJ360721
<i>nr1h3</i>	GCATCTGGACGAGGCTGAATAC	ACTTAGTGTGCGAAGGCTCACC	FJ502320
<i>pck1</i>	CAGCGATGGAGGAGTGTGGTGGGA	GCCCATCCCAATTCCCGCTTCTGTGC TCCGGCTGGTCAGTGT	AF427868
<i>pfkfb1</i>	TGCTGATGGTGGGACTGCCG	CTCGGCGTTGTCGGCTCTGAAG	U84724
<i>pfk1</i>	TGCTGGGGACAAAACGAACTCTTCC	AAACCCTCCGACTACAAGCAGAGCT	KF857580
<i>pklr</i>	CAAAGTGAAAGCCGGCAAGGG	GTCGCCCCTGGCAACCATAAC	KF857579

<i>ppara</i>	GTGAGTCTTGTGAGTGAGGGGTTG	AGTGGGGATGGTGGGCTG	AY590299
<i>srebfl</i>	CAGCAGCCCGAACACCTACA	TTGTGGTCAGCCCTTGGAGTTG	JQ277709
<i>scd1a</i>	TCCCTTCCGCATCTCCTTTG	TTGTGGTGAACCCTGTGGTCTC	JQ277703
<i>18s</i>	TTACGCCCATGTTGTCCTGAG	AGGATTCTGCATGATGGTCACC	AM490061

2.7. Fatty acid methyl ester (FAME) analysis

Fatty acid profiles of liver and muscle were analysed by gas chromatography with flame ionisation detection as previously described (Silva-Marrero et al., 2019), using GC-2025 (Shimadzu, Kyoto, Japan) with capillary column BPX70, 30 m × 0.25 mm × 0.25 µm (Trajan Scientific and Medical, Ringwood, Australia). Oven temperature started at 60 °C for 1 min and then it was raised to 260 °C (rate: 6 °C/min). Injector (AOC-20i, Shimadzu, Japan) and detector temperatures were 260 °C and 280 °C, respectively. Sample (1 µL) was injected with helium as carrier gas and split ratio 1:20. Supelco 37 Component FAME Mix (Sigma-Aldrich, St. Louis, MO, USA) was used as reference for identifying fatty acids.

2.8. Statistics

To identify significant differences between treatments, the SPSS Version 25 software (IBM, Armonk, NY, USA) was used to submit experimental data to one-way analysis of variance followed by the Duncan post-hoc test (>2 groups). Statistical significance was considered when $P < 0.05$.

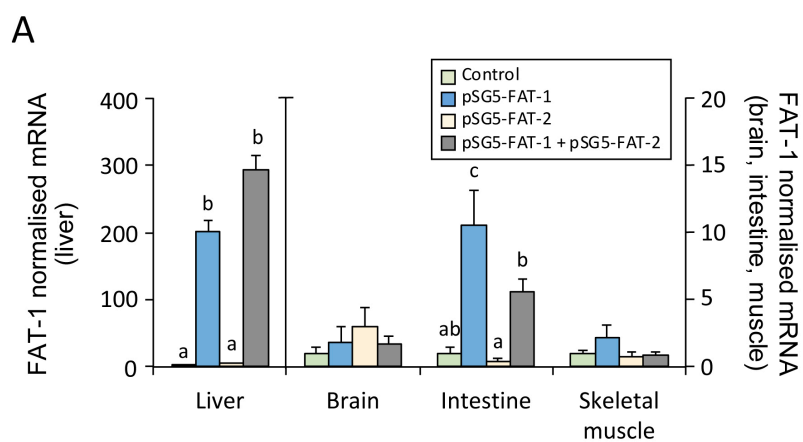
3. Results

3.1. Delivery of chitosan-TPP complexed with pSG5-FAT-1 and pSG5-FAT-2 increases fish codon-optimised FAT-1 and FAT-2 mRNA levels in *S. aurata*

To assess the metabolic effects resulting from expression of *C. elegans* FAT-1 and FAT-2 in the liver of *S. aurata*, we designed fish codon-optimised *C. elegans* FAT-1 and FAT-2 cDNA sequences for further ligation into pSG5 and prepared chitosan-TPP nanoparticles complexed with empty pSG5 (control), pSG5-FAT-1, pSG5-FAT-2 and pSG5-FAT-1 + pSG5-FAT-2 by ionic gelation. Particle size and Z potential of naked chitosan-TPP, expressed as mean ± SEM ($n = 3$), was 214.6 nm ± 20.2 and 37.5 mV ± 0.6, respectively.

Incorporation of plasmid DNA to chitosan-TPP did not significantly modify particle size, which was $262.7 \text{ nm} \pm 74.0$ (mean \pm SEM, $n = 3$), but decreased Z potential to $12.0 \text{ mV} \pm 0.8$ (mean \pm SEM, $n = 3$).

For long-term sustained expression of fish codon-optimised FAT-1 and FAT-2 in the liver of *S. aurata*, each experimental group of fish received every 4 weeks up to 3 intraperitoneal injections of chitosan-TPP complexed with $10 \text{ } \mu\text{g/g}$ BW of the corresponding plasmid (pSG5, pSG5-FAT-1, pSG5-FAT-2 or pSG5-FAT-1 + pSG5-FAT-2). The dosing schedule was based on preliminary studies showing that 28 days post-administration of chitosan-TPP-pSG5-FAT-1 and chitosan-TPP-pSG5-FAT-2 ($10 \text{ } \mu\text{g/g}$ BW of plasmid) to *S. aurata* increased the hepatic mRNA levels of fish codon-optimised FAT-1 and FAT-2 to levels even higher than those found at 72 h post-treatment. Expressed as mean \pm SEM ($n = 3$), fold increase over control values at 72 h and 28 days post-treatment were 31.6 ± 4.1 and 74.8 ± 29.0 , respectively, for FAT-1 mRNA levels, while for FAT-2 mRNA levels fold increase was 20.3 ± 2.8 and 70.2 ± 7.0 , respectively. Seventy days after the beginning of the experiment (14 days following the last injection), the mRNA levels of fish codon-optimised FAT-1 and FAT-2 were determined by RT-qPCR in several tissues of treated fish, including the liver, intestine, skeletal muscle and brain (Fig. 1).



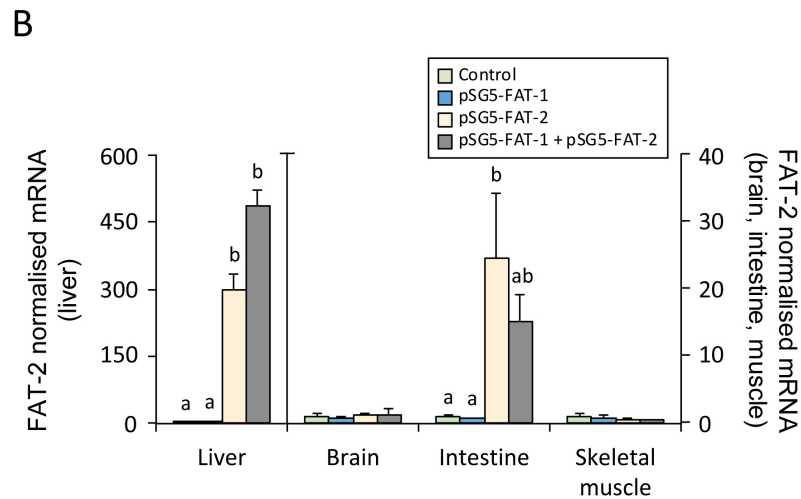


Fig. 1. Effect of long-term treatment with chitosan-TPP nanoparticles complexed with pSG5 (control), pSG5-FAT-1, pSG5-FAT-2 and pSG5-FAT-1 + pSG5-FAT-2 on the mRNA levels of fish-codon optimised *C. elegans* FAT-1 and FAT-2 in *S. aurata* tissues (brain, skeletal muscle, liver and intestine). Fifteen days after the last injection and 24 h following the last meal, exogenous FAT-1 and FAT-2 expression was assayed by RT-qPCR, normalised to the *S. aurata* *18s* mRNA levels and represented as mean \pm SEM ($n = 4$). For each tissue, homogeneous subsets for the treatment are shown with different letters ($P < 0.05$).

When compared with control fish, chitosan-TPP nanoparticles complexed with pSG5-FAT-1 and pSG5-FAT-2 significantly increased the mRNA levels of FAT-1 and FAT-2, respectively, in the liver and intestine of *S. aurata*. Specifically, FAT-1 mRNA abundance in the liver of fish administered with pSG5-FAT-1 was 201.8-fold higher than in control fish, while treatment with pSG5-FAT-2 upregulated FAT-2 297.4-fold. For the intestine, pSG5-FAT-1 and pSG5-FAT-2 upregulated 10.6-fold FAT-1 and 24.7-fold FAT-2, respectively. Nanoparticle administration did not exert effects on the skeletal muscle and brain.

3.2. Effect of fish codon-optimised FAT-1 and FAT-2 expression on whole-body composition, growth performance and serum metabolites in *S. aurata*

Sustained expression of fish codon-optimised FAT-1 + FAT-2 in the liver of *S. aurata* caused a moderate but significant 7.6 % decrease of whole-body crude protein values observed in control fish. No effect was observed in moisture, ash and crude lipid body composition (Table 2). Analysis of growth performance parameters showed significantly increased weight gain values in fish expressing FAT-1 (18 % of increase) and FAT-1 + FAT-2 (26 % of increase) compared to control fish. No significant difference was found between controls and treatment with FAT-2. Similarly, the highest SGR was found in fish treated with FAT-1 + FAT-2, followed by fish treated with FAT-1, controls and fish treated with FAT-2. Fish expressing FAT-2 also presented the lowest PER. HSI significantly decreased in fish treated with FAT-1 and FAT-1 + FAT-2 to 72 % of control values. No significant differences were observed in PR and LR.

Table 2

Growth performance, nutrient retention and body composition of *S. aurata* after intraperitoneal injection of chitosan-TPP complexed with empty vector (pSG5, control), pSG5-FAT-1, pSG5-FAT-2 and pSG5-FAT-1 + pSG5-FAT-2.

	Control	FAT-1	FAT-2	FAT-1 + FAT-2
Initial body weight (g)	9.97±0.69	11.42±0.90	9.74±0.44	11.04±0.55
Final body weight (g)	34.64±1.03 ^a	40.51±1.63 ^b	31.46±1.57 ^a	42.15±1.25 ^b
Weight gain (g)	24.67±0.51 ^a	29.09±1.06 ^b	21.73±1.23 ^a	31.11±0.73 ^b
SGR (%)	1.79±0.05 ^{ab}	1.85±0.08 ^{ab}	1.59±0.04 ^a	2.01±0.03 ^b
FCR	1.40±0.03 ^{ab}	1.36±0.04 ^{ab}	1.53±0.08 ^b	1.29±0.03 ^a
HSI (%)	1.55±0.12 ^b	1.12±0.08 ^a	1.49±0.18 ^{ab}	1.12±0.15 ^a
PR (%)	24.98±3.24	21.96±0.85	18.90±2.45	21.81±1.56
LR (%)	28.00±7.50	31.47±1.12	25.17±2.03	26.24±2.02
PER	1.40±0.03 ^{ab}	1.45±0.05 ^{ab}	1.31±0.07 ^a	1.52±0.04 ^b

Moisture (%)	71.34±1.22	70.68±0.29	72.03±0.98	71.10±1.28
Ash (%)	13.72±1.47	13.93±0.12	13.07±0.73	12.94±0.45
Protein (%)	62.20±3.88 ^b	58.81±1.80 ^{ab}	57.98±1.04 ^{ab}	57.50±1.24 ^a
Lipid (%)	27.28±1.44	29.28±0.55	26.09±1.85	25.02±2.3

SGR, specific growth rate; FCR, feed conversion ratio; HSI, hepatosomatic index; PR, protein retention; LR, lipid retention; PER, protein efficiency ratio. Data are expressed as mean ± SEM ($n = 3$). Different superscript letters indicate significant differences between groups ($P < 0.05$).

Serum glucose, triglycerides and cholesterol were also determined in 70-day treated *S. aurata*. Any of the treatments assayed affected blood glucose levels. However, co-expression of FAT-1 + FAT-2 significantly decreased 1.8-fold triglycerides and 1.5-fold cholesterol compared to control levels (Fig. 2).

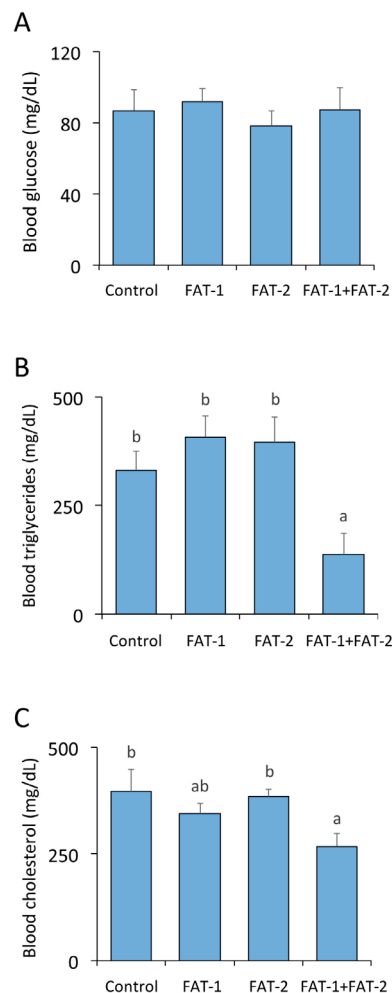


Fig. 2. Effect of long-term treatment with chitosan-TPP nanoparticles complexed with pSG5 (control), pSG5-FAT-1, pSG5-FAT-2 and pSG5-FAT-1 + pSG5-FAT-2 on serum glucose, triglycerides and cholesterol in *S. aurata*. Fifteen days after the last injection and 24 h following the last meal, fish were sacrificed and the blood was collected. Values are represented as mean \pm SEM ($n = 6-7$). Homogeneous subsets for the treatment are shown with different letters ($P < 0.05$).

3.3. Effect of fish codon-optimised FAT-1 and FAT-2 on the fatty acid profile in the liver and skeletal muscle

The effect of long-term expression of FAT-1 and FAT-2 was analysed on the fatty acid profile of the liver and skeletal muscle of *S. aurata*. Table 3 shows the fatty acid composition in the liver of *S. aurata* long-term treated with chitosan-TPP nanoparticles complexed with pSG5 (control), pSG5-FAT-1, pSG5-FAT-2, and pSG5-FAT-1 + pSG5-FAT-2. Among 30 different fatty acids identified in this study, treatment with FAT-1 and FAT-1 + FAT-2 significantly increased EPA (1.5-fold and 1.6-fold, respectively), DHA (2.4-fold and 2.3-fold, respectively) and total $n-3$ fatty acids (1.7-fold in both cases). The $n-6/n-3$ ratio significantly decreased in fish expressing FAT-1 (to 60.3 % of control values), FAT-2 (66.9 %) and FAT-1 + FAT-2 (63.7 %). A moderate 1.2-fold increase of *cis*-10-heptadecenoic acid (17:1 $n-7$) was also observed in FAT-1 + FAT-2 treated fish, while expression of FAT-1 decreased palmitoleic acid (16:1 $n-7$) to 58.4 % of control levels.

Table 3

Effect of chitosan-TPP complexed with empty vector (pSG5, control), pSG5-FAT-1, pSG5-FAT-2 and pSG5-FAT-1 + pSG5-FAT-2 on the fatty acid profile of *S. aurata* liver.

Fatty acid	Control	FAT-1	FAT-2	FAT-1 + FAT-2
14:0	9.38 ± 0.46	7.31 ± 1.45	7.43 ± 0.60	7.40 ± 1.45
15:0	0.10 ± 0.10	0.32 ± 0.12	0.37 ± 0.13	0.32 ± 0.11
16:0	27.49 ± 0.66	27.09 ± 3.37	26.33 ± 1.42	25.29 ± 2.50
17:0	0.21 ± 0.03	0.11 ± 0.04	0.22 ± 0.11	0.11 ± 0.04
18:0	3.73 ± 0.39	3.88 ± 0.30	4.20 ± 0.38	4.03 ± 0.33
20:0	0.02 ± 0.02	0.20 ± 0.13	0.08 ± 0.03	0.08 ± 0.04
21:0	0.06 ± 0.06	0.16 ± 0.06	0.12 ± 0.07	0.11 ± 0.04
22:0	0.00 ± 0.00	0.06 ± 0.04	0.11 ± 0.04	0.05 ± 0.05
23:0	0.02 ± 0.02	0.01 ± 0.01	0.00 ± 0.00	0.01 ± 0.01
24:0	0.01 ± 0.01	0.03 ± 0.02	0.06 ± 0.02	0.04 ± 0.02
14:1 n -5	0.06 ± 0.05	0.00 ± 0.00	0.14 ± 0.09	0.13 ± 0.04
15:1 n -5	0.06 ± 0.02	0.02 ± 0.01	0.05 ± 0.03	0.05 ± 0.02
16:1 n -7	6.93 ^b ± 0.27	4.05 ^a ± 1.23	5.58 ^{ab} ± 0.48	5.38 ^{ab} ± 0.42
17:1 n -7	0.20 ± 0.02	0.22 ± 0.00	0.26 ± 0.02	0.23 ± 0.01
18:1 n -9 _c	21.24 ± 1.24	22.04 ± 1.60	22.45 ± 1.15	21.84 ± 1.89
18:1 n -9 _t	0.06 ± 0.03	0.04 ± 0.01	0.08 ± 0.02	0.04 ± 0.01
20:1 n -9	0.58 ± 0.08	0.83 ± 0.02	0.71 ± 0.13	0.72 ± 0.14
22:1 n -9	0.17 ± 0.03	0.30 ± 0.08	0.25 ± 0.05	0.31 ± 0.08
24:1 n -9	0.00 ± 0.00	0.07 ± 0.05	0.07 ± 0.03	0.05 ± 0.03
18:2 n -6 _c	23.23 ± 0.52	23.55 ± 1.4	22.42 ± 1.36	24.19 ± 1.29
18:2 n -6 _t	0.26 ± 0.22	0.09 ± 0.03	0.09 ± 0.04	0.13 ± 0.05
20:2 n -6	0.17 ± 0.05	0.25 ± 0.03	0.21 ± 0.05	0.19 ± 0.07
22:2 n -6	0.01 ± 0.01	0.02 ± 0.01	0.02 ± 0.01	0.02 ± 0.01

18:3 n -3	1.29 ± 0.10	1.26 ± 0.25	1.76 ± 0.45	1.16 ± 0.20
18:3 n -6	0.76 ± 0.17	0.65 ± 0.14	0.81 ± 0.06	0.72 ± 0.14
20:3 n -3	0.00 ± 0.00	0.06 ± 0.06	0.00 ± 0.00	0.07 ± 0.07
20:3 n -6	0.23 ± 0.04	0.29 ± 0.06	0.21 ± 0.06	0.25 ± 0.02
20:4 n -6	0.22 ± 0.02	0.29 ± 0.10	0.40 ± 0.14	0.30 ± 0.11
20:5 n -3	1.79 ^a ± 0.09	2.76 ^b ± 0.29	2.43 ^{ab} ± 0.26	2.89 ^b ± 0.33
22:6 n -3	1.70 ^a ± 0.15	4.02 ^b ± 0.65	3.15 ^{ab} ± 0.74	3.87 ^b ± 0.66
Saturated	41.02 ± 0.58	39.18 ± 4.49	38.92 ± 1.64	37.45 ± 3.54
Monounsaturated	29.3 ± 1.10	27.57 ± 2.60	29.59 ± 1.30	28.75 ± 1.79
PUFA	29.67 ± 0.60	33.25 ± 2.51	31.49 ± 1.39	33.80 ± 1.94
n -3	4.78 ^a ± 0.28	8.11 ^b ± 0.99	7.34 ^{ab} ± 0.99	8.00 ^b ± 0.93
n -6	24.89 ± 0.47	25.14 ± 1.63	24.15 ± 1.48	25.8 ± 1.54
n -9	22.05 ± 1.18	23.28 ± 1.74	23.56 ± 1.07	22.96 ± 2.06
n -6/ n -3	5.26 ^b ± 0.28	3.17 ^a ± 0.26	3.52 ^a ± 0.65	3.35 ^a ± 0.42

Data are expressed as percentage of total fatty acids and represented as mean ± SEM ($n = 4$).

Different superscript letters indicate significant differences between groups ($P < 0.05$).

The effect of long-term hepatic expression of FAT-1, FAT-2 and FAT-1 + FAT-2 on the fatty acids profile in the skeletal muscle is shown in Table 4. Twenty-one out of 29 fatty acids identified in the skeletal muscle were significantly affected by co-expression of FAT-1 and FAT-2. Total saturated fatty acids significantly decreased to 57.1 % of control levels, mostly resulting from the low content in myristic acid (14:0; 34.4 % of controls), palmitic acid (16:0; 56.3 % of controls) and margaric acid (17:0; 50.0 % of controls). In addition, treatment with FAT-1 and FAT-2 also decreased margaric acid to 50.0 % of control values. In contrast, longer saturated fatty acids (with more than 17 carbons) presented increased values than in controls. Thus, stearic acid (18:0) increased 1.2-fold, while arachidic acid (20:0), behenic acid (22:0), tricosylic acid (23:0) and lignoceric acid (24:0) rised from non-

detectable levels in control fish to low but detectable levels in fish treated with FAT-1 + FAT-2.

Monounsaturated, PUFA and total *n*-3, *n*-6 and *n*-9 fatty acids increased 1.3-fold, 1.3-fold, 2.2-fold, 1.1-fold and 1.5-fold, respectively, in the skeletal muscle of fish expressing FAT-1 + FAT-2. As a result of greater effect on *n*-3 series than in *n*-6 fatty acids, the *n*-6/*n*-3 ratio significantly decreased to 52.0 % of control levels. Considering unsaturated fatty acids with a content greater than 1 % for any assayed treatment, expression of FAT-1 + FAT-2 significantly increased EPA (1.7-fold) and DHA (3.0-fold) from the *n*-3 series, LA (18:2*n*-6c; 1.1-fold) and OA (18:1*n*-9c; 1.5-fold), while decreased palmitoleic acid to 61.5 % of control levels. For less abundant unsaturated fatty acids (content between 0.1 % and 1 %), treatment with FAT-1 + FAT-2 also resulted in significant increases of *cis*-10-heptadecenoic acid (1.5-fold), gondoic acid (20:1*n*-9; 3.2-fold), erucic acid (22:1*n*-9; 5.2-fold), eicosadienoic acid (20:2*n*-6; 5.5-fold) and ARA (20:4*n*-6; 1.4-fold).

Table 4

Effect of chitosan-TPP complexed with empty vector (pSG5, control), pSG5-FAT-1, pSG5-FAT-2 and pSG5-FAT-1 + pSG5-FAT-2 on the fatty acid profile of *S. aurata* skeletal muscle.

Fatty acid	Control	FAT-1	FAT-2	FAT-1 + FAT-2
14:0	8.83 ^b ± 0.37	7.86 ^b ± 1.39	7.44 ^b ± 1.22	3.04 ^a ± 0.10
16:0	29.58 ^b ± 1.31	27.00 ^b ± 3.05	26.93 ^b ± 2.85	16.64 ^a ± 0.34
17:0	0.18 ^b ± 0.01	0.09 ^a ± 0.00	0.09 ^a ± 0.00	0.09 ^a ± 0.00
18:0	2.77 ^a ± 0.04	2.78 ^a ± 0.15	2.96 ^a ± 0.11	3.29 ^b ± 0.08
20:0	0.00 ^a ± 0.00	0.11 ^a ± 0.07	0.09 ^a ± 0.07	0.28 ^b ± 0.03
22:0	0.00 ^a ± 0.00	0.00 ^a ± 0.00	0.00 ^a ± 0.00	0.10 ^b ± 0.01
23:0	0.00 ^a ± 0.00	0.00 ^a ± 0.00	0.00 ^a ± 0.00	0.09 ^b ± 0.03
24:0	0.00 ^a ± 0.00	0.01 ^a ± 0.01	0.02 ^a ± 0.02	0.08 ^b ± 0.00

14:1 <i>n</i> -5	0.01 ± 0.01	0.01 ± 0.01	0.01 ± 0.01	0.02 ± 0.00
15:1 <i>n</i> -5	0.02 ± 0.02	0.04 ± 0.02	0.06 ± 0.02	0.05 ± 0.00
16:1 <i>n</i> -7	6.63 ^b ± 0.16	6.42 ^b ± 0.68	6.14 ^b ± 0.56	4.08 ^a ± 0.05
17:1 <i>n</i> -7	0.16 ^a ± 0.01	0.20 ^{ab} ± 0.03	0.20 ^{ab} ± 0.01	0.24 ^b ± 0.00
18:1 <i>n</i> -9c	19.6 ^a ± 0.53	21.98 ^a ± 2.33	21.65 ^a ± 2.01	28.45 ^b ± 0.30
18:1 <i>n</i> -9t	0.11 ^b ± 0.04	0.06 ^{ab} ± 0.03	0.11 ^b ± 0.04	0.00 ^a ± 0.00
20:1 <i>n</i> -9	0.26 ^a ± 0.16	0.48 ^{ab} ± 0.12	0.54 ^{ab} ± 0.10	0.84 ^b ± 0.01
22:1 <i>n</i> -9	0.12 ^a ± 0.01	0.20 ^a ± 0.09	0.21 ^a ± 0.09	0.62 ^b ± 0.05
24:1 <i>n</i> -9	0.00 ^a ± 0.00	0.01 ^a ± 0.01	0.00 ^a ± 0.00	0.08 ^b ± 0.01
18:2 <i>n</i> -6c	24.49 ^a ± 0.62	24.57 ^a ± 0.64	25.29 ^a ± 0.67	27.98 ^b ± 0.26
18:2 <i>n</i> -6t	0.40 ± 0.23	0.16 ± 0.16	0.17 ± 0.17	0.00 ± 0.00
20:2 <i>n</i> -6	0.06 ^a ± 0.02	0.12 ^a ± 0.05	0.13 ^a ± 0.04	0.33 ^b ± 0.02
22:2 <i>n</i> -6	0.00 ^a ± 0.00	0.01 ^a ± 0.01	0.02 ^a ± 0.02	0.10 ^b ± 0.01
18:3 <i>n</i> -3	0.86 ± 0.26	0.89 ± 0.17	0.83 ± 0.16	1.11 ± 0.13
18:3 <i>n</i> -6	0.97 ± 0.13	0.99 ± 0.06	0.90 ± 0.07	1.12 ± 0.04
20:3 <i>n</i> -3	0.00 ± 0.00	0.04 ± 0.04	0.04 ± 0.04	0.09 ± 0.01
20:3 <i>n</i> -6	0.13 ± 0.01	0.13 ± 0.03	0.13 ± 0.02	0.20 ± 0.02
20:4 <i>n</i> -6	0.23 ^a ± 0.01	0.24 ^a ± 0.03	0.28 ^{ab} ± 0.03	0.32 ^b ± 0.01
20:5 <i>n</i> -3	2.36 ^a ± 0.13	2.62 ^a ± 0.44	2.79 ^a ± 0.45	4.07 ^b ± 0.03
22:6 <i>n</i> -3	2.25 ^a ± 0.31	2.97 ^a ± 0.99	2.98 ^a ± 0.98	6.69 ^b ± 0.21
Saturated	41.36 ^b ± 1.46	37.86 ^b ± 4.21	37.53 ^b ± 3.86	23.62 ^a ± 0.38
Monounsaturated	26.9 ^a ± 0.80	29.39 ^a ± 1.95	28.92 ^a ± 1.68	34.38 ^b ± 0.34
PUFA	31.75 ^a ± 0.67	32.75 ^a ± 2.26	33.55 ^a ± 2.19	42.00 ^b ± 0.38
<i>n</i> -3	5.47 ^a ± 0.19	6.52 ^a ± 1.59	6.64 ^a ± 1.62	11.96 ^b ± 0.16
<i>n</i> -6	26.27 ^a ± 0.82	26.23 ^a ± 0.74	26.91 ^a ± 0.76	30.04 ^b ± 0.26
<i>n</i> -9	20.09 ^a ± 0.65	22.73 ^a ± 2.53	22.51 ^a ± 2.16	29.99 ^b ± 0.32
<i>n</i> -6/ <i>n</i> -3	4.83 ^b ± 0.30	4.52 ^b ± 0.69	4.59 ^b ± 0.76	2.51 ^a ± 0.03

Data are expressed as percentage of total fatty acids and represented as mean \pm SEM ($n = 4$). Different superscript letters indicate significant differences between groups ($P < 0.05$).

3.4. Effect of fish codon-optimised FAT-1 and FAT-2 on the expression of key genes in *de novo* lipogenesis and fatty acid oxidation in the liver

The effect of chitosan-TPP-DNA nanoparticles expressing FAT-1 and FAT-2 was also assessed on the hepatic expression of genes involved in *de novo* lipogenesis and fatty acid oxidation. As shown in Fig. 3, treatment with FAT-1 significantly decreased the mRNA levels of elongation of very long chain fatty acids protein 4a (*elovl4a*; to 43.3 % of control values), elongation of very long chain fatty acids protein 4b (*elovl4b*; to 45.4 %), elongation of very long chain fatty acids protein 5 (*elovl5*; to 62.3 %), sterol regulatory element-binding protein 1 (*srebfl*; to 41.3 %) and peroxisome proliferator-activated receptor alpha (*ppara*; to 46.0 %), while treatment with FAT-2 decreased *elovl5* (to 43.6 %) and *ppara* (to 56.3 %) mRNA levels (Figs. 3f-h, k and l). Co-expression of FAT-1 and FAT-2 also significantly downregulated acetyl-CoA carboxylase 1 (*acaca*; to 31.4 % of control values), acetyl-CoA carboxylase 2 (*acacb*; to 65.0 %), acyl-CoA 6-desaturase (*fads2*; to 69.4 %), *elovl4b* (to 59.1 %), *elovl5* (to 41.8 %), 3-hydroxy-3-methylglutaryl-coenzyme A reductase (*hmgcr*; to 64.2 %) and *srebfl* (to 41.9 %) (Figs. 3a, b, e, g, h, j and k). No significant differences were found for fatty acid synthase (*fasn*), stearoyl-CoA desaturase-1a (*scd1a*) and carnitine O-palmitoyltransferase 1, liver isoform (*cpt1a*) (Figs. 3c, d and i).

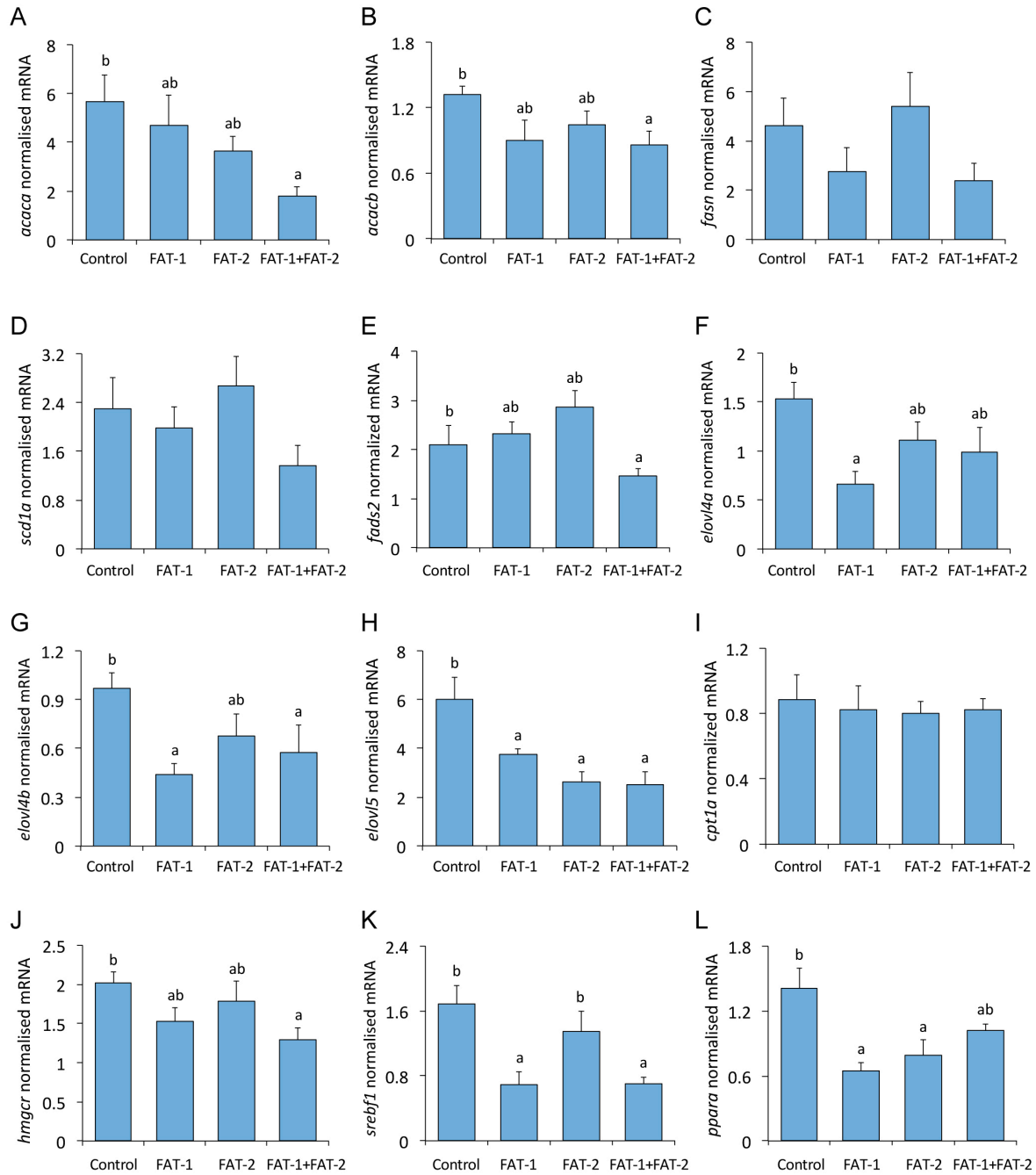


Fig. 3. Effect of long-term treatment with chitosan-TPP nanoparticles complexed with pSG5 (control), pSG5-FAT-1, pSG5-FAT-2 and pSG5-FAT-1 + pSG5-FAT-2 on the expression of key genes in *de novo* lipogenesis and fatty acid oxidation in the liver of *S. aurata*. Fifteen days after the last injection and 24 h following the last meal, fish were sacrificed and the liver were collected. Data are means \pm SEM ($n = 6$). Expression data were normalised by the geometric mean of *S. aurata* *18s*, *actb* and *eef1a* mRNA levels. Homogeneous subsets for the treatment are shown with different letters ($P < 0.05$).

3.5. Effect of fish codon-optimised FAT-1 and FAT-2 on glycolysis-gluconeogenesis, the pentose phosphate pathway, *hnf4a* and *nr1h3* in the liver

Fig. 4a-h shows the effect of long-term expression of fish codon-optimised FAT-1 and FAT-2 on the hepatic expression of rate-limiting enzymes in glycolysis-gluconeogenesis. Due to the pivotal role of the enzymes that control the flux through the fructose-6-phosphate/fructose-1,6-bisphosphate cycle in the regulation of glycolysis-gluconeogenesis, we measured both the mRNA levels and the enzyme activity of PFKL and FBP1. Gene expression of *pfkl* and *fbp1* was not significantly affected by the treatments (Figs. 4d and e). However, when considering the PFKL/FBP1 activity ratio, fish treated with FAT-1 + FAT-2 exhibited a significant increased glycolytic flux (29.9 %) compared to control fish (Fig. 4f). Similarly, treatment with FAT-2 showed a trend to increase the PFKL/FBP1 activity ratio (22.7 %).

In regard of other glycolytic-gluconeogenic enzymes, expression of FAT-2 and FAT-1 + FAT-2 significantly upregulated 1.5-fold and 1.8-fold, respectively, the mRNA levels of liver pyruvate kinase (*pklr*) and 1.4-fold those of 6-phosphofructo-2-kinase/fructose-2,6-bisphosphatase (*pfkfb1*) (Fig. 4c). Compared to controls, the expression levels for glucokinase (*gck*), glucose-6-phosphatase catalytic subunit (*g6pc1*) and phosphoenolpyruvate carboxykinase (*pck1*) were not affected (Figs. 4a, b and h).

In addition, expression of FAT-2 also significantly increased the hepatic mRNA levels (2.0-fold) of glucose-6-phosphate dehydrogenase (*g6pd*), the rate-limiting enzyme in the oxidative phase of the pentose phosphate pathway (Fig. 4i), while treatment with FAT-2 and FAT-1 + FAT-2 upregulated hepatocyte nuclear factor 4-alpha (*hnf4a*; 1.5-fold) and oxysterols receptor LXR-alpha (*nr1h3*; 1.6-fold) mRNA levels, respectively (Figs. 4j-k).

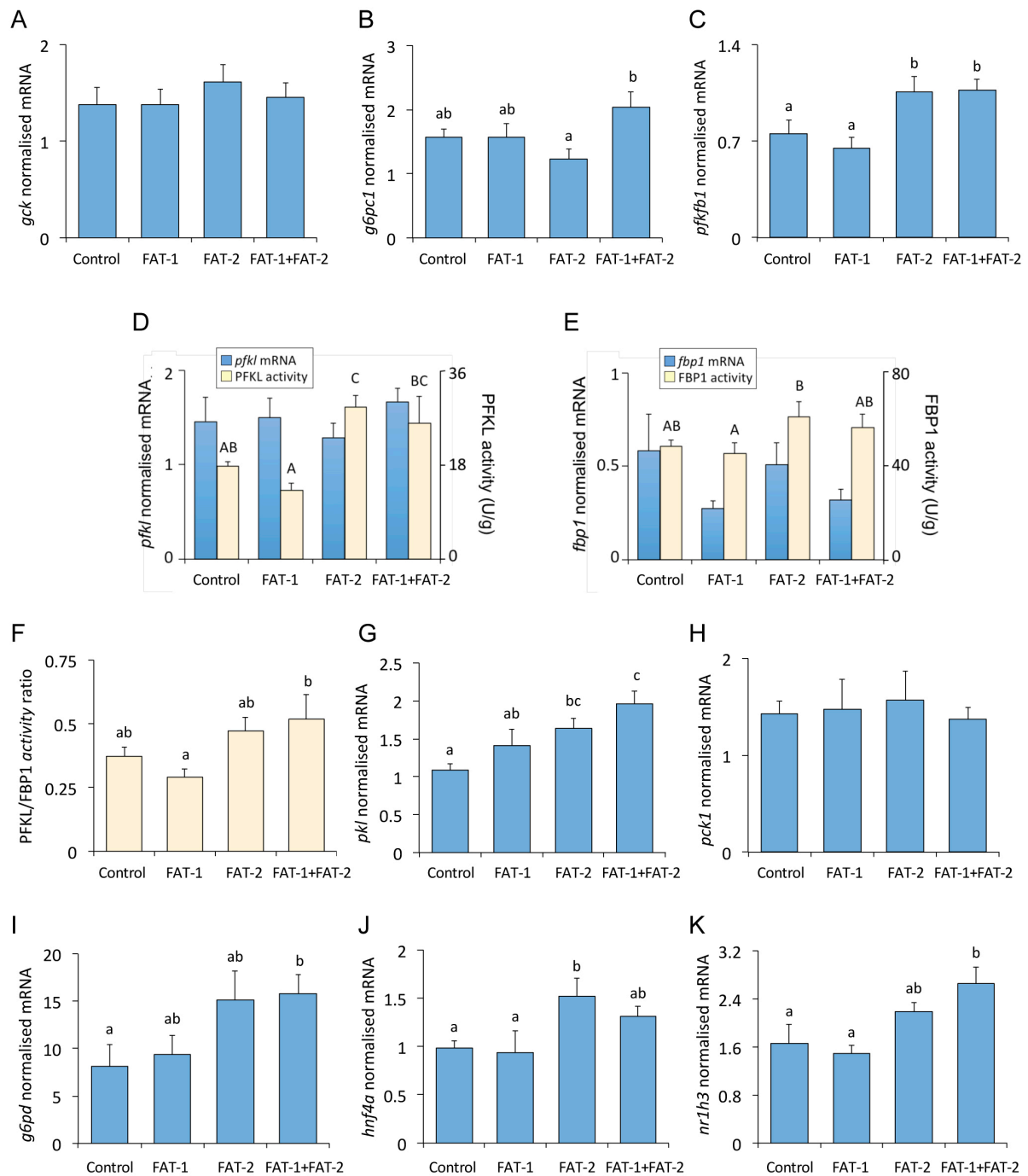


Fig. 4. Effect of long-term treatment with chitosan-TPP nanoparticles complexed with pSG5 (control), pSG5-FAT-1, pSG5-FAT-2 and pSG5-FAT-1 + pSG5-FAT-2 on the expression of key genes in glycolysis-gluconeogenesis and the pentose phosphate pathway, *hnf4a* and *nr1h3* in the liver of *S. aurata*. Fifteen days after the last injection and 24 h following the last meal, fish were sacrificed and the liver were collected. Hepatic mRNA levels and enzyme activity of PFKL and FBP1 are presented as mean \pm SEM ($n = 6$). Expression data were normalised by the geometric mean of *S. aurata 18s*,

actb and *eef1a* mRNA levels. Homogeneous subsets for the treatment are shown with different letters ($P < 0.05$).

4. Discussion

With the aim to induce sustained production of *n*-3 LC PUFA in *S. aurata*, the ionotropic gelation technique was used to obtain chitosan-TPP nanoparticles complexed with plasmids expressing fish codon-optimised *C. elegans* FAT-1 and FAT-2. Monthly intraperitoneal administration of 3 doses of the resulting nanoparticles allowed long-standing high expressional levels of the exogenous proteins in the liver, mild expression in the intestine and barely detectable levels in the skeletal muscle and brain. Biodistribution of fish codon-optimised FAT-1 and FAT-2 expression shows that the particle size of chitosan-TPP-DNA complexes used in the present study favoured liver retention in *S. aurata*, which confirms previous reports where we analysed the acute effect of expressing exogenous SREBP1a and silencing of endogenous cytosolic alanine aminotransferase and glutamate dehydrogenase (Gaspar et al., 2018; González et al., 2016; Silva-Marrero et al., 2019). Possibly, discontinuous endothelia of the intestine enables chitosan-TPP-DNA nanoparticle absorption and transportation to the liver through portal circulation (Hagens et al., 2007), while the tight morphology of capillary endothelium in the muscle and brain may limit the transfer of nanoparticles and result in the scarce levels of transcript (Kooij et al., 2005).

Transgenesis of FAT-1, a gene that facilitates the conversion of *n*-6 to *n*-3 fatty acids, scarcely affected body growth in zebrafish, common carp, mice, pig and lamb (Bhattacharya et al., 2006; Ji et al., 2009; Liu et al., 2016; Sun et al., 2020; Zhang et al., 2018, 2019). However, in the present study long-term hepatic expression of FAT-1 and FAT-1 + FAT-2 significantly increased weight gain but not lipid content in *S. aurata*. A trend to increase SGR values was also observed in fish co-expressing FAT-1 and FAT-2. Our findings suggest that

increased levels of *n*-3 LC-PUFA and decreased *n*-6/*n*-3 fatty acid ratio resulting from expression of fish codon-optimised FAT-1 and FAT-2 may contribute to increased growth performance in *S. aurata*. In support of this hypothesis, substitution of fish oil (rich in *n*-3 LC-PUFA) by vegetable oil enhances the *n*-6/*n*-3 ratio and lowers *n*-3 LC-PUFA and weight gain in *S. aurata* (Houston et al., 2017), as well as in other marine fish such as cobia (Trushenski et al., 2012) and the anadromous Atlantic salmon (Qian et al., 2020). However, dietary fish oil does not significantly affect growth in freshwater fish such as zebrafish (Meguro and Hasumura, 2018), common carp (Ljubojević et al., 2015), red hybrid tilapia (Al-Souti et al., 2012) and rainbow trout (Richard et al., 2006). Greater capacity of freshwater fish than marine fish for converting *n*-3 and *n*-6 C₁₈ PUFA into highly unsaturated long-chain fatty acids (Castro et al., 2016), may explain different adaptative responses to dietary *n*-3 LC-PUFA. Better growth performance of *S. aurata* submitted to sustained expression of fish codon-optimised FAT-1 and FAT-1 + FAT-2 may also result from improved health condition due to increased *n*-3 LC-PUFA and decreased *n*-6/*n*-3 ratio. Consistently, FAT-1 transgenesis prevents liver steatosis and lipid deposition in the abdominal cavity of zebrafish by a mechanism involving hepatic downregulation of lipogenic-related genes and upregulation of steatolysis-related genes (Sun et al., 2020). Moreover, FAT-1 transgenesis prevents glucose intolerance, insulin resistance, non-alcoholic fatty liver disease and allergic airway responses in mice (Bilal et al., 2011; Boyle et al., 2020; Kim et al., 2012; Romanatto et al., 2014), and exerts protective vascular effects on pigs and cattle by reducing inflammatory factors and improving the immune system (Liu et al., 2016, 2017). Accordingly, *S. aurata* treated with FAT-1 and FAT1 + FAT-2 showed decreased HSI levels, which therefore may essentially result from lower lipid deposition in the liver of fish expressing FAT-1.

Body fatty acid composition is affected by multiple factors, including *de novo* fatty acid synthesis, physiological requirements and dietary fatty acid profile. Single-gene expression of

either FAT-1 or FAT-2 enhanced fatty acid desaturation and, consequently, *n*-3 LC-PUFA synthesis in transgenic mice (Pai et al., 2014), pig (Tang et al., 2019), zebrafish (Pang et al., 2014), and common carp (Zhang et al., 2019). Similarly, *S. aurata* long-term treated with chitosan-TPP-DNA nanoparticles expressing either FAT-1 or FAT-2 showed a general trend to increase liver and muscle EPA, DHA, and total *n*-3 fatty acids and PUFA, while decreased the *n*-6/*n*-3 ratio and saturated fatty acids, conceivably by conversion into unsaturated fatty acids. Most of these effects were potentiated by hepatic co-expression of FAT-1 and FAT-2. Combined activities of FAT-1 and FAT-2 decreased saturated fatty acids such as 14:0, 16:0 and 17:0, while increased unsaturated fatty acids, particularly *n*-3, and to a lesser extent *n*-9 and *n*-6. Thus, co-expression of FAT-1 and FAT-2 promoted a synergistic effect that favoured liver production of *n*-3 LC-PUFA and its accumulation in the muscle, particularly EPA and DHA. Given that FAT-1 and FAT-2 mRNA levels were scarcely detected in the skeletal muscle of *S. aurata*, changes in the muscle fatty acid profile between treatments may ascribe to hepatic fat exportation forming part of very low density lipoproteins (VLDL).

Among biochemical parameters improved by FAT-1 transgenesis, reduced circulating levels for triglycerides and cholesterol were reported in mice (Romanatto et al., 2014), pigs (Liu et al., 2016), and cattle (Liu et al., 2017), while decreased hepatic triglycerides and cholesterol ester were found in zebrafish (Sun et al., 2020). Similarly, hepatic co-expression of FAT-1 and FAT-2 reduced serum triglycerides and cholesterol in *S. aurata*. In this regard, the present study showed that long-term co-expression of FAT-1 and FAT-2 promoted a general decrease of the expression of key enzymes for *de novo* lipogenesis in the liver of *S. aurata*. In addition, decreased serum triglycerides may also be attributed in part to the increase of *n*-3 LC-PUFA in the liver, where *n*-3 fatty acids are generally thought to reduce the production of VLDL and induce fatty acid β -oxidation (Shearer et al., 2012).

Treatment with FAT-1 + FAT-2 significantly downregulated *hmgcr*, which encodes the rate-limiting enzyme in cholesterol synthesis, and key genes in fatty acid synthesis, such as *acaca* and *acacb*, which catalyse conversion of acetyl-CoA into malonyl-CoA in the cytosol and mitochondrion, respectively, fatty acid elongases (*elovl4b* and *elovl5*) and *fads2* desaturase. Although not significant, the expression of *scd1a*, which catalyses the insertion of a *cis* double bond at the $\Delta 9$ position into saturated C₁₆ and C₁₈ fatty acyl-CoA (Wang et al., 2005), also showed a trend to decrease in fish treated with nanoparticles expressing FAT-1 + FAT-2. Furthermore, the expression of the three fatty acid elongases herein analysed (*elovl4a*, *elovl4b* and *elovl5*) strongly decreased by sustained expression of FAT-1. In transgenic animals, the effect of FAT-1 seems to depend on a variety of factors including the species, environmental conditions and dietary lipid content. Similarly as in *S. aurata*, a high-fat diet (13.4 % of crude lipid *versus* 18.0 % used in the present study) downregulated the hepatic expression of *acaca*, *fasn* and *scd1* in FAT-1 transgenic zebrafish. However, a low-fat diet (3.1 % of crude lipid) caused the opposite effects, upregulating the expression of the three genes (Sun et al., 2020). In line with our findings, FAT-1 transgenesis in mice decreased the levels of phosphorylated ACACA and FASN (Romanatto et al., 2014). However, FAT-1 transgenic common carp showed upregulation of *fads2*, *elovl5* and *elovl2* in the liver, and transgenic pigs co-expressing FAT-1 and FAT-2 also presented increased expression levels of *elovl5* and *elovl2* in the muscle, skin and fat (Tang et al., 2019; Zhang et al., 2019).

Downregulation of *acacb* in *S. aurata* treated with FAT-1 + FAT-2 suggests a limited synthesis rate of mitochondrial malonyl-CoA. Any of the treatments affected the mRNA abundance of *cpt1a*, which is essential for the mitochondrial uptake of long-chain fatty acids and their subsequent β -oxidation in the mitochondrion. However, given that malonyl-CoA is a potent allosteric inhibitor of CPT1A (Saggerson, 2008), our data suggest that in addition to decrease *de novo* lipogenesis, sustained co-expression of FAT-1 and FAT-2 may increase

fatty acid oxidation in the liver of *S. aurata* fed medium- or high-fat diets. Hence, transgenesis of FAT-1 and double transgenesis of FAT-1 and FAT-2 increased expression of *cpt1a* in zebrafish (Pang et al., 2014; Sun et al., 2020).

In mammals, alternate promoters in the *srebf1* gene generate SREBP1a and SREBP1c, which constitute transcription factors with a major role in *de novo* lipogenesis activation. SREBP1c primarily transactivates genes required for fatty acid and triglyceride synthesis while SREBP1a is a potent activator of all SREBP-responsive genes, including genes associated with cholesterol synthesis. Consistent with the role of *srebf1* in the transcription of lipogenic genes both in fish and mammals (Carmona-Antoñanzas et al., 2014; Silva-Marrero et al., 2019), downregulation of *srebf1* in the liver of *S. aurata* submitted to long-term expression of fish codon-optimised FAT-1 and FAT-1 + FAT-2 led to a trend to decrease the expression of genes involved in cholesterol synthesis (*hmgcr*) and fatty acid synthesis (*acaca*, *acacb* and *fasn*), desaturation (*scd1a* and *fads2*) and elongation (*elovl4a*, *elovl4b* and *elovl5*). In agreement with our findings, transgenic zebrafish expressing FAT-1, FAT-2 and FAT-1 + FAT-2 and double transgenic pigs for FAT-1 and FAT-2 also showed downregulated expression levels of *srebf1*. Since DHA suppresses *srebf1* expression and enhances its protein degradation (Jump, 2008), increased levels of DHA seem the main responsible for decreased expression of *srebf1* and *de novo* lipogenic genes in the liver of *S. aurata* expressing FAT-1 and FAT-1 + FAT-2. Consistently, substitution of fish oil, rich in DHA, by vegetable oil leads to upregulation of *srebf1* and fatty acid synthesis-related genes in *S. aurata* (Ofori-Mensah et al., 2020).

In the present study, FAT-1 and FAT-2 downregulated *ppara* in the liver of *S. aurata*. PPARA is a nuclear receptor activated by a wide range of ligands including fatty acids and fatty acid metabolites, such as eicosanoids. In the mammalian liver, PPARA controls the expression of genes involved in fatty acid uptake, intracellular transport, acyl-CoA formation

and fatty acid mitochondrial and peroxisomal oxidation, ketogenesis and lipoprotein metabolism (Bougarne et al., 2018). Supplementation of fish oil to rodents enhances *ppara* expression in the liver (Hein et al., 2010; Kamisako et al., 2012), possibly as a result of increased availability of *n*-3 LC-PUFA, particularly EPA. However, the effect of dietary fish oil on *ppara* expression in fish depends on the species. Similarly as in *S. aurata* expressing FAT-1 and FAT-2, fish oil was shown to decrease the hepatic mRNA levels of *ppara* in *S. aurata* and juvenile turbot (Ofori-Mensah et al., 2020; Peng et al., 2014), while the opposite effect was reported in large yellow croaker and lean, but not fat, Atlantic salmon (Du et al., 2017; Morais et al., 2011). As pointed out by Peng et al. (Peng et al., 2014), fatty acid-derived factors other than EPA-mediated activation may contribute to species-specific regulation of *ppara* expression in fishes.

The effect of *C. elegans* FAT-1 and FAT-2 on glucose metabolism remains largely unknown. In the present study, we found that long-term expression of fish codon-optimised *C. elegans* FAT-2 and FAT-1 + FAT-2 stimulated glycolysis and the expression levels of *hnf4a* and *nr1h3* in the liver of *S. aurata*. By controlling the flux through the fructose-6-phosphate/fructose-1,6-bisphosphate substrate cycle, *pfkl* and *fbp1* exert critical roles in hepatic glycolysis-gluconeogenesis. Although the mRNA levels of *pfkl* and *fbp1* were not significantly affected by any of the treatments, expression of FAT-2 and FAT-1 + FAT-2 promoted higher levels of PFKL/FBP1 activity ratio, possibly as a result of *pfkfb1* upregulation. The bifunctional enzyme *pfkfb1* catalyses the synthesis and degradation of fructose-2,6-bisphosphate, which is a major regulator of glycolysis–gluconeogenesis through allosteric activation of PFKL and inhibition of FBP1 (Okar et al., 2004). We previously showed that refeeding and high carbohydrate diets upregulate *pfkfb1* and the kinase activity of the bifunctional enzyme in the liver of *S. aurata*, leading to a concomitant increase in fructose-2,6-bisphosphate levels (Metón et al., 2000, 1999a). As in mammals, fructose-2,6-

bisphosphate is an allosteric activator of *S. aurata* PFKL (Mediavilla et al., 2008). Therefore, our results suggest that *pfkfb1* upregulation in the liver of fish expressing FAT-2 and FAT-1 + FAT-2 may be a key step favouring the glycolytic flux through the fructose-6-phosphate/fructose-1,6-bisphosphate substrate cycle, which in turn will increase the hepatic content of fructose-1,6-bisphosphate, an allosteric activator of PKLR.

The nuclear receptor HNF4A is a master regulator of liver metabolism through transcriptional regulation of target genes involved in glucose metabolism, lipid metabolism and hepatocyte differentiation (Meng et al., 2016). In mammals, HNF4A transactivates both glycolytic and gluconeogenic genes. Thus, HNF4A-binding to the gene promoter is required for insulin-stimulated upregulation of *gck* and *pklr* in the fed state, while a synergistic action of HNF4A and FOXO1 enhances the transcription of *g6pc1* and *pck1* during fasting (Ganjam et al., 2009; Hirota et al., 2008). Furthermore, HNF4A was previously shown to induce the expression of *nr1h3* (Theofilatos et al., 2016), which encodes LXR-alpha, a nuclear receptor stimulated by insulin that is also involved in glucose and lipid metabolism (Zhao et al., 2012). Indeed, LXR-alpha was shown to upregulate *pklr* mRNA levels in mice (Cha and Repa, 2007), and behave as a key regulator of *pfkfb* expression in humans by binding and transactivating the gene promoter of the bifunctional enzyme (Zhao et al., 2012). Therefore, increased *hnf4a* and *nr1h3* mRNA abundance in *S. aurata* expressing FAT-2 and FAT-1 + FAT-2 may enhance hepatic upregulation of *pfkfb1* and *pklr* expression, and thus increase the glycolytic flux in the liver. Consistent with HNF4A-dependent enhancement of glycolysis in *S. aurata*, *hnf4a* expression was previously shown to increase in *S. aurata* under glycolytic conditions *versus* gluconeogenic conditions such as fasting and treatment with streptozotocin (Salgado et al., 2012). Increased levels of *n-3* LC-PUFA may be a key factor leading to *hnf4a* and *nr1h3* upregulation in the *S. aurata* liver. In agreement, FAT-1 transgenic mice presented increased hepatic mRNA levels of *hnf4a* and to a lesser extent *nr1h3* (Kim et al., 2012).

Similarly, dietary supplementation with dried marine algae, rich in *n*-3 LC-PUFA (particularly DHA), induced *hnf4a* expression in the pig liver (Meadus et al., 2011). Furthermore, fish oil upregulated *nr1h3* in *S. aurata* adipocytes (Cruz-Garcia et al., 2011), and in the liver of juvenile turbot, Nile tilapia and mice (Ayisi et al., 2018; Kamisako et al., 2012; Peng et al., 2014).

To our knowledge, the effect of FAT-1 and FAT-2 transgenesis on the pentose phosphate pathway was not previously addressed. In the present study, long-term expression of fish codon-optimised FAT-2 and FAT-1 + FAT-2 promoted higher expression levels of *g6pd*, which encodes the rate-limiting enzyme for the production of NADPH in the oxidative phase of the pentose phosphate pathway. Previous reports indicated that dietary carbohydrates are a key factor that enhances G6PD activity in the liver of *S. aurata* (Metón et al., 1999b). Nevertheless, our findings support that fatty acid composition, particularly the *n*-3/*n*-6 ratio, also seems to regulate the hepatic expression of *g6pd*. In agreement with *g6pd* upregulation by *n*-3 LC-PUFA, fish oil stimulated G6PD activity in the rat liver (Yilmaz et al., 2004), and dietary supplementation with *n*-3 PUFA increased *g6pd* mRNA levels in the pig muscle (Vitali et al., 2018). Furthermore, *n*-6 PUFA, particularly LA, decreased *g6pd* mRNA levels in rat hepatocytes (Kohan et al., 2011). Species-specific regulation of *g6pd* expression by fatty acid composition may occur in other fishes. In this regard, total replacement of fish oil by vegetable oil did not affect G6PD activity but increased the mRNA levels in the liver of Nile tilapia (Ayisi et al., 2018), while enhanced G6PD activity in the liver of Atlantic salmon (Menoyo et al., 2005). Bearing in mind a general trend to downregulate *de novo* hepatic lipogenesis in *S. aurata* co-expressing FAT-1 and FAT-2, NADPH resulting from *g6pd* upregulation by *n*-3 LC-PUFA may reinforce cellular protection from oxidative stress.

5. Conclusions

The present study shows that long-term treatment with chitosan-TPP nanoparticles complexed with plasmids expressing fish codon-optimised *C. elegans* FAT-1 and FAT-2 allowed efficient expression of exogenous FAT-1 and FAT-2 desaturases in the liver of *S. aurata*, which in turn elevated the *n*-3 LC-PUFA content, particularly EPA and DHA, and decreased the *n*-6/*n*-3 ratio both in the liver and the skeletal muscle. Co-expression of fish codon-optimised FAT-1 and FAT-2 promoted the highest weight gain, *n*-3 LC-PUFA accumulation in the muscle and metabolic effect on lipid and glucose metabolism. Expression of fish codon-optimised FAT-1 and FAT-1 + FAT-2 downregulated the hepatic expression of *srebfl* and as a consequence, the mRNA levels of key genes in *de novo* lipogenesis, while FAT-2 and FAT-1 + FAT-2 upregulated *hnf4a*, *nr1h3* and glucose oxidation through glycolysis and the pentose phosphate pathway. Our findings support that chitosan-TPP-DNA nanoparticles co-expressing fish codon-optimised FAT-1 and FAT-2 can alleviate the effect of fish oil replacement with vegetable oil currently occurring in aquafeeds and enable production of functional fish rich in EPA and DHA for human consumption.

CRedit authorship contribution statement

Yuanbing Wu: Formal analysis, Investigation, Methodology, Visualization, Writing – original draft, Writing – review & editing. **Ania Rashidpour:** Investigation, Methodology, Writing – review & editing. **Anna Fàbregas:** Investigation, Methodology, Writing – review & editing. **María Pilar Almajano:** Investigation, Methodology, Resources, Writing – review & editing. **Isidoro Metón:** Conceptualization, Formal analysis, Supervision, Project administration, Funding acquisition, Resources, Visualization, Writing – original draft, Writing – review & editing.

Declaration of competing interest

The authors declare no conflicts of interest.

Acknowledgements

This work was supported by the Ministerio de Economía y Competitividad, Spain (grant no. AGL2016-78124-R; cofunded by the European Regional Development Fund, EC) and the Ministerio de Ciencia e Innovación, Spain (grant no. PID2021-125642OB-I00; cofunded by the European Regional Development Fund, EC). YW and AR are the recipients of China Scholarship Council (P.R. China) and PREDOCS-UB (Universitat de Barcelona, Spain) predoctoral fellowships, respectively. The authors thank Piscicultura Marina Mediterranea (AVRAMAR Group, Burriana, Spain) for providing *S. aurata* juveniles and Eurocoyal S.L. (Sant Cugat del Vallès, Spain) for supplying dietary components.

References

- Al-Souti, A., Al-Sabahi, J., Soussi, B., Goddard, S., 2012. The effects of fish oil-enriched diets on growth, feed conversion and fatty acid content of red hybrid tilapia, *Oreochromis sp.* Food Chem. 133, 723–727.
- Alimuddin, Kiron, V., Satoh, S., Takeuchi, T., Yoshizaki, G., 2008. Cloning and over-expression of a masu salmon (*Oncorhynchus masou*) fatty acid elongase-like gene in zebrafish. Aquaculture 282, 13–18.
- Alimuddin, Yoshizaki, G., Kiron, V., Satoh, S., Takeuchi, T., 2007. Expression of masu salmon $\Delta 5$ -desaturase-like gene elevated EPA and DHA biosynthesis in zebrafish. Mar. Biotechnol. 9, 92–100.
- Ayisi, C.L., Zhao, J.L., Hua, X.M., Apraku, A., 2018. Replacing fish oil with palm oil: Effects on mRNA expression of fatty acid transport genes and signalling factors related to lipid metabolism in Nile tilapia (*Oreochromis niloticus*). Aquac. Nutr. 24, 1822–1833.
- Betancor, M.B., Sprague, M., Montero, D., Usher, S., Sayanova, O., Campbell, P.J., Napier, J.A., Caballero, M.J., Izquierdo, M., Tocher, D.R., 2016. Replacement of marine fish oil with de novo omega-3 oils from transgenic *Camelina sativa* in feeds for gilthead sea bream (*Sparus aurata* L.). Lipids 51, 1171–1191.
- Bhattacharya, A., Chandrasekar, B., Rahman, M.M., Banu, J., Kang, J.X., Fernandes, G., 2006. Inhibition of inflammatory response in transgenic fat-1 mice on a calorie-restricted diet. Biochem. Biophys. Res. Commun. 349, 925–930.
- Bilal, S., Haworth, O., Wu, L., Weylandt, K.H., Levy, B.D., Kang, J.X., 2011. Fat-1 transgenic mice with elevated omega-3 fatty acids are protected from allergic airway responses. Biochim. Biophys. Acta - Mol. Basis Dis. 1812, 1164–1169.

- Bougarne, N., Weyers, B., Desmet, S.J., Deckers, J., Ray, D.W., Staels, B., De Bosscher, K., 2018. Molecular actions of PPAR α in lipid metabolism and inflammation. *Endocr. Rev.* 39, 760–802.
- Boyle, K.E., Magill-Collins, M.J., Newsom, S.A., Janssen, R.C., Friedman, J.E., 2020. Maternal fat-1 transgene protects offspring from excess weight gain, oxidative stress, and reduced fatty acid oxidation in response to high-fat diet. *Nutrients* 12.
- Busacker, G.P., Adelman, I.R., Goolish, E.M., 1990. Growth, in: Schreck, C.B., Moyle, P.B. (Eds.), *Methods for Fish Biology*. American Fisheries Society, Bethesda, pp. 363–387.
- Carmona-Antoñanzas, G., Tocher, D.R., Martínez-Rubio, L., Leaver, M.J., 2014. Conservation of lipid metabolic gene transcriptional regulatory networks in fish and mammals. *Gene* 534, 1–9.
- Carvalho, M., Marotta, B., Xu, H., Geraert, P.-A., Kaushik, S., Montero, D., Izquierdo, M., 2022. Complete replacement of fish oil by three microalgal products rich in n-3 long-chain polyunsaturated fatty acids in early weaning microdiets for gilthead sea bream (*Sparus aurata*). *Aquaculture* 558, 738354.
- Castro, L.F.C., Tocher, D.R., Monroig, O., 2016. Long-chain polyunsaturated fatty acid biosynthesis in chordates: Insights into the evolution of Fads and Elovl gene repertoire. *Prog. Lipid Res.* 62, 25–40.
- Cha, J.Y., Repa, J.J., 2007. The liver X receptor (LXR) and hepatic lipogenesis. The carbohydrate-response element-binding protein is a target gene of LXR. *J. Biol. Chem.* 282, 743–751.
- Chen, Y., Mei, M., Zhang, P., Ma, K., Song, G., Ma, X., Zhao, T., Tang, B., Ouyang, H., Li, G., Li, Z., 2013. The generation of transgenic mice with fat1 and fad2 genes that have their own Polyunsaturated Fatty Acid Biosynthetic Pathway. *Cell. Physiol. Biochem.* 32, 523–532.
- Cheng, C.-L., Huang, S.-J., Wu, C.-L., Gong, H.-Y., Ken, C.-F., Hu, S.-Y., Wu, J.-L., 2015. Transgenic expression of omega-3 PUFA synthesis genes improves zebrafish survival during *Vibrio vulnificus* infection. *J. Biomed. Sci.* 22, 103.
- Cruz-García, L., Sánchez-Gurmaches, J., Bouraoui, L., Saera-Vila, A., Pérez-Sánchez, J., Gutiérrez, J., Navarro, I., 2011. Changes in adipocyte cell size, gene expression of lipid metabolism markers, and lipolytic responses induced by dietary fish oil replacement in gilthead sea bream (*Sparus aurata* L.). *Comp. Biochem. Physiol. Part A Mol. Integr. Physiol.* 158, 391–399.
- Djuricic, I., Calder, P.C., 2021. Beneficial outcomes of omega-6 and omega-3 polyunsaturated fatty acids on human health: An update for 2021. *Nutrients* 13, 2421.

- Du, J., Xu, H., Li, S., Cai, Z., Mai, K., Ai, Q., 2017. Effects of dietary chenodeoxycholic acid on growth performance, body composition and related gene expression in large yellow croaker (*Larimichthys crocea*) fed diets with high replacement of fish oil with soybean oil. *Aquaculture* 479, 584–590.
- Ganjam, G.K., Dimova, E.Y., Unterman, T.G., Kietzmann, T., 2009. FoxO1 and HNF-4 are involved in regulation of hepatic glucokinase gene expression by resveratrol. *J. Biol. Chem.* 284, 30783–30797.
- Gaspar, C., Silva-Marrero, J.I., Fàbregas, A., Miñarro, M., Ticó, J.R., Baanante, I.V., Metón, I., 2018. Administration of chitosan-tripolyphosphate-DNA nanoparticles to knockdown glutamate dehydrogenase expression impairs transamination and gluconeogenesis in the liver. *J. Biotechnol.* 286, 5–13.
- González, J.D., Silva-Marrero, J.I., Metón, I., Caballero-Solares, A., Viegas, I., Fernández, F., Miñarro, M., Fàbregas, A., Ticó, J.R., Jones, J.G., Baanante, I.V., 2016. Chitosan-mediated shRNA knockdown of cytosolic alanine aminotransferase improves hepatic carbohydrate metabolism. *Mar. Biotechnol.* 18, 85–97.
- Hagens, W.I., Oomen, A.G., de Jong, W.H., Cassee, F.R., Sips, A.J.A.M., 2007. What do we (need to) know about the kinetic properties of nanoparticles in the body? *Regul. Toxicol. Pharmacol.* 49, 217–229.
- Hein, G.J., Bernasconi, A.M., Montanaro, M.A., Pellon-Maison, M., Finarelli, G., Chicco, A., Lombardo, Y.B., Brenner, R.R., 2010. Nuclear receptors and hepatic lipidogenic enzyme response to a dyslipidemic sucrose-rich diet and its reversal by fish oil n-3 polyunsaturated fatty acids. *Am. J. Physiol. Endocrinol. Metab.* 298, E429-E439.
- Hirota, K., Sakamaki, J.I., Ishida, J., Shimamoto, Y., Nishihara, S., Kodama, N., Ohta, K., Yamamoto, M., Tanimoto, K., Fukamizu, A., 2008. A combination of HNF-4 and Foxo1 is required for reciprocal transcriptional regulation of glucokinase and glucose-6-phosphatase genes in response to fasting and feeding. *J. Biol. Chem.* 283, 32432–32441.
- Houston, S.J.S., Karalazos, V., Tinsley, J., Betancor, M.B., Martin, S.A.M., Tocher, D.R., Monroig, O., 2017. The compositional and metabolic responses of gilthead seabream (*Sparus aurata*) to a gradient of dietary fish oil and associated n-3 long-chain PUFA content. *Br. J. Nutr.* 118, 1010–1022.
- Ji, S., Hardy, R.W., Wood, P.A., 2009. Transgenic expression of n-3 fatty acid desaturase (fat-1) in C57/BL6 mice: Effects on glucose homeostasis and body weight. *J. Cell. Biochem.* 107, 809–817.

- Jump, D.B., 2008. N-3 polyunsaturated fatty acid regulation of hepatic gene transcription. *Curr. Opin. Lipidol.* 19, 242–247.
- Kamisako, T., Tanaka, Y., Ikeda, T., Yamamoto, K., Ogawa, H., 2012. Dietary fish oil regulates gene expression of cholesterol and bile acid transporters in mice. *Hepato. Res.* 42, 321–326.
- Kang, J.X., Wang, J., Wu, L., Kang, Z.B., 2004. Fat-1 mice convert n-6 to n-3 fatty acids. *Nature* 427, 504–504.
- Kim, E.H., Bae, J.S., Hahm, K.B., Cha, J.Y., 2012. Endogenously synthesized n-3 polyunsaturated fatty acids in fat-1 mice ameliorate high-fat diet-induced non-alcoholic fatty liver disease. *Biochem. Pharmacol.* 84, 1359–1365.
- Kohan, A.B., Qing, Y., Cyphert, H.A., Tso, P., Salati, L.M., 2011. Chylomicron remnants and nonesterified fatty acids differ in their ability to inhibit genes involved in lipogenesis in rats. *J. Nutr.* 141, 171–176.
- Kooij, G., van Horsen, J., de Vries, E., 2005. Tight junctions of the blood–brain barrier, in: de Vries, E., Prat, A. (Eds.), *The Blood-Brain Barrier and Its Microenvironment*. CRC Press, pp. 69–92.
- Lai, L., Kang, J.X., Li, R., Wang, J., Witt, W.T., Hwan, Y.Y., Hao, Y., Wax, D.M., Murphy, C.N., Rieke, A., Samuel, M., Linville, M.L., Korte, S.W., Evans, R.W., Starzl, T.E., Prather, R.S., Dai, Y., 2006. Generation of cloned transgenic pigs rich in omega-3 fatty acids. *Nat. Biotechnol.* 24, 435–436.
- Li, M., Ouyang, H., Yuan, H., Li, J., Xie, Z., Wang, K., Yu, T., Liu, M., Chen, X., Tang, X., Jiao, H., Pang, D., 2018. Site-Specific fat-1 knock-in enables significant decrease of n-6PUFAs/n-3PUFAs ratio in pigs. *G3 (Bethesda)* 8, 1747–1754.
- Liu, X.-F., Wei, Z.-Y., Bai, C.-L., Ding, X.-B., Li, X., Su, G.-H., Cheng, L., Zhang, L., Guo, H., Li, G.-P., 2017. Insights into the function of n-3 PUFAs in fat-1 transgenic cattle. *J. Lipid Res.* 58, 1524–1535.
- Liu, X., Pang, D., Yuan, T., Li, Z., Li, Z., Zhang, M., Ren, W., Ouyang, H., Tang, X., 2016. N-3 polyunsaturated fatty acids attenuates triglyceride and inflammatory factors level in hfat-1 transgenic pigs. *Lipids Health Dis.* 15, 89.
- Ljubojević, D., Radosavljević, V., Puvača, N., Živkov Baloš, M., Dordević, V., Jovanović, R., Čirković, M., 2015. Interactive effects of dietary protein level and oil source on proximate composition and fatty acid composition in common carp (*Cyprinus carpio* L.). *J. Food Compos. Anal.* 37, 44–50.
- Lucas, A. (Albert), 1996. Bioenergetics of organisms: Methods, in: Priede, I.G. (Ed.), *Bioenergetics of Aquatic Animals*. Taylor & Francis, London, pp. 65–81.

- Luo, R., Zheng, Z., Yang, C., Zhang, X., Cheng, L., Su, G., Bai, C., Li, G., 2020. Comparative transcriptome analysis provides insights into the polyunsaturated fatty acid synthesis regulation of fat-1 transgenic sheep. *Int. J. Mol. Sci.* 21, 1121.
- Meadus, W.J., Duff, P., Rolland, D., Aalhus, J.L., Uttaro, B., Dugan, M.E.R., 2011. Feeding docosahexaenoic acid to pigs reduces blood triglycerides and induces gene expression for fat oxidation. *Can. J. Anim. Sci.* 91, 601–612.
- Mediavilla, D., Metón, I., Baanante, I.V., 2008. Purification and kinetic characterization of 6-phosphofructo-1-kinase from the liver of gilthead sea bream (*Sparus aurata*). *J. Biochem.* 144, 235–244.
- Meguro, S., Hasumura, T., 2018. Fish oil suppresses body fat accumulation in zebrafish. *Zebrafish* 15, 27–32.
- Meng, J., Feng, M., Dong, W., Zhu, Y., Li, Y., Zhang, P., Wu, L., Li, M., Lu, Y., Chen, H., Liu, X., Lu, Y., Sun, H., Tong, X., 2016. Identification of HNF-4 α as a key transcription factor to promote ChREBP expression in response to glucose. *Sci. Rep.* 6, 23944.
- Menoyo, D., López-Bote, C.J., Obach, A., Bautista, J.M., 2005. Effect of dietary fish oil substitution with linseed oil on the performance, tissue fatty acid profile, metabolism, and oxidative stability of Atlantic salmon. *J. Anim. Sci.* 83, 2853–2862.
- Metón, I., Caseras, A., Fernández, F., Baanante, I.V., 2000. 6-Phosphofructo-2-kinase/fructose-2,6-bisphosphatase gene expression is regulated by diet composition and ration size in liver of gilthead sea bream, *Sparus aurata*. *Biochim. Biophys. Acta - Gene Struct. Expr.* 1491, 220–228.
- Metón, I., Caseras, A., Mediavilla, D., Fernández, F., Baanante, I.V., 1999a. Molecular cloning of a cDNA encoding 6-phosphofructo-2-kinase/fructose-2,6-bisphosphatase from liver of *Sparus aurata*: nutritional regulation of enzyme expression. *Biochim. Biophys. Acta* 1444, 153–165.
- Metón, I., Mediavilla, D., Caseras, A., Cantó, E., Fernández, F., Baanante, I.V., 1999b. Effect of diet composition and ration size on key enzyme activities of glycolysis-gluconeogenesis, the pentose phosphate pathway and amino acid metabolism in liver of gilthead sea bream (*Sparus aurata*). *Br. J. Nutr.* 82, 223–232.
- Morais, S., Pratoomyot, J., Taggart, J.B., Bron, J.E., Guy, D.R., Bell, J.G., Tocher, D.R., 2011. Genotype-specific responses in Atlantic salmon (*Salmo salar*) subject to dietary fish oil replacement by

- vegetable oil: A liver transcriptomic analysis. *BMC Genomics* 12, 1–17.
- Ofori-Mensah, S., Yıldız, M., Arslan, M., Eldem, V., 2020. Fish oil replacement with different vegetable oils in gilthead seabream, *Sparus aurata* diets: Effects on fatty acid metabolism based on whole-body fatty acid balance method and genes expression. *Aquaculture* 529, 735609.
- Okar, D.A., Wu, C., Lange, A.J., 2004. Regulation of the regulatory enzyme, 6-phosphofructo-2-kinase/fructose-2,6-bisphosphatase. *Adv. Enzyme Regul.* 44, 123–154.
- Osmond, A.T.Y., Colombo, S.M., 2019. The future of genetic engineering to provide essential dietary nutrients and improve growth performance in aquaculture: Advantages and challenges. *J. World Aquac. Soc.* 50, 490–509.
- Pai, V.J., Wang, B., Li, X., Wu, L., Kang, J.X., 2014. Transgenic mice convert carbohydrates to essential fatty acids. *PLoS One* 9, e97637.
- Pang, S.-C., Wang, H.-P., Li, K.-Y., Zhu, Z.-Y., Kang, J.X., Sun, Y.-H., 2014. Double transgenesis of humanized fat1 and fat2 genes promotes omega-3 polyunsaturated fatty acids synthesis in a zebrafish model. *Mar. Biotechnol.* 16, 580–593.
- Peng, M., Xu, W., Mai, K., Zhou, H., Zhang, Y., Liufu, Z., Zhang, K., Ai, Q., 2014. Growth performance, lipid deposition and hepatic lipid metabolism related gene expression in juvenile turbot (*Scophthalmus maximus* L.) fed diets with various fish oil substitution levels by soybean oil. *Aquaculture* 433, 442–449.
- Pfaffl, M.W., 2001. A new mathematical model for relative quantification in real-time RT-PCR. *Nucleic Acids Res.* 29, e45.
- Qian, C., Hart, B., Colombo, S.M., 2020. Re-evaluating the dietary requirement of EPA and DHA for Atlantic salmon in freshwater. *Aquaculture* 518, 734870.
- Richard, N., Kaushik, S., Larroquet, L., Panserat, S., Corraze, G., 2006. Replacing dietary fish oil by vegetable oils has little effect on lipogenesis, lipid transport and tissue lipid uptake in rainbow trout (*Oncorhynchus mykiss*). *Br. J. Nutr.* 96, 299–309.
- Romanatto, T., Fiamoncini, J., Wang, B., Curi, R., Kang, J.X., 2014. Elevated tissue omega-3 fatty acid status prevents age-related glucose intolerance in fat-1 transgenic mice. *Biochim. Biophys. Acta* 1842, 186–191.
- Saggerson, D., 2008. Malonyl-CoA, a key signaling molecule in mammalian cells. *Annu. Rev. Nutr.* 28,

253–272.

- Sales, R., Galafat, A., Vizcaíno, A.J., Sáez, M.I., Martínez, T.F., Cerón-García, M.C., Navarro-López, E., Tsuzuki, M.Y., Acién-Fernández, F.G., Molina-Grima, E., Alarcón, F.J., 2021. Effects of dietary use of two lipid extracts from the microalga *Nannochloropsis gaditana* (Lubián, 1982) alone and in combination on growth and muscle composition in juvenile gilthead seabream, *Sparus aurata*. *Algal Res.* 53, 102162.
- Salgado, M.C., Metón, I., Anemaet, I.G., González, J.D., Fernández, F., Baanante, I.V., 2012. Hepatocyte nuclear factor 4 α transactivates the mitochondrial alanine aminotransferase gene in the kidney of *Sparus aurata*. *Mar. Biotechnol.* 14, 46–62.
- Shearer, G.C., Savinova, O. V., Harris, W.S., 2012. Fish oil -- how does it reduce plasma triglycerides? *Biochim. Biophys. Acta* 1821, 843–851.
- Silva-Marrero, J.I., Sáez, A., Caballero-Solares, A., Viegas, I., Almajano, M.P., Fernández, F., Baanante, I.V., Metón, I., 2017. A transcriptomic approach to study the effect of long-term starvation and diet composition on the expression of mitochondrial oxidative phosphorylation genes in gilthead sea bream (*Sparus aurata*). *BMC Genomics* 18, 768.
- Silva-Marrero, J.I., Villasante, J., Rashidpour, A., Palma, M., Fàbregas, A., Almajano, M.P., Viegas, I., Jones, J.G., Miñarro, M., Tico, J.R., Baanante, I.V., Metón, I., 2019. The administration of chitosan-tripolyphosphate-DNA nanoparticles to express exogenous SREBP1 α enhances conversion of dietary carbohydrates into lipids in the liver of *Sparus aurata*. *Biomolecules* 9, 297.
- Sun, S., Castro, F., Monroig, Ó., Cao, X., Gao, J., 2020. fat-1 transgenic zebrafish are protected from abnormal lipid deposition induced by high-vegetable oil feeding. *Appl. Microbiol. Biotechnol.* 104, 7355–7365.
- Tang, F., Yang, X., Liu, D., Zhang, X., Huang, X., He, X., Shi, J., Li, Z., Wu, Z., 2019. Co-expression of fat1 and fat2 in transgenic pigs promotes synthesis of polyunsaturated fatty acids. *Transgenic Res.* 28, 369–379.
- Theofilatos, D., Anestis, A., Hashimoto, K., Kardassis, D., 2016. Transcriptional regulation of the human Liver X Receptor α gene by Hepatocyte Nuclear Factor 4 α . *Biochem. Biophys. Res. Commun.* 469, 573–579.
- Tocher, D.R., Betancor, M.B., Sprague, M., Olsen, R.E., Napier, J.A., 2019. Omega-3 long-chain

- polyunsaturated fatty acids, EPA and DHA: Bridging the gap between supply and demand. *Nutrients* 11, 89.
- Trushenski, J., Schwarz, M., Bergman, A., Rombenso, A., Delbos, B., 2012. DHA is essential, EPA appears largely expendable, in meeting the n-3 long-chain polyunsaturated fatty acid requirements of juvenile cobia *Rachycentron canadum*. *Aquaculture* 326–329, 81–89.
- Vitali, M., Dimauro, C., Sirri, R., Zappaterra, M., Zambonelli, P., Manca, E., Sami, D., Fiego, D.P. Lo, Davoli, R., 2018. Effect of dietary polyunsaturated fatty acid and antioxidant supplementation on the transcriptional level of genes involved in lipid and energy metabolism in swine. *PLoS One* 13, e0204869.
- Wang, J., Yu, L., Schmidt, R.E., Su, C., Huang, X., Gould, K., Cao, G., 2005. Characterization of HSCD5, a novel human stearoyl-CoA desaturase unique to primates. *Biochem. Biophys. Res. Commun.* 332, 735–742.
- Wu, Y., Rashidpour, A., Almajano, M.P., Metón, I., 2020. Chitosan-based drug delivery system: Applications in fish biotechnology. *Polymers* 12, 1177.
- Yilmaz, H.R., Songur, A., Özyurt, B., Zararsiz, I., Sarsilmaz, M., 2004. The effects of n-3 polyunsaturated fatty acids by gavage on some metabolic enzymes of rat liver. *Prostaglandins. Leukot. Essent. Fatty Acids* 71, 131–135.
- You, W., Li, M., Qi, Y., Wang, Y., Chen, Y., Liu, Y., Li, L., Ouyang, H., Pang, D., 2021. CRISPR/Cas9-mediated specific integration of fat-1 and IGF-1 at the p Rosa26 locus. *Genes* 12, 1027.
- Zhang, J., Cui, M.L., Nie, Y.W., Dai, B., Li, F.R., Liu, D.J., Liang, H., Cang, M., 2018. CRISPR/Cas9-mediated specific integration of fat-1 at the goat MSTN locus. *FEBS J.* 285, 2828–2839.
- Zhang, X., Pang, S., Liu, C., Wang, H., Ye, D., Zhu, Z., Sun, Y., 2019. A Novel Dietary Source of EPA and DHA: Metabolic engineering of an important freshwater species—common carp by fat1-transgenesis. *Mar. Biotechnol.* 21, 171–185.
- Zhao, L.F., Iwasaki, Y., Nishiyama, M., Taguchi, T., Tsugita, M., Okazaki, M., Nakayama, S., Kambayashi, M., Fujimoto, S., Hashimoto, K., Murao, K., Terada, Y., 2012. Liver X receptor α is involved in the transcriptional regulation of the 6-phosphofructo-2-kinase/fructose-2,6-bisphosphatase gene. *Diabetes* 61, 1062–1071.